Title
I. THE THEORY OF ABERRATIONS OF QUADRUPOLE FOCUSING ARRAYS. II. ION OPTICAL DESIGN OF HIGH QUALITY EXTRACTED SYNCHROTRON BEAMS WITH APPLICATION TO THE BEVATRON

Author
Meads Jr., Philip Francis

Publication Date
2011-02-15

F. Selph

UCRL-10807

University of California

Ernest O. Lawrence Radiation Laboratory

I. THE THEORY OF ABERRATIONS OF QUADRUPOLE FOCUSING ARRAYS

II. ION OPTICAL DESIGN OF HIGH QUALITY EXTRACTED SYNCHROTRON BEAMS WITH APPLICATION TO THE BEVATRON

Berkeley, California

UCRL-10807
UC-28 Particle Accel.
and High Volt. Mach.
TID-4500 (19th Ed.)

UNIVERSITY OF CALIFORNIA

Lawrence Radiation Laboratory
University of California

Contract No. W-7405-eng-48

I. THE THEORY OF ABERRATIONS OF QUADRUPOLE FOCUSING ARRAYS

II. ION OPTICAL DESIGN OF HIGH QUALITY EXTRACTED SYNCHROTRON BEAMS WITH APPLICATION TO THE BEVATRON

Philip Francis Meads, Jr.
(Thesis)

May 15, 1963

Printed in USA. Price $4.00. Available from the
Office of Technical Services
U. S. Department of Commerce
Washington 25, D.C.

Table of Contents

Page

Page

Page

I. THE THEORY OF ABERRATIONS OF QUADRUPOLE FOCUSING ARRAYS

II. ION OPTICAL DESIGN OF HIGH QUALITY EXTRACTED SYNCHROTRON BEAMS WITH APPLICATION TO THE BEVATRON

Philip Francis Meads, Jr.

Lawrence Radiation Laboratory
University of California
Berkeley, California

May 15, 1963

ABSTRACT

In Part One we formulate in a general way the problem of analyzing and evaluating the aberrations of quadrupole magnet beam systems, and of characterizing the shapes and other properties of the beam envelopes in the neighborhood of foci. We consider all aberrations, including those due to misalignments and faulty construction, through third order in small parameters, for quadrupole beam systems. One result of this study is the development of analytic and numerical techniques for treating these aberrations, yielding useful expressions for the comparison of the aberrations of different beam systems. A second result of this study is a comprehensive digital computer program that determines the magnitude and nature of the aberrations of such beam systems. The code, using linear programming techniques, will adjust the parameters of a beam system to obtain specified optical properties and to reduce the magnitude of aberrations that limit the performance of that system. We examine numerically, in detail, the aberrations of two typical beam systems.

In Part Two, we examine the problem of extracting the

proton beam from a synchrotron of "H" type magnet construction. We describe the optical studies that resulted in the design of an external beam from the Bevatron that is optimized with respect to linear, dispersive, and aberration properties.and that uses beam elements of conservative design. The design of the beam is the result of the collaboration of many people representing several disciplines. We describe the digital computer programs developed to carry out detailed orbit studies which were required because of the existence of large second order aberrations in the beam.

I. INTRODUCTION TO PART ONE

As the complexity of modern physics experiments increases, more sophisticated beam systems are needed. The aberrations of quadrupole magnets limit the performance of many beam systems. An object of this theoretical study is to formulate in a general way the problem of analyzing and evaluating these aberrations, and of characterizing the shapes and other properties of the beam envelopes in the neighborhoods of foci. Another purpose of this study is to generate, for the use of experimenters, a comprehensive IBM digital computer program which will determine the magnitude and nature of the aberrations of beam systems consisting of quadrupole magnets. This code also provides the means to reduce the magnitude of the aberrations that limit the performance of a beam system.

In the decade since their use was first proposed independently by Christophilos[1] and by Courant, Livingston, and Snyder[2], the quadrupole lens has become the standard focusing device in beam optics.

Quadrupole magnets have two planes of reflection antisymmetry. Symmetry arguments demonstrate that there can be no second-order aberrations in beam systems possessing this symmetry. The calculation of aberrations is restricted to beam systems having the quadrupole symmetry. Thus we exclude bending magnets which already have second-order aberrations.

There are five classic third-order aberrations in light optics, where the lenses possess rotational symmetry. Described by the Seidel coefficients, these five aberrations are spherical aberration, coma, astigmatism, curvature of field, and distortion.[3] Owing to the relaxed symmetry, beam systems consisting of quadrupole lenses have an additional eleven geometric aberrations, making a total of sixteen aberrations of third order.

Burfoot classified the additional aberrations that might occur in electron optics, where the classic rotational symmetry is replaced by two plane reflection antisymmetry.[4] He determined, from geometric symmetry considerations, that a total of 16 distinctive aberration types could occur. He described several of these figures, with the objective of recognizing, by inspection of the image, a particular aberration if it should dominate. He did not attempt to describe figures resulting from the presence of more than one type of aberration, nor did he include any of the chromatic aberrations.

Reisman examined the possibility of using a strong-focusing lens as a sustitute for a rotationally symmetric projector lens.[5] A quadrupole doublet may be adjusted to provide focal points and focal planes which are at the same position in both symmetry planes; such a lens is optically equivalent to an axially symmetric lens. It is always the case for such a lens that the focal points are imbedded within the lens, thus restricting its use. He solved analytically, to third order, the equations of motion for this particular doublet configuration, neglecting all end effects. He concluded that the aberrations of such a quadrupole doublet were of comparable magnitude to those of a good axially symmetric lens.

Bernard and Grivet solved analytically the linear equations of motion for a symmetric doublet, adding an impulse-correction term which corresponds to the action of infinitely sharp fringing fields.[6] Their assumption is appropriate to a very weak lens in which the slopes of trajectories are small. The effect of the infinitely sharp fringing field is to abruptly alter the slope of trajectories passing through the lens. They examined the effect of this correction upon a paraxial line image, determining that the image was "smeared" in the particular cases investigated.

Septier has experimentally measured the detailed fringing field shape for a quadrupole magnet 150 mm long with a bore of 40 mm radius.[7] His paper contains the results in graphical form, showing the dependence of the three field components upon the coordinates. The magnet measured was constructed with poletips of circular contour.

Grivet and Septier traced several initially parallel rays through the same symmetric doublet considered by Bernard and Grivet, numerically integrating the equations through third order.[8] This was first done on an analog machine and then repeated on a digital computer. They found aberrations comparable in magnitude to those obtained by adding the impulse-correction term. This validates their assumption that those aberrations which are highly dependent upon the slopes of the trajectories may be neglected in a weakly excited symmetric doublet. This method is slow and does not readily yield the dependence of the total aberrations upon the initial displacements and slopes. The chromatic aberration is less than the aperture aberration for this lens when used in their linear accelerator.

The work described above has been collected by Septier in a treatise on strong-focusing lenses.[9] The work is divided into four sections. Theoretical linear properties of magnetic and electrostatic quadrupole lenses are covered in the first section. Section II is a review of previous work on the aberrations of such lenses, as described above. Construction of these lenses and field measurements conducted upon them are next reported. The final section reviews experimental results obtained by using quadrupole lenses. A particularly comprehensive inclusion in this work is a list of 101 references.

In the present paper the aberrations are treated by studying the third-order terms in the power-series expansions of the displacements and slopes near the image plane in terms of the relative momentum and the displacements and slopes at the object plane. A method of successive approximations is applied to the trajectory equations which generate explicit expressions for the coefficients of terms through third order in the expansions of the displacements and slopes. These calculations are valid for any beam system that possesses the previously mentioned two-plane reflection antisymmetry. Forty derived coefficients characterize the third-order geometric aberrations. In Chapter VI we show that the canonical nature of the transformations that carry the trajectories between two points restricts the number of independent coefficients to 16, the number determined by Burfoot from symmetry arguments. An additional 16 coefficients describe the chromatic aberrations of second order, which satisfy the quadrupole symmetry, and those of third order. If the characteristic length of the fringing field of a quadrupole magnet is much smaller than the geometric mean of its effective length and its focal length, aberrations due to fringing fiedls may be separated from inherent aberrations of the magnet. These aberrations are characterized by 16 coefficients that depend upon the detailed shape of the fringing field.

Real beam systems may fail to produce pure quadrupole fields, owing to mechanical limitations. Nonalignments and rotations of individual quadrupole lenses introduce additional aberrations. The effects of these aberrations are calculated in the present work. Knowing these effects, one may prescribe tolerances in positioning each quadrupole magnet in a beam system which, if satisfied, insure that displacements in the trajectories due to nonalignments will be smaller than inherent aberrations of the beam system.

Real quadrupole magnets frequently contain several troublesome harmonics in the magnetic field which produce aberrations higher than third order. In section H of Chapter V we derive the approximate magnitude of displacements in the trajectories induced by each harmonic.

The maximum displacements due to aberrations are calculated for all trajectories whose momenta and initial displacements and slopes lie within specified symmetric bounds. Root-mean-square displacements due to the aberrations are calculated for three models of the occupied region of object-plane phase space. These rms displacements are useful quantities for comparing the aberrations of a number of beam systems. Numerical calculations included in this thesis demonstrate that the rms displacements are smaller by an order of magnitude than the maximum aberration displacements.

Because of the aberrations, it is not generally possible to obtain a true line or point image of a point source from a beam system. The location and size of the "region of least confusion" (i.e., the "best image") is calculated for systems with a point source. The results determine the best location for a resolving slit and the degree of mass or momentum resolution that can be attained. The width of this region may be as small as one fourth the width of the beam at the paraxial image.

The detailed imaging of an axial point source is discussed. All possible image shapes are classified and described. However, because of the great variety possible in these images, quantitative results are obtained from the computer program.

In the examples quoted, it is shown that the inherent aberrations of the quadrupole beam systems constitute the limiting factors in their performance. It should be easy to realize the tolerances needed to make the aberrations due to misalignments and higher field harmonics smaller than the inherent aberrations.

Numerical calculations were made on several beam systems which differed only in separation of the constituent quadrupole magnets; the magnification and focusing properties were the same for all systems. In every case examined, all the aberrations were smaller for systems with larger separations, even when the different admittances were taken into consideration.

The digital computer program previously mentioned calculates all the aberration coefficients derived in this thesis, including the coefficients relating to the tolerances in magnet construction and placement. The code calculates all the linear properties of a wide variety of beam systems. By use of the powerful methods of linear programming, all parameters of a beam system may be adjusted to meet any specified optical properties; physically unreal solutions are precluded by constraints placed upon each parameter. The code will also adjust parameters to reduce the aberrations of a beam system.

Many results are presented graphically by use of the cathode-ray tube (CRT) display of the IBM 7090 computer. Much quantitative and qualitative detail about the aberrations is contained in plots of the projections on the three coordinate planes of representative groups of trajectories leaving the beam system. Beam-profile plots and phase-space plots complement the printed output describing the linear beam properties. The accuracy of numerical calculation of the aberration coefficients has been verified by application of 28 relationships derived in Chapter VI.

In Chapter II we discuss the linear properties of beam systems, including the properties of the beam envelope. The symmetry properties characteristic of quadrupole magnets are discussed in Chapter III. In Chapter IV we derive the equations of motion from a Hamiltonian in which distance along the optic axis is the independent variable. The successive-approximations method of solving these equations is the topic of Chapter V. Relations between the coefficients of aberration are derived in Chapter VI. In Chapter VII, we discuss the character of the aberrations. The computer program resulting from this study is described in Chapter VIII. Appendix I contains the detailed expressions for the coefficients of aberration, using a symbolic notation introduced in Chapter V. Instructions for operating the computer program are contained in Appendix II. Several sample calculations are presented in Appendix III.

II. LINEAR THEORY

A beam-transport system generally consists of an array of magneto-optical elements, separated by drift spaces, designed to achieve certain desired optical properties. For a given system, there exists a central trajectory, the <u>optic axis</u>, which provides reference points for the displacements and slopes of other trajectories. Throughout the first part of this paper, the optic axis is identified with the z axis; displacements from this axis are measured along the x and y axes. The z axis is a straight line except in a bending magnet.

The equations for x and y as functions of z are called the <u>trajectory equations</u>. For the commonly used <u>beam elements</u> (quadrupole magnets, drift spaces, and bending magnets) the differential equations in x and y in the first approximation are of the type

$$x'' + \alpha(z)\cdot x = a(z)\cdot\Delta \qquad (\text{II-1})$$

$$\text{and } y'' + \beta(z)\cdot y = b(z)\cdot\Delta \; ; \qquad (\text{II-2})$$

here $\Delta \equiv (p-p_0)/p$, where p_0 is the <u>design momentum</u> of the beam system; primes refer to differentiation with respect to z. That the x and y equations are independent in the first approximation means that motion in one plane is independent of motion in the other plane to this approximation. This simplification is obtained only for beam systems in which the constituent magnets are arranged with their principal axes correlated, as described in Section F of this chapter.

Another type of focusing element used is the solenoid, which does not have this property for any orientation because trajectories rotate about the z axis within an axial field such as that in a solenoid. However, the solenoid may be included within the class of elements listed above provided its placement is restricted to points where the beam is rotationally symmetric.

A. Representation of a Lens System

In each of the two planes, x and y, the optical properties of the beam system for the design momentum are completely determined by any two linearly independent solutions of the trajectory equations. Given x and x' at z_1, we can then determine x and x' at any other point z_2 (similarly for y and y'). Let us choose the two independent solutions to satisfy the following conditions at z_1:

$$x_e(z_1) = 1, \qquad x_e'(z_1) = 0$$
$$x_o(z_1) = 0, \qquad \text{and } x_o'(z_1) = 1. \qquad \text{(II-3)}$$

Then at any other point z we have

$$x(z) = x(z_1)\, x_e(z) + x'(z_1)\, x_o(z)$$
$$x'(z) = x(z_1)\, x_e'(z) + x'(z_1)\, x_o'(z) \;, \qquad \text{(II-4)}$$

or, in matrix notation,

$$\begin{pmatrix} x(z) \\ x'(z) \end{pmatrix} = \begin{pmatrix} x_e(z) & x_o(z) \\ x_e'(z) & x_o'(z) \end{pmatrix} \begin{pmatrix} x(z_1) \\ x'(z_1) \end{pmatrix} \qquad \text{(II-5)}$$

The matrix in x_e and x_o is called the x <u>transfer matrix</u> between z_1 and z. The determinant of this matrix is the Jacobian determinant of the transformation between z_1 and z. In a non-dissipative system, Liouville's theorem requires that volume in 6n-dimensional phase space for a system of n particles must be conserved. To first approximation, the equations of motion of each particle are independent of all others, the motion in one

one plane is independent of the motion in the other two, and the components of momenta are proportional to the slopes x' and y'. Thus Liouville's theorem for 6n-dimensional phase space requires that the area occupied by the beam in two-dimensional space of x and x' be conserved. The Jacobian determinant of the transformation must therefore be unity; hence the determinant of the transfer matrix is identically equal to unity. Thus a transfer matrix always possesses an inverse (which in this case is the matrix that takes the beam backwards from z to z_1). It is easily verified that $T_{13} = T_{23}T_{12}$, where T_{13} is the transfer matrix between z_1 and z_3 while T_{12} and T_{23} are the transfer matrices between z_1 and z_2 and between z_2 and z_3, respectively.

As with the thick lens in optics, the linear behavior of a monoenergetic beam transport system between two points is completely determined by the location of the focal points and the focal length in each plane. There are in each plane three independent quantities that determine the optical behavior; they may be thought of in terms of either focal points or matrix elements. To discover the relationship between matrix elements and the location of the focal points, it is necessary to calculate the location at which an incoming parallel beam is imaged on the axis and that at which a source on the axis is imaged into a parallel beam. The focal length is then determined by applying the Newtonian lens equation $qp=f^2$, with p the distance from the image focal point to the image and q the distance from the object focal point to the object. Let z_o be the location of the object focal point and z_i the location of the image focal point. If (T) is the transfer matrix between the points z_1 and z_2, then

$$(T) = \begin{pmatrix} \frac{b}{f} & \frac{f^2 - ab}{f} \\ -\frac{1}{f} & \frac{a}{f} \end{pmatrix} \quad \text{, where } a = z_1 - z_0 \text{ and } b = z_1 - z_2. \qquad (\text{II}-6)$$

Three equivalent representations of a lens system have been presented, together with the relationship between them; these representations are in terms of (a) linearly independent solutions of a differential equations, (b) transfer matrices, and (c) cardinal points. As stated previously, we have been considering the trajectories in the two planes xz and yz separately. The tranfer matrices and the cardinal points in general differ in the different planes.

B. The Beam Envelope

In characterizing the behavior of a group of trajectories, the concept of a beam envelope is of great value. The beam envelope is that surface which encloses the entire beam and which is tangent to at least one trajectory at every point. Before one can work with the envelope, it is necessary to define the region in phase space occupied by the beam; this region varies with z. As long as we are dealing with independent motion in the two planes, we can consider the product of the two-dimensional phase spaces in each plane. A convenient representation of the curve in x-x' space that contains the beam is an ellipse, for if the bounding figure is an ellipse at one value of z, it is an ellipse at all values. Confining our attention to the x-z and the x-x' planes, we note several properties of the envelope that hold independently for the y-z and y-y' planes.

In what follows we shall require the bounding phase space figure to be an ellipse. Because of Liouville's theorem and the stipulated independence of the x and y trajectory equations, the area of the phase ellipse is a constant that is independent of z. The set of trajectories that forms the bounding phase-space ellipse at one value of z forms the bounding figure for all values.

The displacement of a particle passing through a drift space is changed in proportion to the drift distance while the slope remains constant. The corresponding effect on the phase ellipse for a group of particles is a shear in the x direction. It is apparant that any phase ellipse can be sheared to an upright ellipse by drifting some distance either forward or backward.

The effect of a thin lens, defined as an element that changes the slope of a trajectory while not changing its displacement, is to shear the phase ellipse in the x' direction.

C. Beam Widths

A point along the optic axis at which the phase ellipse is upright is known as a waist; at this point the envelope has a minimum width in x. We may parameterize an upright ellipse as follows:

$$x = \bar{x} \cos \theta, \quad x' = \bar{x}' \sin \theta, \quad 0 \leq \theta < 2\pi. \qquad (\text{II}-7)$$

Let us assume the beam to have a waist at the entrance to the beam system, with maximum displacement, and slope given by $\bar{x}$ and $\bar{x}'$, respectively. If T_{ij} is the transfer matrix to some other point, then the maximum displacement and maximum slope at that point are given by

$$x_{max}^2 = T_{11}^2\bar{x}^2 + T_{12}^2\bar{x}'^2 \text{ and } x'^2_{max} = T_{21}^2\bar{x}^2 + T_{22}^2\bar{x}'^2 \quad (\text{II}-8).$$

This result is easily obtained by differentiation with respect to the parameter Θ. Since the transfer matrix for a drift distance z is given by $T_{ij} = \begin{pmatrix} 1 & z \\ 0 & 1 \end{pmatrix}$, the equation for the beam envelope in a field-free region containing a waist with maximum x and x' equal to $\bar{x}$ and $\bar{x}'$, respectively, is $x(z)^2 = \bar{x}^2 + z^2\bar{x}'^2$ (II-9), in which z is measured from the waist. The envelope is thus a hyperbola in a field-free region.

Conversely, let us assume an upright waist at the input to the beam system. With $\bar{x}$ at the input corresponding to the size of the source, we are able to determine $\bar{x}'$ so that none of the trajectories will strike a boundary at any point within the beam system, provided the source is smaller than the apertures.

At every value of z, the beam may be thought of as having come through a field-free region from a waist. If, because of some intervening focusing element, this waist does not really exist, we will denote it as a <u>virtual waist</u>. The study of the beam envelope is thus reduced to knowing the location of all the virtual waists and waists and their respective widths.

To determine the transfer matrix between any two arbitrary points, we may proceed by locating the virtual waist seen by each point and then determining the transfer matrix that carries one virtual waist into the other. We now know the transfer matrix between the two virtual waists, and the drift distance between each of the original arbitrary points and its virtual waist. We multiply the transfer matrix between the two virtual waists by the matrices appropriate to the two drift spaces to obtain the desired transfer matrix.

If $\bar{x}_1$ and $\bar{x}'_1$ are the maximum displacement and slope at z_1, then the matrix

$$\begin{pmatrix} M \cos \phi & (M/r) \sin \phi \\ (-r/M) \sin \phi & (1/M) \cos \phi \end{pmatrix} \qquad \text{(II-10)}$$

produces an upright ellipse at z_2 with maximum width $\bar{x}_2 = M \bar{x}_1$ and slope $\bar{x}'_2 = (1/M)\ \bar{x}'_1$, provided there is an upright ellipse at z_1.

Here $r = \bar{x}_1{}'/\ \bar{x}_1$ and ϕ is an arbitrary angle whose significance can be seen by operating with the matrix upon the ellipse at z_1:

$$\begin{pmatrix} M \cos \phi & (M/r) \sin \phi \\ (-r/M) \sin \phi & (1/M) \cos \phi \end{pmatrix} \begin{pmatrix} \bar{x}_1 & \cos \theta \\ \bar{x}_1{}' & \sin \theta \end{pmatrix} = \begin{pmatrix} M\ \bar{x}_1 \cos (\theta - \phi) \\ \bar{x}_1{}'/\ M \sin (\theta - \phi) \end{pmatrix}$$

Thus ϕ corresponds to a rotation of points on the ellipse about the ellipse's center, and the matrix provides the specified transformation. We have determined the most general transfer matrix which carries one upright ellipse into another upright ellipse; the parameters M and r are determined by the ellipses. It should be noted that M, the ratio of waist widths, differs from the magnification (which is defined only if z_2 is the image of z_1); they are the same only for $\phi = n\pi$ where n is zero or a positive integer (n=1 corresponds to the first image of the source, n=2 corresponds to the second image, ...).

If T_{ij} is the transfer matrix that takes the upright ellipse at z_1 to some arbitrary point z, then one is interested in knowing the location and width of the equivalent (virtual) waist that would produce the observed ellipse at z by a pure drift. If d is the distance from z to the virtual waist and $\bar{x}$ is the maximum displacement at this waist, then

$$d = -\frac{T_{11}T_{21}\bar{x}_1^{\,2} + T_{12}T_{22}\bar{x}_1'^{\,2}}{T_{21}^2\bar{x}_1^{\,2} + T_{22}^2\bar{x}_1'^{\,2}} \qquad \text{(II-11)}$$

and

$$\bar{x}^2 = \frac{\bar{x}_1^{\,2}\,\bar{x}_1'^{\,2}}{T_{21}^2\bar{x}_1^{\,2} + T_{22}^2\bar{x}_1'^{\,2}} \,. \qquad \text{(II-12)}$$

Note that d=0 if $r^2 = -T_{11}T_{21}/T_{12}T_{22}$.

D. Dispersive Systems

If we now broaden our attention to include beams having a spread in momenta about the design momentum, p_0, and dispersive systems, then it is convenient to abandon the 2x2 transfer matrices in favor of 3x3 transfer matrices operating on the column vector $(X)=\begin{pmatrix} x \\ x' \\ \Delta \end{pmatrix}$, where $\Delta \equiv (p-p_0)/p$. The bottom row of a 3x3 transfer matrix is the same as the bottom row of the unit matrix, since the momentum of a single particle is not changed by any of the beam elements considered in this paper (of course, we exclude those particles which are lost by collision with a wall). If there are no bending magnets in the beam system, the right-hand column is the same as the right-hand column of the unit matrix (in this case, there is no advantage in the 3x3 matrices over the 2x2 matrices). For $-\bar{\Delta} \leq \Delta \leq \bar{\Delta}$, the maximum displacement and slope at any point are increased by the dispersive terms $|T_{13}|\,\bar{\Delta}$ and $|T_{23}|\,\bar{\Delta}$, respectively, where T_{ij} is the 3x3 transfer matrix to the point in question.

It is obvious that the 3x3 transfer matrix also has a determinant of unity. The third column of the matrix provides all the needed information about the first-order dispersive properties of the system. The third column of a transfer matrix for a quadrupole magnet is the same as that of the unit matrix.

E. Circular Apertures

Provided that all the apertures encountered by the beam are rectangular, we may separate the occupied region in x, y, x', y' space into independent products of regions in x-x' space and in y-y' space. If the beam is bounded at any point by a circular aperture (as is frequently the case when beam pipes are involved) then we may no longer make the separation into two independent bounding figures. We now introduce a model for the four-dimensional space which corresponds to a double waist and is very useful for comparing the effects of various types of aberrations.

Let T_{ij} be the transfer matrix in the x plane between z_1 and z, with U_{ij} the corresponding transfer matrix for the y plane. All the trajectories that lie within the hyperellipsoid at z_1 defined by

$$\left(\frac{x_1}{\frac{R}{T_{11}}}\right)^2+\left(\frac{x_1'}{\frac{R}{T_{12}}}\right)^2+\left(\frac{y_1}{\frac{R}{U_{11}}}\right)^2+\left(\frac{y_1'}{\frac{R}{U_{12}}}\right)^2 = 1 \qquad \text{(II-13)}$$

lie within a circular aperture of radius R in the x-y plane at z. In parametric form, the equation for this hyperellispsoid is

$$\begin{aligned} x_1 &= \bar{x}_1 \cos\phi \cos\Theta , & x_1' &= \bar{x}_1' \cos\phi \sin\Theta, \\ y_1 &= \bar{y}_1 \sin\phi \cos\Psi , & y_1' &= \bar{y}_1' \sin\phi \sin\Psi , \end{aligned} \qquad \text{(II-14)}$$

with $\bar{x}_1 = R/T_{11}$, etc., and $0\leq\phi<\pi/2$, $0\leq\Theta<2\pi$, and $0\leq\Psi<2\pi$.

F. Linear Properties of Specific Beam Elements

To conclude this discussion and review of the pertinent linear properties of beam-transport systems and their constituent elements, the following list gives the properties of each type of element treated. For the calculations for each element discussed below, we will need

(a) the independent parameters that determine the optical properties,

(b) several useful derived parameters,

(c) the equations of motion (i.e., the trajectory equations),

(d) the 3x3 transfer matrices in each plane.

1. Drift Space

The single parameter describing the optical properties of a drift space is the length of the drift space, L. Additional parameters pertinent to the drift space are those which determine its aperture: width and height for rectangular cross-section, or radius for circular cross-section. A fictitious element to be used later in this paper is the drift space in either x alone or y alone; inclusion of such elements facilitates the treatment of beams in which a waist in the x plane does not coincide with a waist in the y plane.

The equations of motion in a drift space are $x''=0$ and $y''=0$. The transfer matrix for either plane is

$$T = \begin{pmatrix} 1 & L & 0 \\ 0 & 1 & 0 \\ 0 & 0 & 1 \end{pmatrix} \qquad (\text{II}-15)$$

2. Quadrupole Magnet

The necessary parameters are the effective length, L, (which is generally longer than the physical length, owing to the existence of fringing fields), and the field gradient, G. Three derived quantities are

$$\phi = \frac{e}{p_0 c}\frac{\partial B_x}{\partial y} = \frac{e}{p_0 c}\frac{\partial B_y}{\partial x} = \frac{e}{p_0 c} G = \frac{G}{|B\rho|} , \qquad (\text{II}-16)$$

$$k = \phi^{1/2} ,$$

and $\Theta = kL = \phi^{1/2} L$.

By convention both G and ϕ are taken as positive when the lens is convergent in the x-z plane. A quadrupole lens that is convergent in the y-z plane possesses imaginary values of k and Θ.

The equations of motion in a quadrupole are, to lowest order, $x'' + \phi x = 0$ and $y'' - \phi y = 0$ (II-17). The general solutions are $x = x_0 \cos[k(z-z_0)] + (x_0'/k) \sin[k(z-z_0)]$ (II-18)

and $y = y_0 \cosh[k(z-z_0)] + (y_0'/k) \sinh[k(z-z_0)]$. (II-19)

The case $G<0$ is treated by eliminating all imaginary quantities by use of the relations $\cos(i\Theta) \equiv \cosh(\Theta)$, $\sin(i\Theta) \equiv i \sinh(\Theta)$, etc., which merely interchanges the x and y matrices and changes the sign of ϕ. The transfer matrices are

$$\begin{pmatrix} \cos\Theta & (1/k)\sin\Theta & 0 \\ -k\sin\Theta & \cos\Theta & 0 \\ 0 & 0 & 1 \end{pmatrix} \text{ (x plane)} \qquad (\text{II}-20)$$

$$\begin{pmatrix} \cosh\Theta & (1/k)\sinh\Theta & 0 \\ k\sinh\Theta & \cosh\Theta & 0 \\ 0 & 0 & 1 \end{pmatrix} \text{ (y plane)} \qquad (\text{II}-21)$$

3. Bending Magnet

We first consider a bend in the x-z plane in the x direction. The significance of the five independent parameters describing a bending magnet is more easily seen by reference to Fig. 1. Each of the parameters is positive, as shown. The parameters are

(a) L, the length of the magnet, measured along the perpendicular to the entrance edge of the magnet at the point where the optic axis intersects that edge;

(b) γ, the angle between the entrance and exit edges to the magnet, which is positive when the region of magnetic field increases in the negative x direction;

(c) α, the entrance angle (the angle between the optic axis and the normal to the entrance face), which is positive when particles with $x<0$ pass through a longer field region than do those with $x>0$;

(d) The field strength, B, which is positive when the bend is in the negative x direction (for a positively charged particle);

(e) n, the field exponent, which is measured orthogonal to the optic axis ($n \equiv -\frac{\rho}{B}\frac{\partial B}{\partial \rho}$).

These parameters have been chosen as the primary parameters because each is independent of the others, with the exception of n, which depends upon the location of the optic axis.

Derived parameters include:

(a) ρ, the radius of curvature, which is positive when B is positive;

(b) Θ, the angle of bend, which satisfies $\Theta = \alpha + \beta - \gamma$ (II-22);

(c) β, the exit angle, defined in much the same way as α;

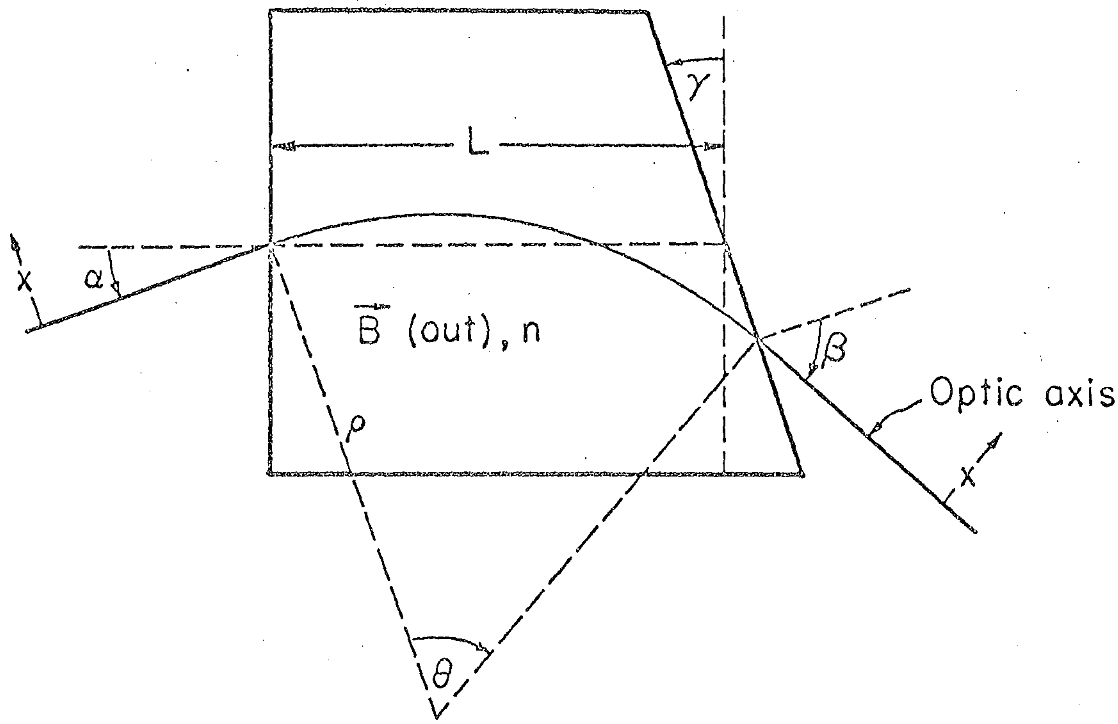

MU-30403

Fig. 1. Parameters of a bending Magnet.

i.e., β is positive when excess field is experienced by a particle with $x<0$. β is derived from the formula

$$\sin\beta = \frac{L}{\rho}\cos\gamma + \sin(\gamma-\alpha) \qquad (\text{II-23})\ .$$

In addition to the focusing in the interior of the bending magnet, there may be focusing by the fringing field at the edge, which acts as a thin lens if the optic axis is not orthogonal to the magnet face. The cause of this focusing in the x-z plane (orthogonal to the magnetic field) at the edge is obvious: a particle displaced in x experiences either a greater or a lesser amount of bending field than needed to turn through the angle Θ. Thin-lens focusing in the vertical plane occurs because the field lines "bulge" at the edge; if the edge is not orthogonal to the optic axis there is a component of field in the x direction which produces a force in the y direction on a particle traveling essentially in the z direction. With the sign conventions given above for α and β, the transfer matrices for the edges are:

$$\begin{array}{lcc} & \text{x-z plane} & \text{y-z plane} \\ \text{in:} & \begin{pmatrix} 1 & 0 & 0 \\ (\tan\alpha)/\rho & 1 & 0 \\ 0 & 0 & 1 \end{pmatrix} & \begin{pmatrix} 1 & 0 & 0 \\ -(\tan\alpha)/\rho & 1 & 0 \\ 0 & 0 & 1 \end{pmatrix} \\ \text{out:} & \begin{pmatrix} 1 & 0 & 0 \\ (\tan\beta)/\rho & 1 & 0 \\ 0 & 0 & 1 \end{pmatrix} & \begin{pmatrix} 1 & 0 & 0 \\ -(\tan\beta)/\rho & 1 & 0 \\ 0 & 0 & 1 \end{pmatrix} \end{array} \qquad (\text{II-24})\ .$$

The equations of motion in the central potion of the magnet are

$$\frac{d^2x}{d\theta^2} + (1-n)\,x = \rho\,\Delta\ , \quad \frac{d^2y}{d\theta^2} + n\,y = 0 \qquad (\text{II-25}).$$

The general solution of the x equation is

$$x = x_0 \cos(\nu_x\theta) + x_0' \frac{\rho}{\nu_x} \sin(\nu_x\theta) + \frac{\Delta}{\nu_x^2}\left[1 - \cos(\nu_x\theta)\right]. \quad \text{(II-26)}$$

That for the y equation is $y = y_0 \cos(\nu_y\theta) + \dfrac{y_0'}{\nu_y} \sin(\nu_y\theta)$. (II-27).

Here $\nu_x \equiv (1-n)^{\frac{1}{2}}$, $\nu_y \equiv n^{\frac{1}{2}}$, $x_0' \equiv \dfrac{dx}{dz} \equiv \dfrac{1}{\rho}\dfrac{dx}{d\theta}$, etc.

The x-z transfer matrix is

$$\begin{pmatrix} \cos(\nu_x\theta) & \frac{|\rho|}{\nu_x}\sin(\nu_x\theta) & \rho/\nu_x^2\left[1-\cos(\nu_x\theta)\right] \\ -\frac{\nu_x}{|\rho|}\sin(\nu_x\theta) & \cos(\nu_x\theta) & \frac{1}{\nu_x}\frac{\rho}{|\rho|}\sin(\nu_x\theta) \\ 0 & 0 & 1 \end{pmatrix} \quad \text{(II-28)}.$$

The y-z transfer matrix is

$$\begin{pmatrix} \cos(\nu_y\theta) & \frac{|\rho|}{\nu_y}\sin(\nu_y\theta) & 0 \\ -\frac{\nu_y}{|\rho|}\sin(\nu_y\theta) & \cos(\nu_y\theta) & 0 \\ 0 & 0 & 1 \end{pmatrix}, \quad \text{(II-29)}$$

which passes to the limit

$$\begin{pmatrix} 1 & \rho\theta & 0 \\ 0 & 1 & 0 \\ 0 & 0 & 1 \end{pmatrix} \quad \text{(II-30)}$$ as n goes to zero.

The total transfer matrix is the properly ordered product of the exit-edge matrix, the matrix for the interior, and the matrix for the entrance edge.

If the entire magnet is physically rotated 180° about the incoming optic axis (α, β, γ, B, and ρ are reversed in sign) then the first and second columns of the transfer matrix are unchanged, whereas the third column is reversed in sign.

If the bending magnet is oriented so that the bend is in the y-z plane, then the above relationships all hold with x and y interchanged everywhere.

4. Solenoid Magnet

Two parameters are required to describe the linear properties of a solenoid magnet; they are the length, L, and the central magnetic field, B, which is axial in the magnet's interior. Two derived quantities are of interest:

$k = eB/2p_0c$,

$\Theta = kL$.

If the condition is imposed that the beam entering a solenoid be rotationally symmetric, the rotation induced by the axial field (which results in mixing the solutions for x and y) can be ignored. The radial equation of motion is $r'' + k^2 r = 0$. The transfer matrix, which is the same in both the x-z plane and the y-z plane, is

$$\begin{pmatrix} \cos\Theta & \frac{1}{k}\sin\Theta & 0 \\ -k\sin\Theta & \cos\Theta & 0 \\ 0 & 0 & 1 \end{pmatrix}. \qquad \text{(II-31)}$$

5. Octupole Magnet

We introduce octupole magnets in the next chapter. Properly oriented octupole magnets in some instances may be adjusted to reduce the magnitude of the aberrations of a beam system of quadrupole magnets. The linear properties of an octupole magnet are the same as those for a drift space, hence the matrices are also the same.

III QUADRUPOLE SYMMETRY PROPERTIES AND THE MAGNETIC SCALAR POTENTIAL

We continue to refer to the Cartesian coordinate frame used in the last chapter in which the optic axis coincides with the z axis and particles travel in the positive z direction.

A. Magnetic Field Symmetries

The ideal quadrupole field possesses several important symmetry properties. The magnetic field is antisymmetric with respect to reflection through both the $x=0$ and $y=0$ planes, and is symmetric with respect to reflection through both the $x=y$ and $x=-y$ planes. The magnitude of the magnetic field in an ideal quadrupole lens is proportional to the radial displacement from the optic axis and is independent of z. The restoring force produced by the ideal quadrupole field is proportional to x in the x-z plane and proportional to y in the y-z plane. Such a magnetic field would be produced by an ideal magnet possessing hyperbolic cylindrical pole pieces of infinite transverse extent, infinite length, and infinite permeability which satisfy the equations $xy = a^2/2$ (north poles) and $xy = -a^2/2$ (south poles) where a is the radius of the inscribed circle. With this choice of polarity, positively charged particles are focused in the y-z plane and defocused in the x-z plane. Reversing the polarity interchanges the converging and the diverging planes.

The scalar magnetic potential appropriate to the <u>linear field</u> produced by the ideal magnet is proportional to the product xy or, alternatively, proportional to $r^2 \sin 2\Theta$, where Θ is the usual angle in cylindrical coordinates ($x = r\cos\Theta$, $y = r\sin\Theta$, $z = z$). The field produced by a magnet having pole pieces of the ideal magnet configuration but finite in extent will contain, in addition to the linear field component, harmonic components proportional to higher powers of x and y. In addition, all the field components, including the linear component, depend upon z.

To treat real (not ideal) quadrupole magnets, we need a general expression for the magneic field.

B. The General Magnetic Field

We first introduce a general expression for a potential giving rise to a magnetic field which possesses the previously stated symmetries, and which approximates the field produced by an ideal quadrupole magnet; this field will be referred to as a "pure quadrupole magnetic field." We then consider field components that may be introduced by failure to achieve the assumed symmetries exactly.

1. General Magnetic Scalar Potential

In terms of cylindrical coordinates, we choose the following general expansion of the scalar magnetic potential V:

$$V(r,\theta,z)=\sum_{m=0}^{\infty}\sum_{n=0}^{\infty} r^m \left\{-\mu_{mn}(z)\sin n\theta - \nu_{mn}(z)\cos n\theta\right\} \qquad \text{(III-1)}$$

This expression is chosen because the field is obviously periodic in θ with period 2π, is dominated near the z axis by a term in r^2 that approximates the ideal field, and is nearly independent of z except in the regions near a magnet edge.

Applying Laplace's equation,

$$V = \frac{1}{r}\frac{\partial}{\partial r}\left(r\frac{\partial V}{\partial r}\right) + \frac{1}{r^2}\frac{\partial^2 V}{\partial \theta^2} + \frac{\partial^2 V}{\partial z^2} = 0, \qquad \text{(III-2)}$$

we obtain

$$\sum_{m=0}^{\infty}\sum_{n=0}^{\infty} r^{m-2}\left\{\left[\mu''_{m-2,n}+(m^2-n^2)\mu_{m,n}\right]\sin n\theta+\left[\nu''_{m-2,n}+(m^2-n^2)\nu_{m,n}\right]\cos n\theta\right\}=0 .$$

As r approaches zero, terms in the above expression with m=0 or m=1 increase without bound except for those terms for which m=n, hence $\mu_{0,n}\equiv\nu_{0,n}\equiv 0$ for n>0 and $\mu_{1,n}\equiv\nu_{1,n}\equiv 0$ for n>1 .

Since Laplace's equation must be satisfied at all values of r, Θ, and z, we have

$$\mu''_{m-2,n} + (m^2-n^2)\mu_{m,n} = 0 \quad \text{for } n=0,\ 1,\ 2,\ \cdots$$

$$\nu''_{m-2,n} + (m^2-n^2)\nu_{m,n} = 0 \quad \text{for } n=0,\ 1,\ 2,\ \cdots .$$

For each n, the lowest-order nonvanishing term which appears is that for m=n, yielding the following general expression for V:

$$V(r,\ \theta,\ z) = \qquad \text{(III-3)}$$

$$-\sum_{k=0}^{\infty}\sum_{n=0}^{\infty} r^n \frac{n!\ r^{2k}}{k!(n+k)!(-4)^k}\left\{\sin n\theta\,\mu_n(z)+\cos n\theta\,\nu_n(z)\right\}^{(2k)} .$$

Here $f^{(2k)}$ denotes the 2kth derivative of f with respect to z, $f^{(0)}\equiv f$, and μ_n and ν_n are functions of z which must be chosen to fit the boundary conditions and the symmetries of the problem.

2. Pure Quadrupole Magnetic Scalar Potential

We first apply eq. (3-3) to the pure quadrupole field. All terms in cos nΘ must vanish owing to the required antisymmetry for reflection through the x=0 plane. Reflection antisymmetry through the y=0 plane rules out all terms in sines of odd multiples of Θ. Finally, the required symmetry for reflection through either th x=y or the x= -y planes rules out all terms except those containing a factor $\sin[2(2\ell+1)\theta]$ with $\ell=1, 2, 3, \ldots$. The general expansion of the pure quadrupole field is

$$V(r,\theta,z) = -r^2 \sin 2\theta \left\{ \mu_2 - \frac{r^2}{12}\mu_2'' + \frac{r^4}{384}\mu_2^{(4)} - \cdots \right\}$$
$$- r^6 \sin 6\theta \left\{ \mu_6 - \frac{r^2}{28}\mu_6'' + \cdots \right\}$$
$$- r^{10} \sin 10\theta \left\{ \mu_{10} - \cdots \right. \qquad \text{(III-4)}$$
$$+ \cdots .$$

Only the leading term of this expression would appear in the potential of an ideal quadrupole magnet of infinite extent; this term would be independent of z. The higher-order terms in the coefficient of sin 2θ appear as a consequence of the finite extent of the magnet in the z direction. The higher harmonics in θ are induced by truncating the poles of an ideal magnet in the x and y direction. An object of much effort has been the design of magnet pole-face contour and coil placement so that these higher harmonics are minimized. Quadrupole magnets have been constructed for which the contribution to the magnetic field due to the higher harmonics is less the 0.5% of the contribution due to the sin 2θ term at maximum radius.[10]

Dropping terms that do not contribute to the trajectory equations when trucated to third order in the displacements and slopes, and expressing in terms of x, y, and z, we have

$$\frac{e}{p_0 c} V(x,y,z) = -xy\,\phi(z) + \frac{1}{12}(x^2 + y^2)\, xy\,\phi''(z) \qquad \text{(III-5)}$$

where $\phi = e\mu_2(z)/p_0 c$.

3. The Octupole Field Component

It may be desireable to consider quadrupole magnets that possess all symmetries listed above except for reflection through the x=y and x= -y planes. Such is the case in quadrupole magnets that have been shimmed in such a manner that the reflection anti-symmetries are preserved, and in octupole magnets oriented so that the x=0. y=0, x=y, and x= -y planes are planes of reflection anti-symmetry. The terms in the scalar potential possessing antisymmetry about each of the four planes mentioned are those in sin 4kΘ, k= 1, 2, 3, ... Including these terms yields the scalar potential

$$\frac{e}{p_0 c} V = -xy\,\phi(z) + \frac{1}{12}\,xy\,(x^2+y^2)\,\phi''(z) - \frac{1}{3}\,xy\,(x^2-y^2)\,\Psi(z) + \cdots ,$$

$$\text{where } \Psi(z) \equiv 12\,\frac{e}{p_0 c}\,\mu_4(z). \tag{III-6}$$

4. Failure to Achieve Quadrupole Symmetries

Finally, real beam systems may fail to achieve the above symmetries owing to nonalignment, rotation, etc. Therefore, we add several terms to the scalar potential which will be used later to calculate the tolerances permitted in the construction and placement of the constituent magnets in particular beam system. Truncating to fourth order, we have

$$\begin{aligned} V(r,\theta,z) = &-\mu_0(z) - r\sin\theta\left[\mu_1 - \frac{r^2}{8}\mu_1''\right] - r\cos\theta\left[\nu_1 - \frac{r^2}{8}\nu_1''\right] \\ &- r^2\sin 2\theta\left[\mu_2 - \frac{r^2}{12}\mu_2''\right] - r^2\cos 2\theta\left[\nu_2 - \frac{r^2}{12}\nu_2''\right] \\ &- r^3\mu_3\sin 3\theta - r^3\nu_3\cos 3\theta - r^4\mu_4\sin 4\theta - r^4\nu_4\cos 4\theta \end{aligned} \tag{III-7}$$

In terms of x and y,

$$\begin{aligned} \frac{e}{p_0 c} V(x,y,z) = &-xy\,\phi(z) + \frac{1}{12}\,xy\,(x^2+y^2)\,\phi''(z) - \frac{1}{3}\,xy\,(x^2-y^2)\,\Psi(z) \\ &-xy\,\delta\phi(z) - y\mu(z) - x\nu(z) - (x^2-y^2)\,\lambda(z) + \Omega(z) \end{aligned} \tag{III-8}$$

These extra terms are assumed to be unwanted and therefore small; in particular, the following assumptions have been made. The coefficients μ_5, ν_2, and ν_3 are assumed to be smaller by at least one order of magnitude than the coefficient μ_2. The terms in sin 3Θ and cos 3Θ (sextupole terms) are not the result of a simple displacement or rotation; they are treated separately as field errors in the same way as the 6Θ and 10Θ terms are treated. The term in cos 4Θ is also treated as a field error, since it does not satisfy the basic quadrupole antisymmetry. However, the sin 4Θ term is treated with the pure quadrupole field terms, since the sin 4Θ term may be adjusted in some instances to reduce objectionable aberrations due to the 2Θ terms. The coefficients Ω, ν_1, and μ_1, are assumed to be smaller by two orders of magnitude than μ_2, which is consistent with the assumption made throughout this paper that the r^2 sin 2Θ term represents the dominant field component.

As an example of how these terms may enter, consider the field produced by a quadrupole; the potential is given by Eq. (III-5) with x and y referred to the magnet's axis of symmetry. If this magnet is now translated so that its center axis is the line $x = \delta x$ and $y = \delta y$, and if the magnet is rotated about the optic axis by an angle ω (positive when the magnet is rotated in the direction of increasing Θ), the added terms in the scalar potential take the values $\mu = \delta x \cdot \phi(z)$, $\nu = \delta y \cdot \phi(z)$,

$$\delta\phi = \phi(z)\left[\cos 2\omega - 1\right], \quad \lambda = \tfrac{1}{2}\phi(z)\sin 2\omega \quad . \qquad \text{(III-9)}$$

Here δx, δy, and ω are assumed to be an order of magnitude smaller than the displacements and slopes of trajectories to be considered.

The term in Ω gives rise to a uniform z component of the field which can occur as the result of tilting a particular magnet so that the axis of symmetry of the magnet ceases to be parallel with the optic axis.

C. Symmetry Restrictions on Aberrations

Returning to a field which possesses reflection antisymmetry about the planes x=0 and y=0, let us consider what types of terms may be present in the expressions giving the displacements and slopes at any chosen point in terms of the displacements and slopes at some initial point (the object). Since a linear relationship is assumed to dominate (this is the lens assumption), we are justified in expanding x, y, x', and y' at an arbitrary value of z in a power series in x_o, x_o', y_o, y_o' and Δ taken at z_o (the initial point).

Since the trajectories cannot depend upon the coordinate system in which they are represented, we find that all even-order terms in the displacements and slopes are absent in the power series as a consquence of the reflection antisymmetry. The same reasoning demonstrates that the expansion of x cannot contain any terms that are odd in y_o or y_o' nor can the expansion of y contain any terms that are odd in x_o or x_o'. Thus the following terms are the only terms, to third order, which may appear in the power series expansions; these terms are grouped according to aberration type

Aberration Type	Terms in x and x'	Terms in y and y'
generalized dispersion	Δx_o, $\Delta^2 x_o$, $\Delta x_o'$, $\Delta^2 x_o'$	Δy_o, $\Delta^2 y_o$, $\Delta y_o'$, $\Delta^2 y_o'$

generalized spherical (aperture) aberration	$x_o'^3$, $x_o' y_o'^2$	$y_o'^3$, $y_o' x_o'^2$
generalized coma	$x_o x_o'^2$, $x_o y_o'^2$, $y_o x_o' y_o'$	$y_o y_o'^2$, $y_o x_o'^2$, $x_o x_o' y_o'$
generalized astigmatism	$x_o^2 x_o'$, $y_o^2 x_o'$, $x_o y_o y_o'$	$y_o^2 y_o'$, $x_o^2 y_o'$, $x_o y_o x_o'$
generalized distortion	x_o^3, $x_o y_o^2$	y_o^3, $y_o x_o^2$
<u>Linear terms</u>	x_o, x_o'	y_o, y_o' (III-10)

Thus there are many more terms to be considered than in light optics, where complete rotational symmetry rules out all third-order terms except seven corresponding to the five Seidel coefficients and two chromatic aberration terms, the seven classic optical aberrations. Although a total of 40 terms appears in third order for x, x', y, and y' (excluding dispersion terms), only 16 of these coefficients are independent, as is shown in Ch. VI. The classical aberrations of light optics are described in most textbooks on optics, such as that by Jenkins and White.[3]

The expressions for the coefficients to the 40 aberration terms are derived in Ch. V.. The equations for the coefficients, in terms of the symbolic notation introduced in Ch. V., are listed in Appendix I.

The significance of the aberration coefficients is discussed in Ch. VII.

IV. THE EQUATIONS OF MOTION

In preparation for derivations presented in Ch. V, we need certain results which are obtained from the following derivations of the equations of motion. A single charged particle of mass m and charge e, under the influence of a magnetic field, $\vec{B}$, possesses the following Lagrangian, L, and Hamiltonian, H.

$$L = \frac{1}{2} mv^2 + \frac{e}{c} \vec{A} \cdot \vec{v} \quad , \tag{IV-1}$$

$$H = \frac{1}{2m} \left[\vec{p} - \frac{e}{c} \vec{A} \right]^2 \quad , \tag{IV-2}$$

where $\vec{v} = \dot{\vec{r}} = (\dot{x}, \dot{y}, \dot{z})$ and $\vec{B} = \nabla \times \vec{A}$.

As long as the only force the particle experiences is due to the field, B, the velocity of the particle will be a constant of the motion; the nonrelativistic equations of motion that would be derived from either the Lagrangian or the Hamiltonian given above may be extended to relativistic particles by merely replacing the mass m by the so-called "relativistic transverse mass," $m_r \equiv m(1-v^2/c^2)^{-\frac{1}{2}}$. Through the rest of this paper, the symbol m will always refer to the transverse mass. The variational principle known as Hamilton's principle from which both LaGrange's equations and Hamilton's canonical equations of motion are derived is generally stated in terms of t as the variable of integration:

$$\delta \int_{t_1}^{t_2} L\, dt \equiv \delta \int_{\vec{r}_1}^{\vec{r}_2} \vec{p} \cdot d\vec{r} - \delta \int_{t_1}^{t_2} H\, dt \equiv 0 \ . \tag{IV-3}$$

To obtain the trajectory equations, we replace t by z, the variable measuring distance along the optic axis, as the independent variable. For all the orbits of interest, the transformation from t to z is single-valued, with a well-defined derivative everywhere. We may then rewrite Hamilton's principle in terms of z as the variable of integration. From this point primes refer to differentiation with respect to z, and dots to differentiation with respect to time:

$$f' \equiv \frac{df}{dz} \quad , \quad \dot{f} \equiv \frac{df}{dt} \; . \quad \text{We now proceed:}$$

$$\delta \int_{t_1}^{t_2} L\,dt \equiv \delta \int_{z_1}^{z_2} L \frac{dt}{dz}\,dz \equiv \delta \int_{z_1}^{z_2} \mathcal{L}\,dz \equiv \delta \int_{z_1}^{z_2} [x' p_x + y' p_y - t' H - \mathcal{H}]\,dz = 0 \qquad \text{(IV-4)},$$

$$\mathcal{L} = \frac{1}{2} \frac{m}{t'} (1 + x'^2 + y'^2) + \frac{e}{c} (x' A_x + y' A_y + A_z) , \qquad \text{(IV-5)}$$

$$\mathcal{H} = - p_z .$$

Having made this transformation, we follow the same procedure, which reduces this variational principle to the equations of motion in the case of the standard Lagrangian or Hamiltonian, yielding

$$\frac{d}{dz} \frac{\partial \mathcal{L}}{\partial x'} - \frac{\partial \mathcal{L}}{\partial x} = 0 \; , \quad \frac{d}{dz} \frac{\partial \mathcal{L}}{\partial y'} - \frac{\partial \mathcal{L}}{\partial y} = 0 , \quad \frac{d}{dz} \frac{\partial \mathcal{L}}{\partial t'} - \frac{\partial \mathcal{L}}{\partial t} = 0 ,$$

$$x' = \frac{\partial \mathcal{H}}{\partial p_x} \; , \quad p_x' = - \frac{\partial \mathcal{H}}{\partial x} , \qquad \text{etc.} \qquad \text{(IV-6)}$$

In terms of z as the independent variable, the canonical momenta are

$$p_x = \frac{\partial \mathcal{L}}{\partial x'} = m v x' (1 + x'^2 + y'^2)^{-\frac{1}{2}} + \frac{e}{c} A_x ,$$

$$p_y = \frac{\partial \mathcal{L}}{\partial y'} = m v y' (1 + x'^2 + y'^2)^{-\frac{1}{2}} + \frac{e}{c} A_y , \qquad \text{(IV-7)}$$

$$p_t = - \frac{1}{2} m v^2 = - E .$$

Two easily derived relationships are

$$v^2 = \dot{z}^2 (1 + x'^2 + y'^2) , \qquad \text{(IV-8)}$$

$$m\dot{z} = \left[m^2 v^2 - (p_x - \frac{e}{c} A_x)^2 - (p_y - \frac{e}{c} A_y)^2 \right]^{\frac{1}{2}} \qquad \text{(IV-9)}$$

In terms of the canonical set of coordinates and momenta, the Hamiltonian becomes

$$\mathcal{H} = x' p_x + y' p_y - t' E - \mathcal{L} \; ; \qquad \text{(IV-10)}$$

$$\mathcal{H} = - [2mE - (p_x - \frac{e}{c} A_x)^2 - (p_y - \frac{e}{c} A_y)^2]^{\frac{1}{2}} - \frac{e}{c} A_z = - p_z \qquad \text{(IV-11)}$$

Applying the modified Hamilton's equations for x (IV-7), we obtain

$$\frac{\partial \mathcal{H}}{\partial p_x} = x' = (p_x - \frac{e}{c} A_x) / m\dot{z} , \qquad \text{(IV-12)}$$

$$y' = (p_y - \tfrac{e}{c}A_y)/m\dot{z},$$

$$t' = m\left[2mE - (p_x - \tfrac{e}{c}A_x)^2 - (p_y - \tfrac{e}{c}A_y)^2\right]^{-\frac{1}{2}},$$

and $E' = -\dfrac{\partial \mathcal{H}}{\partial t} = 0$.

Thus $p_x' = -\dfrac{\partial \mathcal{H}}{\partial x} = \dfrac{e}{c}\left[(p_x - \tfrac{e}{c}A_x)\dfrac{\partial A_x}{\partial x} + (p_y - \tfrac{e}{c}A_y)\dfrac{\partial A_y}{\partial y}\right]/m\dot{z} + \dfrac{e}{c}\dfrac{\partial A_z}{\partial x}$, (IV-13)

the latter reducing to

$$\frac{d}{dz}\, mvx'(1+x'^2+y'^2)^{-\frac{1}{2}} + \frac{e}{c}\frac{dA_x}{dz} = \frac{e}{c}\,\frac{(p_x - \frac{e}{c})\frac{\partial A_x}{\partial x} + (p_y - \frac{e}{c})\frac{\partial A_y}{\partial y}}{m\dot{z}} + \frac{e}{c}\frac{\partial A_z}{\partial x}, \quad \text{(IV-14)}$$

and then to

$$(1+y'^2)x'' - x'y'y'' = \frac{e}{c}\,\frac{(p_x - \frac{e}{c}A_x)\frac{\partial A_x}{\partial x} + (p_y - \frac{e}{c}\frac{\partial A_y}{\partial y})}{m\dot{z}} + \frac{e}{c}\frac{\partial A_z}{\partial x}\ . \quad \text{(IV-15)}$$

Using $\vec{B} = \nabla \times \vec{A}$ and $\dfrac{dA_x}{dz} = \dfrac{\partial A_x}{\partial z} + x'\dfrac{\partial A_x}{\partial x} + y'\dfrac{\partial A_y}{\partial y}$, (IV-16)

we obtain $(1+y'^2)x'' - x'y'y'' = \dfrac{e}{p\ c}\,(1+x'^2+y'^2)^{3/2}(-B_y + y'B_z)$. (IV-17)

Similarly, $-x'y'x'' + (1+x'^2)y'' = \dfrac{e}{p\ c}\,(1+x'^2+y'^2)^{3/2}(B_x - x'B_z)$. (IV-18)

Solving for x" and then y", we obtain

$$x'' = \frac{e}{p\ c}\,(1+x'^2+y'^2)^{\frac{1}{2}}\left\{-(1+x'^2)B_y + x'y'B_x + y'B_z\right\},$$

$$y'' = \frac{e}{pc}\,(1+x'^2+y'^2)^{\frac{1}{2}}\left\{-(1+y'^2)B_x + x'y'B_y + x'B_z\right\}. \quad \text{(IV-19)}$$

These are the exact trajectory equations for a particle under the influence of a magnetic field, $\vec{B}$. That they are identical to the equations obtained from first principles confirms the correctness of the procedure and the choice of new canonical variables.

The expansions for the magnetic field components, in terms of the scalar magnetic potential (III-8) are

$$\frac{e}{p_0c}B_x = \frac{-e}{p_0c}\frac{\partial V}{\partial x} = y\phi \;-x^2y\phi''/4 \;-y^3\phi''/12 \;+x^2y\psi \;-y^3\psi/3 \;+y\delta\phi+\nu \;+2x\lambda \;+\cdots,$$

$$\frac{e}{p_0c}B_y = x\phi \;-x^3\phi''/12 \;-xy^2\phi''/4 \;+x^3\psi/3 \;-xy^2\psi \;+x\delta\phi+\mu \;-2y\lambda \;+\cdots,$$

$$\frac{e}{p_0c}B_z = xy\phi' \;+\Omega' \;+\cdots. \qquad \text{(IV-20)}$$

With the insertion of these fields and the trucation of terms of fourth order and higher (fourth order of smallness in x, y, x', y'), we obtain the following equations of motion:

$$x'' + \phi x = -3xx'^2\phi/2 \;-xy'^2\phi/2 \;+yx'y'\phi+xyy'\phi' \;+xy^2\phi''/4 \;+x^3\phi''/12$$
$$-x^3\psi/3 \;+xy^2\psi \;-x\delta\phi \;-\mu \;+2y\lambda \;+\cdots, \qquad \text{(IV-21)}$$

$$y'' - \phi y = 3yy'^2\phi/2 \;+yx'^2\phi/2 \;-xy'x'\phi \;-xyx'\phi' \;-x^2y\phi''/4 - y^3\phi''/12$$
$$-y^3\psi/3 \;+x^2y\psi + y\delta\phi + \nu \;+2x\lambda + \cdots. \qquad \text{(IV-22)}$$

With respect to the terms in μ, ν, Ω, and λ, the following assumptions have been made:

(a) μ, ν, and λ are piecewise constant functions in this approximation;

(b) $r^2\mu''$, $r^2\nu''$, $r^2\lambda''$, and $r'\Omega'$ are smaller than third order and may be dropped;

(c) μ, ν, and $r\lambda$ are of higher order in "smallness" than $r\phi$ which gives rise to the main field. In V. C. we discuss further the relative orders of magnitude of the terms in the equations of motion. These assumptions restrict the application of these equations only to situations where the displacement or rotation of any quadrupole magnet from the correct alignment is small compared with typical displacements and slopes of the trajectories. Any flutter in μ, ν, or λ is assumed to average to zero to third order in the parameters of smallness.

For pure quadrupole fields, the equations of motion are

$$x'' + \phi x = -3xx'^2\phi/2 \quad -xy'^2\phi/2 \quad +yx'y'\phi' + xyy'\phi' \quad +xy^2\phi''/4 \quad +x^3\phi''/12 + O(5) \tag{IV-23}$$

$$y'' - \phi y = \quad 3yy'^2\phi/2 \quad +yx'^2\phi/2 \quad -xx'y'\phi \quad -xyx'\phi' \quad -x^2y\phi''/4 \quad -y^3\phi''/12 + O(5) \tag{IV-24}$$

In the next chapter we solve these equations by an iterative method to obtain expressions for the coefficients of aberration.

V. THE CALCULATION OF THE COEFFICIENTS OF ABERRATION

In order to separate most clearly and to characterize the different aberrations in a beam system, it will be our purpose to obtain the coefficients in the power-series expansions of the displacements and slopes of a trajectory at some arbitrary value of z (such as the image) as functions of the initial (object plane) displacements and slopes. We further would like to separate aberrations that depend upon the shape of the fringing field from those which appear even in an ideal model magnet with infinitely sharp fringing fields. Finally, we shall examine the effect of misalignments, rotations, and other defects in the constituent magnets.

A. Separation of Equations

We first turn our attention to solving the equations of motion for particles in a pure quadrupole field [Eqs. (IV-23) and (IV-24)]. These equations are expressed in terms of the function $\phi(z)$, which is proportional to the radial field gradient along the z axis. Applying the method of successive approximations to the equations in x, we obtain three equations, one entirely linear, one containing all the dispersive and fringing field effects, and the third containing the aberrations that are cubic in the initial slopes and displacements. Only the x-z equations will be treated explicitly here, as the corresponding equations in y can be obtained from them by interchanging x and y and changing the sign of ϕ.

Let $x = x_s + x_c + x^a$, where

$$x_s'' + \phi_s x_s = 0 \quad , \qquad \text{(V-1)}$$

$$x_c'' + \phi_s x_c = -\phi_c(x_s + x_c) + \Delta(\phi_s + \phi_c)(x_s + x_c) \quad , \qquad \text{(V-2)}$$

$$x^{a\prime\prime} + (\phi_s+\phi_c)x^a = -3xx'^2\phi/2 - xy'^2\phi/2 + yx'y'\phi + xyy'\phi' + xy^2\phi''/4 + x^3\phi''/12 + \cdots, \qquad \text{(V-3)}$$

$\Delta=(p-p_0)/p$ and ϕ is given by (II-16).

The gradient function $\phi(z)$ has been split into two parts

$$\phi(z) \equiv \phi_s(z) + \phi_c(z) ; \qquad \text{(V-4)}$$

ϕ_s ("phi simple") is a piecewise constant-step-function; ϕ_c ("phi complicated") describes the field behavior in the fringing field regions. The function, ϕ_c, is assumed to vanish well inside a magnet as well as in the field-free regions. For reasons to be given later (V. D.), the locations of the discontinuities in $\phi_s(z)$ are chosen so that the integral, $\int_{z_1}^{z_2} \phi_c(z)\, dz$, vanishes when taken over any fringing field region, (between z_1 and z_2 such that $\phi_c(z_1)= \phi_c(z_2)= \phi_c'(z_1)= \phi_c'(z_2)= 0$. Figure 2 shows $\phi(z)$ and its division into ϕ_s and ϕ_c. The graphs are taken over a single quadrupole magnet.

In the event that the fringing fields are very large, this separation need not be made; greater accuracy is thereby achieved at the loss of the desired separation of the fringing-field effects. When retaining the separation, we shall show that the solution to Eq. (V-3) is not affected, within the approximation already made, by taking the limit $\phi \to \phi_s$ (corresponding to neglecting the detailed shape of the fringing field in these terms).

B. The Integral Equations of Motion

In order to proceed to solve equations (V-2), and (V-3) by the method of successive approximations, we form integral equations by means of Green's functions. we define two Green's functions, one appropriate to each equation; the Green's functions

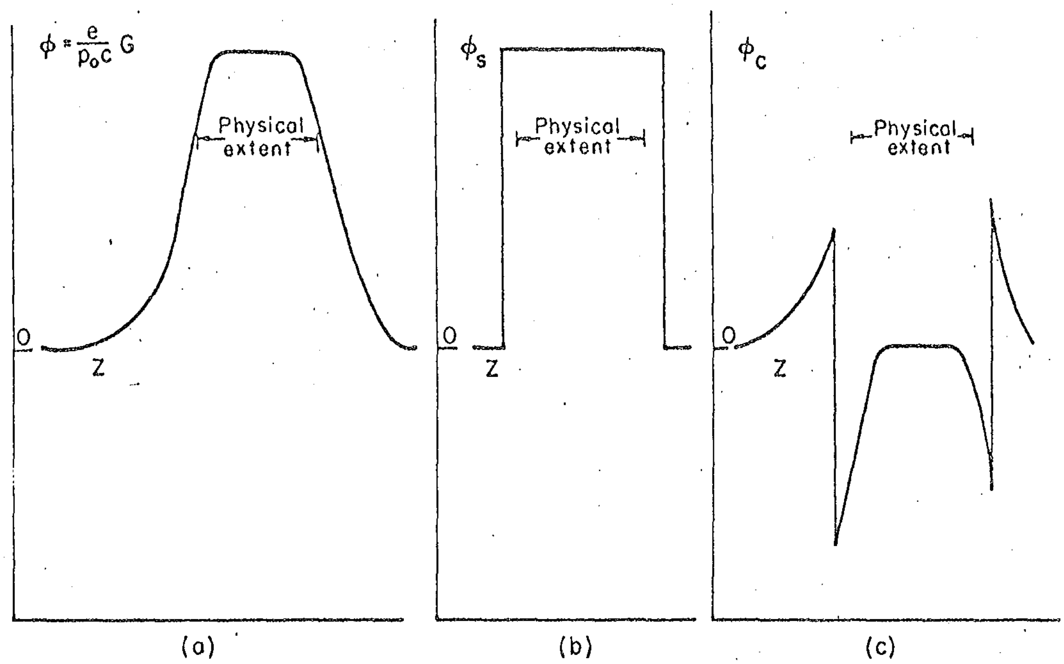

Fig. 2. The gradient function over a quadrupole magnet; (a) the total function, $\phi(z)$; (b) the step function, $\phi_s(z)$; (c) the difference function, $\phi_c(z)$.

satisfy $$\frac{d^2}{dz^2}\, g(z,\zeta) + \phi_s(z)\, g(z,\zeta) = -\delta(z-\zeta) \qquad \text{(V-5)}$$

and $$\frac{d^2}{dz^2}\, g_c(z,\zeta) + [\phi_s(z)+\phi_c(z)]\, g_c = -\delta(z-\zeta), \text{ respectively.} \qquad \text{(V-6)}$$

Green's functions can be constructed from pairs of linearly independent solutions of the equations. Let $x_{so}(z)$ and $x_{se}(z)$ be two linearly independent solutions of Eq. (V-1) for which the initial conditions at the object plane are

$$x_{se}(0)=1,\; x_{so}(0)=0,\; x_{se}'(0)=0, \text{ and } x_{so}'(0)=1 \;. \qquad \text{(V-7)}$$

Any solution of (V-1) may be written as

$$x_s(z) = x(0)\, x_{se}(z) + x'(0)\, x_{so}(z) \;. \qquad \text{(V-8)}$$

Furthermore, the Green's function is

$$g(z,\zeta) = x_{so}(z)\, x_{se}(\zeta) - x_{se}(z)\, x_{so}(\zeta) \quad \text{for } \zeta \leq z,$$
$$g(z,\zeta) = 0 \quad \text{for } \zeta \geq z \;. \qquad \text{(V-9)}$$

Since the equation does not contain terms in x', the Wronskian, $W(x_{se},x_{so})$, is constant: $W = x_{se}x_{so}' - x_{so}\, x_{se}' \equiv 1$.

Similar independent solutions, x_e and x_o, will be defined for the equation $x'' + (\phi_s+\phi_c)x = 0$ (V-10)

such that the general solution can be written

$$x(z) = x(0)\, x_e(z) + x'(0)\, x_o(z), \qquad \text{(V-11)}$$

while the Green's function for Eq. (V-10) may be written as

$$g_c(z,\zeta) = x_o(z)\, x_e(\zeta) - x_e(z)\, x_o(\zeta) \quad \text{for } \zeta \leq z. \qquad \text{(V-12)}$$

The implicit solutions of (V-2) and (V-3) written as integral equations are

$$x_c(z) = \int_0^z g(z,\zeta)\left[X_s(\zeta)+X_c(\zeta)\right]\left\{-\phi_c(\zeta) + \Delta\left[\phi_s(\zeta)+\phi_c(\zeta)\right]\right\} d\zeta \,, \qquad \text{(V-13)}$$

$$x^a(z) = \int_0^z g_c(z,\zeta)\left\{-\tfrac{3}{2}xx'^2\phi - \tfrac{1}{2}xy'^2\phi + yx'y'\phi + xyy'\phi' + \tfrac{1}{4}xy^2\phi'' + \tfrac{1}{12}x^3\phi''\right\} d\zeta \,, \qquad \text{(V-14)}$$

where $\phi = \phi(\zeta) = \phi_s(\zeta) + \phi_c(\zeta)$ and $x = x(\zeta) = x_s + x_c + x^a$, etc.

C. Parameters of Smallness

Let ε be characteristic of the magnitude of the slopes x' and y'; we assume that ε is small compared with unity. For each magnet, we define a characteristic length,

$$L = (\ell f)^{1/2} \approx \phi_s^{-1/2}, \tag{V-15}$$

where ℓ is the effective length of the magnet and f is the absolute value of its focal length. Then x/L and y/L are considered small, of the order of magnitude of ε.

Further, $\Delta = (p-p_0)/p$ is assumed small compared with unity.

Let h be a characteristic length of a fringing field, such as the half width of the fringing field. Then $\lambda = h/L$ is assumed small compared with unity when we separate ϕ into ϕ_s and ϕ_c.

In the treatment that follows, all terms are of third or lower order in these three parameters of smallness, ε, Δ, and λ, are retained, while those of higher order are dropped. For example, $\Delta^2\varepsilon$, ε^3, and $\lambda^2\varepsilon$ are retained while $\lambda^2\Delta\varepsilon$, $\lambda\Delta^2\varepsilon$, and $\lambda\varepsilon^3$ are dropped.

Some magnets in use barely qualify for the classification "quadrupole magnet," since the characteristic length of their fringing field is the same order of magnitude as their effective length. This is due to their large aperture-to-length ratio. In such magnets the approximation made above with respect to the extent of the fringing field is invalid and may easily be abandoned by replacing ϕ_s by ϕ and then dropping all terms in ϕ_c in the final expressions. One then loses the ready identification of the effects of the fringing field and also loses the calculational advantage of simple known first-order solutions.

D. The Dispersion and Fringing-Field Terms

We turn first to Eq. (V-13) whose solution yields the dispersive and fringing field terms. The term x_c can be written as the sum of the expressions

$$I_a = \int_0^z g(z,\zeta)\{-\phi_c(\zeta) X_s(\zeta)\}d\zeta = -\int_0^z [X_{s0}(z) X_{se}(\zeta) - X_{se}(z) X_{s0}(\zeta)]\phi_c X_s d\zeta, \quad \text{(V-16)}$$

$$I_b = \Delta \int_0^z g(z,\zeta)\, \phi_s(\zeta)\, X_s(\zeta) d\zeta, \quad \text{(V-17)}$$

$$I_c = -\int_0^z g(z,\zeta)\, \phi_c(\zeta)\, X_c(\zeta)\, d\zeta, \quad \text{(V-18)}$$

$$I_d = \Delta \int_0^z g(z,\zeta)\, \phi_s(\zeta)\, X_c(\zeta)\, d\zeta, \quad \text{(V-19)}$$

$$I_e = \Delta \int_0^z g(z,\zeta)\, \phi_c(\zeta)\, X_s(\zeta) d\zeta, \quad \text{(V-20)}$$

$$I_f = \Delta \int_0^z g(z,\zeta)\, \phi_c(\zeta)\, X_c(\zeta)\, d\zeta. \quad \text{(V-21)}$$

The integral I_b contains two parameters of smallness, thus x_c has at least one component which is of second order in magnitude. We will show that, under the assumption that λ is a small parameter, I_b, is the only second-order term in x_c.

Integrals that contain ϕ_c as a factor have contributions only in the fringing field regions. These integrals may be split into sums of integrals taken over each magnet entrance and exit. A typical term in the integral I_a is

$$\int_0^z \phi_c(\zeta) X_{s0}(\zeta) X_{se}(\zeta) d\zeta = \sum_k \int_{z_{k-}}^{z_{k+}} \phi_c X_{s0} X_{se}\, d\zeta = \sum_k I_k, \quad \text{(V-22)}$$

where the sum is taken over each entrance and exit. At each fringing field, the integrand may be expanded about the point of discontinuity in ϕ_s. Let ζ_- and ζ_+ be the ends of one fringing field region with $\zeta_- < \zeta_+$. Then we have

$$I_k = \int_{Z_{k-}}^{Z_{k+}} \phi_c X_{so} X_{se}\, d\zeta$$
$$= \int_{\zeta_-}^{\zeta_+} \phi_c(\zeta) \left\{ X_{so}\Big|_{\zeta=0} X_{se}\Big|_{\zeta=0} + \zeta (X_{so}X_{se})'\Big|_{\zeta=0} + \tfrac{1}{2}\zeta^2 (X_{so}X_{se})''\Big|_{\zeta=0} + \cdots \right\} d\zeta \qquad \text{(V-23)}$$

However, the integrand has a discontinuous second derivative, hence

$$I_k = X_{so}\Big|_0 X_{se}\Big|_0 \int_{\zeta_-}^{\zeta_+} \phi_c\, d\zeta + (X_{so}X_{se})'\Big|_0 \int_{\zeta_-}^{\zeta_+} \zeta \phi_c\, d\zeta$$
$$+ \tfrac{1}{2}(X_{so}X_{se})''\Big|_{\zeta=0-\epsilon} \int_{\zeta_-}^{0} \zeta^2 \phi_c\, d\zeta + \tfrac{1}{2}(X_{so}X_{se})''\Big|_{\zeta=0+\epsilon} \int_{0}^{\zeta_+} \zeta^2 \phi_c\, d\zeta \,. \qquad \text{(V-24)}$$

We now invoke the definition of the location of the discontinuity in ϕ_s which was chosen so that $\int_{\zeta_-}^{\zeta_+} \phi_c\, d\zeta = 0$. Using $x_{so}'' + \phi_s x_{so} = 0$ and $x_{se}'' + \phi_s x_{se} = 0$, we have

$$I_k = c_k \lambda_k^2 \phi_s (X_{so}X_{se})'\Big|_0 + (X_{so}'X_{se}')\Big|_0 \int_{\zeta_-}^{\zeta_+} \zeta^2 \phi_c\, d\zeta - (X_{so}X_{se})\Big|_0 \int_{\zeta_-}^{\zeta_+} \zeta^2 \phi_s \phi_c\, d\zeta, \qquad \text{(V-25)}$$

where the coefficient $c_k\lambda_k^2$ depends only upon the detailed shape of the fringing field. The expression for this "shape coefficient" is:

$$c_k \lambda_k^2 = \frac{1}{\phi_s} \int_{\zeta_-}^{\zeta_+} \zeta \phi_c(\zeta)\, d\zeta < \tfrac{1}{2}(\zeta_+ - \zeta_-)^2 \approx h^2. \qquad \text{(V-26)}$$

Let us determine the order of magnitude of this expression for a typical example. A good approximation to the actual fringing field shape is the "bell shape," for which

$$\phi = \phi_s \quad \text{for } \zeta \le -\pi h/4 \,,$$
$$\phi = \phi_s \left\{ 1 + (\zeta + \pi h/4)^2/h^2 \right\}^{-2} \quad \text{for } \zeta > -\pi h/4 \,, \qquad \text{(V-27)}$$

$\zeta = 0$ at the effective ends, and h is the "half width." Figure 3 shows the parameters used in the calculation of the shape coefficient for the exit fringing field of a quadrupole magnet. One half of the

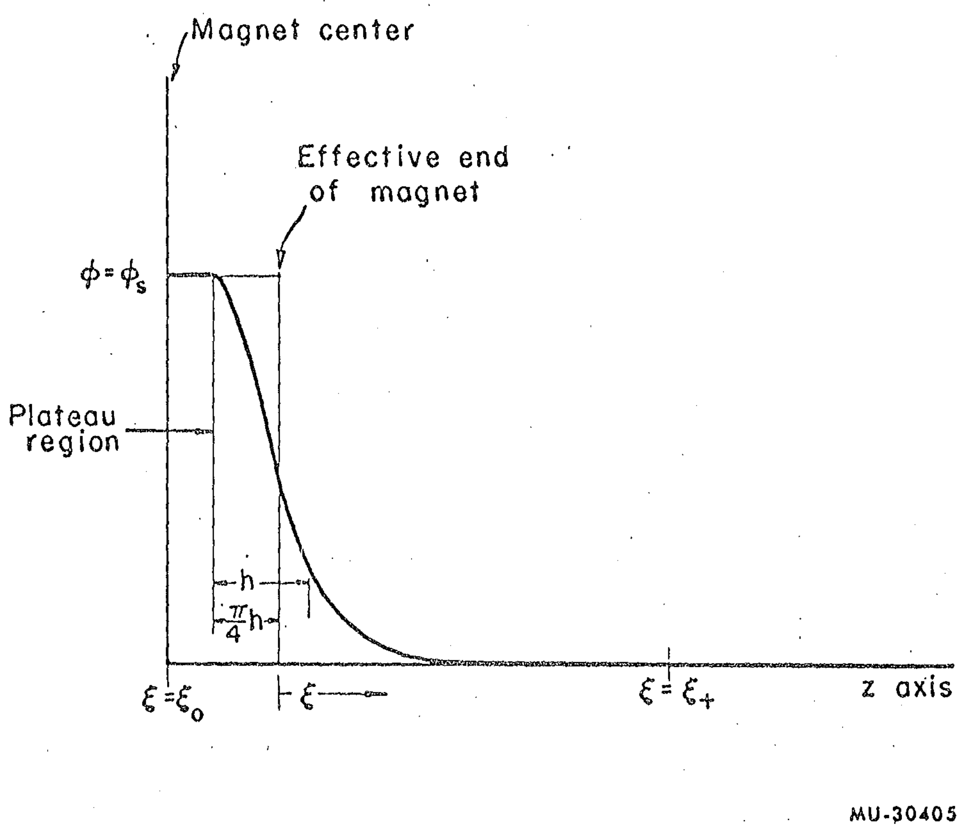

Fig. 3. Calculating the shape coefficient with the bell-shape curve.

magnet is shown. The function ϕ, as shown, obeys the "bell shape" formula. With this model, we find $c_k\lambda_k^2 = h^2(1-\pi^2/16)/2 \approx h^2/5$. (V-28)
The comparable coefficient for the other end of the magnet is just the negative of the one above.

To calculate the order of magnitude of the terms in ϕ_c we should compare them with the comparable terms in ϕ_s. For an example, consider

$$R = \frac{\int_{z_1}^{z_2} \phi_c x_1 x_2 dz}{\int_{z_1}^{z_2} \phi_s x_1 x_2 dz} \qquad \text{(V-29)}$$

with the integral taken over one magnet. Applying (V-25) and (V-26) to the expression for R, we obtain (V-30)

$$R = \frac{ch^2 \phi_s \left\{ (x_1x_2)'\big|_{z_2} - (x_1x_2)'\big|_{z_1} \right\}}{\phi_s \overline{(x_1x_2)}\ (z_2-z_1)} = \frac{ch^2 \phi_s \overline{(x_1x_2)''}\,\ell}{\phi_s \overline{(x_1-x_2)}\,(z_2-z_1)},$$

where $\bar{f}$ is the average value of the function f, defined by

$\bar{f} = \left\{ \int_a^b f\ dz \right\} (b-a)^{-1}$. We approximate further, using Eq. (V-1):

$$R \approx \frac{-h^2 \phi_s^2 \overline{(x_1x_2)}\,\ell}{\phi_s \ell\ \overline{(x_1x_2)}} \approx \frac{-h^2}{\ell f} = -\lambda^2 . \qquad \text{(V-31)}$$

This demonstrates that $\lambda = \frac{h}{L} = h(\ell f)^{-1/2} = h(\phi_s)^{-1/2}$ is the appropriate parameter of smallness for treating the fringing field terms.

We are now in a position to evaluate all the integrals appearing in x_c:

$$I_a = \sum_{\substack{K \\ (\text{ends})}} \left[-C_K \lambda_K^2 \phi_{s_K} \right] \left\{ \frac{\partial}{\partial \varsigma} \left[g(z,\varsigma)\ x_s(\varsigma) \right] \Big|_{\varsigma = z_K} \right\}, \qquad \text{(V-32)}$$

$$I_b = \Delta \int^z g(z,\varsigma)\phi_s(\varsigma)x_s(\varsigma)\ d\varsigma\ , \qquad \text{(V-33)}$$

$$I_c = O(\Delta \lambda_\varepsilon^2)\ ,$$

$$I_d = \Delta^2 \int^z d\varsigma\, \phi_s(\varsigma)\, g(z,\varsigma) \int^{\varsigma} d\gamma\, \phi_s(\gamma)\, g(\varsigma,\gamma) \quad , \tag{V-34}$$

$$I_e = O(\Delta^{2}\varepsilon),$$

$$I_f = O(\Delta^2 \lambda^2 \varepsilon).$$

The integrals I_c, I_e, and I_f, being smaller than third order, are dropped. The remaining integrals are readily evaluated.

E. The ε^3 Aberrations

All of the integrals in the expression for x^a (V-14) are continuous, as ϕ has not been separated into $\phi_s + \phi_c$. Consequently, we may integrate by parts to eliminate the terms in ϕ' and ϕ''; this has the advantage of leading to increased accuracy and simplicity of subsequent numerical calculations. The presence of the Green's function poses no difficulty, as it is readily expressed in terms of x_o and x_e (V-12); we retain g in the expressions only for brevity. All the integrated terms resulting from the integration by parts vanish, since ϕ and its derivatives all vanish at the end points, which have been chosen to lie well outside of any field region. Thus we have

$$\int_0^z \phi' g\, x y y'\, d\varsigma + \int^z \phi'' g \left(\tfrac{1}{4} x y^2 + \tfrac{1}{12} x^3\right) d\varsigma$$

$$= \left[\phi' g \left(\tfrac{1}{4} x y^2 + \tfrac{1}{12} x^3\right)\right]\Big|_0^z + \int_0^z \phi' g \left(-\tfrac{1}{4} x' y^2 - \tfrac{1}{4} x' x^2 + \tfrac{1}{2} x y x'\right) d\varsigma + \int_0^z \phi' g' \left(-\tfrac{1}{4} x y^2 - \tfrac{1}{12} x^3\right) d\varsigma$$

$$= \left\{\phi' g \left(\tfrac{1}{4} x y^2 + \tfrac{1}{12} x^3\right) + \phi g \left(-\tfrac{1}{4} x' y^2 - \tfrac{1}{4} x^2 x' + \tfrac{1}{2} x y y'\right) + \phi g \left(-\tfrac{1}{4} x y^2 - \tfrac{1}{12} x^3\right)\right\}\Big|_0^z$$

$$+ \int_0^z d\varsigma\, \phi^2 g \left(-x y^2 - \tfrac{1}{3} x^3\right) + \int_0^z d\varsigma\, \phi g' \left(\tfrac{1}{2} x' y^2 + \tfrac{1}{2} x' x^2\right) + \int_0^z d\varsigma\, \phi g \tfrac{1}{2} \left(x x'^2 - x y'^2\right),$$

where $g = \frac{\partial}{\partial \varsigma} g(z,\varsigma) \equiv x_o(z)\, x_e'(\varsigma) - x_e(z)\, x_o'(\varsigma)$,

$$x'' = -\phi x + \cdots, \quad y'' = \phi y + \cdots, \quad g'' = -\phi g. \tag{V-35}$$

The integrated term does vanish. The entire expression for x^a is

$$x^a = \int_0^z d\varsigma\, \phi^2 g(-xy^2 - \tfrac{1}{3}x^3) + \tfrac{1}{2}\int_0^z d\varsigma\, \phi g' x'(x^2+y^2)$$
$$+ \int_0^z d\varsigma\, \phi g\, (-xx'^2 - xy'^2 + x'yy') \quad . \tag{V-36}$$

Each of the terms in x^a is already of order ε^3, hence we may drop x^a wherever it occurs in the integrands without affecting the solution to third order.

If the fringing fields are small, i.e., if λ is truly a parameter of smallness, then we may replace ϕ by $\phi_s + \phi_c$, x by $x_s + x_c$, etc. and then keep only the terms in ϕ_s, x_s, x_s', y_s, and y_s'. The terms dropped are of order $\lambda\varepsilon^3$, $\Delta\varepsilon^3$ at most. We have now put all the terms giving the aberrations into integrals of products of the first-order solutions multiplied by piecewise constant functions [(V-33), (V-34), and (V-36)], and a fringing field term which is evaluated from a sum of products of first-order solutions multiplied by "shape coefficients" (V-32). Each of the expressions may be explicitly evaluated from known functions.

F. Octupole Terms

The same Green's-function approach yields the contribution to x due to the octupole fields (III-6), if any. These terms are added to x^a; they are

$$\int_0^z g(z,\varsigma)\ (xy^2 - x^3/3)\,\Psi(\varsigma)\ d\varsigma \ . \tag{V-37}$$

In evaluating these integrals, which are already small (of order ε^3), we replace $\Psi(\varsigma)$ by the mean value of Ψ, which is then piecewise constant.

G. Tolerances

In addition to the components of the magnetic field which have either the quadrupole or the octupole symmetry, we may find others present owing to misalignment of magnets, etc. In developing the equations of motion, we included these effects in the terms in $\mu, \nu, \delta\phi$, and λ [(IV-21), (III-8)]. The treatment is exactly the same as for the other aberration terms. Let x_t and y_t be the contributions to x and y, respectively, due to these terms; then we have

$$x_t = -\int^z \delta\phi\, g x\, ds - \int^z ds\, g\mu + z\int^z \lambda g y\, ds,$$

$$y_t = \int^z \delta\phi\, g y\, ds + \int^z g \nu\, ds + z\int^z \lambda g x\, ds\,. \tag{V-38}$$

Each of these integrals may be separated into a sum of integrals, each of which has contributions from only a single magnet. Hence we obtain the effect of misalignments, etc. of each magnet independent of the rest.

H. Higher Harmonics

Real quadrupole magnets frequently contain several troublesome higher harmonic components corresponding to n=3, 4, 5, 6, ···, 10, ··· in the general scalar magnetic potential expansion given by Eq. (III-3). Let us now consider the effect of these harmonics. Keeping only the lowest-order term in each harmonic, we may write the increment in the scalar potential due to the higher harmonics as

$$\frac{e}{p_0 c}\Delta V(r,\theta,z) = -a^2 \sum_{n=3}^{\infty} \frac{1}{n} \rho^n \phi(z) f_n(z) \sin(n\theta + \delta_n) \quad . \tag{V-39}$$

Here $\rho = r/a$, a is the maximum radius, f_n are arbitrary functions whose significance will be seen below, and δ_n are arbitrary phase angles.

The field components due to this potential increment are

$$\frac{e}{p_0 c}\,\Delta B_x = a \sum_{n=3}^{\infty} \rho^{n-1} f_n(z)\phi(z) \sin\left[(n-1)\theta+\delta_n\right] ,$$

$$\frac{e}{p_0 c}\,\Delta B_y = a \sum_{n=3}^{\infty} \rho^{n-1} f_n(z)\phi(z) \cos\left[(n-1)\theta+\delta_n\right] . \qquad \text{(V-40)}$$

Since the magnitude of the pure quadrupole field at maximum radius is $(p_0c/e)a\phi$, it is clear that f_n is the ratio of the maximum field component, due to the nth harmonic in the potential, to the maximum pure quadrupole component.

The displacements due to these field components are

$$\Delta x = -\int_0^z g_x(z,\zeta)\,\frac{e}{p_0 c}\,\Delta B_y\, d\zeta = -\frac{e}{p_0 c}\,\overline{\Delta B}_y \int^z_{\text{kth magnet}} g\, d\zeta ,$$

$$\Delta y = +\int_0^z g_y(z,\zeta)\,\frac{e}{p_0 c}\,\Delta B_x\, d\zeta = \frac{e}{p_0 c}\,\overline{\Delta B}_x \int^z_{\text{kth magnet}} g\, d\zeta . \qquad \text{(V-41)}$$

The integrals are taken over the kth magnet, and $\overline{\Delta B}$ is the average field increment experienced by the trajectory of interest. These integrals have already been calculated (V-38); they are the same integrals as determine the displacements in x and y due to displacing the kth magnet from the optic axis. Let T_1^0 and T_2^0 be the coefficients that determine the effects of displacing the kth magnet ($\Delta x = T_1^0 \frac{\mu_\kappa}{\phi_\kappa}$ and $\Delta y = T_2^0 \frac{\nu_\kappa}{\phi_\kappa}$). We express the displacements due to the higher harmonic terms in terms of the coefficients

$$\Delta x = aT_1^0 \sum_{n=3}^{\infty} f_n \rho^{n-1} \sin\left[(n-1)\theta+\delta_n\right] ,$$

$$\Delta y = aT_2^0 \sum_{n=3}^{\infty} f_n \rho^{n-1} \cos\left[(n-1)\theta+\delta_n\right] . \qquad \text{(V-42)}$$

We now have the effect of each harmonic for different regions of the k*th* quadrupole. That is, for any radius, $r=\rho a$, we can calculate the displacements due to any harmonic component in the field, providing we know the fractional magnitude of that component and the phase angle appropriate to that harmonic. Of course, we have neglected all but the lowest-order effect for these components. Lacking specific knowledge of a particular field component, we can specify the upper bound on the effect of that component. This calculation can be repeated for each quadrupole magnet in the beam system under consideration.

I. Symbolic Expressions

In the subsequent paragraphs, we introduce a useful short-hand for the independent functions (V-7) and those integrals which are required to evaluate the aberration coefficients. All of the coefficients may be evaluated from sums of integrals whose integrands are proportional to combinations of the four independent solutions to Eq. (V-1) and the corresponding equation in y, and the derivatives of these four solutions.

Let the eight-element array, χ_k, denote the independent funtions and their derivatives:

$$\chi_1(z)=x_{se}(z),\ \chi_2(z)=y_{se}(z),\ \chi_3(z)=x_{so}(z),\ \chi_4(z)=y_{so}(z)$$

$$\chi_5(z)=x_{se}'(z),\ \chi_6(z)=y_{se}'(z),\ \chi_7(z)=x_{so}'(z),\ \chi_8(z)=y_{so}'(z)\ . \qquad \text{(V-43)}$$

We introduce an array ψ_m for the initial conditions at the object plane: $\psi_1=x(0)$, $\psi_2=y(0)$, $\psi_3=x'(0)$, $\psi_4=y'(0)$,

$$\psi_5=\Delta\equiv(p-p_0)/p,\ \psi_o\equiv\psi_6\equiv 1\ . \qquad \text{(V-44)}$$

All of the terms in the expressions for x^a and y^a (with the fringing field taken out) are of two types:

$$K\psi_i\psi_j\psi_k\int_0^z \phi_s^2(\varsigma)\, \chi_m(\varsigma)\chi_n(\varsigma)\chi_p(\varsigma)\chi_q(\varsigma)\, d\varsigma,$$

$$K\psi_i\psi_j\psi_k\int_0^z \phi_s(\varsigma)\, \chi_m(\varsigma)\chi_n(\varsigma)\chi_{p+4}(\varsigma)\chi_{q+4}(\varsigma)\, d\varsigma,$$

for $m<5$, $n<5$, $p<5$, and $q<5$. (V-45)

We denote these integrals by the symbol

$$(mnpq) = \int_0^z \phi_s^2 \chi_m\chi_n\chi_p\chi_q\, d\varsigma \quad \text{or} \quad \int_0^z \phi_s \chi_m\chi_n\chi_p\chi_q\, d\varsigma \tag{V-46}$$

Whether ϕ_s or ϕ_s^2 is indicated depends upon whether all the indices are less than five or not (equivalent to selecting the power of ϕ which puts the integrand into dimensionless units).

We write

$$x^a(z) = \sum_{1\le i\le j\le k\le 4} C^{kji}(z)\,\psi_i\psi_j\psi_k \quad , \tag{V-47}$$

where the coefficients C^{kji} are sums of integrals multiplied by one of the four independent functions (V-7), evaluated at z.

The terms comprising x_c are also sums of integrals with the exception of the fringing field terms. We also introduce a symbolic expression for these integrals:

$$(mn) = \int_0^z \phi_s(\varsigma)\,\chi_m(\varsigma)\,\chi_n(\varsigma)\, d\varsigma \quad , \tag{V-48}$$

$$(mn\,|\,pq) = \int_0^z d\varsigma\, \phi_s(\varsigma)\chi_m(\varsigma)\chi_n(\varsigma)\int_0^\varsigma d\tau\, \phi_s(\tau)\,\chi_p(\tau)\,\chi_q(\tau) \quad . \tag{V-49}$$

The fringing field sums are denoted by

$$S_{mn} = \sum_{\substack{\text{all } k \\ \text{(fringing fields)}}} c_k\phi_{sk}\,\chi_m(z_k)\,\chi_n(z_k) \quad . \tag{V-50}$$

Then we have $x_c = \sum_{i=1}^{4}\left\{ C^{5i}\psi_5\psi_i + C^{55i}\psi_5{}^2\psi_i + C^{66i}\psi_i \right\}$, (V-51) where C^{5i} and C^{55i} are the coefficients for second-order and third-order dispersion terms, respectively; C^{66i} are the coefficients describing the fringing-field effects.

As shown in Ch. III, reflection symmetry forces certain coefficients to vanish. For example, there can be no term in $x(0)^2 y'(0)$ in the expansion of x^a, although there is such a term in the expansion of y^a; hence the coefficient C^{411} appears only in the expansion of y^a. In fact, for any combination of indices, it can be proven from symmetry considerations that the coefficient corresponding to those indices can appear in only one of the expansions, that for x^a or that for y^a. We combine x^a and x_c [(V-47) and (V-51)] and write

$$x=\psi_1\chi_1(z)+\psi_3\chi_3(z)+\sum_{1\le k\le j\le i\le 6} C^{ijk}(z)\psi_i\psi_j\psi_k,$$
$$y=\psi_2\chi_2(z)+\psi_4\chi_4(z)+\sum_{1\le k\le j\le i\le 6} C^{ijk}(z)\psi_i\psi_j\psi_k, \tag{V-52}$$

with the following "rule of thumb" for determining in which expression a particular coefficient C^{ijk} belongs: excluding indices of five or six, if $(i+j+k)$ is even then C^{ijk} is a factor in the expansion of y; if $(i+j+k)$ is odd then it is a factor in the expansion of x.

A complete list of coefficients and expressions that yield them are found in Appendix I.

The octupole integrals are denoted by

$$\langle ijkm\rangle = \int_0^z \psi(\zeta)\,\chi_i(\zeta)\,\chi_j(\zeta)\,\chi_k(\zeta)\,\chi_m(\zeta)\,d\zeta\ . \tag{V-53}$$

We denote the displacements due to the nonsymmetrical field components μ, ν, $\delta\phi$, and λ by x_t. To lowest order in these effects we have

$$x^t = \frac{\mu}{\phi} T_1^0 + \frac{\delta\phi}{\phi} T_1^1 \psi_1 + \frac{\lambda}{\phi} T_1^2 \psi_2 + \frac{\delta\phi}{\phi} T_1^3 \psi_3 + \frac{\lambda}{\phi} T_1^4 \psi_4 \, , \qquad \text{(V-54)}$$

$$y^t = \frac{\nu}{\phi} T_2^0 + \frac{\lambda}{\phi} T_2^1 \psi_1 + \frac{\delta\phi}{\phi} T_2^2 \psi_2 + \frac{\lambda}{\phi} T_2^3 \psi_3 + \frac{\delta\phi}{\phi} T_2^4 \psi_4 \, . \qquad \text{(V-55)}$$

There is a set of tolerance coefficients T_j^i for each quadrupole magnet in the beam system. The tolerance coefficients on magnet placement required to insure $|x^t| < T_{max}$, where T_{max} is the maximum aberration due to permissible tolerances.

J. Numerical Methods of Calculation

All the coefficients of aberration may be calculated by summing a number of terms, each of which consists of three factors: (a) a numerical factor, (b) one of the functions $\mathcal{X}_i(z)$ (i=1, 2, 3, or 4), and (c) an integral of one of the types mentioned. The coefficients describing the fringing field differ only in that the integral is replaced by a sum.

A digital computer code for the IBM 7090 digital computer has been written which includes the calculation of the coefficients of aberration within its scope. The entire scope of the code is described in Ch. VIII, and its operation is described in Appendix II.

In calculating the aberrations, the code must evaluate numerically 113 integrals taken over the beam system [16 of the type (mn|pq), 6 of the type (mn), 72 of the type (mnpq), and 19 of the type <ijkm>], in addition to 14 integrals required for the tolerance coefficients, which must be integrated separately over each magnet in the system.

The total number of terms to be formed and summed is 244, exclusive of the tolerance coefficients. An additional 244 terms are summed to evaluate the 32 coefficients in the expansions of the slopes, x' and y'.

All the terms in the expansions of x' and y' are the same as the corresponding terms in the expansions for x and y (V-52) except that the factor $\chi_i(z)$ is replaced by its derivative, $\chi_{i+4}(z)$. We have $x'(z)=\psi_1\chi_5(z)+\psi_3\chi_7(z)+\sum_{1\leq k\leq j\leq i\leq 6} D^{ijk}(z)\psi_i\psi_j\psi_k$, (V-56)

and $x_t'(z)= T_3^0\frac{\mu}{\phi}+T_3^1\frac{\delta\phi}{\phi}+\cdots$, etc.; the coefficients D^{ijk} are obtained by differentiating the equations for C^{ijk} (Appendix I) with respect z.

The integrals are evaluated by ten-point Gaussian integration, which corresponds to fitting a 21st-degree polynomial to the integrand and evaluating the integral of that polynomial. Since there are 16 double integrals to be evaluated, each of the intervals used in the Gaussian integration must be further subdivided. In all, the first-order solutions and derivatives, $\chi_i(z)$ (with i=1, 8) must be evaluated at 111 points for each quadrupole magnet.

The first-order solutions, $\chi_i(z)$, are evaluated from the entrance of the magnet to each of the 111 points using Eqs. (II-18) and (II-19)(the accuracy is improved by calculating each time from the beginning of the magnet rather than from the preceding point;, this procedure is just as fast). At each point certain products are formed and the code runs through a table of 94 entries which specifies the factors in the integrands of each integral. The integrands are evaluated, weighted with the appropriate Gaussian factor, and added into the partial sums that comprise the integrals.

After the integrals have been evaluated for the entire beam system, a second table consisting of 244 entries is consulted. Each entry in this table lists a factor k, one of the functions $\mathcal{X}_i(z)$, and one of the integrals (mn), (mn|pq), (mnpq), or <mnpq>, and a coefficient C^{ijk} into which the product, $k \cdot \mathcal{X}_i(z) \cdot \int(-)d\zeta$, is added. All the coefficients C^{ijk} and D^{ijk} are calculated with no octupole contributions and are listed. The octupole contributions (if there are any) are then added into the coefficients, which are then listed again.

For a beam system consisting of three quadrupole magnets and four drift spaces, the entire process of calculating the aberration coefficients takes approximately 0.01 minute on the IBM 7090 computer.

The code will also calculate the shape coefficients and the locations of the effective ends of quadrupole magnets. The required input consists of a table of $\Phi(z)$ at uniform intervals in z, the locations of the magnet centers, and the physical lengths of the magnets. The code evaluates the integrals $\int \Phi dz$ and $\int z \Phi dz$ over both ends of each magnet and the adjacent drift spaces. From these integrals, the required data can be derived.

If desired, the code will construct the table of $\Phi(z)$ using the bell-shape approximation previously described (V-27). The locations of the magnet centers, the relative excitation of each magnet, the length of the central plateau (constant-gradient region) of each magnet, and the half width, h, (characteristic of the fringing field extent) for each magnet constitute the input data.

VI. RELATIONS BETWEEN THE GEOMETRICAL COEFFICIENTS OF ABERRATION

In the preceding chapters we have calculated 56 coefficients which completely describe the aberrations through third order for a beam system possessing two planes of reflection antisymmetry. Of these, 40 characterize the geometrical aberrations of monoenergetic beams; the remaining 16 describe the chromatic aberrations. (If the scalar potential is separated into two parts, one a step function in z and the other a difference function, as described in Chapter V, then eight additional coefficients are obtained; these coefficients describe the thrid-order effects of the fringing fields. In this chapter we ignore the fringing field coefficients. They are not fundamental, but have been included to clearly demonstrate the effects of the fringing fields.) Not all these coefficients are independent. Burfoot has shown that the third-order geometric aberrations of a monoenergetic beam system possessing the above symmetry properties are completely described by 16 independent numbers.[4] In this chapter we derive 28 relationships, of which 24 are independent, among the 40 geometrical aberration coefficients in the third-order terms in the power-series expansions of x, y, x', and y' in terms of x_o, y_o, x_o', and y_o'. These relationships are derived by making use of certain Poincaré integral invariants which express the fact that the transformations carrying the trajectories between two points are restricted to the special class of canonical transformations.

A. Number of Independent Coefficients

Burfoot's method of classifying aberration types follows a classical method of treating aberrations. This is fully described in Chapter 16 of the book by Zworykin et al.[11]

Instead of expanding the displacements, x and y, in a power series in the object plane displacements and slopes, this method describes the trajectories in terms of a power series in x_o, y_o, x_a, and y_a. The latter two quantities are the displacements of a trajectory at the aperture plane. The aperture plane is defined as a plane in field-free space near the image plane. All trajectories are straight lines between the aperture plane and the image plane.

It is well known that the system of trajectories issuing from a monoenergetic point source are all orthogonal to a particular family of surfaces, on each of which Hamilton's characteristic function takes a constant value. For each trajectory one value of Hamilton's characteristic function, W, corresponds to the surface orthogonal to that trajectory at the point where the trajectory intersects the aperture plane. If we know the value of W as a function of the coordinates of the source and the coordinates of the intersection with the aperture plane of trajectories issuing from that source, then we know all there is to know about the optical properties, including aberrations, of the beam system considered.

Since the family of surfaces described above must also have the symmetries of the quadrupole magnet array, the power-series expansion of W in terms of x_o, y_o, x_a, and y_a may contain only terms of even power. The trajectories are determined by the derivatives $\frac{\partial W}{\partial x_a}$ and $\frac{\partial W}{\partial y_a}$ of W, evaluated at x_a and y_a. Thus third-order terms in the image-plane displacements are derived from fourth-order terms in the power series for W. Since there are only 16 independent fourth-power combinations of x_o, y_o, x_a, and y_a that contain at least one power of x_a or y_a and satisfy the symmetries, there can be only 16 independent numbers describing the geometrical aberrations of third-order.

In III. C. we listed the 20 third-order terms that describe the geometric aberrations to that order. The coefficients to eight of these terms are derived from the following four terms in the expansion of W: $x_a^2 y_a^2$, $x_o y_o x_a y_a$, $x_o x_a y_a^2$, and $y_o y_a x_a^2$. (four terms from differentiating with respect to x_a and four from y_a). There are three numbers characterizing generalized spherical aberrations, four numbers characterizing generalized coma, five numbers characterizing generalized astigmatism, and four numbers characterizing generalized distortion. In systems possessing rotational symmetry, these 16 independent numbers reduce to five.

B. Derivation of the Relationships

We now return to our description of the aberrations, which employs coefficients of the third-order terms in the power-series expansions of x, y, x', and y' in terms of x_o', y_o', x_o, and y_o. We derive the desired relationships by utilizing the Poincare integral invariants, using the coordinate frame introduced in Chapter IV. With z as the independent variable, the canonical coordinates and momenta are x, y, t, p_x, p_y, and p_t; the expressions for the canonical momenta are given by Eq. (IV-7). These quantities are the Cartesian coordinates in our six-dimensional phase space. The magnetic field is assumed to vanish in the neighborhoods of the object and image planes, so that the following expansions are valid in these regions

$$p_x = Mvx' \ (1-x'^2/2-y'^2/2+\cdots),$$
$$p_y = Mvy' \ (1-x'^2/2-y'^2/2+\cdots). \qquad \text{(VI-1)}$$

The Poincare invariance theorem states that the integral

$$J \equiv \iint_S \sum_{i=1}^{3} dq_i \ dp_i \ , \qquad \text{(VI-2)}$$

taken over any arbitrary surface in phase space, is invariant under all canonical trasformations, such as the canonical transformation that takes the coordinates from their initial values to their final values. Similar invariants exist for integrals taken over any even-dimensional subspace of phase space.

The method we use is an adaptation of the proof of the invariance found in the textbook by Goldstein.[12] We may calculate an invariant in terms of the initial coordinates and slopes at the object plane and also in terms of the coordinates and slopes at the image plane. We can then express the invariant at the image plane in terms of the initial coordinates and slopes, using the power-series expansions of the image-plane coordinates and slopes in terms of the object-plane coordinates and slopes. Equating the value of the invariant at the image plane with the value at the object plane, we obtain the desired relationships between the coefficients as required by invariance.

Points on a two-dimensional surface may be located by two curvilinear coordinates. Let u and v be any curvilinear coordinates appropriate to the arbitrary two-dimensional surface on which we evaluate the integral to obtain the invariant. In terms of u and v, the integral may be written

$$J=\iint_S \sum_{n=1}^{3} \frac{\partial(q_i, p_i)}{\partial(u,v)} \, du \, dv \; . \qquad \text{(VI-3)}$$

We now see that, owing to the invariance of the integral over an arbitrary surface, S, the integrand must be invariant. The integrand is the Lagrange bracket of u and v,

$$\sum_i \frac{\partial(q_i, p_i)}{\partial(u,v)} = \{u, v\}_{q,p} \; . \qquad \text{(VI-4)}$$

Although we have been referring to an "image" plane, there is no need to restrict the subsequent discussion to systems that form a point image of a point source. Let there be a line image parallel to the y axis at z_x and a line image parallel to the x axis at z_y. Either of these images may be virtual.

At some arbitrary point z, in a field-free region, we expand the displacements and slopes of a trajectory, obtaining to first order [from (II-6)]

$$\begin{aligned} x'(z) &= x_o'/m - x_o/f_x, \quad x(z) = m\,x_o + (z-z_x)x'(z) \; , \\ y'(z) &= y_o'/n - y_o/f_y, \quad y(z) = n\,y_o + (z-z_y)y'(z) \; . \end{aligned} \qquad \text{(VI-5)}$$

Here m and n are the magnifications in the x-z plane and the y-z plane, respectively, and f_x and f_y are the two focal lengths.

Letting the superscript a denote the correction due to aberrations, we find the corresponding expressions that include the aberrations are

$$\begin{aligned} x'(z) &= x_o'/m - x_o/f_x + x'^a(x_o, y_o, x_o', y_o'), \\ x(z) &= m\,x_o + (z-z_x)\,x'(z) + x^a(x_o, y_o, x_o', y_o'). \end{aligned} \qquad \text{(VI-6)}$$

In restricting this discussion to monoenergetic beams, we limit ourselves to surfaces in phase space on which E is a constant. Thus we shall always have

$$\frac{\partial(t, -E)}{\partial(u, v)} \equiv 0. \tag{VI-7}$$

In the subsequent derivations, we shall have ocassion to use the following properties of Jacobian determinants; these properties are easily derived. If α, β, and ε are three arbitrary functions of u and v, and if x is a function of α and β, then

$$\frac{\partial(\alpha,\beta)}{\partial(u,v)} = -\frac{\partial(\beta,\alpha)}{\partial(u,v)} = \frac{\partial\alpha}{\partial u}\frac{\partial\beta}{\partial v} - \frac{\partial\beta}{\partial u}\frac{\partial\alpha}{\partial v}, \tag{VI-8}$$

$$\frac{\partial(a\alpha+\varepsilon,\beta)}{\partial(u, v)} = a\frac{\partial(\alpha,\beta)}{\partial(u,v)} + \frac{\partial(\varepsilon,\beta)}{\partial(u,v)} \text{ (where a is a constant),} \tag{VI-9}$$

$$\frac{\partial(x,\varepsilon)}{\partial(u,v)} = \frac{\partial x}{\partial\alpha}\frac{\partial(\alpha,\varepsilon)}{\partial(u,v)} + \frac{\partial x}{\partial\beta}\frac{\partial(\beta,\varepsilon)}{\partial(u,v)}, \tag{VI-10}$$

$$\frac{\partial(\alpha,\alpha)}{\partial(u,v)} = 0 . \tag{VI-11}$$

When evaluated at the object plane, the integrand of the invariant becomes

$$I = \left\{u,v\right\}_{q,p} = \frac{\partial(x_o, p_{xo})}{\partial(u, v)} + \frac{\partial(y_o, p_{yo})}{\partial(u, v)}, \tag{VI-12}$$

where, applying (VI-1),

$$\frac{\partial(x_o, p_{xo})}{\partial(u, v)} = Mv(1 - 3x_o'^2/2 - y_o'^2/2)\frac{\partial(x_o,x_o')}{\partial(u,v)} - Mv\, x_o' y_o' \frac{\partial(x_o,y_o')}{\partial(u,v)}. \tag{VI-13}$$

to third order; a similar expression is obtained fromthe term in y_o and p_{yo}.

At the arbitrary point z, the integrand in terms of the initial conditions, is $I = \dfrac{\partial(x,p_x)}{\partial(u,v)} + \dfrac{\partial(y,p_y)}{\partial(u,v)}$, (VI-14) where $$\frac{\partial(x,p_x)}{\partial(u,v)} = Mv\ (1 - 3x'^2/2 - y'^2/2)\ \frac{\partial(x,x')}{\partial(u,v)}$$

$$-Mvx'y'\ \frac{\partial(x,y')}{\partial(u,v)} - x'y'\ (z-z_x)\ \frac{\partial(x'y')}{\partial(u,v)}\ , \qquad \text{(VI-15)}$$

$$\frac{\partial(x,x')}{\partial(u,v)} = \frac{\partial(x_o,\ x_o')}{\partial(u,\ v)} + m\ \frac{\partial(x_o,x'^a)}{\partial(u,\ v)} - \frac{1}{m}\ \frac{\partial(x_o',x^a)}{\partial(u,\ v)} + \frac{1}{f}\ \frac{\partial(x\ \ ,x^a)}{\partial(u,\ v)}\ ,$$

$$\frac{\partial(x,y')}{\partial(u,v)} = \frac{m}{n}\ \frac{\partial(x_o,y_o')}{\partial(u,v)} - \frac{m}{f_y}\ \frac{\partial(x_o,y_o)}{\partial(u,v)} + \cdots\ , \quad \text{and}$$

$$\frac{\partial(x',y')}{\partial(u,v)} = \frac{1}{mn}\ \frac{\partial(x_o',y_o')}{\partial(u,v)} - \frac{1}{mf_y}\ \frac{\partial(x_o',y_o)}{\partial(u,v)} - \frac{1}{nf_x}\ \frac{\partial(x_o,y_o')}{\partial(u,v)} + \frac{1}{f_xf_y}\ \frac{\partial(x_o,y_o)}{\partial(u,v)}\ ;$$

these expressions are obtained from Eq. (VI-1) and Eq. (VI-6) using Eqs. (VI-8) through (VI-11).

Let D be the difference between the integrands evaluated at the two points. As stated previously, this integrand is an invariant and D therefore is identically zero. We write D as

$$D=Mv\left\{\frac{\partial(x,p_x)}{\partial(u,v)} + \frac{\partial(y,p_y)}{\partial(u,v)} - \frac{\partial(x_o,p_{xo})}{\partial(u,v)} - \frac{\partial(y_o,p_{yo})}{\partial(u,v)} + \cdots\right\}. \qquad \text{(VI-16)}$$

Each of the aberration terms can be expanded, using (V-47) (this expansion is not made until later for reasons of brevity), and each term can be written so that the only Jacobian determinants remaining involve pairs of initial parameters. We write D as

$$D = Mv\left\{S_1\ \frac{\partial(x_o,x_o')}{\partial(u,v)} + S_2\ \frac{\partial(x_o,y_o)}{\partial(u,v)} + S_3\ \frac{\partial(x_o,y_o')}{\partial(u,v)}\right.$$

$$\left. + S_4\ \frac{\partial(x_o',y_o)}{\partial(u,v)} + S_5\frac{\partial(x_o',y_o')}{\partial(u,v)} + S_6\ \frac{\partial(y_o,y_o')}{\partial(u,v)}\right\}\ , \qquad \text{(VI-17)}$$

$$\text{where } S_1 = m\frac{\partial x'^a}{\partial x_0'} + \frac{1}{m}\frac{\partial x^a}{\partial x_0} + \frac{1}{f_x}\frac{\partial x^a}{\partial x_0'} + \frac{3}{2}\left\{x_0'^2 - \left(\frac{x_0'^2}{m^2} - \frac{2}{m f_x}x_0 x_0' + \frac{1}{f_x^2}x_0^2\right)\right\}$$
$$+ \frac{1}{2}\left\{y_0'^2 - \left(\frac{y_0'^2}{n^2} - \frac{2}{n f_y}y_0 y_0' + \frac{1}{f_y^2}y_0^2\right)\right\}, \tag{VI-17}$$

$$S_2 = m\frac{\partial x'^a}{\partial y_0} - n\frac{\partial y'^a}{\partial x_0} + \frac{1}{f_x}\frac{\partial x^a}{\partial y_0} - \frac{1}{f_y}\frac{\partial y^a}{\partial x_0} + \left\{\frac{x_0' y_0'}{mn} - \frac{x_0 y_0'}{n f_x} - \frac{x_0' y_0}{m f_y} + \frac{x_0 y_0}{f_x f_y}\right\}\left\{-\frac{n}{f_x} + \frac{m}{f_y} + \frac{L}{f_x f_y}\right\},$$

$$S_3 = m\frac{\partial x'^a}{\partial y_0'} + \frac{1}{n}\frac{\partial y^a}{\partial x_0} + \frac{1}{f_x}\frac{\partial x^a}{\partial y_0'} + x_0' y_0' + \left\{\frac{x_0' y_0'}{mn} - \frac{x_0 y_0'}{n f_x} - \frac{x_0' y_0}{m f_y} + \frac{x_0 y_0}{f_x f_y}\right\}\left\{-\frac{m}{n} - \frac{L}{n f_x}\right\},$$

$$S_4 = -\frac{1}{m}\frac{\partial x^a}{\partial y_0} - n\frac{\partial y'^a}{\partial x_0'} - \frac{1}{f_y}\frac{\partial y^a}{\partial x_0'} - x_0' y_0' + \left\{\frac{x_0' y_0'}{mn} - \frac{x_0 y_0'}{n f_x} - \frac{x_0' y_0}{m f_y} + \frac{x_0 y_0}{f_x f_y}\right\}\left\{\frac{n}{m} - \frac{L}{m f_y}\right\},$$

$$S_5 = -\frac{1}{m}\frac{\partial x^a}{\partial y_0'} + \frac{1}{n}\frac{\partial y^a}{\partial x_0'} + \left\{\frac{x_0' y_0'}{mn} - \frac{x_0 y_0'}{n f_x} - \frac{x_0' y_0}{m f_y} + \frac{x_0 y_0}{f_x f_y}\right\}\frac{L}{mn},$$

$$S_6 = n\frac{\partial y'^a}{\partial y_0'} + \frac{1}{n}\frac{\partial y^a}{\partial y_0} + \frac{1}{f_y}\frac{\partial y^a}{\partial y_0'} + \frac{3}{2}\left\{y_0'^2 - \left(\frac{y_0'^2}{n^2} - \frac{2 y_0 y_0'}{n f_y} + \frac{y_0^2}{f_y^2}\right)\right\} + \frac{1}{2}\left\{x_0'^2 - \left(\frac{x_0'^2}{m^2} - \frac{2 x_0 x_0'}{m f_x} + \frac{x_0^2}{f_x^2}\right)\right\}.$$

The integral, J, is invariant over any two-dimensional surface in phase space. Among these surfaces are those on which two of the four parameters x_0, y_0, x_0', y_0' take constant values. On such a surface only one of the six Jacobian determinants in Eq. (VI-17) is nonvanishing. For example, consider the surface $x_0 \equiv a$ and $y_0' \equiv b$. Here we find that the coefficients of S_1, S_2, S_3, S_5, and S_6 each vanish as the Jacobian determinants contain constants. Thus, for this choice of surface, we see that $S_4 \equiv 0$. By applying this argument to other surfaces, it is clear that each of the coefficients S_1, S_2, S_3, S_4, S_5, and S_6 must vanish identically.

Let us now group the terms withing these six expressions as follows:

$$S_1 = S_{11}\, x_0^2 + S_{12}\, x_0 x_0' + S_{13}\, x_0'^2 + S_{14} y_0^2 + S_{15}\, y_0'^2, \tag{VI-18}$$

$$S_2 = S_{21}x_o y_o + S_{22}\, x_o y_o' + S_{23}\, x_o' y_o + S_{24}\, x_o' y_o' \quad ,$$

$$S_3 = S_{31}x_o y_o + S_{32}\, x_o y_o' + S_{33}\, x_o' y_o + S_{34}\, x_o' y_o' \quad ,$$

$$S_4 = S_{41}x_o y_o + S_{42}\, x_o y_o' + S_{43}\, x_o' y_o + S_{44}\, x_o' y_o' \quad ,$$

$$S_5 = S_{51}x_o y_o + S_{52}\, x_o y_o' + S_{53}\, x_o' y_o + S_{54}\, x_o' y_o' \quad ,$$

$$S_6 = S_{61}x_o^{\,2} + S_{62}\, x_o x_o' + S_{63}\, x_o'^{\,2} + S_{64}\, y_o^{\,2} + S_{65}\, y_o y_o' + S_{66}\, y_o'^{\,2} .$$

Since the region of integration is completely arbitrary, S_1 through S_6 can all vanish identically only if each of the $S_{ij}=0$. These conditions yield 28 relations between the coefficients of aberration, of which only 24 are independent. The derived relationships, in the notation introduced in V.I. [the aberration corrections are expanded, using Eq. (V-47)], are

$$S_{11} = mD^{311} + 3C^{111}/m + C^{311}/f_x - 3/2f_x^{\,2} = 0 \;, \qquad \text{(VI-19)}$$

$$S_{12} = 2mD^{331} + 2C^{311}/m + 2C^{331}/f_x + 3/mf_x = 0 \;,$$

$$S_{13} = 3mD^{333} + C^{331}/m + 3C^{333}/f_x + 3(m^2-1)/2m^2 = 0,$$

$$S_{14} = mD^{322} + C^{211}/m + C^{322}/f_x - 1/2f_y^{\,2} = 0 \;,$$

$$S_{15} = mD^{432} + C^{421}/m + C^{432}/f_x + 1/nf_y = 0 \;,$$

$$S_{16} = mD^{443} + C^{441}/m + C^{443}/f_x + (n^2-1)/2n^2 \;,$$

$$S_{21} = 2mD^{221} - 2nD^{211} + 2C^{221}/f_x - 2C^{211}/f_y - n/f_x^{\,2}f_y + m/f_xf_y^{\,2} + L/f_x^{\,2}f_y^{\,2} = 0,$$

$$S_{22} = mD^{421} - 2nD^{411} + C^{421}/f_x - 2C^{411}/f_y + 1/f_x^{\,2} - m/nf_xf_y - L/f_x^{\,2}f_y = 0,$$

$$S_{23} = 2mD^{322} - nD^{321} + 2C^{322}/f_x - C^{321}/f_y + n/mf_xf_y - 1/f_y^{\,2} - L/mf_xf_y^{\,2} = 0,$$

$$S_{24} = mD^{432} - nD^{431} + C^{432}/f_x - C^{431}/f_y - 1/mf_x + 1/nf_y + L/mnf_xf_y = 0,$$

$$S_{31} = mD^{421} + 2C^{211}/n + C^{421}/f_x - m/nf_xf_y - L/nf_x{}^2f_y = 0,$$

$$S_{32} = 2mD^{441} + 2C^{411}/n + 2C^{441}/f_x + m/n^2f_x + L/n^2f_x{}^2 = 0,$$

$$S_{33} = mD^{432} + C^{321}/n + C^{432}/f_x + 1/nf_y + L/mnf_xf_y = 0,$$

$$S_{34} = 2mD^{443} + C^{431}/n + 2C^{443}/f_x + 1 - 1/n^2 - L/mn^2 = 0,$$

$$S_{41} = -nD^{321} - 2C^{221}/m - C^{321}/f_y + n/f_xf_y + L/mf_xf_y{}^2 = 0,$$

$$S_{42} = -nD^{431} - C^{421}/m - C^{431}/f_y - 1/mf_x + L/mnf_xf_y = 0,$$

$$S_{43} = -2nD^{332} - 2C^{322}/m - 2C^{332}/f_y - n/m^2f_y + L/m^2f_y{}^2 = 0,$$

$$S_{44} = -2nD^{433} - C^{432}/m - 2C^{433}/f_y - 1 + 1/m^2 + L/m^2nf_y = 0,$$

$$S_{51} = C^{321}/n - C^{421}/m + L/mnf_xf_y = 0,$$

$$S_{52} = C^{431}/n - 2C^{441}/m - L/mn^2f_x = 0$$

$$S_{53} = 2C^{332}/n - C^{432}/m - L/m^2nf_y = 0,$$

$$S_{54} = 2C^{433}/n - 2C^{443}/m + L/m^2n^2 = 0,$$

$$S_{61} = nD^{411} + C^{211}/n + C^{411}/f_y - 1/2f_x{}^2 = 0,$$

$$S_{62} = nD^{431} + C^{321}/n + C^{431}/f_y + 1/mf_x = 0,$$

$$S_{63} = nD^{433} + C^{332}/n + C^{433}/f_y + (m^2-1)/2m^2 = 0,$$

$$S_{64} = nD^{422} + 3C^{222}/n + C^{422}/f_y - 3/2f_y{}^2 = 0,$$

$$S_{65} = 2nD^{442} + 2C^{422}/n + 2C^{442}/f_y + 3/nf_y = 0,$$

$$S_{66} = 3nD^{444} + C^{442}/n + 3C^{444}/f_y + 3(n^2-1)/2n^2 = 0.$$

These 28 relationships, derived from the Poincare integral invariance, are a consequence of the assumed symmetry of the beam system and the requirement that the transformations between the object plane and the plane at the arbitrary point z be a canonical transformation. In Chapter V we have derived the expressions for the 40 coefficients appearing in the above relationships. We may now apply these relationships to any numerical values of the coefficients we may calculate, in order to verify the accuracy of our calculations. This is a powerful check, as these relationships involve the five first-order quantities m, n, f_x, f_y, and L in addition to the aberration coefficients.

These relationships are satisfied by the aberration coefficients calculated by the 7090 computer code in every instance checked. In most cases, the relations are valid to five of six significant figures. As we are easily able to test the accuracy of the linear calculations of the code, we are now able to completely verify the accuracy of the aberration calculations.

The expressions S_{51} through S_{54} yield one relationship between the four coefficients describing generalized spherical aberration, one relationship between the six coefficients describing generalized astigmatism, and two relationships between the six coefficients describing generalized coma. The remaining independent terms agree with the distribution described by Burfoot.

The other 24 conditions we have derived relate the coefficients in the expansions of the slopes x' and y' to the coefficients in the expansions of the displacements x and y.

VII. THE CHARACTER OF THE ABERRATIONS

In the preceding chapters we have developed power-series expansions of the displacements of trajectories that have passed through a quadrupole magnet beam system. The aberrations of such a system are described by 64 coefficients, many of which are not independent. In addition to the aberrations of a beam system possessing the two-plane reflection symmetry properties assumed in the aberration calculations, beam systems with real quadrupole magnets have defects due to their failure to achieve exactly the assumed symmetry. These defects can be characterized by further coefficients. We have referred to a digital computer code that calculates all these coefficients, but we have not yet examined the qualitative and quantitative effects of the aberrations. This we shall now do.

We are interested in aberrations only in a region where the displacements due to linear terms are small. We therefore restrict our discussion to the neighborhood of an image or a waist produced by the beam system. The actual character of the beam in such a neighborhood is strongly dependent on the distribution of the trajectory points in the object-plane phase space, because some components in the displacements, which are cubic in the object-plane parameters, may be dominant in such a neighborhood.

A complete solution would provide the exact shape of the three-dimensional beam envelope near the image, but a more practical description, even though not quite so general, consists of the knowledge of the projections of the envelope on each of the coordinate planes. In addition to the projections of the envelope, our description must consider the distribution of trajectories within the envelope. In most applications a system in which relatively few trajectories suffer large aberration displacements would be preferred to one in which many trajectories suffer large aberration displacements, even though the maximum displacement due to the aberrations might be the same for both systems. Finally, we would like to represent the aberrations by a few characteristic numbers in order that we can compare several beam systems. The maximum displacements due to the aberrations and the root-mean-square displacements due to the aberrations are good quantities for use in making comparisons. For beam systems in which a line or a point image is desired, one would like to know the width of the best image attainable when aberrations are considered.

In the remainder of this chapter, we calculate the average and maximum aberration displacements and the location and size of the best image attainable for a given beam system; we also examine the effects of aberrations on the image of a point source. In the course of these discussions we refer to two sample problems which have been solved by use of the digital computer code. Significant portions of the computer printouts obtained for these examples are reproduced in Appendix III, together with instructions for further interpretation. Instructions for using the code are given in Appendix II.

The first example consists of a beam system composed of a symmetric quadrupole triplet which is adjusted to provide a point image of a point source, the symmetric triplet being located midway between the source and the image. Obviously, unit magnification is obtained in both planes in this example. We then examine the imaging of a small circular diffuse source by this system.

The second example consists of a quadrupole doublet which is adjusted to provide a line image of an incoming parallel beam in one plane and a parallel outgoing beam in the other plane. For each of these examples, we determine the coefficients that dominate the aberrations displacements and then calculate the tolerances permitted in positioning the magnets so that the aberrations due to failure to achieve quadrupole symmetry are smaller than the inherent aberrations.

A. The Average Aberration Displacements

In this section, we calculate the maximum and average displacements due to the aberrations obtaining expressions that enable us to compare the contributions of the different coefficients of aberrations. We first must stipulate the occupied region in phase space. For this purpose, we introduce three models. Some calculations result in relatively simple expressions for one model but not for others. Each of the three models represents a reasonable approximation to a real beam distribution.

1. Models for the Occupation of Object-Plane Phase Space

As stated previously, we always assume an effective source at the input to the beam system, since this assumption entails no real restriction. We restrict the distribution of trajectories to those which are symmetric with respect to reflection through any of the five coordinate planes in x_o, y_o, x_o', y_o', Δ

space.

Model #1 is a rectangular distribution with each coordinate ranging between a minimum and a maximum value independent of the other four coordinates. For this model, we have (VII-1)

$$-\bar{x}\leqslant x_o\leqslant\bar{x},\ -\bar{y}\leqslant y_o\leqslant\bar{y},\ -\bar{x}'\leqslant x_o'\leqslant\bar{x}',\ -\bar{y}'\leqslant y_o'\leqslant\bar{y}',\ \text{and}\ -\bar{\Delta}\leqslant\Delta\leqslant\bar{\Delta}\ .$$

This model is used by the computer program to evaluate the maximum displacement due to aberrations.

Model #2 is the product of elliptical distributions in x-x' space and y-y' space with Δ taken as zero. This model is appropriate to a beam system bounded by rectangular apertures. We parameterize this distribution as

$$x_o=\bar{x}_o\zeta\cos\theta,\ x_o'=\bar{x}_o'\zeta\sin\theta,\ 0\leqslant\zeta\leqslant 1,\ 0\leqslant\theta<2\pi\ ,$$
$$y_o=\bar{y}_o\eta\cos\phi,\ y_o'=\bar{y}_o'\eta\sin\phi,\ 0\leqslant\eta\leqslant 1,\ \text{and}\ 0\leqslant\phi<2\pi. \qquad \text{(VII-2)}$$

Although helpful for comparing with model #1, this model is not used by the computer code.

Model #3 consists of a hyperellipsoid in x_o, x_o', y_o, and y_o' with Δ taken as zero. As mentioned in Chapter II, this model is appropriate to a beam limited by a circular aperture, which is usually the case when beam pipes of circular cross section are employed. The code uses this model to calculate the rms aberration displacements. We parametrize this distribution by

$$x_o=r\,\bar{x}_o\cos\phi\cos\theta,\quad x_o'=r\,\bar{x}_o'\cos\phi\sin\theta,$$
$$y_o=r\,\bar{y}_o\sin\phi\cos\psi,\quad y_o'=r\,\bar{y}_o'\sin\phi\sin\psi, \qquad \text{(VII-3)}$$
$$0\leqslant\phi<\pi/2,\ 0\leqslant\theta<2\pi,\ 0\leqslant\psi<2\pi,\ \text{and}\ 0\leqslant r\leqslant 1.$$

2. Normalized Aberration Coefficients

As each of these models involves the maximum values the parameters can attain (i.e., $\bar{x}_o$), we find it convenient to normalize the aberration coefficients by multiplying them by such powers of $\bar{x}_o$, $\bar{y}_o$, $\bar{x}_o'$, $\bar{y}_o'$, and $\bar{\Delta}$ as are required to scale to a space in which each parameter achieves a maximum value of 1.0 and a minimum value of -1.0. We denote the normalized coefficients by an underscore, for example, $\underline{C}^{111}=C^{111}\bar{x}_o^{\,3}$, $\underline{C}^{554}= C^{554}\bar{y}_o'\,\bar{\Delta}^2$, and $\underline{D}^{421}= D^{421}\bar{y}_o'\bar{y}_o\bar{x}_o$. With the coefficients in this form, we may immediately compare the relative effect of the various coefficients acting upon the beam described by this object-plane phase space distribution.

3. Symmetry Groups in Displacement Expansions

In the expansion of x in terms of object-plane parameters, we may separate the terms according to the reflection symmetries about various coordinate planes:

$$
\begin{aligned}
x^a = {} & x_o(C^{111}x_o^{\,2}+ C^{331}x_o'^{\,2} + C^{221}y_o^{\,2} + C^{441}y_o'^{\,2} + C^{551}\Delta^2) \\
& +x_o'(C^{432}y_oy_o') \\
& +x_o'(C^{311}x_o^{\,2} + C^{333}x_o'^{\,2} + C^{322}y_o^{\,2} + C^{443}y_o'^{\,2} + C^{553}\Delta^2) \qquad \text{(VII-4)} \\
& +x_o\ (C^{421}y_oy_o') \quad .
\end{aligned}
$$

The first line is antisymmetric under reflection through the plane $x_o=0$ while symmetric under reflection through any other plane containing two coordinate axes. The other three lines have similar properties. Notice that, with the exception of the dispersion terms, the first two lines contain only terms in spherical aberration and astigmatism. This separation, arising from the symmetry properties assumed in the five-dimensional object-plane space, appears in each of the later results of this section. In the expressions for maximum and mean aberration displacements, this separation into symmetry groups demonstrates that the distortion and coma terms contribute in exactly the same way as the spherical aberration and astigmatism terms. If the corresponding terms were equal (i.e., $\underset{\sim}{C}^{111} = \underset{\sim}{C}^{333}$, $\underset{\sim}{C}^{432} = \underset{\sim}{C}^{421}$, ...) then the distortion terms would contribute exactly the same amount as the spherical aberrations terms, and the astigmatism terms would contribute exactly the same amount as the coma terms toward the maximum and rms aberrations.

4. Maximum Aberration Displacement

Let us calculate the upper bound on the magnitude of the displacements due to the aberration terms. It is clear from the symmetry properties that for model #1 we must replace each parameter by its maximum value and take the sum of the absolute values of the four lines to obtain the maximum displacement, given by

$$
\begin{aligned}
|x^a| \leqslant\ & |\underset{\sim}{C}^{111} + \underset{\sim}{C}^{331} + \underset{\sim}{C}^{221} + \underset{\sim}{C}^{441} + \underset{\sim}{C}^{551}| + |\underset{\sim}{C}^{432}| \\
& + |\underset{\sim}{C}^{311} + \underset{\sim}{C}^{333} + \underset{\sim}{C}^{322} + \underset{\sim}{C}^{443} + \underset{\sim}{C}^{553}| + |\underset{\sim}{C}^{421}| \quad .
\end{aligned}
\tag{VII-5}
$$

This value is obviously larger than the maxima that would be appropriate either to model #2 or to model #3. Note that the symmetry separations have occurred as discussed above. The maximum displacement $|y^a|$ is calculated in exactly the same manner.

We obtain an upper limit on the beam width at the image by adding $|x^a|$ to the maximum obtained from the terms that are linear in x_o and x_o'; this limit in general is larger than the maximum displacement actually obtained in a typical beam.

Only a very small proportion of the trajectories will suffer aberration displacements nearly as large as $|x^a|$. The rms aberration displacement to be calculated next has been found to be an order of magnitude smaller than this maximum displacement in the examples mentioned above. The rms value is the more interesting figure in applications in which the quadrupole magnets are placed to form a point or line image on a scintillator or resolution slit.

5. Root-Mean-Square Aberration Displacement

The rms displacement is defined as the square root of the average of the squares of the displacements of a representative set of trajectories given by the following ratio of integrals taken over the object-plane phase space:

$$\langle x^a \rangle = \frac{\int \rho(\tau)\,(x^a)^2\,d\tau}{\int \rho(\tau)\,d\tau} . \tag{VII-6}$$

Here $\rho(\tau)d\tau$ is the number of trajectories originating in the volume element $d\tau$ at τ. The denominator is the total number of trajectories considered. We restrict $\rho(\tau)$ to have the same reflection symmetry as has been imposed upon the three models of the object-plane phase space, so that the expression for $\langle x^a \rangle$ separates into the four symmetry groups, each term being positive definite and containing only coefficients from a single symmetry group. This result follows because the cross-terms between terms in different symmetry groups must integrate to zero; every contribution is balanced by an equal contribution with opposite sign.

We now evaluate the rms displacement for model #3. The transformation Jacobian for this choice of parameters is

$$\frac{\partial(x_o, y_o, x_o', y_o')}{\partial(r, \emptyset, \Theta, \ \ )} = r^3\ \bar{x}\ \bar{x}'\ \bar{y}\ \bar{y}'\ \cos\emptyset\ \sin\emptyset. \qquad \text{(VII-7)}$$

If we assume the trajectory density function, ρ, to depend only upon the dimensionless variable r, then (VII-8)

$$\langle x^a\rangle^2 = \frac{\bar{x}_o\bar{x}_o'\ \bar{y}_o\bar{y}_o'\ \int_0^1 dr\ r^3\rho(r)\int_0^{\pi/2}d\emptyset\ \cos\emptyset\ \sin\emptyset\ \int_0^{2\pi}d\Theta\int_0^{2\pi}d\ \ x^a(r,\emptyset,\Theta)^2}{\bar{x}_o\bar{x}_o'\ \bar{y}_o\bar{y}_o'\ \int_0^1 dr\ r^3\rho(r)\int_0^{\pi/2}d\emptyset\ \cos\emptyset\ \sin\emptyset\ \int_0^{2\pi}d\Theta\int_0^{2\pi}d} .$$

Upon carrying out the indicated operations, we find

$$\begin{aligned} x^a = \Bigg\{\frac{F}{480}\Big[&(3\underline{C}^{333}+\underline{C}^{311}+\underline{C}^{443}+\underline{C}^{322})^2+6(\underline{C}^{333})^2+2(\underline{C}^{311})^2+2(\underline{C}^{443})^2 \\ &+2(\underline{C}^{322})^2+(\underline{C}^{432})^2 \\ &+(3\underline{C}^{111}+\underline{C}^{331}+\underline{C}^{221}+\underline{C}^{441})+6(\underline{C}^{111})+2(\underline{C}^{331})+2(\underline{C}^{221}) \\ &+2(\underline{C}^{441})^2+(\underline{C}^{421})^2\Big]\Bigg\}^{\frac{1}{2}} . \end{aligned} \qquad \text{(VII-9)}$$

Here $F = \frac{5}{2}\,\frac{\int_0^1 \rho(r)\ r^9\ dr}{\int_0^1 \rho(r)\ r^5\ dr}$; if $\rho(r) \equiv$ constant the F=1, as has been assumed in all the examples quoted below.

Note that the four symmetry groups separate as discussed above. The additional symmetry between x_o, y_o and x_o', y_o' is expected, since the expansions for x^a and y^a are similar and the coefficients are labeled in a symmetric way. This symmetry may be described by stating that the expressions for the maximum aberration displacement and mean aberration displacement are invariant under the permutation of indices: 12345 $\longrightarrow$ 34125. What this means is that the spherical aberration and astigmatism contributions are as important as the distortion and coma contributions, respectively, in determining the characteristic size of the aberration displacements provided the normalized coefficients are comparable in magnitude.

The expression for $\langle x^a \rangle$ reveals the relative importance of the coefficients. For instance, the coefficients $\underline{C}^{333}$ and $\underline{C}^{111}$ are the most important contributions; these terms correspond to the contribution from $x_o'^3$ and x_o^3, respectively.

For a numerical comparison of the maximum and rms aberration displacements, refer to example #1 in Appendix III. This system consists of a symmetrical quadrupole triplet of 8 in. diameter aperture, with elements having lengths 16 in., 32 in., and 16 in., respectively. The separation of elements and the excitations are adjusted to produce a point image of a point source, with source and image symmetrically located at 275 in. from the triplet. The maximum slopes of trajectories that can pass through an 8 in. bore beam tube are $\overline{x}_o' = 14.3$ mr, $\overline{y}_o' = 9.30$ mr. Let us assume a source 1.50 in. in diameter and a relative momentum spread $\overline{\Delta} = 2.5 \times 10^{-4}$. We find that the maximum displacements due to aberrations are 0.94 in. in the x plane and 1.35 in. in the y plane; these figures do not include the second-order chromatic aberration terms. The rms aberration displacements, when model #3 is used, are $\langle x^a \rangle = 0.053$ in., $\langle y^a \rangle = 0.073$ in.. If we next assume a point source with $\overline{x}_o'$, $\overline{y}_o'$, and $\overline{\Delta}$ unchanged, we find the maximum displacements are 0.54 in. and 0.77 in. in the x and y planes, respectively, while the rms displacements are 0.050 in. and 0.068 in.. We discuss these examples at length at the end of this chapter.

We can also calculate the rms aberration displacements for the other two models. For model #1, we find

$$\begin{aligned}\langle x^a\rangle^2 \approx \frac{1}{30}\Big\{&(2\underline{C}^{333}+\underline{C}^{311}+\underline{C}^{443}+\underline{C}^{322}+\underline{C}^{553})^2+2(\underline{C}^{311})^2+2(\underline{C}^{443})^2\\ &+2(\underline{C}^{322})^2+2(\underline{C}^{553})^2+2(\underline{C}^{432})^2\\ &+(2\underline{C}^{111}+\underline{C}^{331}+\underline{C}^{221}+\underline{C}^{441}+\underline{C}^{551})^2+2(\underline{C}^{331})^2+2(\underline{C}^{221})^2\\ &+2(\underline{C}^{441})^2+2(\underline{C}^{551})^2+2(\underline{C}^{421})^2\Big\} \quad .\end{aligned} \tag{VII-10}$$

For model #2 we find

$$\begin{aligned}\langle x^a\rangle^2 = \frac{1}{192}\Big\{&(3\underline{C}^{333}+\underline{C}^{311}+2\underline{C}^{443}+2\underline{C}^{322})^2+2(\underline{C}^{443}-\underline{C}^{322})^2\\ &+6(\underline{C}^{333})^2+2(\underline{C}^{311})^2+2(\underline{C}^{432})^2\\ &+(3\underline{C}^{111}+\underline{C}^{331}+2\underline{C}^{221}+2\underline{C}^{441})^2+2(\underline{C}^{221}-\underline{C}^{441})^2\\ &+6(\underline{C}^{111})^2+2(\underline{C}^{331})^2+2(\underline{C}^{421})^2\Big\} \quad .\end{aligned} \tag{VII-11}$$

By inspection of these two expressions, we can determine the relative importance of different coefficients for the different models. Continuing with the point source in the above example, we find $\langle x^a\rangle = 0.161$ in. with model #1 and $\langle x^a\rangle = 0.102$ in. with model #2.

B. Region of Least Confusion

In classical optics for rotationally symmetric systems, the best image, known as the "circle of least confusion", is not generally found at the paraxial image plane but at another value of z. Quadrupole beam systems, lacking the rotational symmetry, do not generally form a "circle" of least confusion; however, there is a region of least confusion near the paraxial image where the beam width is a minimum.

For a paraxial point image, the best focus in the x-z plane is usually found at one value of z, whereas that in the y-z plane is found at another value. For a line image, we are interested only in the region of least confusion in the plane orthogonal to the image line. We wish to determine the width of the region of least confusion as well as its location. If our purpose is to use the beam system to provide a momentum or mass resolution, we place the resolving slit at the region of least confusion. The smaller this region, the better resolution we attain.

1. The Beam Envelope Near an Image --Single-Parameter Trajectory Distribution

If z is measured from the image plane, the equation for the family of trajectories issuing from a point source and restricted to single values of y_o' and Δ is

$$\Phi_{x_o'}(x,z)=x-cx_o'^3-dx_o'-hzx_o'/m + O(4) = 0. \qquad \text{(VII-12)}$$

As x_o' varies the family of trajectories is swept out. In Eq. (VII-12), m is the magnification, d and h depend upon y_o' and Δ, and c, d, and r represent spherical and chromatic aberration contributions.

In the absence of aberrations, all the trajectories would lie within the envelope formed by the two extreme trajectories $\Phi_{-\bar{x}_o'} = 0$ and $\Phi_{\bar{x}_o'} = 0$. The aberration terms alter the envelope in the region near the image plane; in this region the envelope is defined by the characteristic points of the family of trajectories.

The characteristic point is defined by the intersection of the trajectories $\Phi_{x'}=0$ and $\Phi_{x'+dx'}=0$, or equivalently by the equations $\Phi_{x'}=0$ and $\frac{\partial}{\partial x'}\Phi_{x'}=0$. (VII-13)

The caustic is tangent to the extreme trajectories at some value of z which we will call z_1 and tangent to the z axis at z_2. Between z_1 and z_2 the caustic exists, and at every value of z is tangent to that trajectory for which $|x|$ is a maximum.

We eliminate x_o' from Equations (VII-13) to obtain the equation of the caustic, $x^2=-(4/27c)(\,d + hz/m)^3$. (VII-14)

At this point it is convenient to introduce the dimensionless parameters $\phi \equiv x/c\bar{x}_o'^3 h$ and $\psi \equiv v(w+\zeta)$, where $\zeta=z/mc$, (VII-15)
$w=d/rc + 3\bar{x}_o'^2/4h$, and $v=h/\bar{x}_o'^2>0$. This choice of parameters yields relatively simple expressions and at the same time avoids dividing the results into a number of separate cases according to the sign of m and the sign of c.

In terms of these parameters, the equation for the caustic takes the form $\phi^2=\frac{1}{16}(\,1-\frac{4}{3}\psi)^3$; (VII-16)

The total envelope consists of three parts and is referred to as the "three-part envelope." The equation for the extreme trajectories ($x_o' = \pm\,\bar{x}_o'$) is $\phi^2=(\frac{1}{4}+\psi)^2$. (VII-17)

The envelope is drawn in dimensionless coordinates in Fig. 4. The part of the envelope defined by (VII-16) is between $\psi=-9/4$, where the caustic is tangent to the extreme trajectories, and $=0$, where it intersects the extreme trajectories. The caustic lies within the extreme trajectories between $\psi=0$ and $\psi=3/4$;

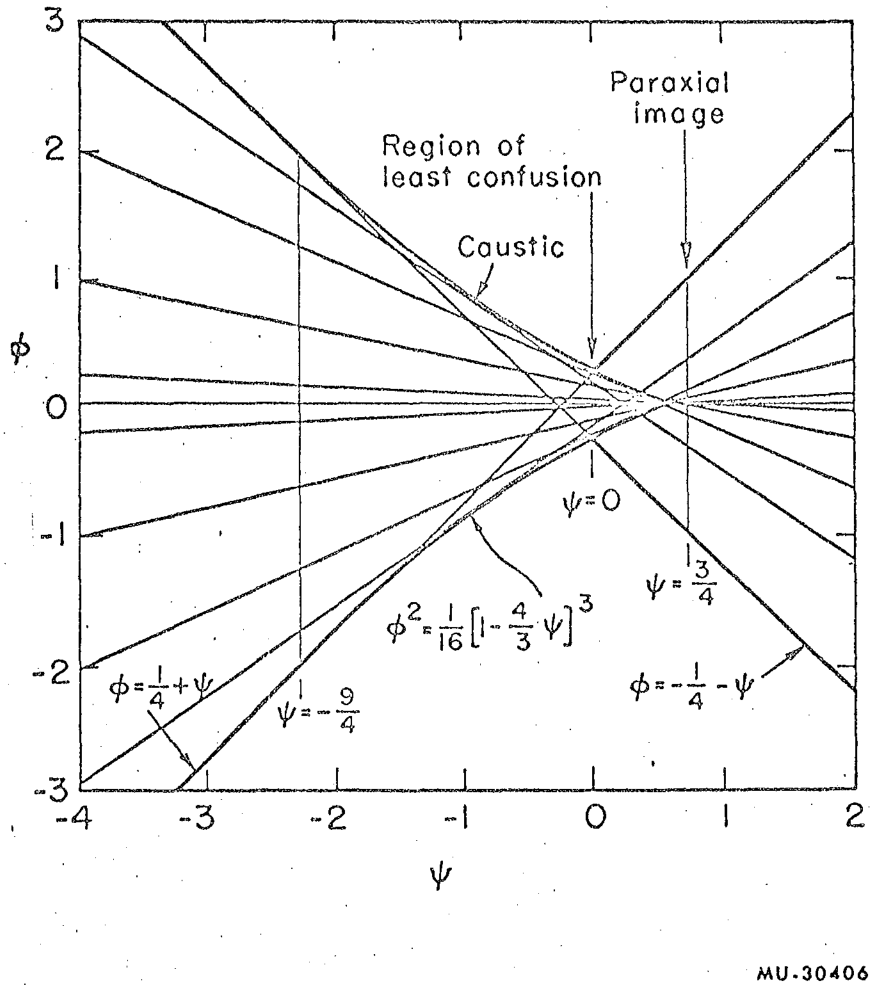

Fig. 4. The three-part envelope in dimensionless coordinates.

it is tangent ot the z axis at $\psi=3/4$, the paraxial image for this choice of h, d, and c. The minimum beam width, the <u>region of least confusion</u>, occurs at $\psi=0$, where the caustic intersects the extreme trajectories.

Between $(\psi,\phi) = (-9/4, 2)$ and $(\psi,\phi) = (0, 1/4)$ the envelope is defined by Eq. (VII-16); elsewhere, it is defined by the extreme trajectories (VII-17).

The half width of the region of least confusion at $\psi=0$ is $\phi = 1/4$; this is one-fourth of the half width at the paraxial focus ($\psi = 3/4$). The half width of the beam at the other end of the caustic ($\psi = -2$) is twice the width at the paraxial focus. Since $x = c\phi\bar{x}_o'^3$, it is clear that the beam widths at these points depend only upon the coefficient c and the maximum initial slope $\bar{x}_o'$; these widths do not depend upon the coefficients d, h, and m. However, the location of the paraxial focus does depend upon d and r, and, in addition, upon c. If $m \cdot c > 0$, the caustic will be on the upstream side of the paraxial focus, and vice versa.

We will illustrate the three-part envelope by giving numerical results for the double-focusing triplet referred to previously. Consider a point source on the axis with no momentum spread, and assume that the trajectories are constrained by a slit to lie entirely in the x-z plane. For this example $c\bar{x}_o'^3 = \underline{C}^{333}$ $= -0.162$ in. The half width at the paraxial image is 0.162 in., while the half width at the region of least confusion is 0.041 in. Here $m= -1$, $h=1$, and $d=0$; hence $w=0.000154$ and $z= (55434)\zeta$.

The location of the region of best focus ($\psi=0$) is $z=(55434)(-0.000154)= -8.53$ in. These figures may be verified by referring to cathode-ray tube (CRT) plot #42 in Appendix III.

2. The General Beam Envelope Near the Image For a Point Source

We now consider a more general situation in which we have spreads in y_o' and Δ as well as in x_o'. For each choice of y_o' and Δ, we obtain a unique value for both d and h; the envelope obtained by varying x_o' differs from the three-part envelope discussed above only in scale and in origin of the abscissa (ζ axis). Our goal is to obain the envelope that contains the entire beam in the region near the image plane for the range of parameters $-\bar{x}_o'\leqslant x_o'\leqslant\bar{x}_o'$, $-\bar{y}_o'\leqslant y_o'\leqslant\bar{y}_o'$, $-\bar{\Delta}\leqslant\Delta\leqslant\bar{\Delta}$.

As y_o' and Δ are varied within the stated bounds, the parameters w and v vary within the bounds $-\underline{w}\leqslant w\leqslant\bar{w}$ and $0<\underline{v}\leqslant v\leqslant\bar{v}$. The parameter w determines the point where the caustic is tangent to the z axis, and v is a scaling factor. For any value of w, all the trajectories for $-\bar{x}_o'\leqslant x_o'\leqslant\bar{x}_o'$ and $\underline{v}\leqslant v\leqslant\bar{v}$ lie within the three-part envelope:

$$\begin{aligned}\phi^2&=\left[1-\tfrac{4}{3}\bar{v}\,(w+\zeta)\right]^3 \text{ for } -9/4\leqslant\bar{v}(w+\zeta)\leqslant 0,\\ \phi^2&=\left[\tfrac{1}{4}+\bar{v}(w+\zeta)\right]^2 \text{ elsewhere.}\end{aligned}\qquad\text{(VII-18)}$$

(As v and w are not necessarily independent, we may have $\underline{v}<\underline{\underline{v}}(w_1)\leqslant v(w_1)\leqslant\bar{\bar{v}}(w_1)<\bar{v}$ for a particular w_1).

A variation in w now merely translates this envelope along the ζ axis. The total envelope, containing the entire beam, consists of a portion of the three-part envelope with $w=\bar{w}$ for $\zeta\geqslant\zeta_o$ and a portion of the three-part envelope for $w=\underline{w}$ for $\zeta\leqslant\zeta_o$, where ζ_o is the intersection of the envelope for $w=\underline{w}$ with the envelope for $w=\tilde{w}$. (VII-19)

We now define ψ as $\psi=\tilde{v}(\underset{\sim}{w}+\zeta)$ and introduce $\Delta\psi\equiv\tilde{v}(\tilde{w}-\underset{\sim}{w})>0$. The quantity $\Delta\psi$ determines whether the total envelope consists solely of two pairs of extreme trajectories or whether it contains a cautic region. For $\Delta\psi\geq 4$, the total envelope consists of two pieces, both of which are pairs of trajectories; this is the case when the dispersive effects completely overshadow the spherical aberration effects. The envelope is given by

$$\begin{aligned} \phi^2 &= (\tfrac{1}{4}+\psi)^2 \text{ for } \psi\leq\psi_0, \\ \phi^2 &= (\tfrac{1}{4}+\Delta\psi+\psi)^2 \text{ for } \psi\geq\psi_0, \end{aligned} \tag{VII-20}$$

where ψ_0 is the location of the region of least confusion;

$$\psi_0 = -\frac{1}{4}-\frac{1}{2}\Delta\psi < -\frac{9}{4} . \tag{VII-21}$$

If $\Delta\psi<4$ (but $\Delta\psi\neq 0$), the total envelope consists of three parts, the additional part being a caustic because of the spherical aberration terms

$$\begin{aligned} \phi^2 &= (\tfrac{1}{4}+\psi) && \text{for } \psi\leq -\tfrac{9}{4}, \\ \phi^2 &= \tfrac{1}{16}(1-\tfrac{4}{3}\psi)^3 && \text{for } -\tfrac{9}{4}\leq\psi\leq\psi_0, \\ \phi^2 &= (\tfrac{1}{4}+\psi+\Delta\psi)^2 && \text{for } \psi\geq\psi_0 . \end{aligned} \tag{VII-22}$$

Here ψ_0, the location of the region of least confusion, is given by

$$(1-\tfrac{4}{3}\psi_0)^3 = (1+\tfrac{1}{4}\psi_0+\tfrac{1}{4}\Delta\psi)^2 ; \tag{VII-23}$$

this equation has the approximate solution

$$= -2/3\ \Delta\psi + 14/384\ (\Delta\psi)^2 - (\Delta\psi)^3/384 . \tag{VII-24}$$

In Fig. 5, we plot both the minimum half-width (at the region of least confusion) and (the location of the region of least

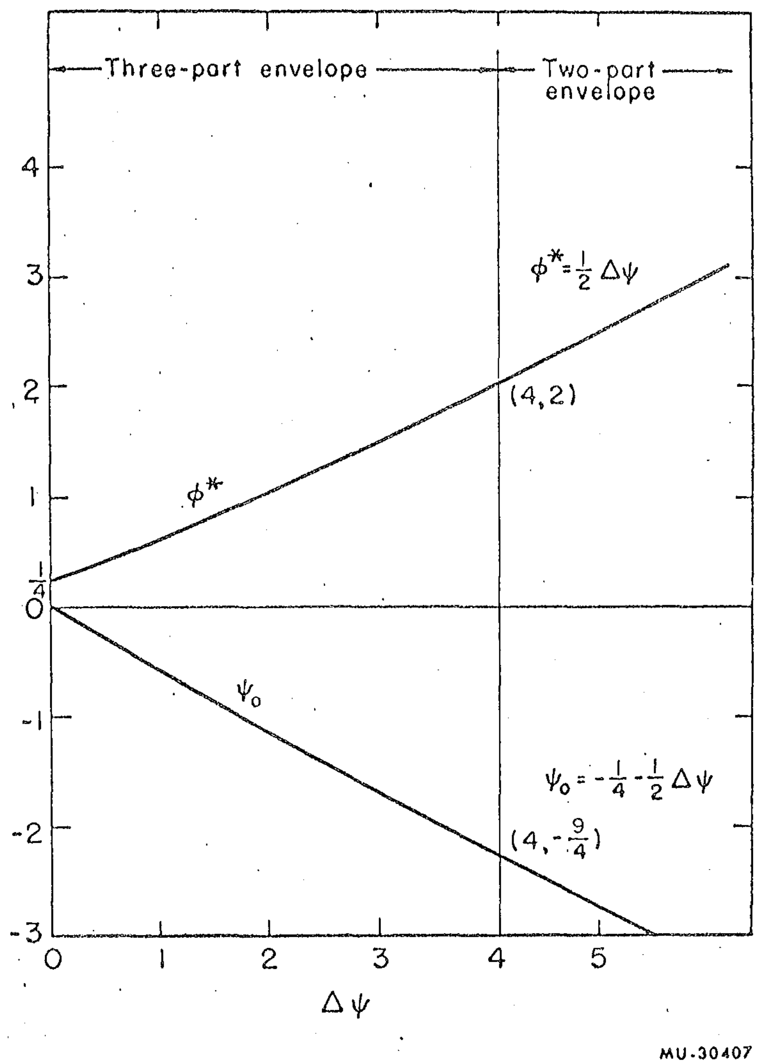

Fig. 5. The determination of the location and size of the best image.

confusion) as functions of $\Delta\psi$. Figure 6 shows the composite envelope for $\Delta\psi = 5/8$.

For any value of $\Delta\psi$, the minimum half-width, ϕ^*, is given by $\phi^* = \frac{1}{4} + \psi_0 + \Delta\psi$. (VII-25)

We have now determined the location of the region of least confusion and the beam width at that point for a beam issuing from a source on the axis with a spread in momentum. If the purpose of the beam system is to produce a line image at a slit for momentum or mass resolution, we have determined where the slit should be placed and the resolution achieved.

The power-series expansion of x near the image for trajectories issuing from a point source [Eq. (V-52)] is

$$x = C^{333}x_0'^3 + C^{443}x_0'y_0'^2 + C^{53}\Delta x_0' + C^{553}\Delta^2 x_0' + C^{663}x_0'$$
$$+ z \cdot x_0'/m + z \cdot D^{53}\Delta x_0' + \cdots, \qquad \text{(VII-26)}$$

with z again measured from the paraxial image plane. In terms of these coefficients, we find $c = C^{333}$, whence $x = \phi\,\underline{C}^{333}$, $h = 1 + m\Delta D^{53}$,

$$d = C^{443}y_0' + C^{53}\Delta + C^{553}\Delta^2 + C^{663}, \text{ and} \qquad \text{(VII-27)}$$

$$\Delta\psi = \left|\frac{\underline{C}^{443}}{\underline{C}^{333}}\right| + 2\left|\frac{\underline{C}^{53}}{\underline{C}^{333}}\right| + \cdots.$$ The location of the region of least confusion is given by

$$z_0 = \frac{m}{x_0'}\,\underline{C}^{333}\left\{\psi_0 - \frac{3}{4} - \frac{\underline{C}^{663}}{\underline{C}^{333}} + \left|\frac{\underline{C}^{53}}{\underline{C}^{333}}\right| + s\cdot\frac{\underline{C}^{443}}{\underline{C}^{333}} + \cdots\right\} \text{ for } \Delta < 4, \qquad \text{(VII-28)}$$

and by $z_0 = \frac{m}{x_0'}\,\underline{C}^{333}\left\{-1 - \frac{\underline{C}^{663}}{\underline{C}^{333}} + (s - \frac{1}{2})\frac{\underline{C}^{443}}{\underline{C}^{333}}\right\}$, for $\Delta \geq 4$.

Here $s=1$ if $\underline{C}^{443}\underline{C}^{333} < 0$; $s=0$ if $\underline{C}^{443}\underline{C}^{333} > 0$.

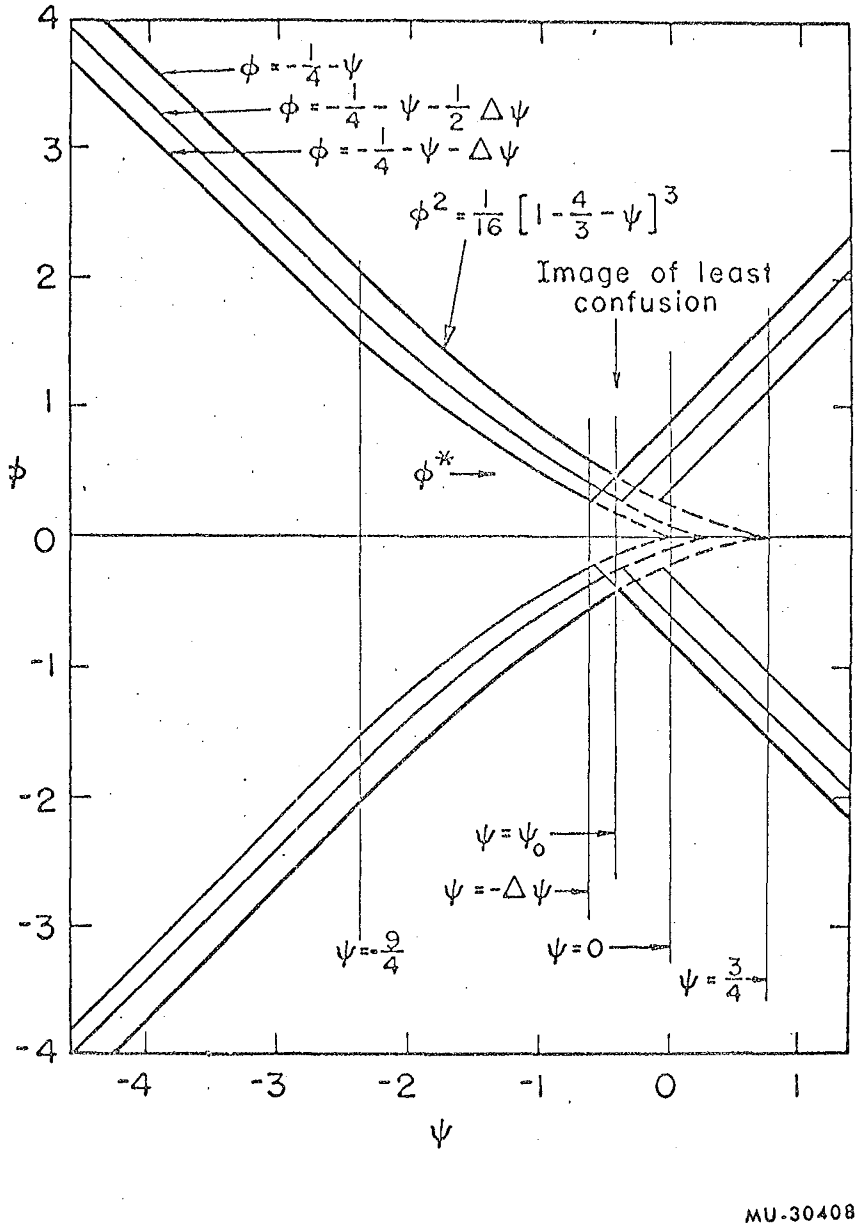

Fig. 6. The composite envelope.

3. Example of the Region of Least Confusion

For an example, let us return to the double-focusing triplet referred to previously; we now consider a spread in y_o', x_o' and Δ. We have $\bar{x}_o'=0.0143$, $\bar{y}_o'=0.0093$ (determined by the 8 in. bore), and $\Delta=0.00025$. The normalized coefficients calculated by the digital computer are $\underline{C}^{333}=-0.1621$, $\underline{C}^{443}=-0.3768$, $\underline{C}^{53}=0.000301$, and $\underline{C}^{553}= 10^{-8}$. We calculate $\Delta\psi = 2.36$, which shows that the total envelope consists of three pieces. From Fig. 5, we determine $\phi^* = 1.2$ and $\psi_o= -1.4$. The minimum half width is then $1.2\ \underline{C}^{333}=0.19$ in.; the region of least confusion is located at $z = -24$ in.. The family of trajectories corresponding to the values of $\bar{x}_o'$, $\bar{y}_o'$, and $\bar{\Delta}$ given above is shown on CRT plot #34 in Appendix III.

Provided the momentum spread is less than $\pm$ 1.13% in this example, there will be a three-part envelope, the middle piece being a caustic of spherical aberration type. A larger momentum spread will result in the entire caustic region being buried within the extreme trajectories.

As another illustration, we give numerical results for the doublet system described above which provides a line image 275 in. from the doublet of an incoming parallel beam. The two quadrupole magnets are 16 in. long with 8 in. diameter apertures; they are separated by 9.25 in. To study the envelope in this example we replace x_o' by x_o, y_o' by y_o, C^{333} by C^{111}, etc., because the trajectories forming the envelope all have zero initial slope but vary in initial displacement. We consider a monoenergetic beam with $\bar{x}_o=\bar{y}_o=3.0$ in. We find $\underline{C}^{111}= -0.017$ in.

and $\underline{C}^{221}$ = -0.072 in.; the beam half width at the paraxial line image is the sum of the absolute values of these two numbers, or 0.089 in.. $\Delta\Psi$, their ratio is 4.25; thus the envelope consists of the extreme trajectories only. We find $\phi^* = \Delta\Psi/2 = 2.12$; hence the minimum beam width is 0.0361 in.; $\Psi_o = -2.38$. The quantity corresponding to m may be determined from the expression for x near the line image: $x = C^{111} x_o^{\ 3} + C^{221} x_o y_o^{\ 2} - z\, x_o/f + \cdots$, where f is the focal length of the lens. We replace m by -f in the expression for the location of the region of least confusion, obtaining z= -6.52 in.. This agrees with the graph, CRT plot #51, in Appendix III. For comparison, the calculated rms displacement at the paraxial image is 0.00755 in.

For more general object-plane distributions, calculation of the width and location of the region of least confusion becomes more complicated, generally involving all the coefficients of aberration. The computer plots representative sets of trajectories to scale, thus allowing easy determination of both the width and the location of the image of least confusion from the resulting graph. All the preceding formulas, which have been presented for the x-z plane, hold for the y-z plane when the appropriate substitutions are made.

Having discussed the projection of the envelope on the y=0 plane, and (by symmetry) the projection of the envelope on the x=0 plane, let us now turn our attention to the projection of the envelope on planes near the image that are orthogonal to the optic axis.

C. The Aberration Figure

In classic optics for rotationally symmetric systems, a point source on the optic axis is not imaged to a point in an uncorrected system, because of spherical aberration. Rather, the set of trajectories that form a given angle with the optic axis at the source are imaged on a circle whose radius depends upon the initial slope and also upon the point of observation. The image of a point source produced by a beam system lacking rotational symmetry is generally more complicated. The image produced by a quadrupole magnet system retains the two-plane reflection symmetry characteristic of the magnets. In this section, we analyze the shape of the figure traced out by the portion of the beam from an axial point source which passes through an elliptical aperture. The parametric equations for the group of trajectories that pass through this aperture are $x_o = y_o = 0$, $x_o' = \bar{x}_o' \cos\Theta$, $y_o' = \bar{y}_o' \sin\Theta$, and $\Delta = 0$. (VII-29)

At the paraxial image plane the linear terms vanish, yielding, for the aberration figure traced out by this group of trajectories, the equations

$$x = \underline{C}^{333} \cos^3\Theta + \underline{C}^{443} \cos\Theta \sin^2\Theta,$$
$$y = \underline{C}^{444} \sin^3\Theta + \underline{C}^{433} \sin\Theta \cos^2\Theta, \qquad \text{(VII-30)}$$

with $0 \leqslant \Theta < 2\pi$.

The scale of this figure is proportional to the cube of the scale of the elliptical aperture; all the trajectories that would pass through the interior of the aperture region, if the interior aperture were removed, would also pass through the interior of the figure in the paraxial image plane define by the foregoing parametric equations.

We may write these equations in the form

$$x = \underline{C}^{333}\cos\Theta + (\underline{C}^{443} - \underline{C}^{333})\cos\Theta\sin^2\Theta,$$
$$y = \underline{C}^{444}\sin\Theta + (\underline{C}^{433} - \underline{C}^{444})\sin\Theta\cos^2\Theta. \qquad \text{(VII-31)}$$

Since the linear terms, the fringing-field terms, and the chromatic aberration terms are proportional to x_o' in the x-z plane and y_o' in the y-z plane, we see that we may include them without increasing the complexity of the family of figures to be studied. However, if these terms are added or if the plane of observation is not the paraxial image plane, the scale of the figure will not be directly proportional to the cube of the size of the elliptical aperture. To treat the general case of the figure traced out by the set of trajectories passing through the elliptical aperture on some plane orthogonal to the optic axis and near the image plane, we must consider the equations

$$x = A\cos\Theta + B\cos\Theta\sin^2\Theta,$$
$$y = C\sin\Theta + D\sin\Theta\cos^2\Theta. \qquad \text{(VII-32)}$$

These equations contain four parameters which determine the shape and size of the aberration figure.

Two of these parameters may be effectively removed by scaling the x and y axes; the qualitative shape of the figure is not changed by this scaling. We set $x = (AD+BC)X/2D$ (VII-33) and $y = (AD+BC)Y/2B$; then

$$X = (1+\varepsilon)\cos\Theta + \alpha\sin^2\Theta\cos\Theta,$$
$$Y = (1-\varepsilon)\sin\Theta + \alpha\cos^2\Theta\sin\Theta, \qquad \text{(VII-34)}$$

where $$\varepsilon = \frac{AD-BC}{AD+BC} \quad\text{and}\quad \alpha = \frac{2BD}{AD+BC}. \qquad \text{(VII-35)}$$

The shape of the aberration figure depends upon the two parameters ε and α. Changing the sign of ε is equivalent to interchanging x and y; hence we need only consider positive ε to classify all possible aberration figures.

Let $X = r \cos \phi$ and $Y = r \sin \phi$; (VII-36)

then we find

$$r^2 = \varepsilon^2 + (\alpha/2+1)^2 + 2\varepsilon \cos 2\Theta - \alpha(1+\alpha/4) \cos^2 2\Theta, \tag{VII-37}$$

$$r\frac{dr}{d\Theta} = \frac{1}{2}\left[(\alpha+4)\alpha \cos 2\Theta - 4\varepsilon\right] \sin 2\Theta \quad , \tag{VII-38}$$

and

$$\frac{d\phi}{d\Theta} = -1 + (\alpha+2)(1+\varepsilon \cos 2\Theta)/r^2 \quad , \tag{VII-39}$$

providing $\tan \phi$ is defined. By examining these equations and the equations for X and Y, we can determine the desired characteristics of the aberration figure as function of the parameters α and ε.

1. Illustrative Aberration Figures

We first note some distinctive figures that are obtained for certain integral values of the two parameters; several figures are reproduced in Fig. 8.

With $\varepsilon=0$, we obtain several highly symmetric figures. A circle is obtained with $\alpha=0$, corresponding to the pure spherical aberration characteristic of systems with rotational symmetry. A circle is also obtained with $\alpha=-4$; however, this circle has the interesting property that ϕ is swept through three revolutions when Θ advances through one revolution. With $\alpha=-2$ the figure is a rosette with the tips of the leaves lying on the coordinate axes. As $|\alpha| \to \infty$, a rosette is obtained which is rotated 45° relative to the rosette obtained with $\alpha = -2$.

As the plane of observation is moved further from the image plane, α is diminished, becoming small in comparison with unity; the resulting aberration figure approaches an ellipse with semiaxes of lengths $1+\varepsilon$ and $1-\varepsilon$ respectively. As α is increased in comparison to $1+\varepsilon$ and $1-\varepsilon$, the complexity of the figure increases, with as many as four loops or leaves developing in the figure. We now turn our attention to classifying figure types.

2. Classification of Figure Types

As the parameters ε and α are varied, the aberration figure varies assuming shapes intermediate to the characteristic special cases described above. Figure 7 shows the division of the ε, α space into 22 regions, each of which yields a characteristic aberration figure. The significance of the curves that divide these regions is discussed below.

The number of loops in the figure is determined by the number of roots in the equations $X(\Theta)=0$ and $Y(\Theta)=0$. There are no loops if the only roots to these equations are $\Theta=0$, $\pi/2$, π, $3\pi/2$, $\cdots$, in which case the aberration figure may be considered a distorted ellipse with a maximum extent in the X direction of $1+\varepsilon$ and in the Y direction of $1-\varepsilon$. For $1+\varepsilon+\alpha<0$, X also vanishes at $\sin^2\Theta = (1+\varepsilon)/(-\alpha)$; here $Y = (2+\alpha)\left[(1+\varepsilon)/(-\alpha)\right]^{1/2}$. $Y=0$ has additional roots provided either $-\alpha>1-\varepsilon>0$ or $-\alpha<1-\varepsilon<0$. X and Y will both vanish at the same Θ provided $\alpha=-2$ and $0<\varepsilon<1$, yielding a generalized rosette. These regions have been separated in Fig. 7 by the appropriate straight lines.

Another distinctive feature of the aberration figures is whether they are concave or convex at the X axis and at the Y axis. For $2\alpha>\varepsilon+1$, the figure is concave at the X axis; it is

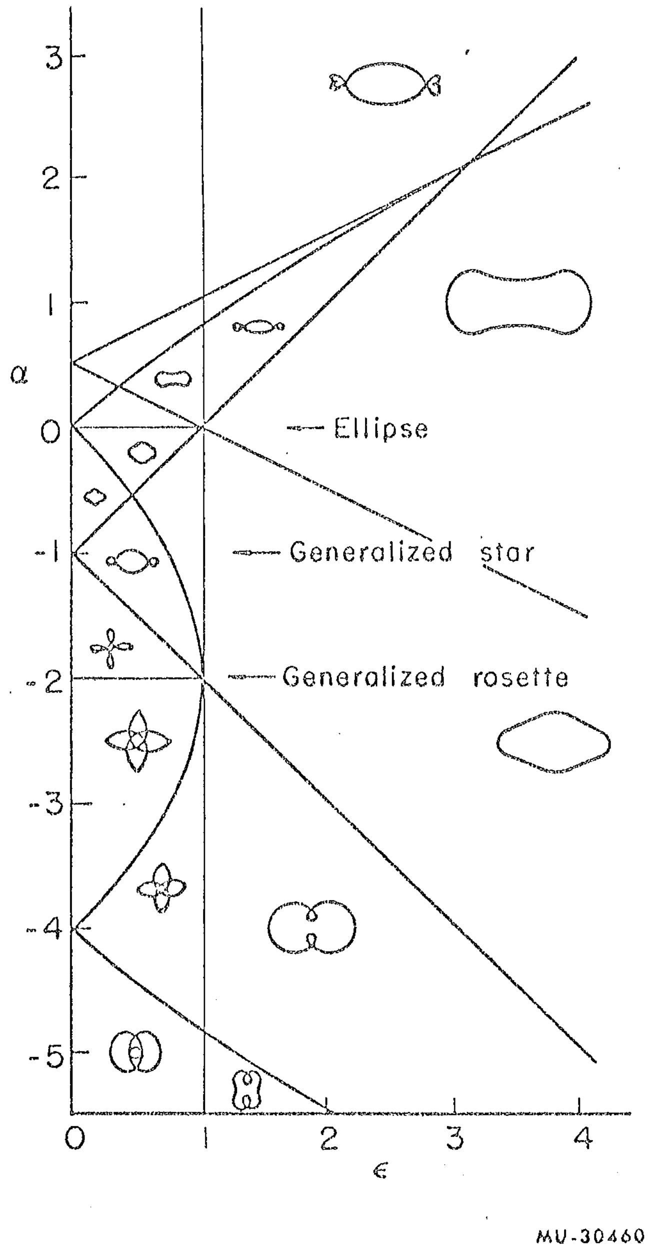

Fig. 7. Division of ε, α space into regions yielding different aberration figures.

at the Y axis only for $2\alpha > 1-\varepsilon$.

A rosette-type figure is characterized by the fact that $r^2(\Theta)$ has four maxima and four minima in the interval $0 \leqslant \Theta < 2\pi$. This is characteristic of all figures in the region for which $|4\varepsilon| \leqslant |(\alpha+2)^2-4|$. The curves separating the ε, α space into regions with four maxima and minima and region with two maxima and minima are the two parabolas shown on Fig. 7.

Finally, for $-4 \leqslant \alpha \leqslant 0$, $r^2 \leqslant (1+\varepsilon)^2$ everywhere on the figure, and $r^2 \geqslant (1-\varepsilon)^2$ for $\alpha \geqslant 0$ or $\alpha \leqslant -4$.

With the above criterea, the figure corresponding to any pair α, ε can easily be drawn. Figure 8 is an array of figures for six different values of ε (that is, ε=0, 0.5, 0.75, 1.0, 2.0, and 3.0) and 12 different values of α (that is, α= -6, -5, -4, -3, -2, -1, -0.25, 0, 0.25, 0.375, 1.0, and 2.0); the figure is in three parts, 8a, 8b, and 8c.

3. Incoming Parallel Beam to Point Image

In the discussion above, we have been referring to the image of a point source on the axis, so that $x_o=0$, $y_o=0$, while x_o' and y_o' were varied. An incoming parallel beam, passing through the same elliptical aperture and then focused to a point (for paraxial trajectories), produces exactly the same types of aberration figures on planes orthogonal to the optic axis and close to the image plane. For a parallel beam, we set $x_o'=y_o'=0$, $x_o = \bar{x}_o \cos\Theta$, and $y_o = \bar{y}_o \sin\Theta$, and scale as before. The coefficients involved are those of x_o and y_o ($\underline{C}^{111}$, $\underline{C}^{221}$, etc.); the same separation into figure types applies.

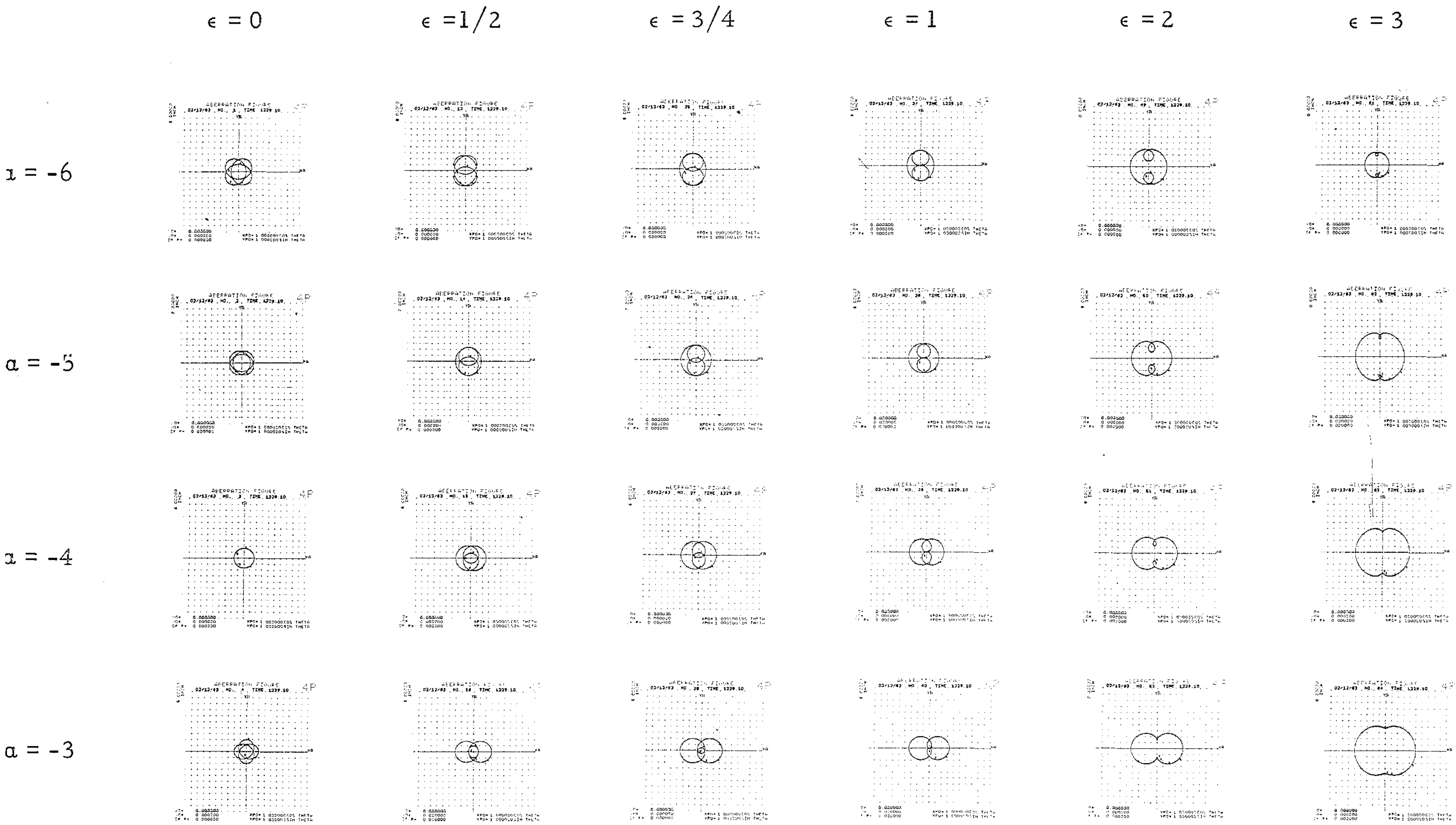

MUB-1892

Fig. 8a. Illustrative aberration figures.

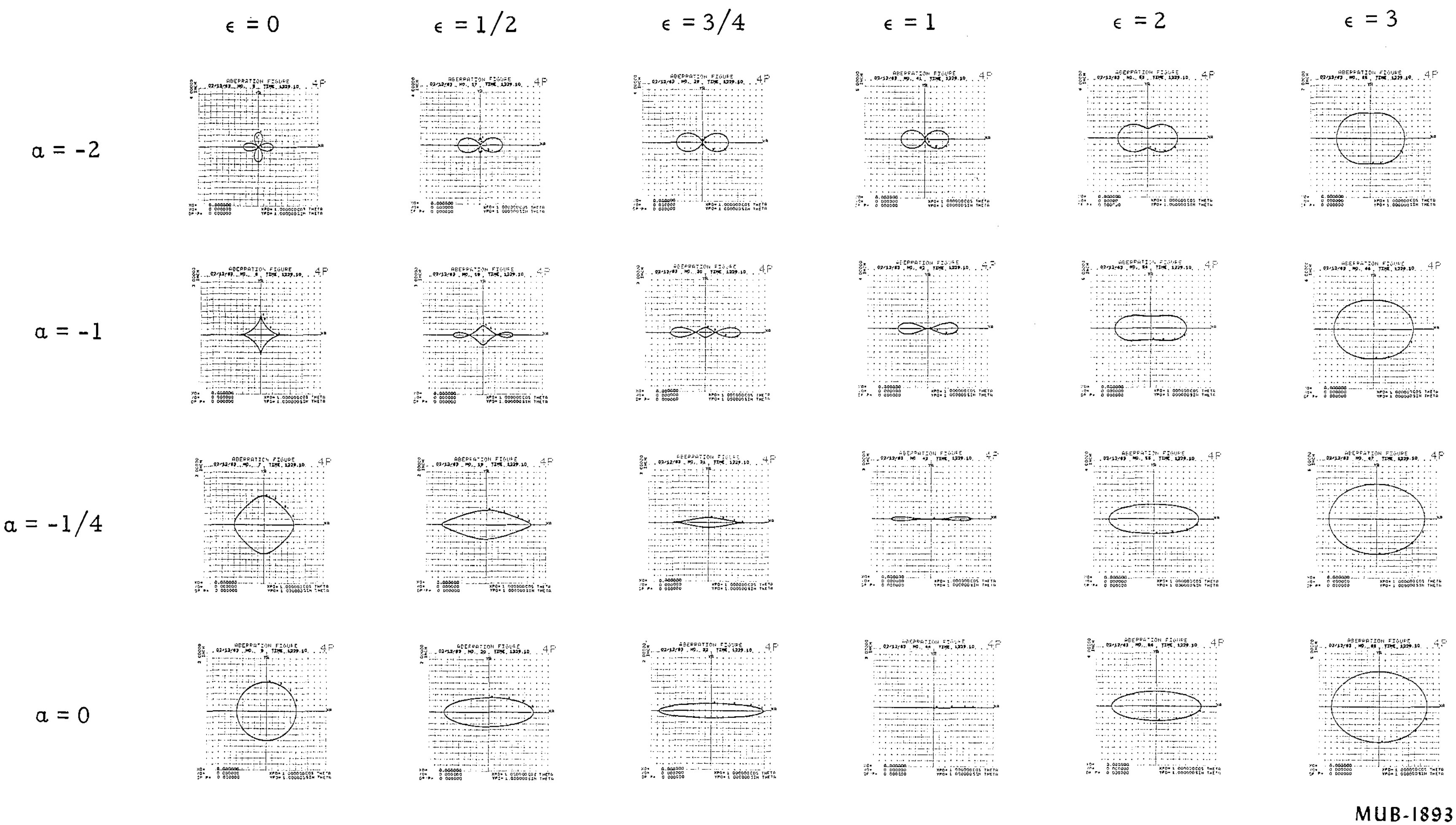

Fig. 8b. Illustrative aberration figures.

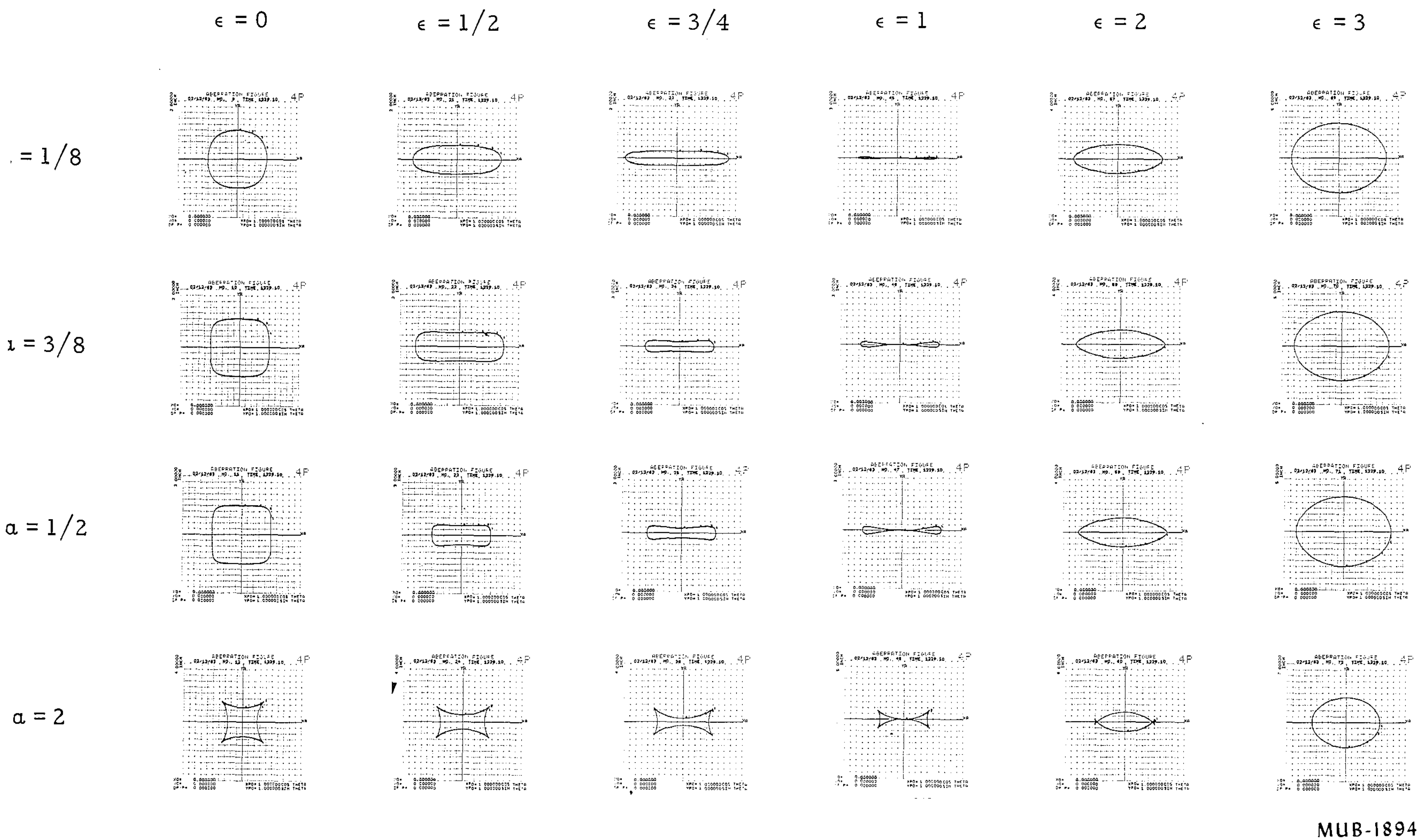

Fig. 8c. Illustrative aberration figures.

4. Remarks on the General Figure Types

In the above pages, we have discussed the considerations that lead to a great many distinctive figure types. Although some quantitative statements were made about the size of the figure, complete expressions for the maximum extent in the x, y, and radial directions would have to be divided into so many cases that this type of description would have little usefulness. As an alternative, the computer program was equipped to plot the aberration figure to scale, thus immediately showing quantitatively every characteristic of the figure.

D. Concluding Remarks on the Two Examples

In the previous parts of this chapter, we have examined the projections of the beam envelope in the neighborhood of an image. We have also developed expressions for the maximum and rms aberration displacements, which are useful for comparing aberrations of different beam systems. In this section we compare the aberrations due to misalignments, etc., with the inherent aberrations. We also discuss an improvement in the point-source to point-image beam system which reduces the aberrations.

1. Tolerances

The measure of tolerances required is that the effects due to misalignments, etc. should be smaller than the maximum aberration displacement. We use example #1, the double-focusing quadrupole triplet with unit magnification in both planes to illustrate the use of our results. In this example the maximum aberration displacements are 0.94 in. in the x direction and 1.35

in. in the y direction.

The most important tolerance coefficients (V-54) for the middle magnet are

$$T_1^0 = 5.61,\quad T_2^0 = -10.3,\quad T_1^2 = -14.7,\quad T_1^4 = -4500. = T_2^3 \text{ and}$$

$T_2^1 = 13.1$. If δx and δy are the displacements of the middle magnet and ω its rotation, the displacements introduced are

$$\Delta x = 5.61\,\delta x - 14.7\,\omega y_o - 4500\,\omega y_o' + \cdots \quad , \qquad \text{(VII-40)}$$

$$\Delta y = -10.3\,\delta y + 13.1\,\omega x_o + 4500\,\omega x_o' + \cdots \quad .$$

Thus, a displacement of 0.17 in. in the x direction would displace the image by an amount equal to the maximum aberration displacement in the x direction; a displacement of 0.14 in. in the y direction would displace the image by an amount equal to the maximum aberration displacement in that direction.

A rotation of 1.3° in the second magnet will smear the image in both directions by an amount equivalent to the maximum aberration displacements. This damages image quality more than the simple displacement caused by the shifting of the magnet.

The smearing in the image due to the higher harmonic components present in this magnet is

$$\Delta x = 5.6 \sum_{n=3}^{\infty} f_n \rho^{n-1} \sin\left[(n-1)\theta + \delta_n\right] \qquad \text{(VII-41)}$$

and $$\Delta y = 10.3 \sum_{n=3}^{\infty} f_n \rho^{n-1} \cos\left[(n-1)\theta + \delta_n\right] \quad ,$$

where $a = 4$ in. . If these effects are to be less than the maximum aberration displacements then we must have

$\sum_{n=3}^{\infty} f_n < 0.035$. That is to say, the total contribution

to the magnetic field at full radius due to the harmonics must be less than 3.5%.

It is important to note that all the above figures have been based on a comparison with the maximum aberration displacements. A comparison with the rms displacements would yield tolerances that are smaller, by an order of magnitude.

The corresponding tolerances for the first and third magnets are slightly larger than the tolerances stated above for the middle magnet. For example, $T_1^0 = -3.80$ for both the first and the third magnets.

Since none of these tolerances should prove difficult to meet, it is clear that the inherent aberrations limit beam system performance in the example considered.

2. The Reduction of Aberrations

In III.D.4 it was noted that the introduction of octupole magnetic field components frequently can be used to advantage to reduce offensive aberrations. Although we have tried to do so with the computer code in the examples described above, the results were poor. Improvement of the linear programming techniques used in the code could probably enable it to prescribe octupole field components in a beneficial way.

The triplet magnet used for the calculations in example #1 may be replaced by two doublets; this is equivalent to splitting the center magnet of the triplet into two magnets. The effect of separating the two doublets up to 150 inches while maintaining the same location of the source and image points was studied with the code. For each separation the quadrupoles were readjusted so as to retain the double-focusing properties with unit magnification in both planes. A separation of 50 in. reduces the distances to the source and image from 275 in. to 250 in., thus increasing the maximum slopes of the trajectories that pass through the magnets without encountering a wall along the way. With equal solid angles, the aberrations for the system with a 50 in. separation are 25% to 30 % less than the aberrations for the system with no separation.

Even if the aperture of these magnets remains filled, the aberrations are reduced as the separation is increased. The tolerances in displacing a magnet are relaxed by about 4%; since the same figure applies to the higher harmonic influence, those tolerances are reduced by the same amount. The tolerances on rotating a magnet are relaxed 13%. The maximum aberration displacements are reduced about 5% though some coefficients are reduced by as much as 30 % (C^{333}, C^{444}, and C^{111}, for example). The maximum aberrations are reduced by small amounts because the maximum slopes permitted are larger than in the case with no separation between the doublets. Other than the increased power requirements, the only cost in this separation is that of replacing one 32-in. magnet by two-16 in. magnets. In this example the excitation of the center quadrupole magnets is increased from 1.79 kg/in. to 1.86 kg/in., and that of the other quadrupoles is increased from 1.95 kg/in. to 2.05 kg/in..

The effects of changing the separation of the quadrupole magnets in a triplet were also studied with the code. The quadrupole magnets in example #1 are separated by an effective length of 8.5 in.. If this separation is increased to 20 in., retaining the image and object drift lengths at 275 in., the aberrations are reduced by 30% to 35%; the power requirements are also reduced, since the gradients are 20% smaller. If the separation is eliminated, the aberrations are 60% to 70% larger than those described in example #1; the required gradients are increased by 34%. The solid angle admitted by the quadrupole magnets was assumed to remain unchanged in these illustrations.

VIII. IBM 7090 QUADRUPOLE ABERRATION PROGRAM

To calculate aberrations and other properties of beam systems, a computer program has been written for the IBM 7090 digital computer.

A. Program Scope

Known as "4P", this program calculates first-order optical properties, including dispersion, of an arbitrary beam system consisting of no more than thirty of the following types of beam elements:

(a) drift space;

(b) quadrupole magnet;

(c) octupole magnet;

(d) bending magnets with bends in either plane, with arbitrary angles of entry and exit, and with an arbitrary field exponent;

(e) pseudo-elements, which provide a drift space in one plane but not in the other, providing a handy device for specifying properties that occur at a different location in the x-z plane than in the y-z plane;

(f) solenoid magnets;

(g) any other type of element whose optical properties are described solely by fixed 3x3 transfer matrices in each plane.

In addition, the program calculates all the aberrations, through third-order in the previously defined small parameters, of a beam system consisting of quadrupole and octupole magnets and drift spaces. The tolerance requirements on placements and construction of all constituent quadrupole magnets are also calculated. Convenient and easily interpreted output is provided by a flexible complement of cathode-ray-tube plots.

The program is equipped to execute very general variations of all designated parameters of the beam system in order to obtain, as closely as possible, desired first order optical properties while restricting each varied parameter to previously determined bounds. In addition, the program will seek to minimize objectionable aberrations while keeping the first-order properties unchanged. Many other features of the code allow the widest latitude in its application while retaining simplicity in its use.

Control of the flow through the program is specified by a sequence of "CALL cards" that are put in a mnemonic format similar to mnemonic computer instructions. Input and output options are mainly controlled through a series of internal switches that are set by a single card and that may be independently changed at any time.

B. Basic Computer Required

The present version of the program is designed to operate under the FORTRAN-II monitor on a 7090 computer equipped with seven index-registers, a cathode-ray-tube (CRT), and a direct data clock on channel D. The code is approximately one-half FAP coded and one-half FORTRAN coded, with FAP coding on most of the highly repetitive calculations and on the supervisor routines.

C. Required Input Data

The input data needed to calculate the first-order optical properties of a beam system consist of the appropriate parameters of length and field for each constituent beam element:

length, gradient for quadrupoles;

length, field, field exponent, orientation angles for bending magnets;

length, field for solenoid magnets;

length for drift spaces and octupole magnets.

Elements described solely by their transfer matrices require the input of those matrices.

A beam system consisting solely of quadrupole magnets and drift spaces may be completely described by giving the field gradient as a function of distance along the optic axis. Given these data and a minimum of information about magnet locations, the code will calculate effective magnet and drift-space lengths, effective field gradients for the magnets, and the shape coefficients required for the calculation of aberrations. An additional feature provides for the construction of the field-gradient function, given the location and length of each quadrupole magnet and the "half width" characteristic of the fringing field of each magnet

A subsidiary feature of the code provides for direct integration of the differential equations for several trajectories by using the field gradient function, $\phi(z)$.

If it is desired to alter the parameters to effect a desired optimization, then the following additional data are required:

(a) list of the parameters that may be varied including designation of parameters to be varied together;

(b) minimum and maximum constraints upon each parameter to be varied;

(c) list of conditions to be satisfied, the desired properties.

D. Output Produced by the Program

1. Field Data

When the beam system parameters are derived from a gradient dunction, either given or calculated by the code, the code plots graphs showing the gradient function and showing the separation, for each magnet, into a step function and a difference function.

2. Linear Properties

The primary output describing the linear properties consists of a full description of each element in the beam system and the 3x3 transfer matrices in each plane. If desired, transfer matrices to intermediate points may be provided.

Beam widths may be calculated and listed as well as the location and size of the virtual waists seen by each element in the system. In addition, the code may be directed to plot the beam profile in each plane for the entire system and also to plot the phase ellipses, in each plane, between each constituent element.

3. Optimization of Linear Properties

When asked to adjust certain parameters to achieve specified first-order properties, the code provides the usual data yielded by linear programming techniques. These data include initial and final errors in meeting the specified properties, the variations made in the parameters, the dependence of the error upon the constraints imposed, and the errors in meeting the constraints.

4. Aberrations

Additional data needed to calculate the aberrations of a system including only quadrupole and octupole magnets and drift-spaces consist of the field-shape coefficients for the quadrupole magnets and the third derivative of the magnetic field for magnets having octupole field components.

The primary output for the aberration calculations consists of a list of the coefficients describing the tolerances of each magnet with respect to displacements, rotations, and undesired harmonics of the magnetic field, followed by a list of the coefficients in the expansions of x, y, x', and y' in terms of x_o, y_o, x_o', y_o', and Δ grouped by type of aberration. These data are followed by the normalized aberration coefficients appropriate to the given bounds on the object-plane parameters. The maximum displacements in x and y due to the aberrations, assuming a rectangular object space, are calculated as are the rms displacements, which assume a hyperellipsoid object-plane distribution.

If desired, the code will plot the aberration figure which is the image of a point source on the axis.

A five-dimensional raster of coordinates (x_o, y_o, x_o', y_o', Δ) may be specified by giving upper and lower bounds and increments in each parameter. The code will then calculate the linear and aberration terms in x, y, x', and y' for each trajectory whose object-plane coordinates are given by one of the points in the five-dimensional raster. Data may be plotted in addition to being listed. If they are plotted, one may specify any or all of the three projections of the trajectories upon the coordinate planes. With the scales given upon the plots, the location and sizes of the "images of least confusion" may be quickly determined. The plots also show whether a small or large proportion of the trajectories is adversely affected by the system's aberrations. Frequently the virtual sources are distinctively shown upon the plots. As all of these data are highly dependent upon the region of object-plane phase space occupied, provisions are included for changing this region and observing the effects of this change.

With the exception of the plots, all the other data are calculated very rapidly. The code initiates a beam system, adjusts it to provide the specified first-order properties, and then calculates all the first-order properties and the aberration properties in a fraction of a minute. Plotting is considerably slower, taking between 2 seconds and a half minute, depending upon the complexity of the plot.

APPENDIX I. EQUATIONS FOR ABERRATION COEFFICIENTS

A complete list of the expressions that yield the coefficients of aberration follows. The symbolic notation used is that introduced in Chapter V, and is here redefined for convenience. The following integral types are referred to:

$$(mn) = \int_0^z \phi(\zeta)\, x_m(\zeta)\, x_n(\zeta) d\zeta \ , \quad \text{for example}$$

$$(22) = \int_0^z \phi\, x_2^{\,2}\, d\zeta = \int_0^z \phi\, y_e^{\,2}\, d\zeta \ ,$$

$$(mnpq) = \begin{cases} \displaystyle\int_0^z \phi^2(\zeta) x_m(\zeta) x_n(\zeta) x_p(\zeta) x_q(\zeta) d\zeta & \text{if} \quad m \leqslant 4,\ n \leqslant 4,\ p \leqslant 4, \\ & \text{and} \quad q \leqslant 4 \\ \displaystyle\int_0^z \phi(\zeta) x_m(\zeta) x_n(\zeta) x_p(\zeta) x_q(\zeta) d\zeta & \text{if any} \quad m,n,p,q > 4, \end{cases}$$

$$(mnpq) = \int_0^z \psi(\zeta)\, x_m(\zeta)\, x_n(\zeta)\, x_p(\zeta)\, x_q(\zeta) d\zeta \ ,$$

$$(mn|pq) = \int_0^z d\zeta\, x_m(\zeta)\, x_n(\zeta) \phi(\zeta) \int_0^\zeta d\xi\, x_p(\xi)\, x_n(\xi) \phi(\xi) \ .$$

The sums taken over the fringing fields are denoted by

$$Smn = \sum_{i \atop \text{(all fringe fields)}} c_i \phi_{si}\, x_m(z_i) x_n(z_i) \quad \text{for example}$$

$$S42 = \sum_i c_i \phi_{si}\, y_o(z_i) y_e(z_i) \ ,$$

where

$$\chi_1(z) = x_e(z), \quad \chi_3(z) = x_o(z), \quad \chi_5(z) = x_e'(z), \quad \chi_7(z) = x_o'(z),$$

$$\chi_2(z) = y_e(z), \quad \chi_4(z) = y_o(z), \quad \chi_6(z) = y_e'(z), \quad \chi_8(z) = y_o'(z).$$

We have

$$x_c(z) + x^a(z) = \sum_{1 \le k < j < i \le 6} C^{ijk}(z) \; \psi_i \; \psi_j \; \psi_k \; ,$$

where

$$\psi_1 = x(0), \quad \psi_2 = y(0), \quad \psi_3 = x'(0), \quad \psi_4 = y'(0), \quad \psi_5 = \frac{\Delta p}{p}, \quad \psi_6 \equiv \psi_0 \equiv 1 \; .$$

The tolerance coefficients are defined by:

$$x^t = \frac{\mu}{\emptyset} T_1^{\,o} + \frac{\delta\emptyset}{\emptyset} T_1^{\,1} \psi_1 + \frac{\lambda}{\emptyset} T_1^{\,2} \psi_2 + \frac{\delta\emptyset}{\emptyset} T_1^{\,3} \psi_3 + \frac{\lambda}{\emptyset} T_1^{\,4} \psi_4 \; ,$$

and

$$y^t = \frac{\nu}{\emptyset} T_2^{\,o} + \frac{\lambda}{\emptyset} T_2^{\,1} \psi_1 + \frac{\delta\emptyset}{\emptyset} T_2^{\,2} \psi_2 + \frac{\lambda}{\emptyset} T_2^{\,3} \psi_3 + \frac{\delta\emptyset}{\emptyset} T_2^{\,4} \psi_4 \; .$$

The equations defining the coefficients are

$$C^{444} = \frac{1}{3} \chi_2(4444) - \frac{1}{3} \chi_4(4442) + \frac{1}{2} \chi_2(8844) - \frac{1}{2} \chi_4(8644)$$

$$- \chi_2(8844) + \chi_4(8842) + \frac{1}{3} \chi_2\langle 4444\rangle - \frac{1}{3} \chi_4\langle 4442\rangle \; ,$$

$$c^{333} = \frac{1}{3} x_1(3333) - \frac{1}{3} x_3(3331) - \frac{1}{2} x_1(7733) + \frac{1}{2} x_3(7533) + x_1(7733)$$

$$- x_3(7731) + \frac{1}{3} x_1\langle 3333\rangle - \frac{1}{3} x_3\langle 3331\rangle ,$$

$$c^{222} = -\frac{1}{3} x_4(2222) + \frac{1}{3} x_2(42222) - \frac{1}{2} x_4(6622) + \frac{1}{2} x_2(8622) + x_4(6622)$$

$$- x_2(6642) - \frac{1}{3} x_4\langle 2222\rangle + \frac{1}{3} x_2\langle 4222\rangle ,$$

$$c^{111} = -\frac{1}{3} x_3(1111) + \frac{1}{3} x_1(3111) + \frac{1}{2} x_3(5511) - \frac{1}{2} x_1(7511) - x_3(5511)$$

$$+ x_1(5531) - \frac{1}{3} x_3\langle 1111\rangle + \frac{1}{3} x_1\langle 3111\rangle ,$$

$$c^{422} = x_2(4422) - x_4(4222) + x_2(8642) - x_4(6642) + \frac{1}{2} x_2(8822) - \frac{1}{2} x_4(8622)$$

$$- 2x_2(8642) + 2x_4(8622) - x_2(6644) + x_4(6642) + 1\cdot x_2\langle 4422\rangle$$

$$- x_4\langle 4222\rangle ,$$

$$c^{311} = x_1(3311) - x_3(3111) - x_1(7531) + x_3(5531) - \frac{1}{2} x_1(7711) + \frac{1}{2} x_3(7511)$$

$$+ 2x_1(7531) - 2x_3(7511) + x_1(5533) - x_3(5531) + x_1\langle 3311\rangle$$

$$- x_3\langle 3111\rangle ,$$

$$c^{442} = -x_4(4422) + x_2(4442) - \frac{1}{2}x_4(6644) + \frac{1}{2}x_2(8644) - x_4(8642)$$

$$+ x_2(8842) + 2x_4(8642) - 2x_2(8644) + x_4(8822) - x_2(8842)$$

$$- x_4\langle 4422\rangle + x_2\langle 4442\rangle \,,$$

$$c^{331} = -x_3(3311) + x_1(3331) + \frac{1}{2}x_3(5533) - \frac{1}{2}x_1(7533) + x_3(7531)$$

$$- x_1(7731) - 2x_3(7531) + 2x_1(7533) - x_3(7711) + x_1(7731)$$

$$- x_3\langle 3311\rangle + x_1\langle 3331\rangle \,,$$

$$c^{433} = x_2(4433) - x_4(4332) + \frac{1}{2}x_2(8833) - \frac{1}{2}x_4(8633) - x_2(7744)$$

$$+ x_4(7742) + x_2(8743) - x_4(8732) - x_2\langle 4433\rangle + x_4\langle 4332\rangle \,,$$

$$c^{443} = x_1(4433) - x_3(4431) - \frac{1}{2}x_1(7744) + \frac{1}{2}x_3(7544) + x_1(8833)$$

$$- x_3(8831) - x_1(8743) + x_3(8741) - x_1\langle 4433\rangle + x_3\langle 4431\rangle \,,$$

$$c^{211} = -x_4(2211) + x_2(4211) - \frac{1}{2}x_4(6611) + \frac{1}{2}x_2(8611) + x_4(5522)$$

$$- x_2(5542) - x_4(6521) + x_2(6541) + x_4\langle 2211\rangle - x_2\langle 4211\rangle \,,$$

$$C^{221} = -X_3(2211) + X_1(3221) + \frac{1}{2}X_3(5522) - \frac{1}{2}X_1(7522) - X_3(6611)$$
$$+ X_1(6631) + X_3(6521) - X_1(6532) + X_3\langle 2211\rangle - X_1\langle 3221\rangle ,$$

$$C^{411} = X_2(4411) - X_4(4211) + \frac{1}{2}X_2(8811) - \frac{1}{2}X_4(8611) - X_2(5544)$$
$$+ X_4(5542) + X_2(8541) - X_4(8521) - X_2\langle 4411\rangle + X_4\langle 4211\rangle ,$$

$$C^{322} = X_1(3322) - X_3(3221) - \frac{1}{2}X_1(7722) + \frac{1}{2}X_3(7522) + X_1(6633)$$
$$- X_3(6631) - X_1(7632) + X_3(7621) - X_1\langle 3322\rangle + X_3\langle 3221\rangle ,$$

$$C^{332} = -X_4(3322) + X_2(4332) - \frac{1}{2}X_4(6633) + \frac{1}{2}X_2(8633) + X_4(7722)$$
$$- X_2(7742) - X_4(7632) + X_2(7643) + X_4\langle 3322\rangle - X_2\langle 4332\rangle ,$$

$$C^{441} = -X_3(4411) + X_1(4431) + \frac{1}{2}X_3(5544) - \frac{1}{2}X_1(7544) - X_3(8811)$$
$$+ X_1(8831) + X_3(8541) - X_1(8543) + X_3\langle 4411\rangle - X_1\langle 4431\rangle ,$$

$$C^{321} = 2X_2(4321) - 2X_4(3221) + X_2(8631) - X_4(6631) - 2X_2(7542)$$
$$+ 2X_4(7522) + X_2(6543) - X_4(6532) + X_2(7641) - X_4(7621)$$
$$- 2X_2\langle 4321\rangle + 2X_4\langle 3221\rangle ,$$

$$c^{421} = 2X_1(4321) - 2X_3(4211) - X_1(7542) + X_3(5542) + 2X_1(8631)$$

$$- 2X_3(8611) - X_1(6543) + X_3(6541) - X_1(8532) + X_3(8521)$$

$$- 2X_1\langle 4321\rangle + 2X_3\langle 4211\rangle ,$$

$$c^{431} = 2X_4(4321) - 2X_2(4431) - X_4(8631) + X_2(8831) + 2X_4(7542)$$

$$- 2X_2(7544) - X_4(8532) + X_2(8543) - X_4(8721) + X_2(8741)$$

$$+ 2X_4\langle 4321\rangle - 2X_2\langle 4431\rangle ,$$

$$c^{432} = -2X_3(4321) + 2X_1(4332) + X_3(7542) - X_1(7742) - 2X_3(8631)$$

$$+ 2X_1(8633) + X_3(7641) - X_1(7643) + X_3(8721) - X_1(8732)$$

$$+ 2X_3\langle 4321\rangle - 2X_1\langle 4332\rangle ,$$

$$c^{52} = - X_4(22) + X_2(42) ,$$

$$c^{51} = X_3(11) - X_1(31) ,$$

$$c^{54} = X_2(44) - X_4(42) ,$$

$$c^{53} = - X_1(33) + X_3(31) ,$$

$$C^{552} = -X_4(22|42) + X_2(42|42) + X_4(42|22) - X_2(44|22) ,$$

$$C^{551} = -X_3(11|31) + X_1(31|31) + X_3(31|11) - X_1(33|11) ,$$

$$C^{554} = -X_2(44|42) + X_4(42|42) + X_2(42|44) - X_4(22|44) ,$$

$$C^{553} = -X_1(33|31) + X_3(31|31) + X_1(31|33) - X_3(11|33) ,$$

$$C^{661} = -X_1 S71 - X_1 S53 + 2X_3 S51 ,$$

$$C^{662} = X_2 S82 + X_2 S64 - 2X_4 S62 ,$$

$$C^{663} = X_3 S53 + X_3 S71 - 2X_1 S73 ,$$

and

$$C^{664} = -X_4 S64 - X_4 S82 + 2X_2 S84 .$$

The coefficients in the expansions for x'^a and y'^a are obtained from the corresponding coefficients in the expansions for x^a and y^a by replacing each X_k appearing in the expression by its derivative, X_{k+4}. For example:

$$D^{444} = \frac{1}{3} X_6(4444) - \frac{1}{3} X_8(4442) + \frac{1}{2} X_6(8844) - \frac{1}{2} X_8(8644) - X_6(8844)$$

$$+ X_8(8842) + \frac{1}{3} X_6\langle 4444\rangle - \frac{1}{3} X_8\langle 4442\rangle .$$

Tolerance Coefficients

The tolerance coefficients for the kth quadrupole magnet are given by the following expressions with the integrals taken over the kth quadrupole, having no contributions elsewhere.

The tolerance coefficients are given by

$$T_1^{\,0} = X_1 \int_k \phi_k X_3 - X_3 \int_k \phi_k X_1 \,, \qquad T_2^{\,0} = -X_2 \int_k \phi_k X_4 + X_4 \int_k \phi_k X_2 \,,$$

$$T_1^{\,1} = X_1 \int_k \phi_k X_3 X_1 - X_3 \int_k \phi_k X_1 X_1 \,, \qquad T_2^{\,1} = 2X_2 \int_k \phi_k X_4 X_1 - 2X_4 \int_k \phi_k X_2 X_1 \,,$$

$$T_1^{\,2} = -2X_1 \int_k \phi_k X_3 X_2 + 2X_3 \int_k \phi_k X_2 X_1 \,, \qquad T_2^{\,2} = -X_2 \int_k \phi_k X_4 X_2 + X_4 \int_k \phi_k X_2 X_2 \,,$$

$$T_1^{\,3} = X_1 \int_k \phi_k X_3 X_3 - X_3 \int_k \phi_k X_3 X_1 \,, \qquad T_2^{\,3} = 2X_2 \int_k \phi_k X_4 X_3 - 2X_4 \int_k \phi_k X_3 X_2 \,,$$

$$T_1^{\,4} = -2X_1 \int_k \phi_k X_4 X_3 + 2X_3 \int_k \phi_k X_4 X_1 \,, \qquad T_2^{\,4} = -X_2 \int_k \phi_k X_4 X_4 + X_4 \int_k \phi_k X_4 X_2 \,.$$

APPENDIX II

OPERATING INSTRUCTIONS FOR QUADRUPOLE ABERRATION CODE

The scope of the code as described in Chapter VIII consists of two primary functions: (a) calculation of the linear and aberration properties of a beam system, and (b) adjustment of specified parameters of the beam system to provide desired optical properties. These calculations are executed by a large number of subroutines which operate under the direction of the program supervisor; it in turn is governed by a sequence of cards directing the order of calculations to be performed.

A. Supervisor

1. Call Cards

The cards that control the sequence of calculations are called "CALL cards". Each CALL card contains four fields, the first of which contains a mnemonic word of from one to six letters. This word is matched against a table in the supervisor known as the "call list". For each name on the list, a location in the program is given; this location may be the entry point of some subroutine or the start of some calculational sequence within the supervisor. The name given on the call card must be left adjusted in the field and must contain no blanks. Upon recognition of the name on the card, the supervisor transfers control to the location corresponding to that name. If the name is not contained in the call list, that fact is noted and the supervisor reads the next card and again examines the call list.

The second and third fields of the call card each contain an integer whose function depends upon the particular call card involved. The last field is a print control field which is described, under subroutine

TRAP, in section D.4.b. The names that may be used on CALL cards are listed at the end of the next section.

2. Repeating groups of CALL cards

A sequence of CALL cards may be repeated a specified number of times by means of a subroutine in the supervisor called into action by the CALL card, REPEAT. The card, REPEAT m n, is followed by m CALL cards. The m CALL cards are stored and each is executed in sequence, the sequence being repeated a total of n times. For example, the sequence of cards

```
REPEAT0275
DESIGN
SYSTEM
```

would cause the execution of 75 iterations of the linear programming problem set up by subroutine DESIGN, and the resultant beam system is listed after each iteration under control of the SYSTEM card. Further description of the CALL cards DESIGN and SYSTEM is deferred until later.

Following the CALL cards under the control of a REPEAT card, all data cards to be read by the CALL cards must appear in the order in which they will be called. Many CALL cards may not be included in the domain of a REPEAT card -- for instance, a second REPEAT card or a CALL card that uses data in the second and third fields (these fields are not read for CALL cards in the domain of a REPEAT). Those cards which can be used in the domain of REPEAT are so noted in the CALL list.

Prior to the execution of the first CALL card in the domain of a REPEAT card, the following line is written; "REPEAT THE NEXT m CARDS n TIMES."

In some instances the REPEAT sequence can be terminated before the normal exit. For example, if the error in meeting specifications in the optimization routines is sufficiently small at the end of a given iteration, the optimization routine exists to CALL, which executes the next call card after the REPEAT sequence.

When the execution of one CALL card has been completed, the code reads the next CALL card and initiate execution of this card. This is also true of REPEAT cards.

3. The CALL list

The following names comprise the CALL List; they are listed in three groups. The first group consists of those names which may be used on CALL cards in the domain of a REPEAT card as well as on CALL cards not in the domain of a REPEAT card. The second group are those names which should not be used on CALL cards in the domain of a REPEAT card but which may be used on other CALL cards. The third group consists of names which may not be used on any CALL card but which may be used as reference names on ALTER, PEEK, and TEST cards.

a. Names that may be used on CALL cards in the domain of a REPEAT card

RKY3--integrates orbits through system using exact equations,

BELL--creates gradient function for beam system using bell shape,

INCHI--clears all aberration integrals,

SHAPE--calculates quadrupole magnet parameters from gradient function,

SUM1--forms aberration coefficients without octupole terms,

SUM2--adds octupole term contributions to aberration coefficients,

STATE--outputs aberration calculations, written and plotted,

EXIT--terminates calculations and returns control to monitor,

FIRST--calculates first-order displacements and slopes of a trajectory,

THIRD--calculates higher-order terms in displacements and slopes, FOCUS--adjusts two parameters to meet two conditions,

DESIGN--sets up and executes linear programming problem to adjust many parameters to meet many specifications,

PAUSE--executes halt and proceed, with clock disconnected, for operator action,

NORM--calculates normalized coefficients and mean aberrations,

SENSE--changes program switches controlling various options,

TIME--writes line showing time remaining for job,

EJECT--starts new page with heading, shows time remaining,

TITLE--enters new heading text,

ALTER--modifies stored instructions or constants,

READ--enters parameters of beam system,

TRACE--calculates first-order properties of beam system,

SOLVE--claculates aberrations for system and lists them,

SYSTEM--writes system parameters and calculates first-order properties,

DUMPC--dumps COMMON region and exits to monitor

DUMPAL--dumps COMMON region and program region, exits to monitor,

PREID--plots CRT identification preceding plotting, sets IF(10) to 0,

POSTID--plots CRT identification completing film, sets IF(10) to 1,

PUNCH--punches beam-system parameter cards,

PEEK--sets up and executes snapshot dump,

VARY--changes the parameters of a single beam-system element,

ASSIGN--assigns dummy variables to system parameters for optimization,

ERRSET--sets specifications to be met by optimization routines,

INITER--calculates initial errors in meeting desired specifications,

REFINE--adjusts parameters to minimize aberrations,

NEWP--enters new design momentum,

SAVE--writes current beam-system parameters on select tape, NOTE--reads text and prints on-line for operator instruction,

OBJECT--reads object-plane parameters,

SCWRIT--writes object-plane parameters

SHOW--writes transfer matrices and locations of focal points.

b. Names that may be used on CALL cards not in the domain of REPEAT card

SCAN--scans five-dimensional object-plane space, print, plot,

REPEAT--executes a group of CALL cards several times in succession,

CHANGE--same as REPEAT except that the parameters of one element change,

UNLOAD--writes end of file and unloads selected tape,

OUTTAP--selects new output tape,

TEST--skips or executes a group of call cards, depending upon test outcome,

REMOVE--removes selected element from beam system,

INSERT--inserts additional element into beam system,

SAVTAP--selects utility tape for saving system parameters,

RELOAD--reloads system parameters from tape, locates "best" system,

SELECT--assigns two utility tapes for use of SCAN, STATE, and RESCAN

DEFINE--defines an user-chosen function to be used by optimization routines.

c. Subroutine names that may not be used on CALL cards

STEP--directs stepping linear or abberation calculations through elements of beam system,

SIMPLX, DEL, ERR, GET, JMY, MIN, NEW, PIV, ROW, VER, XCK--subroutines in RS MSUB linear programming subroutine,

SHAPES--sets up calculation of parameters of quadrupole magnet,

LABEL2--CRT plotting routine called BELL,

GRID--CRT plotting routine to plot coordinate grids,

SOLVES--calculates aberration integrals and tolerance coefficients, CHICHI--carries first-order solutions through quadrupole magnet,

INT--interpolation subroutine,

COEFT--determines five-point interpolation coefficients,

FPSI--calculates bell function in creating gradient curve,

WRKY--Runge-Kutta integration routine,

W--calculates higher-order terms for Runge-Kutta integration,

WWRK--calculates derivatives for Runge-Kutta routine,

ABS--dummy entry point corresponding to location zero,

RESCAN--plots aberration envelopes from data on utility tapes.

4. Program Options--SENSE cards

Thirty-one locations in the code are reserved for switches that are tested by the program to determine which options should be executed. Thirty of these switches form the array IF(k), k=1, 30. The other cell contains a single word, BOOL, which is always interpreted as a collection of bits and is usually inserted into the SENSE INDICATOR register for testing.

All these switches are set and reset from a single card which follows the CALL card, SENSE (which instructs the supervisor to read the SENSE card). The first thirty columns of the SENSE card are interpreted as the thirty integers IF(k). A blank in one of these columns signifies that the corresponding IF(k) is to remain unchanged; thus only those columns containing punches change the switch settings.

BOOL is always inserted as a twelve-digit octal word. Only the left half of the word is interpreted and stored. The right half of BOOL can be changed only by the program (or through an ALTER card). The word consists of 36 bits or binary digits, each of which may take the value zero or one. Groups of three bits are represented by a single octal digit. The correspondence is: 000=0, 001=1, 010=2, 011=3, 100=4, 101=5, 110=6, and 111=7. BOOL must contain no blanks when entered on the SENSE card.

Some of the switch settings are changed by the program, particularly when conflicts arise.

Also on the SENSE card is the CHIF field; CHIF is a floating-point number which is used only in the Runge-Kutta integration routines. CHIF is the value of z at which a new SENSE CARD is to be read (to set new output options).

a. Significance of IF(k) settings. The listing of the significance of the switches which follows is for convenience; fuller explanations will be found in the description of the calculations affected by a particular switch.

IF(1) selects linear programming problem and is normally zero,

=0 minimizes maximum error and sum of errors,

1= minimizes sum of errors,

=2 minimizes sum of errors and prevents errors from changing sign.

IF(2) determines recovery procedure from EXEM (normally 1),

=0 read-write error terminates current CALL card, reads next one,

=1 code attempts to salvage data and continue calculations.

IF(3) debug output from WWRK if nonzero (prints derivatives);

IF(5) normally zero; subroutine BELL prints PHI(z) if nonzero.

IF(7) frequency of printing of solutions under RKY3,

=0 no printing,

=k, $k \neq 0$ then print every kth Runge-Kutta step.

IF(9) number of times trajectory points are plotted in "Beam Cross-section" plots; IF(9)=4 is satisfactory.

IF(10) CRT plotting switch; no plotting can be done unless IF(10)=0.

IF(11) relative intensity of plotted lines (as the magnet locations in BELL and SHAPE plots); intensity is proportional to exp [-IF(11)]; IF(11)=1 is satisfactory.

IF(12) intensity of grid lines is proportional to exp(-IF(12)); IF(12)=6 gives optimum appearance.

IF(13) number of times curves are plotted; IF(13)=3 is good.

IF(14) intensity of trajectories in "Aberration Envelope" plots; intensity is proportional to exp[-IF(14)]. IF(14)=6 is good provided about 100 trajectories are plotted.

IF(15) number of times heading text is plotted; IF(15)=3 is good.

IF(16) normally zero. If nonzero, transfer matrices and error are printed every time the linear properties of the beam system are calculated (TRACE, SYSTEM).

IF(17) normally zero. If not zero, the constraint matrix for the linear programming problems set up by DESIGN and REFINE are printed.

IF(18) controls output of DESIGN and REFINE,

=0 minimal output printed--initial and final errors and the arrays INFIX and KOUT,

=1 medium output lists solutions, errors, basis (suggested output),

=2 advances page and prints constraints in addition to above.

IF(20) normally zero. If nonzero, aberration coefficients are printed after each magnet under SOLVE, showing partial contributions due to that magnet.

IF(21) controls plotting of phase ellipses under SYSTEM or TRACE,

=0 no phase ellipses are plotted,

=1 phase ellipses before the first element and after the last element are plotted,

=2 phase ellipses between elements are also plotted.

IF(22) controls output of beam envelope properties under SYSTEM

≠1 no output of envelope properties,

=1 virtual waists at the end of the system are printed,

≧2 virtual waists seen by each element are printed,

=3 or 4 --beam widths are printed for entire system

=4 or 5 --beam envelope is plotted.

Those switches which are not listed above are presently not used.

b. Significance of BOOL options. The bits are numbered from left to right with the sign bit denoted as bit number 1. Following each bit number is the octal word which place a 1 in that bit. Bits 1-18 are set from the SENSE card while 19-36 are set by the program.

Bit	Octal equivalent	Significance
1	400000 000000	normally 0; debug dump of integral formulation by SOLVES if 1.
2	200000 000000	normally 0; debug dump of partial sums for coefficient formulation by SUM1, SUM2 if 1.
3	100000 000000	normally 0; if 0, then aberration coefficients calculated at intermediate points (IF(20)≠0) refer to the expansions at the end of the system; if 1, then coefficients refer to expansions at that

		intermediate point.
4	040000 000000	normally 0; if 1, double integrals for third-order dispersion terms will not be calculated.
5	020000 000000	set by STEP; 0 denotes quadrupole field; 1 denotes no quadrupole field in given magnet.
6	010000 000000	set by STEP; 0 denotes octupole field; 1 denotes no octupole field component.
7	004000 000000	if 0, the third column of the transfer matrices will not be calculated through quadrupoles, if 1, the third column will be calculated.

Bits 4-7 are set by the program to avoid calculations that are not needed, such as calculating dispersive terms when there are no dispersive elements in the beam system, calculating the quadrupole components of the coefficients through octupole magnets, or calculating octupole contributions in pure quadrupole magnets. Obvious time savings result. We now continue with the listing of the bits.

Bit	Octal equivalent	Significance
8	002000 000000	not used.
9	001000 000000	not used.
10	000400 000000	if 1, then partial sums in the formulation of the mean aberrations and maximum aberrations will be listed by STATE; if 0, sums not listed.
11	000200 000000	if 1, linear and total displacements and slopes will be listed for each trajectory in the SCAN raster by STATE; if 0, trajectories not listed.
12	000100 000000	if 1, aberration figure will be plotted by STATE; if 0, abberation figure not plotted.

13	000040 000000	not used.
14	000020 000000	if 1, excessive printing for job will not suppress subsequent printing; if 0, printing beyond 2300 lines will be suppressed.
15	000010 000000	if 1, calculation interrupted by expiration of time will be completed (this option is not presently available).
16	000004 000000	if 1, STATE will plot beam cross section; if 0, beam cross section will not be plotted.
17	000002 000000	if 1, STATE will plot x-z plane aberration envelope (requests utility tapes); if 0, x-z plane aberration envelope will not be plotted.
18	000001 000000	if 1, STATE will plot y-z plane aberration envelope; not plotted if 0.
19	000000 400000	if 1, control is under call card REFINE (suppresses output from SOLVE during iterations).
20	000000 200000	if 0, no octupole fields in system--SOLVE does not call SUM2, STATE; if 1, there is octupole field--SOLVE calls STATE twice.
21	000000 100000	if 1, there is a beam specification at some interior location; TRACE then calls MIDERR after every element.
22	000000 040000	if 1, both utility tapes required for aberration envelope plots are available and have been written; if 0, tapes are not available (indicates either no SELECT card or error in SELECT card).
23	000000 020000	if 1, utility tapes have been requested by STATE

		(request granted by SCAN if tapes are available); if 0, tapes have not been requested.
24	000000 010000	indicates which utility tape is being written (SCAN)
25	000000 004000	
	through	not used.
30	000000 000100	
31	000000 000040	if 1, too much printing has been attempted under current CALL card.
32	000000 000020	if 1, more than 2300 lines have been written.
33	000000 000010	if 1, time is about to expire (<0.15 min remains).
34	000000 000004	controls calculation of beam envelope properties by TRACE; if 0, envelope not calculated.
35	000000 000002	if 1, at least one print line has been suppressed because of exceeding 2300 printed lines.
36	000000 000001	if 1, x and y transfer matrices are interchanged for current beam element (used for BENDY).

5. General Considerations in Operating Code

The first card in the data deck must be a MOMENTUM card which contains the design momentum. A TITLE card with the heading text may be inserted following this card. A SENSE card should follow next since all switches are initially zero. The suggested first five cards are demonstrated in the following example.

```
*        DATA
8.0            1700.0         1.72          0.1           1.0
TITLE
THIS IS A SAMPLE PROBLEM BEING RUN ON THE QUADRUPOLE CODE
SENSE
01000000401636300100140000     004527000000
```

The sense card should be followed by the CALL card, which initiates the first calculation. EJECT cards should be freely interspersed among the subsequent CALL cards to improve the clarity of the output . TITLE cards may also be inserted to denote different calculations.

All the cathode-ray tube output should be executed after a PREID card and before a POSTID card. The plots will be numbered; the corresponding number will appear on the printed output, showing exactly where in the calculations a particular plot occured. All plots will be dated and labeled with the identification "4P".

Every page of the printed output will be dated and identified. The current heading text will appear at the top of each page along with the page number.

Utility tapes must be assigned by SAVTAP or SELECT before they are needed; if they are not assigned, the calculations requiring their use will be skipped.

The card deck should end with one of the cards EXIT, DUMPC, or DUMPAL, followed by the monitor end-of-file card.

B. Calculation of Beam Properties

1. Input and Output of Beam-System Parameters

The code is currently equipped to execute calculations on beam systems containing no more than thirty elements. Of the thirty elements, no more than five may be "black-box" elements whose optical properties are determined by (input) transfer matrices. Because of the number of parameters that may be varied in a bending magnet, the code considers a bending magnet to consist of two elements.

The parameters are stored in six one-dimensional arrays. For element k, ITYPE(k) determines the type of element (QUAD, DRIFT, ...) and also identifies the transfer matrices used with a black-box element. The three arrays ZL(k), XPHI(k), and XPSI(k) contain the primary parameters for element k, i.e., those which can be varied. The remaining two arrays, XCL(k) and XCR(k), contain parameters that cannot be independently varied. Of course many types of beam elements do not have this many parameters.

a. READ. The primary means of entering the parameters of the beam system is by means of the CALL card, READ, followed by one card giving the number of elements in the beam system and scaling parameters. This card is followed by one card for each beam element, giving the type of element and the parameters for that element (bending magnets, each thought of as two elements, require two cards). These cards, called ELEMENT cards, are fully described in Section E.5 of this appendix.

Each parameter may be entered directly by means of the ELEMENT cards. If desired the previous value of any parameter may be retained upon entering a new beam system merely by putting a -1 immediately to the left of the parameter's field on the ELEMENT card.

Section B.4, below, describes the method of calculating the parameters of a quadrupole magnet, or series of quadrupole magnets, given the gradient as a function of distance along the optic axis. This calculation is executed by the subroutine SHAPE, and the results are stored in COMMON.

Any of the four parameters effective length, gradient, left shape coefficient, and right shape coefficient for any quadrupole magnet in the beam system (including magnets with octupole field components called 4PLUS8 types) can be loaded from the stored results of the SHAPE calculations. The quadrupole magnets considered in SHAPE are numbered 1, 2, 3, ···; to enter a parameter from quadrupole magnet number 3, for example, a 3 is placed immediately to the left of the parameter field on the ELEMENT card for that element. Suppose we wish to enter the effective length and the left and right shape coefficients from the third quadrupole magnet (in SHAPE) while entering the gradient directly. If this same magnet occurs at two different locations in the beam system, the deck could be as follows:

```
SHAPE
READ
07
DRIFT   300.0
QUAD    3              2.0              3          3
DRIFT   9.75
QUAD    34.0           -3.0             8.0        -8.0
DRIFT   9.75
QUAD    3              2.0              3          3
DRIFT   600.0
SYSTEM
```

The significance of other cards in this deck is described elsewhere.

The same means may be used to enter the length of the drift space between two adjacent magnets in the SHAPE calculations. The code calculates the length between the effective ends of the <u>k</u>th and the <u>k+1</u>th quadrupole magnets and inserts this length as the length of the intervening drift space. This is accomplished by placing the integer k immediately to the left of the ZL field in the element card, DRIFT. An example of a doublet follows.

```
SHAPE
READ
04
QUAD   01          01                            01          01
DRIFT  01
QUAD   02          02                            02          02
DRIFT    500.0
```

In the above example, the system analyzed by SHAPE has been inserted as the beam system. The last element, the 500-inch drift space, had to be specified directly, since it does not lie between two quadrupole magnets.

The first card following the READ card is written in the format (I2, 7F10.5). The first field contains the number of elements in the beam system, KMAX; KMAX element cards must follow this card. The next five fields describe the object-plane phase space, giving the largest displacements and slopes in the two planes and the bounds on $\Delta p/p$. These quantities are $\overline{x}$ (columns 3-12), $\overline{y}$ (13-22), $\overline{x'}$(23-32), $\overline{y'}$ (33-42), and $\overline{\Delta}$ (43-52). These maxima are interpreted as the semi-axis lengths for the phase ellipes and the phase-space hyperellipsoid in X, X', Y, and Y' introduced in Chapter II. They are also the quantities used to normalize the aberration coefficients to refer to a unit hypersphere in the normalized phase space (Chapter VII). Any one of these five maxima may be later changed by insertion of the call card, OBJECT. The last two fields on the first card following the READ card determine the scaling to be used in the "beam profile" plot and the "beam phase space" plots. The scaling factor for displacements (which must be larger than any displacement encountered along the beam system) appears in columns 53-62. The scaling factor for slopes is placed in columns 63-72 and is the upper bound of the slopes encountered in the beam system.

Black-box elements, described by matrices, are entered into the beam system by inserting the element card MATRIX, followed by three cards on which the twelve nontrivial elements of the two 3x3 transfer matrices are punched. The element card, MATRIX, may contain a length in the ZL field which will be printed when the beam system is listed but otherwise enters into no calculation. Five matrices may be stored and each call card, MATRIX, must contain one of the integers 1, 2, 3, 4, or 5 which determines where the matrices are to be stored. It is possible to store one matrix that refers to two elements by this scheme. Of course, different matrices should not be stored in the same locations. If this integer is negative, the matrices are not read, and the code assumes that the matrices were inserted by a previous READ sequence and are stored in the same location. This is consistent with the treatment of other parameters; they remain unchanged when a -1 is inserted just to the left of the field that would otherwise have replaced them.

b. PUNCH. The call card, PUNCH, causes the beam system to be written on the punch tape in the format described above. The resultant cards, when preceded by a READ card, may be used to insert the beam system for a subsequent job. The punched cards are labeled in columns 73-80 with the date and sequential numbering. A card containing the current page heading text, for identification, precedes the card sequence. The card, PUNCH, should be inserted following optimization sequences so that the optimized system can be loaded at some future time for additional calculations.

c. INSERT. At any time the existing beam system may be augmented by reading the call card, INSERT m, which inserts a new beam element between elements m and m+1 of the current beam system. INSERT 0 places the new element in front of the current beam system, while INSERT m with m=KMAX places the new element after the current beam system.

The INSERT card must be followed by one ELEMENT card punched in exactly the same manner as the ELEMENT cards for READ. If the new element is a bending magnet, then there must be a second ELEMENT card following the first. If the new element is a matrix, then three MATRIX cards must follow the ELEMENT card, MATRIX.

d. REMOVE. Any beam element can be removed from the beam system by inserting the call card, REMOVE m. The mth element is removed and the following line is written: "REMOVE BEAM ELEMENT 13 (BENDY)." In this example the call card would be REMOVE 13 and the 13th beam element is a bending magnet. To remove a bending magnet, the first element of the two should always be the element referenced; removing a bending magnet reduces the number of elements in the beam system by two.

e. VARY. The call card, VARY, is designed to allow the replacement of the parameters ZL, XPHI, and XPSI of a beam element. The card contains the number of the element which is to be varied in the first two columns.

The parameters ZL, XPHI, and XPSI are placed in the same locations as they would appear in on an ELEMENT card. To change the parameters of a bending magnet, the card must distinguish between the two elements comprising the bending magnet.

f. CHANGE. Frequently one wishes to observe the behavior of beam properties as the parameters of a single beam element are systematically changed. The call card, CHANGE m n, executes a group of m call cards, in sequence, a total of n times. Before each execution of the sequence of call cards, the parameters of a selected beam element are incremented. Immediately following the call card, CHANGE, (preceding the first call card in the domain of CHANGE) a single card appears designating the element, k, to be changed and containing the numbers to be added to the parameters of that element. The number k is placed in the first two columns while the numbers to be added to ZL(k), XPHI(k), and XPSI(k) appear in the same locations as those in which ZL, XPHI, and XPSI are punched in the ELEMENT cards. In the repetition aspects CHANGE m n is equivalent to REPEAT m n.

g. SAVE, RELOAD. Provisions have been incorporated into the code for writing the important parameters of many beam systems on binary tapes for future reference. Any one of these beam systems may be "reloaded", becoming the current beam system. The code may be requested to reload the "best" beam system, which is defined as the system satisfying the beam specifications (set up by one of the subroutines ERRSET, DESIGN, REFINE, or FOCUS) with the minimum error. The use of these provisions is described in Section D.1 of this appendix.

2. Calculation of the First-Order Properties

After a beam system has been installed by one of the methods described above, all the desired first-order properties are calculated when the CALL card, SYSTEM, is read.

a. SYSTEM. The output obtained from SYSTEM depends upon the switches, IF(21) and IF(22), which are set by the SENSE card. SYSTEM first causes the listing of the elements contained in the beam system, giving the primary and derived parameters for each element. The total length of the beam system concludes this part of the written output. TRACE is then called to calculate the optical properties.

b. TRACE. The primary function of TRACE is to calculate the transfer matrices for the beam system. TRACE may be called by the call card TRACE; it is also called by the optimization routines. When called in these two ways, TRACE normally does not produce any written output. If the switch IF(16) is not zero, the transfer matrices are printed every time TRACE is called; this provision allows checking of the optimization routines.

When TRACE is called by the CALL card, SYSTEM, general output options apply. These range from as little as the transfer matrices, error in beam specifications, and the virtual waists at the end of the system to as much as a complete set of cathode-ray tube plots showing the envelope and phase-space ellipses throughout the system. The switch IF(21) controls the plotting of the phase-space ellipses. The switch IF(22) controls the listing and plotting of the beam envelope. The IF(22) options include: (a) the listing of the virtual waists seen by each element and the transfer matrices between object plane and each element,

(b) the listing of the beam half-widths at five equally spaced locations within each element, and (c) the beam envelope plot.

The beam envelope plot assumes a double waist to be present at the object plane; this represents no restriction, since the pseudo elements, DRIFTX and DRIFTY, may be used to provide a virtual double waist at the object plane for any system. Each beam element is divided into five equal parts, the widths calculated at each of the five locations, and the envelope constructed of line segments between these points.

If a beam envelope plot is specified by IF(22), the code resets IF(21), if necessary, to prevent phase-space plots from appearing at intermediate points in the system. If both the profile and the intermediate phase-space plots are desired, the call card SYSTEM must appear twice, separated by a SENSE card changing IF(21) and IF(22).

TRACE calls subroutine MERR, described in Section C below, to calculate the error in meeting the beam specifications. MIDERR is called to calculate beam specifications involving DEFINE type functions.

The transfer matrices are printed by subroutine SHOW which also calculates and lists the locations of the focal points.

c. STEP. Subroutine STEP is the master routine that guides the calculations of the beam properties. Coded in FORTRAN, STEP occupies nearly 2000_{10} (subscript indicates base of 10 as opposed to base of 8) locations in the core. STEP operates in three modes: the SYSTEM mode, the TRACE mode, and the SOLVE mode. Its primary function is to guide the calculations through the beam system, calling the necessary subroutines to carry out the requested calculations for each type of beam element encountered.

In the SYSTEM mode, STEP lists the current beam system as described above.

In the TRACE mode, STEP calculates the envelope data and executes the profile and phase-space plots. It calls the following subroutines to carry the first-order solutions of the trajectory equations through the various element types:

(1) CHICHI for quadrupole magnets, octupole magnets, and drift spaces.

(2) AXIAL for solenoid magnets.

(3) EDGE for the entrance and exit thin-lens effects of bending magnets.

(4) BEND to carry the solutions through the interior regions of a bending magnet.

(5) MPYMAT for black-box elements. MPYMAT is also called by AXIAL, EDGE, BEND, and DRIFT.

(6) DRIFT for the pseudo elements DRIFTX and DRIFTY.

(7) JNCHI to initialize the solution vectors, CHI(k) and DCHI(k), at the start of the system.

(8) FSCHI, which moves the solution vectors from CHI(k) and DCHI(k) to CHIO(k) and DCHIO(k) before each element.

All of these subroutines comprise a single package requiring 370_{10} locations in memory. This package is FAP coded and is optimized with respect to space required and speed of calculation.

The SOLVE mode of subroutine STEP differs from the TRACE mode in two respects. The envelope properties are not calculated. The calculations for quadrupole and octupole magnets are carried out by the subroutine SOLVE. Aberrations induced by other beam elements are ignored;

the same routines are used in the SOLVE mode as in the TRACE mode to carry the calculations through these elements.

3. Calculation of Aberrations

a. SOLVE. The single call card, SOLVE, causes the code to calculate all the aberrations of the beam system. If bending magnets or solenoid magnets are included in the beam system, the aberration calculations are conducted as if these elements had no aberrations. The call card, SOLVE, causes two passes through subroutine STEP, the first in the trace mode and the second in the solve mode. The trace mode is required to obtain the final values of the solution vectors which are needed for the tolerance coefficients; these final values of CHI(k) are stored in the array SAVCHI(k).

In the solve mode, STEP first initializes the solution vectors by calling JNCHI and clears the aberration integrals by calling INCHI. For each quadrupole or octupole magnet in the system, SOLVE is called to carry the integrals through that magnet. CHICHI is used by SOLVE to calculate the first-order solutions; one pass through SOLVE requires 111 passes through CHICHI. When the aberration integrals have been calculated, STEP calls SUM1 and STATE to give the output of the aberration calculations in the absence of octupole components. If there are any octupole components SUM2 and STATE are called to repeat the output, this time with the octupole components.

When aberrations are being minimized under subroutine REFINE, the aberrations are calculated in the same manner except that no output is produced. When the integrals have been calculated, SUM1 and SUM2 are called to calculate the coefficients of aberration, NORM is called to calculate the mean and maximum aberration displacements, and SCAN is called to calculate the data required by REFINE.

Once the aberration integrals have been calculated they remain available to the program until they are recalculated. This is also true of the aberration coefficients. The normalized aberration coefficients are destroyed by either DESIGN or REFINE; these coefficients can be restored by entering the call card NORM. The tolerance coefficients, calculated by SOLVE for each quadrupole magnet, are not available for use by the program. They are listed as they are calculated.

b. STATE. Subroutine STATE lists the aberration coefficients, calls NORM, and then lists object-plane phase-space parameters, several derived quantities characterizing the aberrations, and the normalized aberration coefficients. BOOL is examined and, depending upon the switch setting in BOOL, additional output data may be provided, primarily as plots.

The derived quantities characterizing the aberrations listed consist of:

(a) The maximum displacements and slopes, including the fringing field aberrations and the second-order chromatic aberrations. These maxima are calculated for the model of object-plane phase space in which the beam is contained in the region enclosed by ellipses in the x-x' and y-y' planes.

(b) The maximum aberration displacements, calculated from the rectangular model of the object-plane phase space using Eq. (VII-5). The second-order chromatic aberration and the fringing-field terms are excluded.

(c) The sums of (a) and (b), which give an upper bound to the total beam half-width, including aberration terms.

(d) The root-mean-square aberration displacements calculated for the hyperellipsoid model of the object-plane phase space by using Eq. (VII-9).

These quantities are all available to the program for subsequent calculations, such as minimizing by REFINE.

Depending upon the setting of BOOL, STATE next calls SCANS to plot the beam cross section or list the final coordinates and slopes of the raster of trajectories considered in SCAN (see c, below).

Following the above, STATE then plots the aberration figure if instructed to do so by the setting of BOOL. The aberration figure is that figure which is traced out by the parametric equations $x = x^a$, $y = y^a$, $x^a = x^a(0, 0, \overline{x_o'} \cos\theta, \overline{y_o'} \sin\theta, 0) = x^a(x_o, y_o, x_o', y_o', \Delta_o)$, $0 \leq \theta < 2\pi$, and $y = y^a(0, 0, \overline{x_o'} \cos\theta, \overline{y_o'} \sin\theta, 0)$. This is the image of an axial point source in a double-focusing system with an elliptical annular aperture.

Following the aberration figure, STATE calls RESCAN twice if instructed to do so by BOOL. RESCAN plots the aberration envelope in the x-z plane and then in the y-z plane. The aberration envelope consists of trajectories in the neighborhood of the end of the system. The trajectories plotted are those considered in SCAN. In the event that an error occurs in assigning the two utility tapes required for these plots, RESCAN immediately returns control to STATE. The tapes are assigned by the call card, SELECT m n.

c. SCAN. The call card, SCAN m, is equivalent to the FORTRAN statement, Q = SCANSF(m); both cause the execution of calculations upon a group of trajectories originating from a raster of points in the object-plane phase space. The raster is constructed by defining lower bounds, XINF(k); upper bounds, XSUP(k); and increments, XDEL(k) in the five object-plane coordinates x_o, y_o, x'_o, y'_o, and Δ. In each of these coordinates, we then consider the initial values, XINF(k), XINF(k)+XDEL(k), XINF(k)+2*XDEL(k), ···XINF(k)+[n(k)-1]*XDEL(k), where XINF(k)+n(k)*XDEL(k) ≤ XSUP(k)<XINF(k)+[n(k)+1]*XDEL(k). SCAN then performs the specified calculations on the N = n(1)*n(2)*n(3)*n(4)*n(5) trajectories which are obtained by including all the possible combinations of the object-plane coordinates obtained in the above manner. Note that if XINF(m)=XSUP(m) and XDEL(m)>0 for some m two groups of trajectories are run, one with the mth coordinate set to XINF(k), the other with the mth coordinate set to XINF(m)+XDEL(m). If one wishes to include just one value of that coordinate, then XSUP(m)<XINF(m). XDEL(k) must always be positive, never zero.

These quantities, together with two others to be defined below [XMEAN(k) and XDEV(k)] are loaded by inserting the call card, OBJECT, followed by five cards containing the coordinates. The maximum values of the object-plane coordinates, which are used in calculating the beam widths and the quantities characterizing the aberrations, may also be entered on these cards (i.e., $\overline{x_o}$, $\overline{y'_o}$, etc.). Blank fields on these cards are ignored; the corresponding quantities remain as they were before the card was read. To set a quantity to zero, an explicit zero must appear in the corresponding field. Following reading of the cards, the values of these parameters are listed in the same order as they are punched in the cards. This listing is also produced by STATE, and may be written at any other time by the insertion of the call card, SCWRIT.

The calculations performed by SCAN depend upon the integer m punched on the card, SCAN m, or that which is the argument in the calling sequence, Q=SCANSF(m). The possibilities are as follows.

(a) m=0. SCAN calculates the final displacements and slopes for every trajectory in the set considered. For each trajectory, a line is written containing Δ and the initial displacements and slopes, followed by the final values separated into linear and aberration parts (written as x= 2.34004 + 0.04502..).

(b) m=1. The same calculations are excuted as above, but the resultant total displacements are both plotted (beam cross-section plot) and written on the output tape. If requested by a flag in BOOL (set by STATE), the final coordinates and slopes are written on the utility tapes assigned by SELECT. In order not to delay the tapes that are written at the same time the trajectories are plotted, the printed output contains the final slopes and trajectories, separated into linear and (linear+aberration) terms. Plotting may be overridden by BOOL.

(c) m=2. The calculations are as above, but there is no printed output. Plotting may be overridden by BOOL.

(d) m=3. The root-mean-square displacement due to both linear terms and aberrations is calculated. For each trajectory, the radial displacement is calculated, weighted as described below, and added to the others to form the mean displacement.

(e) m=4. The root-mean-square displacement due to the aberration terms alone is calculated as above.

(f) m=5. The weighting coefficients are calculated and stored. This is done once to save time in calculations. The weighting coefficients used are calculated as follows. Let XIN(k) be the object-plane coordinates of the trajectory, then if N is the total number of trajectories considered, the weighting factor w, is

$$w=\frac{1}{N}\prod_{k=1}^{5} \quad \mathrm{EXP} \left\{ \left[\mathrm{XIN(k)}-\mathrm{XMEAN(k)}\right]^2 \quad / \quad \mathrm{XDEV(k)}^2 \right\}$$

(g) m=6. Calculate aberration function specified on the condition card with condition no. zero.

The limit on the number of values permitted for each coordinate is 7, putting the maximum number of trajectories treated at 7^5=3x10^8. The number of values permitted is not limited for the plotting of the trajectories. It is obvious that a great deal of care must be exercised in the selection of the number of trajectories to be considered, since it is quite easy to set up calculations requiring hours to complete because of the excessive number of trajectories.

The calculation of the mean displacements as described above is time-consuming. The rms values, calculated by NORM from the formulas given in chapter VII, are preferable for calculational use.

Subroutines FIRST and THIRD calculate the linear and aberration components, respectively, of the trajectory whose object-plane coordinates are stored at XIN(k). The final displacements and slopes are stored at XOUT(m) with XOUT(1)=x^1, XOUT(2)=y^1, XOUT(3)=x'^1, XOUT(4)=y'^1 (linear parts) XOUT(5)=x^a, XOUT(6)=y^a, XOUT(7)=x'^a, and XOUT(8)=y'^a.

4. Calculation from Gradient Plot

An alternative method of calculating the optical properties of a beam system that consists solely of quadrupole magnets and drift spaces, is the direct integration of the equations of motion using field values derived from stored values of the magnetic field gradient along the z axis. This method is also available to the user of the code, primarily to check the calculations carried out by the main body of the code.

The function (z), which is proportional to the field gradient, is stored in the array, POT(k), K=1, KKMAX. The spacing in z between consecutive values in the array, DELTAZ, is entered on the MOMENTUM card. The first value in the array corresponds to z=0 (this defines z=0), and the last value in the array corresponds to z=ZEND. The dimension of the array is 2000, hence (ZEND/DELTAZ)<2000.

The gradient array is entered by subroutine BELL, which constructs it from "bell-shaped" curves for each magnet. Provisions will be made for entering this array directly should one possess the required measurements of the gradient as a function of distance along the optic axis.

a. BELL. To calculate the gradient array, the call card, BELL, is entered, followed by one MAGNET card for each quadrupole magnet in the system. The magnet cards are followed by a single card giving ZEND. Prior to calling BELL, the system BORE the increment between gradient values, DELTAZ, a reference gradient, GRAD, and the design momentum p_o must have been read on a MOMENTUM card such as the first card following the *DATA card.

The magnet cards contain a nonzero integer; the location of the center of the magnet, ZMID(k) (relative to z=0); the magnet's length, ZLONG(k); a factor FR(k) that determines the length of the central plateau of constant gradient within the magnet; the "half-width", of the magnet's fringing field, BW(k); and a relative exitation, EX(k). EX(k) is chosen so that the gradient at the center of the magnet is EX(k)*GRAD. The gradient is assumed to be constant in the center of the magnet, starting to fall at a distance of FR(k)*BORE from either end. If ZZ2(k)>ZZ1(k) and the plateau region extends between ZZ1(k) and ZZ2(k), then the magnetic field gradient function for z>ZZ2(k) is given by

$$\mathrm{PHI}(z)=\mathrm{EX}(k)*\mathrm{GRAD}*\left[1+(z-\mathrm{ZZ2}(k))^2/\mathrm{BW}(k)^2\right]^{-2}.$$

The gradient function for z<ZZ1(k) is given by

$$\mathrm{PHI}(z)=\mathrm{EX}(k)*\mathrm{GRAD}*\left[1+(z-\mathrm{ZZ1}(k))^2/\mathrm{BW}(k)^2\right]^{-2}.$$

There should be no more than ten magnets in all. The gradient array, POT(k), is obtained by calculating the gradients separately for each magnet and then adding them together. If the magnets are separated by a distance greater than three times their bore, this is a reasonable approximation. If the magnets are closer together, then the approximation suffers to the extend that there is leakage flux between neighboring magnets.

The resultant gradient function is plotted provided IF(10)=0. The physical extents of the magnets are shown on the plot, and the locations of the magnet centers are listed. In each fringing-field region the half-width of the bell curve is shown by a line segment of length BW(k), plotted slightly above the z axis.

b. SHAPE. With the gradient array, calculated by BELL, stored in POT(k), the program calculates the parameters of the quadrupole magnets which produce that gradient. To execute this calculation, the call card SHAPE is inserted. No computations other than the direct integration of the trajectory equations under control of the call card RKY3 should intervene between the call cards BELL and SHAPE; this is because some of the data needed by SHAPE would be destroyed by some of the other calculational routines, particularly the optimization routines, DESIGN and REFINE, which use the array, POT(k), to store the linear programming constraint matrices.

For each quadrupole magnet entered by BELL, SHAPE calculates the locations on either side of the magnet where the gradient vanishes. These two points define the region of integration to be used in the calculation of the effective lengths of the magnet and the shape coefficients describing the fringing field. This calculation fails if the gradient does not vanish between consecutive magnets, a limitation in the code which will be overcome in a future version.

The integrals $\int \phi \, dz$ and $\int z\phi \, dz$ are calculated by a ten-point Gaussian integration formula; the integrals are taken over both the entrance- and the exit-field regions. From these integrals, the code determines the locations of the effective ends of the magnet, which are defined to be those points which would yield the same value to the integral $\int \phi \, dz$ were ϕ a constant between the effective ends and zero beyond them.

The output consists of a listing, for each magnet, of the physical length, the effective length, the difference in the two lengths, the shape coefficients, the location of the effective ends, and the region of integration. For convenience, the physical and effective lengths are also listed separately for each half of the magnet. ZMID(k) is taken to be the center of the magnet for this purpose even though ZMID(k) may not bisect the effective length.

If IF(10)=0, additional output in the form of cathode-ray tube plots is produced. There is one plot for each magnet considered. On each plot, the physical extent of the magnet is shown by a pair of horizontal lines, one near the top of the plot and the other near the bottom. The curve plotted is ϕ_c, "PHI complicated," which has been defined as the difference between the actual scalar potential and the step-function scalar potential, ϕ_s, which vanishes outside the effective ends of the magnet. The left and right shape coefficients (entrance and exit, respectively) are listed on the plot. The portion of the z axis shown on the plot is the region of integration.

The results of the SHAPE calculations would be destroyed by the execution of any of the optimizing routines, and must therefore be used prior to the calling of an optimizing routine.

c. <u>Direct integration of the equations of motion.</u> The code provides for the direct integration of up to twenty-five trajectories using the Runge-Kutta method. This calculation uses the gradient array developed by BELL. No optimization routine may intervene between BELL and the direct integration calculations. The Runge-Kutta calculations are invoked by the call card RDY3. This card is followed by a single card containing DRIN and DROUT, defined as the initial drift distant to the point z=0 (defined in BELL) and the final drift distance after the point z=ZEND, respectively. DRIN and DROUT may be negative as well as positive.

The card containing DRIN and DROUT is followed by cards containing the inital displacements and slopes and the momentum of the trajectories to be integrated. There is one card for each trajectory. These cards must contain no punches in the first two columns except the last card of the group, which must contain a positive integer in those columns. The first two trajectories, corresponding to the first two cards, are calculated from the linearized equations

$$x''+\frac{p}{p_o}\cdot\varphi(Z)\cdot x=0 \text{ and } y''-\frac{p}{p_o}\cdot\ \varphi(z)\ y=0.$$

The remaining trajectories are calculated from the complete equations (to third order).

The trajectories are brought through a drift space to Z= DELTAZ and are integrated from this point to the point $Z=z_1$ where ZEND-4*DELTAZ$<Z_1\leq$ ZEND-3*DELTAZ. They are brought through a drift space from Z_1 to ZEND+DROUT. The region of integration is chosen so that gradient values are always available forthe five-point interpolation formulas.

The trajectories are listed before and after both the inital drift and the final drift. The listing at intermediate points is under the control of the switch IF(7). They are listed at every Runge-Kutta step exactly divisible by IF(7) unless IF(7)=0, in which case they are not listed at all. If IF(7)=5, for example, then they are listed at z=5H, z=10H, z=15H, etc. The field CHIF on the SENSE card permits changing switches during the course of the integration. At each Runge-Kutta step, CHIF is examined; a new SENSE card is read if z $\geq$ CHIF.

The Runge-Kutta method of solution is much slower than the Green's function power-series method used in SYSTEM, TRACE, and SOLVE. Calculation of twenty-five trajectories takes approximately one hundred times as much time using RKY3, as does calculation of the same trajectories to third order by SYSTEM, SOLVE, and SCAN(0). In addition, the output is much less useful, since few statements about the quantitative nature of the aberrations can be made from these trajectories.

C. Optimization of Parameters

The code contains three optimizing subroutines; two of these routines, DESIGN and REFINE, perform the desired optimization by the methods of linear programming (L.P.). The third subroutine, FOCUS, adjusts two parameters to meet two specified conditions by elementary methods. The methods using linear programming are very powerful; the number of independent variables considered and the number of conditions which may be specified are limited only by the number of storage locations available and time considerations. With linear programming, constraints may be imposed upon the variables to prevent the construction of nonphysical or undesirable solutions.

1. Linear Programming Theory and Application

a. The linear programming problem.

The general statement of the L.P. problem is, "choose a set of variables such that a given linear functional of the variables is minimized while a set of linear constraints upon the variables is satisfied."

Let x^j, $j=1,\ldots,n$ be the set of variables. Let the functional to be minimized be

$$z = \sum_{j=1}^{n} c_j x^j \qquad \text{(A-1)}$$

and the constraints be

$$\sum_{j=1}^{n} a_j^{\ i} x^j = b^i, \quad i=1,\ldots,m, \text{ where } m<n$$

and $x^j \geqq 0$, $j=1,\ldots,n$. This is the standard form of the L.P. problem and is known as the primal problem.

An equivalent problem, known as the dual problem, is the more useful problem for our purposes. The statement of the dual problem is, "choose the values of the variables w_i, $i=1,\ldots,m$ that minimize the functional

$$y = \sum_{i=1}^{m} b^i w_i \tag{A-2}$$

subject to the constraints

$$\sum_{i=1}^{m} a_j^{\,i} w_i \geq -c_j, \qquad j=1,\ldots,n \quad .$$

The arrays $a_j^{\,i}$, c_j, and b^i are the same for both forms of the problem. The value of z which is obtained as the solution to the primal problem is the negative of the value of y obtained as the solution to the dual problem. The relationship between the primal and dual solution vectors is

$$w_i = -\frac{\partial z}{\partial b^i} \qquad \text{and} \qquad x^j = -\frac{\partial y}{\partial c_j} \quad . \tag{A-3}$$

Referring to the primal problem, any set of the variables, $x^1,\ldots,x^n$, that satisfies the equations of constraint is called a <u>feasible solution</u>. The feasible solution which also minimizes the linear functional is known as the <u>optimal feasible solution</u>. A feasible solution with no more than m of the n variables x^j positive (the rest being zero) is termed a <u>basic feasible solution</u>; a basic feasible solution for which exactly m of the variables x^j are positive is nondegenerate.

Let us visualize the n-dimensional space of the variables, x^j. Each of the equations of constraint defines a plane in this space. It can be shown that the region of this space that satisfies all equations of constraint is either void, a convex polygon (called a <u>simplex</u>), or a convex region which is unbounded in some direction. A void solution space is realized if there is no feasible solution of the problem. An unbounded region may lead to an unbounded solution.

The region of the n-dimensional space, for which the linear functional takes a constant value, is also a plane. Parallel planes correspond to different values of the linear functional.

A convex region is defined to be a region for which every point, lying on the line connecting any two points in the region, also lies in the region. The family of planes, on which the linear functional takes constant values, progresses toward a vertex of the convex region, with each succeeding plane yielding a smaller value for the linear functional. Thus the minimum value of the linear functional (the optimal feasible solution) will occur at a vertex or along the line connecting two vertices, in which case the planes corresponding to constant values of the linear functional are parallel to the line connecting the two vertices. If no bound exists in the direction of decreasing values of the linear functional, then the solution is unbounded.

It can be shown that each vertex in the convex region of feasible solutions corresponds to a basic feasible solution. Each basic feasible solution corresponds to setting (n-m) of the x^j to zero, reducing the equations of constraint to m equations in m unknown variables to which there is a unique solution, the vertex. The m columns of the constraint matrix, $A = |a_j^{\ i}|$, belonging to the positive x^j constitute the basis B corresponding to the vertex.

The solution procedure is to move from an extreme point to a neighboring extreme point by replacing a column in the basis with one not in the basis. There is a test to select the column to be replaced; this is, "the column to be replaced shall be the one which yields the greatest reduction in the linear functional". Another test determines when the optimal feasible solution has been found.

For further information on the formulation, solution, and theory of the linear programming problem, one should turn to a text on the subject such as that by Gass.[13]

b. The Application of Linear Programming to Beam Design

We now turn our attention to the problem of adjusting the parameters of a beam system to provide specified optical properties while satisfying a number of constraints. Let $f_k = f_k(v_1, v_2, \ldots v_N)$, $K=1, M$ be a set of functions of the variables $v_1 \ldots v_N$. The f_k describe certain optical properties and may be chosen to be particular transfer matrix elements or functions of the transfer matrix elements. We define a set of errors, $E_k \equiv f_k(v_1 \ldots v_N) - F_k$ where F_k is the desired value of the function f_k. Define the set λ_k by $(-\lambda_k \leqq E_k \leqq \lambda_k)$. We define the upper bound of the errors to be λ; i.e., $\lambda \geqq \lambda_k$, $k=1, M$. We define a total error, E, as follows: $E = \sum_{k=1}^{M} w^k \lambda_k + \mu\lambda$. Here the w^k $(w^k > 0)$ are arbitrary weighting factors that determine the relative importance of the errors E_k; the factor $\mu (\mu \geqq 0)$ is also an arbitrary number that may be chosen to relate the importance of the largest error to the importance of the weighted sum of errors. We shall assume the following constraints on the variables, v_i: $\underline{v_i} \leqq v_i \leqq \overline{v_i}$, $i=1, N$.

Our problem is to choose the set $v_1 \ldots v_N$, satisfying the constraints that minimizes E. From the definition of E, it is clear that we desire E=0 (E cannot be negative). We will assign the variables $V_1 \ldots v_N$ to vary in proportion to specified parameters of the beam system with $v_i=0$, i=1, corresponding to the parameters of the initial beam system. For small variations in these parameters, i.e., for small v_i, we have

$$E_k(v_1 \ldots v_k) = E_k(0, \ldots 0) + \sum_{i=1}^{N} v_i \frac{\partial E_k}{\partial v_i} + \cdots, \quad k=1, M \quad . \qquad \text{(A-4)}$$

If this expansion is terminated with the linear terms then the problem which has been described is the dual problem to a linear programming problem. The constraints on this problem force the solution vector to lie within a closed surface, a <u>simplex</u>, in the N dimensional v_i space. An optimal feasible solution must exist to the problem as stated, since the constraints prevent an unbounded solution whereas there always exists at least one feasible solution, namely $v_i=0$, i=1, N, that yields the initial beam system parameters. Since the actual expansion of the error functions includes terms of higher order than the linear terms, we need to iterate the procedure of setting up the linear programming problem, solving it, and making the specified adjustment in the parameters.

In addition to the constraints $\underline{v_i}$ and $\overline{v_i}$ already introduced, more constraints may be added to the problem to maintain other properties of the system within certain bounds. We constrain the total length of the beam system to remain fixed; this constraint may be relaxed or removed if desired.

The variables, v_i, are brought into the problem as follows. Letting P_r be the <u>r</u>th physical property of the beam system (length, gradient, field, etc.), we set $p_r = p_{r_o}(1+v_i)$ for some i; the <u>r</u>th physical property then varies in direct proportion to v_i with $v_i=0$ corresponding to the initial value, p_{r_o}. In this manner we indirectly obtain the error functions E_k , and thus E, as functions of the variables $v_1 \dots v_N$. Any group of parameters may be forced to remain in proportion by assigning them to the same variable, v_i .

The minimum and maximum constraints upon each v_i ($\underline{v_i}$ and $\overline{v_i}$) are calculated so that each length assigned to v_i will remain within the minimum and maximum values permitted, and each field and gradient will remain less than or equal in magnitude to the maximum value specified.

The standard linear programming tableau for the problem as outlined is shown in table I. The first row of this tableau is known as the <u>cost row</u>. Each column except the last one determines one constraint in the dual problem. The N rows following the cost row contain the coefficients of the N independent variables v_i. The next M rows contain the coefficients of the λ_j whereas the last row contains the coefficients of λ. For each column, the sum of the entry from the cost row and the entries from the other rows, each multiplied by the appropriate v_i, λ_j or λ is constrained to be nonnegative. The last column, called the "right hand side" (B), contains the coefficients of $v_1 \dots v_N, \lambda_1 \dots \lambda_\mu$, and λ used to calculate the total error, E, which is to be minimized. The columns 2N+1 and 2N+2 constrain the total length to remain fixed. l_k is the sum of the lengths which are allowed to vary with the variable v_k.

2. DESIGN

The call card, DESIGN, will cause one linear programming problem to be set up and solved. Except as noted below, DESIGN will call subroutine ASSIGN which reads the variable assignment from cards; DESIGN then calls subroutine ERRSET which reads the cards containing the specified

Table I. Standard linear programming tableau for beam-design problem.

			Upper and lower bounds on independent variables		Fix Total Length		Upper and lower bounds on error magnitude (define)		Upper bound on magnitude of max. error	B
			minimum	maximum			minimum	maximum		
		i \ j	1 . p . N	N+1 . . , 2N	2N+1	2N+2	2N+3 . . . 2N+3 +M	2N+4 +M . . . 2N+3 +2M	2N+4 +2M . . . 2N+3 +3M	
cost row →		1	$\underline{V_1}$. $\underline{V_p}$. $\underline{V_N}$	$\overline{V_1}$. $\overline{V_p}$. $\overline{V_N}$	0	0	E_1^o . E_q^o . E_M^o	$-E_1^o$. $-E_q^o$. $-E_M^o$	0 . 0 . 0	0
Independent Variables (var(p))	V_1	2	1 . 0 . 0	-1 . 0 . 0	1_1	-1_1	$\frac{\partial E_1}{\partial V_1}$. $\frac{\partial E_q}{\partial V_1}$. $\frac{\partial E_M}{\partial V_1}$	$-\frac{\partial E_1}{\partial V_1}$. $-\frac{\partial E_q}{\partial V_1}$. $-\frac{\partial E_M}{\partial V_1}$	0 . 0 . 0	0
	.	.	. . . . .	. . . . .	.	.	. . . . .	. . . . .	. . . . .	.
	V_p	p+1	0 . 1 . 0	0 . -1 . 0	1_p	-1_p	$\frac{\partial E_1}{\partial V_p}$. $\frac{\partial E_q}{\partial V_p}$. $\frac{\partial E_M}{\partial V_p}$	$-\frac{\partial E_1}{\partial V_p}$. $-\frac{\partial E_q}{\partial V_p}$. $-\frac{\partial E_M}{\partial V_p}$	0 . 0 . 0	0
	.	.	. . . . .	. . . . .	.	.	. . . . .	. . . . .	. . . . .	.
	V_N	N+1	0 . 0 . 1	0 . 0 . -1	1_N	-1_N	$\frac{\partial E_1}{\partial V_N}$. $\frac{\partial E_q}{\partial V_N}$. $\frac{\partial E_M}{\partial V_N}$	$-\frac{\partial E_1}{\partial V_N}$. $-\frac{\partial E_q}{\partial V_N}$. $-\frac{\partial E_M}{\partial V_N}$	0 . 0 . 0	0
Upper and lower bounds on error magnitude	λ_1	N+2	0 . 0 . 0	0 . 0 . 0	0	0	1 . 0 . 0	1 . 0 . 0	$-w_1$. 0 . 0	w_1
	.	.	. . . . .	. . . . .	.	.	. . . . .	. . . . .	. . . . .	.
	λ_q	N+q+1	0 . 0 . 0	0 . 0 . 0	0	0	0 . 1 . 0	0 . 1 . 0	0 . $-w_q$. 0	w_q
	.	.	. . . . .	. . . . .	.	.	. . . . .	. . . . .	. . . . .	.
	λ_M	N+M+1	0 . 0 . 0	0 . 0 . 0	0	0	0 . 0 . 1	0 . 0 . 1	0 . 0 . $-w_M$	w_M
bound on max. error	λ	N+M+2	0 . 0 . 0	0 . 0 . 0	0	0	0 . 0 . 0	0 . 0 . 0	1 . 1 . 1	μ

optical properties that are to be achieved. ASSIGN and ERRSET are described later; the instructions for punching the cards are given in Sections E9 and E10 of this appendix. These cards are not read (the variable assignments and specified optical properties are not changed) when DESIGN is in the domain of a REPEAT card or when columns 7-8 of the call card DESIGN contain a nonzero integer.

After the parameters have been entered as noted above, DESIGN calls subroutine VSAVE to save the current parameters of the beam system. Subroutine INITER is then called to calculate the errors in the specified optical properties for the current parameters of the beam system. The constraint matrix is set up next, using subroutine VPRIME which calculates the derivatives of the errors in each specified optical property with respect to the variables, v_i. In order to improve accuracy, each column of the constraint matrix is scaled so that the geometric mean of the column is unity. The first 2N columns are not scaled since they contain two identity matrices, one of which can be used as the initial basis for the solution of the linear programming problem.

The linear programming problem which has been formulated is then solved by the RAND Corporation linear programming subroutine, MSUB.[14] The entire adjustment, specified by the solution to the L.P. problem, need not be made. The code calculates the new error, after the parameters have been adjusted by $\frac{1}{2} v_i$, i=1, N where the v_i are the solutions to the linear programming solution. If the error is smaller than the initial error, the parameters are adjusted by $\frac{3}{4} v_i$. However, if the error is larger than the initial error, the parameters are adjusted by $\frac{1}{4} v_i$. This procedure is repeated a total of twelve times with the factor multiplying the v_i increased by $\frac{1}{2} \cdot 2^{-k}$ if the resultant error after the kth adjustment is smaller than the error before the adjustment; a decrease in the factor by the same amount is made if the error increased after the last adjustment.

If there is no optimal feasible solution (due to an error in input), the original system is restored and the parameters punched.

The output follows, according to the setting of IF(18). The minimum and maximum constraints on the variables, the solution, right-hand-side, current basis, primal solution, and constraint errors may be written. The initial and final errors, the calculated improvement (the error calculated by the linear programming subroutine), and the factor multiplying the variables v_i (chosen as outlined above) are always written, followed by the two arrays, INFIX and KOUT, described in the write-up to the MSUB routine.

VARMAX is reduced as the solution is approached; VARMAX is set to seven times the maximum adjustment made, if this results in a reduction. The absolute values of the variables, v_i , are constrained to be less than VARMAX.

If no optimal feasible solution exists, DESIGN exits to CALL; this results in terminating the REPEAT sequence if DESIGN was called in the domain of a REPEAT. This exit will also occur if no further improvement can be made.

In order to execute a second iteration of the linear programming problem set up in design, a second DESIGN call card must be inserted. By placing a non-zero integer in columns 7-8 of this call card, the code will continue with the same problem. A large number of iterations can be executed under a REPEAT card; when so executed, no ASSIGN card or CONDITION cards will read. The REPEAT will be terminated before its normal conclusion if the code is unable to make any further improvement.

The subroutines which are used in the calculations controlled by DESIGN are described in the following paragraphs.

a. ASSIGN. ASSIGN is called by the subroutines DESIGN, FOCUS, and REFINE unless these subroutines are executed in the domain of a REPEAT card. ASSIGN may also be called by the call card, ASSIGN. This subroutine assigns the parameters of the beam system, which are to be varied, to the specified v_i. It also reads the constraints upon each parameter that is allowed to vary. The cards read are described in Section E9 of this appendix. The reading of cards is terminated by a card with -1 punched in the first two columns. The variable assignment is printed offline; (the index k of the variables $v_k \equiv \mathrm{VAR}(k)$ is printed in octal).

b. ERRSET. Subroutine ERRSET reads the CONDITION cards; each of these specifies one optical property to be satisfied, the desired value of the specified parameter, and the weighting factor which determines the relative importance of the specified parameter. The group of CONDITION cards is terminated by a card with -1 punched in the first two columns. The directions for punching these cards are given in Section E10 of this appendix.

c. INITER. Subroutine INITER calculates the initial error in each specified optical property and prints the desired value, initial value, error, and weight for each condition. The subroutine returns the total error to the calling subroutine.

d. MERR. Subroutine MERR is called by subroutines TRACE and STEP and indirectly by subroutine INITER to calculate the errors in the specified optical properties. If more than 12 conditions have been assigned, no errors will be calculated, as the limit on the number of conditions permitted is 12.

e. VPRIME. The derivatives needed by the optimizing routines are calculated by subroutine VPRIME. Four point derivative formulas are used; the functions whose derivatives are required are evaluated for VAR(k) = -2*VARFIX, -VARFIX, VARFIX, and 2*VARFIX. VARFIX is set to .0001, but may be changed by an ALTER card (VARFIX is located at MERR+124_8). VPRIME is called once for each independent variable VAR(k). The derivatives of the specified conditions (set by ERRSET) are stored in the array DMAT(j). If the REFINE problem is being solved, the derivative of the aberration function being minimized is calculated and returned in ZEND.

f. VSAVE. Subroutine VSAVE saves the initial parameters; ZL(k) is stored at SZL(k), XPHI(k) is stored at SPHI(k), and XPSI(k) is stored at SPHI(k).

g. VRESET. Subroutine VRESET restores the initial values of the parameters of the beam system and then alters the parameters as needed to calculate the derivatives under VPRIME. VRESET also calculates $\underline{v}_k$ and $\bar{v}_k$ from the constraints entered on the ASSIGN cards.

h. VSET. Subroutine VSET is called at the conslusion of the optimizing calculations to make the directed changes in the system parameters.

i. DEFINE. Twenty optical properties of the beam system are normally available for reference by the CONDITION cards. These twenty include the twelve nontrivial elements in the two 3x3 transfer matrices, and certain functions of these elements that determine the locations and widths of the (virtual) waists. Subroutine DEFINE enables additional functions to be constructed when the program is executed. Up to seven functions may be defined by this subroutine. Each function is defined by a maximum of twenty arithmetic operations. To define the nth function (n=1, .., 7), the call card, DEFINE n, is entered, followed by three cards which define the function; the function number, n, must be placed in column 8 of the DEFINE card. The first card following the DEFINE card contains the constants used in the arithmetic operations. The second card locates the parameters which are required. The third card contains the arithmetic statements which define the function; each of these statements is of the form: $A \otimes C$ where $\otimes$ is one of the operations (+, *, /, ., -). The format for punching these cards is explained in Section F14. The functions defined by DEFINE cards can be referenced by CONDITION cards to specify some optical property; these functions may be calculated at some intermediate point in the beam system, if desired.

j. MIDERR. If any conditions require one of the define functions, MIDERR is called to calculate the error in that condition. MIDERR is called once for each element in the beam system.

3. FOCUS.

A second optimization routine, that adjusts two parameters to meet two specified conditions, is called by the call card, FOCUS. The parameter assignment and condition specifications are entered in exactly the same manner as are those for DESIGN. If FOCUS is not in the domain of a REPEAT card, then ASSIGN and ERRSET will be called provided columns 7-8 of the FOCUS card are blank. The assign cards must assign VAR(1) and VAR(2); no other variables may be assigned. There must be exactly two condition cards. FOCUS calls VPRIME to calculate the derivatives of the two specified conditions with respect to the two independent variables. The initial errors are calculated by INITER. The equations, $E_{1_0} + v_1 \frac{\partial E_1}{\partial v_1} + v_2 \frac{\partial E_2}{\partial v_2} = 0$ and $E_{2_0} + v_1 \frac{\partial E_1}{\partial v_1} + v_2 \frac{\partial E}{\partial v_2} = 0$, are solved for v_1 and v_2. The adjustments are made by subroutine VSET. There can be no constraints on this problem. If the initial error is less than 0.000001 of if an error has been made in assigning parameters or conditions, FOCUS exits to CALL; this will terminate a REPEAT.

4. REFINE.

Subroutine REFINE is called to minimize aberrations. REFINE operates through subroutine DESIGN and solves the same problem except that the total error is defined as follows;

$$E = \nu \sum_{i=1}^{N} v_i \frac{\partial A}{\partial v_i} + \sum_{j=1}^{M} w_j \lambda_j + \mu\lambda \text{ ; } \quad \nu \text{ is an arbitrary constant.}$$

The aberration function, A, is defined by a CONDITION card on which the first two columns are blank or zero; A may be defined as XRMS, YRMS, RRMS, XAMAX, YAMAX, ... (these quantities are defined in chapter VII). If IF(2)=2 , REFINE will minimize the aberration function but will hold the special optical properties fixed.

The other operating instructions for REFINE are the same as those for DESIGN.

D. Utility Routines

In this section, we discuss the remaining routines available to the user of the code. The first group of routines is designed to enable wide latitude in the assignment and use of tape units for output use and utility use.

1. Tape Manipulating Routines

a. Outtap.

In the event that a large amount of output printing may not be used but should be available in case it is needed, provisions have been made to put this output on a tape separate from the monitor output tape. The second tape can be saved and subsequently printed if the data is needed.

To change the output tape to logical tape m, the call card, OUTTAP m, is inserted: Subsequent output then appears on tape m provided that that tape is available. Should tape m not be listed in the IOU table, the call card, OUTTAP m, will be ignored. The message, "*** OPERATOR *** DIAL TAPE C3 (LOGICAL 23) TO RECEIVE OUTPUT -- SAVE TAPE." is printed both on-line and off-line to notify the operator to hang the tape (this example is appropriate to the call card, OUTTAP23).

This card may be followed by the call card, PAUSE, if the operator has not previously been instructed to prepare the tape.

The output may be returned to the monitor output tape or put on a third tape by inserting another OUTTAP card.

b. Unload.

The call card, UNLOAD m, causes logical tape m to be terminated with an end of file, rewound and unloaded. If logical tape m is not listed in the IOU table, then the UNLOAD card is ignored.

Since non-monitor output tapes are not unloaded, each tape assigned by an OUTTAP card should be subsequently unloaded by inserting an UNLOAD card when the tape is no longer needed.

c. Savtap.

The subroutine group, SAVTAP, SAVE, and RELOAD, makes possible storing the parameters of several beam systems so that a particular beam system may be restored for subsequent calculations. For example, one may wish to design a beam system to meet certain specifications, and to try several magnet arrangements. He may optimize the parameters, by subroutine DESIGN, for each magnet arrangement, storing the result on tape. When all arrangements have been optimized, the code may then be asked to restore that arrangement which best met the specifications.

The call card, SAVTAP m, prepares logical tape m to receive system parameters. The card is ignored if logical tape m is not included in the IOU table. If the tape is available, the operator will be notified to hang the selected tape. For instance, inserting SAVTAP13 will select logical tape 13 (machine tape B3 for the Lawrence Radiation Laboratory Fortran monitor) and print the following message on-line and off-line, "DIAL TAPE B3 (LOGICAL 13) FOR UTILITY TAPE USE". It is recommended that utility tapes normally dialed for the monitor system be used.

d. Save.

The call card, SAVE, causes the parameters of the current beam system to be written on the tape selected by the last preceeding SAVTAP card. While writing the current system on the tape, the code checks to see whether it is a better system than all of the systems previously stored on the tape. A system is said to be "better", if the total error in meeting specifications calculated by DESIGN, FOCUS, or REFINE is smaller than the total error for any other stored beam system.

Upon completion of writing, the accuracy is checked; if an error is detected, the tape is backspaced and the writing done over. This process will be repeated until no redundancy check is detected.

In the event that the utility tape has not been selected by a previously executed SAVTAP m card, a SAVE card will be ignored. A subsequent SAVTAP card will reset the register containing the location of the "best" system on the current tape.

e. Reload.

The call card, RELOAD m n, reloads the nth beam system from logical tape m. If m=0 and n=0 (or both blank), then the best system from the current utility tape is reloaded as the current beam system. If the selected tape is not available, the RELOAD card is ignored.

If a system is reloaded, the tape and the record read is printed off-line. For example the card, RELOAD2307, reads the 7th beam system from tape C3 and prints the following message off-line, "SYSTEM NO. 7 FROM TAPE C3 HAS BEEN RELOADED."

As is the case when the beam systems are written on the utility tape by SAVE, the system read by RELOAD is checked for accuracy in reading, and will be reread until read accurately.

No more than 129_{10} beam systems should be placed on one tape. If one desires to locate the best system among a greater number of systems, he should enter a RELOAD card after about 100 systems have been stored on the tape, reassign the tape by a SAVTAP card, store the system just reloaded by a SAVE card, and then continue with the comparisons.

Several utility tapes may be used in sequence, but the code will be able to locate the best system only on the last tape assigned.

f. <u>Select.</u>

If "aberration envelopes" in either the x-z or the y-z planes are to be plotted by subroutine STATE, then two utility tapes must be assigned prior to entering that subroutine. The call card, SELECT m n, assigns logical tapes m and n as utility tapes for this purpose. If either of the logical tapes m or n is not listed in the IOU table, a flag is set which prevents any subsequent attempt to use the tapes.

An on-line message is printed requesting each tape specified.

The tapes chosen must be distinct, must be on a different channel than the cathode ray tube, and should not be any of the monitor input or output tapes or the current output tape assigned by a SAVTAP card. For the most efficient use, both tapes should be on channel B since the input and output tapes are on channel A whereas the cathode ray tube is on channel C. These tapes may be changed at any time.

The tapes greatly speed up plotting the aberration plots, since the same data must be calculated for three separate plots. Two tapes are available so that one may be used while the other is being rewound, eliminating waiting for a tape to be rewound. Writing and reading of the tapes is fully buffered. While the last record read is being plotted, a new record is being transmitted. The new record is then checked for accuracy and reread if necessary. In most cases, both the tape units and the cathode ray tube are in continuous simultaneous use. The tapes are always left in the rewound position.

Example: The call card, SELECT1109, will assign logical tapes B1 and A9 for utility tape use for cathode ray tube plotting.

2. Output Control Utility Routines

Several Call Cards control off-line and on-line printed output and Cathode Ray Tube Output. These cards and their functions are described below.

a. Eject.

The call card, EJECT, starts a new page of off-line printed output by writing a line of heading which includes the time remaining on the interupt clock. This card also resets the line count that determines when a page is full (see h., below).

b. Time.

The call card, TIME, causes the time remaining to be calculated and written on the output tape.

c. Title.

The page heading contains 72 arbitrary characters which are entered by the call card, TITLE, followed by a single card with the heading text in columns 1-72. A new page is started with the new heading text. The text may be changed at any time by inserting another TITLE card.

d. Note.

Occasionally one desires to instruct the computer operator regarding operation of the program. The call card NOTE followed by a single card with Hollerith text in column`1-72, causes that text to be printed on-line and also off-line. If desired, this card may be followed by the call card PAUSE to halt the computer while the instructions printed on-line are carried out.

e. Pause.

The call card PAUSE halts the computer, with HPR 11111_8 in the storage register, to notify the operator that some instruction, to be carried out, has been printed on-line. Depressing the start key will cause calculation to proceed. The interrupt clock is suspended during the halt.

f. Preid.

When the cathode ray tube is used, the film must be labelled to identify it. The call card PREID causes initial labelling of the film output and should precede all CRT plots. This card will also set the "switch" IF(10) to zero, thus allowing the CRT to be used.

g. Postid.

The call card, POSTID, causes the final labelling of CRT output and should follow the last plot. This card will also prevent future CRT use by setting IF(10) to a non-zero value.

h. Automatic Page Advance.

Every time a "WRITE OUTPUT TAPE 3" statement is executed, the program checks to see whether the current output page is full; if it is full, a new page is started by the EJECT subroutine. The current number of lines allowed on a page is 50; this may be changed by placing the desired number of lines per page in the address portion of location FULL (= TRAP-23_8) by means of the ALTER routine (section 7, below).

3. Exit Routines

When calculations are concluded, several options are available with regard to terminating the job.

a. Exit.

The call card, EXIT, immediately returns control back to the monitor.

b. Dumpc.

The call card, DUMPC, dumps the common area of the program in both floating point and octal formats after which control is returned to the monitor.

c. Dumpal.

The call card, DUMPAL, dumps the program in octal with mnemonics in addition to the DUMPC dumps.

4. Print Subroutines

The following subroutines are used by other parts of the program and are mentioned for completeness.

a. Print Routine.

The subrouting CVRT converts up to twelve BCD words to a binary card image and then prints this card image on-line. Control is returned to the calling routine while the line is still being printed so that, in most cases, no time need be wasted for on-line printing.

b. Octal to BCD Conversion.

Subroutine OCTAL converts a single octal word to two binary coded decimal words for output purposes.

c. Elimination of Preceding Zeros.

A 16 place table is located at A.. in the supervisor routine for use with a CRQ instruction to replace leading zeros in BCD words with blanks.

d. Printing IOH Buffer.

Subroutine PRINTB will print the IOH buffer on-line, thereby reproducing on-line the last line of off-line output.

5. Test Subroutine

Provisions have been incorporated in the program for a general conditional branching of program control. The subroutine TEST allows skipping or execution of a number of call cards, depending on the result of several tests which are specified.

Each test specifies a location in the core (relative to one of the names given in the call list), a value, and a tolerance. The test is passed if the absolute value of the difference between the number stored at the specified core location and the specified value is less than the tolerance. The test is failed if the difference is greater than the tolerance.

This routine is executed by entering the call card, TEST m n, followed by m cards, each of which specifies one test. Whether or not the n cards following the test cards are skipped depends on the outcome of the tests.

If all the tests are passed then the next $|n|$ cards are listed and skipped if $n<0$; no cards are skipped if $n>0$. If any one of the m tests results in a failure, then the next n cards are skipped if $n>0$; no cards are skipped if $n<0$.

The format of the test card is described in Section E.11, below.

EXAMPLE: The error in meeting the specified beam conditions is stored at location 70712 by subroutine DESIGN. We wish to plot phase ellipses for the system only if the conditions have been met sufficiently well; if the error is less than 0.001, we will plot the ellipses. The following cards are entered:

```
SENSE
          1                                    IF(10)=1
TEST  01-3
ABS   70712     0.          0.001
SENSE
          0                                    IF(10)=0
SYSTEM
```

The first SENSE card prevents cathode ray tube plotting by setting IF(10) to 1. If the floating point number stored at location 70712_8 is less than 0.001 in absolute value, the next three cards will be executed. The SENSE card following the TEST card resets IF(10) to zero, permitting plotting during the execution of the following SYSTEM card. If the number stored at 70712 is larger than 0.001 in absolute value, the three cards following the TEST card will be skipped (but listed off-line), and the call card immediately following the SYSTEM card will be executed next.

If any of the TEST cards refer to a subroutine name that is not found on the call list, the test comparison specified on that card is ignored.

6. Alter Routine

No matter how general a code may be, the user will frequently wish to change constants used by the code or portions of the code itself to accomplish a particular aim. The ALTER routine provides for the replacement of part or all of any instruction or constant in any subroutine by a word entered in any format on an "ALTER" card.

The call card, ALTER, is followed by a single card which specifies the subroutine name (any name in the call list) and the octal location of the word being altered relative to the subroutine entry point. The relative location is defined as the address of the word being modified minus the address corresponding to the subroutine name in the call list. To change constants or other data in COMMON, a pseudo-subroutine ABS is specified; the octal address relative to ABS is the absolute address of the word to be modified. If the subroutine name specified is not in the call list, no changes will be made.

The name and location fields are followed by an octal word that is used as a mask; a bit in any location of this word prevents the corresponding bit in the word being modified from being changed. for example if the mask is 777777700000 only the address portion of the word will be modified.

The next field contains a variable format such as A6, F8.3, O12, I5, ... This format specifies how the new word is to be read. If one is changing a floating point decimal constant, he obviously wants to enter the replacement word in an E or F format. But if an instruction is being changed then the O format is more convenient.

A single digit field follows the format field. If this field is blank or zero, the address of the replacement word is not relocated. If, however, the field is not blank, the address field of the replacement word will be relocated relative to the location of the word being modified. The relocation will be ignored if the address portion is masked out by the mask word.

The next field on the card is the replacement word, to be read by the variable format described above. The variable format also specifies the length of this field.

Immediately following the replacement word, 24 characters of descriptive text may be added. This text is reproduced off-line in addition to data showing what was altered. The subroutine name, the octal location relative to the entry point corresponding to that name, and the absolute location of the word being modified are printed off-line together with the octal digits of the word before and after modification. Examples of the use of ALTER cards are reproduced in Appendix III.

7. Peek Routine---Arbitrary Snapshot Dumps

A variable snapshot dump may be executed at any time by inserting the call card, PEEK, followed by a card giving the region to be dumped and the type of conversion to be employed.

The first two fields on the card contain the subroutine name (which must be in the call list) and the octal address, relative to the subroutine entry point, of the first word to be dumped, exactly as in the case of the ALTER card. The third field is the address of the last word to be dumped minus the address of the first word to be dumped, in octal (this is one less than the number of words to be dumped). The fourth field contains one of the integers 0, 1, 2, or 3; this field specifies the conversion to be followed: 0 results in octal conversion, 1 results in floating point decimal conversion, 2 results in decimal conversion with decrements interpreted as decimal quantities, and 3 results in octal conversion with mnemonic machine instructions printed. Thus the card PEEK is equivalent to the Fortran statement, "CALL PDUMP (FWA, LWA, I)".

If the subroutine named in the PEEK card does not appear in the call list the octal address will be taken as an absolute address.

EXAMPLE: Some numerical quantities are stored between locations SOLVES+624 and SOLVES+654 which are used in calculating the aberration integrals; we can dump these numbers by inserting the cards:

```
PEEK
SOLVESbb624bbb301
```

Note that 654-624 = 30.

8. Error Routines

The most likely errors are those relating to input and output functions. Most of these errors are detected by the Fortran input-output routines IOH, RER, WER, or IOS; detection of errors by one of these routines results in a transfer to subroutine EXEM after the error code and return address have been loaded into the SENSE INDICATORS. The standard Fortran monitor EXEM routine will correct some errors, but in most cases, a transfer to EXEM results in termination of the job.

a. EXEM.

In order to attempt to continue with calculations, a separate EXEM routine has been built into the supervisor routine for the code. This routine prints the message, "(EXEM) CALLED...BUFFER CONTENTS ARE..", off-line, followed by the Fortran IOH buffer in BCD; this is the card image or output line image that was being processed when the error was detected. The buffer data is followed by the octal contents of:

(a) The SENSE INDICATORS; the address and tag portions contain the error code while the decrement portion contains the return address.

(b) The LOGICAL ACCUMULATOR

(c) The MULTIPLIER-QUOTIENT; the acc and MQ generally contain the portion of the input-output text which caused the trouble.

(d) Location zero--address of calling sequence

(e) Location two--address transferred to by the STR instruction

(f) ACCUMULATOR--in BCD

(g) MQ--in BCD

The code then attempts recovery in the same manner as if the START key were pressed when under non-monitor control. For further information refer to Appendix VII of the IBM 7090 FORTRAN OPERATIONS MANUAL.

The common errors and the actions taken are as follows:

(a) 0,1 illegal character in formal; treated as end of format

(b) 1,1; 2,1; 3,1; 4,1; 5,1 illegal character in data field; the offending character is treated as zero.

b. Trap.

Every WRITE OUTPUT TAPE 3 statement is trapped before it is executed. Subroutine TRAP tests for too much writing for the job; the current limit is 2300 lines. If the line about to be printed off-line is the first line to exceed the limit, then the warning, "EXCESSIVE WRITING CURTAILED" is written and all subsequent writing is suppressed with the exception of important results. This feature may be over-ridden at any time by inserting a 2 in the fifth octal digit of BOOL on the SENSE card (i.e. BOOL=BOOL+000020000000). The limit of 2300 lines may be changed to any other number of lines by inserting the desired limit in the address portion of location LNTEST (LNTEST=TRAP+77757_8) by an ALTER card.

The last field on each CALL card gives the maximum number of lines which may be printed during the execution of that card. An attempt to print a greater number of lines results in terminating the execution of that CALL card and the reading of the next CALL card. If this field is zero or blank, no limit is placed on the amount of writing permitted under the CALL card.

These two tests may be used to prevent unforseen loops involving large amounts of writing; their main use was in debugging the code.

Subroutine TRAP also advances the output page when the current page is full. Each page starts with a heading line, giving the data and time of the run, the amount of time remaining, the page number, and the text entered by the last TITLE card.

If the output tape has been reassigned by an OUTTAP card, TRAP inserts the correct output tape in place of logical tape 3 called for in the WRITE OUTPUT TAPE 3 statement.

E. Input Card Formats

In this section, the exact placement of all data on the various types of input cards is described. The use of these cards is described in preceding sections. All lengths are in inches, all gradients in kilogauss/in., all magnetic fields in kilogauss, all momenta in MeV/c, and all slopes in radians.

1. CALL Card

The CALL card controls the execution of the many different parts of the program. Its format is (A6, 2I2, I5).

column	description of use
1-6	Name of subroutine or program section called (left adjusted); the name must be one of those in the call list.
7-8	MREP field; integer (right-adjusted).
9-10	NREP field; integer (right-adjusted). The two fields above are used in REPEAT, CHANGE, INSERT, DELETE, VARY, SAVTAP, OUTTAP, UNLOAD, RELOAD, etc., cards.
11-15	LINMAX field; this is the maximum number of lines that can be written under the control of this card. If blank or zero, no limit will be imposed. The field is right-adjusted.

2. SENSE Card

The SENSE card controls program options; its format is (30I1, 012, 8XF6.1).

column	description of use
1,2,3,···,30	IF(k); the first thirty columns give the changes to be made in the switches, IF(1) to IF(30). A blank

column indicates that the corresponding switch is not to be changed. If a switch is to be reset to zero, the corresponding column must contain an explicit zero. Refer to A.3 for the switch assignments.

31-42 BOOL; these twelve columns may contain no blanks; they form an octal word which is loaded into the SENSE indicators. Only the first six columns are interpreted; the right half of this word is set by internal subroutines.

51-56 CHIF; this field is used only by subroutine RKY3.

3. TITLE Card

Following the call card, TITLE, a TITLE card, containing the Hollerith text to be inserted into the output page heading, must appear. The text is to be written in the format (12A6) and consequently must appear in the first 72 columns of the card.

4. MOMENTUM Card

The first card in the data deck must be the MOMENTUM card. This card also follows the call card, NEWP. The format for this card is (5F14.6)

columns	description of use
1-14	BORE; the diameter of the quadrupole magnets to be used. This quantity is used only by subroutine BELL.
15-28	p_O, the design momentum in MeV/c; the momentum is required for most calculations.
29-42	GRAD; a reference gradient in Kgauss/in. used by BELL.
43-56	DELTAZ, the increment in inches between values of PHI(k) (used by BELL and RKY3).

57-70	H, the Runge-Kutta step size (increment in z) in inches. H is required only if the call card, RKY3, is used.

5. ELEMENT Cards

Following the call cards, READ, INSERT, CHANGE, and VARY, one or more cards containing beam system parameters must appear. For READ and INSERT, these cards are read by the format (A6, 5(I2,F11.7)). The first field gives the element type whereas the remaining five groups, of two fields each, specify up to five parameters. The element cards read by VARY or CHANGE differ slightly; they are described later. The locations and names of the fields for the element cards read by READ or INSERT are:

column	field, description of use
1-6	TYPE, type of element, must be left-adjusted and one of the following words: DRIFT, QUAD, 4PLUS8, OCT, BENDX, BENDY, DRIFTX, DRIFTY, AXIAL, or MATRIX.
7-8	IZL; directs loading of ZL (normally zero or blank).
9-19	ZL; length of element (in.)(a floating point no.).
20-21	IPHI; directs loading of XPHI (normally blank).
22-32	XPHI; parameter of element.
33-34	IPSI; directs the loading of XPSI; always blank or zero.
35-45	XPSI; parameter of element.
46-47	ICL; directs loading of XCL (normally blank).
48-58	XCL; left shape coefficient for quadrupole (entrance).
59-60	ICR; directs the loading of XCR (normally blank).

61-71 XCR; the right shape coefficient for quadrupole (exit).

The integers IZL, IPHI, IPSI, ICL, and ICR are normally zero; if they are zero then the next field is read into its normal location (for example, if IZL=0 then ZL is loaded from the ZL field on the card). If any of the integers are negative then the field following is ignored and the parameter corresponding to that field retains the value it had before the card was read (if IPHI=-1 then XPHI is unchanged). If any of the integer fields are positive then the corresponding parameter is located in COMMON as described in B.1.a above; this option should not be used except for the elements DRIFT, 4PLUS8, or QUAD.

If the element type is not one of those in the above list, then the element will be taken to be a drift space.

<u>a. QUAD.</u> To enter a quadrupole magnet the name "QUAD" is placed in columns 1-4 on the element card. ZL is the effective length in inches, XPHI is the gradient in Kgauss/in. (positive if convergent in the x-z plane). XCL and XCR are the fringing field shape coefficients for the entrance and exit ends of the magnet, respectively. They are the $c_k \lambda_k^2$ described in V.D and have units of in^2.

<u>b. DRIFT, DRIFTX, or DRIFTY.</u> To enter a drift space in both planes or in the x plane alone or the y plane alone, the element type is DRIFT, DRIFTX, or DRIFTY, respectively. The length of the drift space is placed in the ZL field.

<u>c. OCT.</u> To enter an octupole magnet, the name "OCT" is placed in columns 1-3 of the element card. The effective length of the magnet is placed in the ZL field. The strength of an octupole magnet is

determined by the third radial derivative of the absolute value of the magnetic field, this derivative being constant throughout the aperture of an ideal magnet. The strength is entered in the XPSI field of the element card in units of gauss/ in^3 (positive when the field is converging in the x-z plane and the y-z plane and diverging in the x=y and x= -y planes).

d. 4PLUS8. A quadrupole magnet that has been modified by shims or other means to induce an octupole component in the field may be brought into the beam system by means of the element card, 4PLUS8. The parameters on the card are the same as those on a QUAD card except that the third radial derivative is placed in the XPSI field as is the case in an OCT card.

e. AXIAL. A solenoid magnet is entered into the beam system by means of the element card, AXIAL. The effective length, in inches, is placed in the ZL field; the magnitude of the axial field, in kilogauss, is placed in the XPHI field. The use of a solenoid is restricted to placement where the beam is rotationally symmetric.

f. MATRIX

Beam elements to be described solely in terms of their transfer matrices are entered by the element card, MATRIX, followed by three "MATRIX" cards (Section 6, below) containing the twelve nontrivial elements of the 3x3 transfer matrices. The ZL (length) field on the element card is stored and listed as the "length" of the black-box element described by the transfer matrices; this length does not enter into any calculations.

Each set of transfer matrices is labelled by one of the integers 1, 2, 3, 4, or 5. This integer, appearing in the IPHI field, directs the storing of the transfer matrices. If there are several elements in the beam system described solely by transfer matrices, then no two of these elements may be labelled by the same integer, IPHI, unless the transfer matrices for the two elements are the same. If IPHI is negative, the code assumes that the matrices have been loaded by a previous READ sequence and are not to be replaced. In this case the three matrix cards that normally follow the element card, MATRIX, must not appear. IPHI may not be zero nor may it be an integer larger than five.

g. BENDX or BENDY

A bending magnet is entered on two element cards; the first card has "BENDX" punched in columns 1-5 if the bend is in the x-z plane. BENDY punched in columns 1-5 signifies that the bend is in the y-z plane.

(a) The first card contains the length of the bending magnet, in inches, in the ZL field. The field strength, in kguass, appears in the XPHI field. The XPSI field contains α, the entrance angle, in degrees (refer to Fig. 1).

(b) The second card contains the field exponent, n, in the XPHI field; γ, the angle the entrance edge makes with the exit edge, (in degrees) is placed in the XPSI field. The remainder of the card is ignored. The second element is of zero length.

The conventions on sign for the above quantities are the same as the convention adopted in Chapter II, shown as positive in Fig. 1.

6. MATRIX Cards

The three cards following the element card, MATRIX, are read in the format (4E15.8). The first row of the x transfer matrix, followed by the second row of the x transfer matrix, the first row of the y transfer matrix, and the second row of the y transfer matrix comprise the matrix elements to be placed on these cards. The location of these elements follow.

columns	card #1	card #2	card #3
1-15	MX_{11}	MX_{22}	MY_{13}
16-30	MX_{12}	MX_{23}	MY_{21}
31-45	MX_{13}	MY_{11}	MY_{22}
46-60	MX_{21}	MY_{12}	MY_{23}

7. MAGNET cards

Following the call card, BELL, a card must appear for each quadrupole magnet to be entered into the BELL calculations, resulting in the construction of the gradient array. There may be no more than ten such cards. This group is followed by a single card containing ZEND in columns 2-15 with no other punches on the card. The magnet cards are read by the format statement (I1,5F14.6); the significance of the fields is as follows.

column	field description
1	IC; IC is any positive integer (0 for ZEND card only).
2-15	ZMID, the location of the midpoint of the magnet, in inches, relative to an arbitrary starting point. In order to allow an adequate length for the fringing field, the center of the first magnet should be at least 5*BORE from this starting point.

16-29 ZLONG, the physical length of the magnet, in inches.

30-43 FR; the plateau region of the magnet, where the gradient is constant, extends to a distance FR*BORE from each end of the magnet. Beyond this point the gradient falls from its value in the plateau region.

44-57 BW, the half width characteristic of the extent of the fringing field, in inches. The gradient falls to 1/4 of its value in the plateau region at a distance BW from either end of the plateau.

58-71 EX, the relative excitation of the magnet. The gradient in the plateau region is EX*GRAD.

8. TRAJECTORY Cards.

The cards read by subroutine RKY3, giving the initial displacements and slopes of the trajectories to be integrated, are read by the format statement (I2,5F14.6). Immediately following the call card, READ, a single card is placed, containing DRIN in columns 3 through 16 and DROUT in columns 17 through 30; DRIN and DROUT are the initial and final drift distances, in inches, to the points z=0 and z= ZEND, respectively.

The remainder of the cards is to be punched as follows:

columns	field description
1-2	IC; IC=0 (blank), except for the last card for which IC=1.
3-16	x_o, the initial displacement in x, in inches.
17-30	y_o, the initial displacement in y, in inches.
31-44	x_o', the initial slope in the x-z plane.
45-58	y_o', the initial slope in the y-z plane.
59-72	$(p-p_0)/p$, the relative momentum.

The first two cards give the initial conditions for the two trajectories which will be calculated from the linearized equations. A maximum of 25 trajectories can be integrated.

9. ASSIGN Cards

The ASSIGN cards are called by the optimizing routines, DESIGN, REFINE, and FOCUS, and also be the call card ASSIGN for the purpose of instructing the code which parameters of the beam system may be varied, which dummy variable, VAR(k), is to be assigned to each parameter being varied, and the limits that are to be imposed upon the parameters being varied. There must be one ASSIGN card for each beam element containing a parameter that is to be adjusted. Two ASSIGN cards are therefore required for bending magnets if all the parameters are to be varied. The group of ASSIGN cards must be followed by a single card containing the integer -1 in the first two columns. The format for the ASSIGN cards is (4I2, 2X4F15.6). The cards are to be punched as follows.

columns	field description
1-2	k, the element number for this card (right-adjusted).
3-4	ITT; ZL(k) will be varied in proportion to VAR(ITT(k)); ITT=0 (or blank) prevents ZL(k) from being altered.
5-6	JTT; XPHI(k) will be varied in proportion to VAR(JTT(k)); JTT=0 (or blank) prevents XPHI from changing.
7-8	KTT; XPSI(k) will be varied in proportion to VAR(KTT(k)); KTT=0 (or blank) prevents XPSI(k) from being changed.

The integers used in the ITT, JTT, and KTT fields should be assigned in sequence; i.e., if 4 is punched on some card, then 1, 2, and 3 must appear on one or more ASSIGN cards. Elements, for which no ASSIGN card appears, remain unchanged in subsequent optimization calculations. We now continue with the description of the fields.

columns	field description
11-25	ZLMIN, the minimum length (must be given if ITT $\neq 0$).
26-40	ZLMAX, the maximum length (must be given if ITT $\neq 0$).
	$ZLMIN(k) \leqslant ZL(k) \leqslant ZLMAX(k)$ is the constraint imposed.
41-55	PHIMAX; must be given if JTT is not zero;
	$\lvert XPHI(k) \rvert \leqslant PHIMAX(k)$ is the constraint imposed.
56-70	PSIMAX; must be given if KTT is not zero;
	$\lvert XPSI(k) \rvert \leqslant PSIMAX(k)$ is the constraint imposed.

The constraints are ignored by FOCUS and need not be given for that routine. If the bounds are not given for any parameter which has been specified as a parameter to be varied, then that parameter is held fixed by default by both DESIGN and REFINE.

10. CONDITION Cards

Condition cards form the vehicle for entering the beam specifications to be satisfied by the optimization routines. The maximum number of conditions that may be entered is 12 (excluding assigning the aberration function to be minimized). There is one condition for each card entered. The group of CONDITION cards must be followed by a single card with the integer -1 in the first two columns. The format of the CONDITION cards is (2I2, I1, 2F15.8). The cards are to be punched as follows.

columns	field description
1-2	condition number; this labels which matrix element or

or other quantity specified as a property to be achieved. A zero (or blank) signifies an aberration function to be minimized is entered in columns 3-4. The condition number must be zero or a positive integer less than or equal to 30. Conditions 11 through 30 are described below. Conditions 1 through 10 signify that the corresponding property is to be calculated from the DEFINE function punched in column 5; this function is to be calculated after the element number punched in columns 3-4. No two cards may contain the same condition no.

3-4 These columns are ignored for conditions 11 through 30. If a DEFINE function has been specified by giving a condition number between 1 and 10, then that condition is evaluated after element k, where k is punched in columns 3-4. If condition 0 (aberration function definition) then the function to be minimized is identified in columns 3-4; this number must be taken from the "aberration function" list below.

5 Column 5, interpreted only for conditions 1 through 10, labels the DEFINE function to be used. This is the integer n on the DEFINE n card that defined the function.

6-20 The desired value for the specified quantity (MATTRY); if condition 0 is punched in columns 1-2 then the arbitrary constant ν is punched here; if blank or zero, ν will be set to 1.0 (C.4).

21-35 The weight to be used in multiplying the error in the specified quantity when summing to form the total error. If blank or zero, a weight of 1.0 is assumed.

If condition 0, then the aribtary constant μ is punched in this field. This field may not be negative (MATWT).

CONDITION List. The integers placed in the first field must be between 0 and 31. Conditions 11 through 20 refer to the x-z plane or x transfer matrix whereas conditions 21 through 30 refer to the y-z plane or y transfer matrix. Conditions 1-10 refer to "defined" functions; condition 0 defines the aberration function to be minimized.

No.	quantity specified
11, 21	the transfer matrix element T_{11}
12, 22	the transfer matrix element T_{12}
13, 23	the transfer matrix element T_{13}
14, 24	the transfer matrix element T_{21}
15, 25	the transfer matrix element T_{22}
16, 26	the transfer matrix element T_{23}
17, 27	the ratio of matrix elements, T_{11}/T_{22} [M^2 in (II-10)]
18, 28	r^2 as defined in (II-12): $r^2 = -T_{11}T_{21}/T_{12}T_{22}$.
19, 29	d, the distance to the virtual waist (II-11)
20, 30	$\bar{w}/2$, the maximum half-width in the system.

If any of the numbers 17-20 or 27-30 are specified then the object plane parameters specifying the maximum displacements and slopes must have been entered on the first card following the call card, READ, or on a subsequent sequence of OBJECT cards.

Aberration Function List. The aberration functions defined in Chapter VII are calculated. The code may be directed to minimize one of them by identifying it in columns 3-4 of the condition card with condition number 0 punched in columns 1 and 2. The numbers punched in columns 3-4 must be taken from the following list

<u>No.</u>	<u>aberration function</u>
0	RRMS≡ $(XRMS^2+YRMS^2)^{-1/2}$.
1	XRMS (VII-9),
2	YRMS (VII-9),
3	the maximum aberration displacement in x, XAMAX, (VII-5).
4	the maximum aberration displacement in y, YAMAX.
5	maximum displacement in x due to linear terms, and terms in Δx, $\Delta x'$, $\lambda^2 x$, and $\lambda^2 x'$ (elliptical distribution).
6	maximum displacement in y due to terms in y, y', Δy, ...
7	sum of (3) and (5): the maximum displacement in x.
8	sum of (4) and (6): the maximum displacement in y.
9	XRMS + $\bar{x}$ where $\bar{x}$ is the half-width due to the linear terms.
10	YRMS + $\bar{y}$ (II-8).
11	mean aberration displacement calculated by SCAN.
12	mean total displacement calculated by SCAN.

Numbers 11 and 12 are not recommended as they are very time-consuming.

11. OBJECT Cards.

Five cards follow the call card, OBJECT; these cards specify the parameters describing the object plane phase space. The format for these cards is (5F10.5). A blank in any field signifies that the corresponding parameter is to remain unchanged. The five cards refer to the coordinates x_o, y_o, x_o', y_o' and Δ, respectively. The field specifications are as follows.

column	field specification
1-10	XINF, the lower bound on the coordinate.
11-20	XSUP, the upper bound on the coordinate.
21-30	XDEL, the increment between raster values of the coord.
31-40	XMEAN, the mean value of the coordinate (normally zero)
41-50	XDEV, the standard deviation in the distribution of the coordinate. XMEAN and XDEV are required only if aberration functions 11 and 12 are to be minimized.
51-60	XMAX, the maximum initial value of the coordinate, used in plotting the phase ellipses, beam envelope, and the aberration figure; also used in the normalized aberration coefficients. The array XMAX(k) is the same array that appears on the first card following the call card, READ.

XINF(k), XSUP(k), and XINF(k) determine the trajectories to be run by SCAN by forming a raster of initial values.

12. TEST Cards.

The TEST cards are called by subroutine TEST; each card specifies a location in the memory whose contents are to be compared with the number given on the card. A test is said to have been passed if the absolute value of the difference between the stored number and the number given on the TEST card is less than or equal to the tolerance specified on the card. The format of the TEST cards is (A6, O5, 2E15.8); the field specifications are described below.

columns	field specification
1-6	Subroutine name, left adjusted, containing the number

to be examined.

7-11 Location of the number being tested relative to the subroutine entry point, in octal. This is the address of the core location containing the number less the address corresponding to the subroutine name.

12-26 The value against which the stored number is being compared.

27-41 The tolerance permitted in the comparison.

The number of test cards is given in columns 7 and 8 of the call card, TEST. A defined function may be tested as all defined functions specified on condition cards are automatically calculated by TRACE.

13. PEEK Card

The call card, PEEK, causes one card to be read; this card specifies the dump limits and type of conversion for the PDUMP that is to be executed. The card, read in the format (A6,2O5,I1), is to be punched as directed below.

columns	field specification
1-6	Subroutine name.
7-11	First word address relative to entry point for subroutine.
12-16	Word-count less one.
17	Type of conversion.

14. DEFINE Cards

The first card following the call card, DEFINE n, is punched in the format (7F10.5); it contains up to seven floating-point constants. The constant punched in the kth field is referenced by the symbol (k+1). For example that number punched in columns 1-10 is referenced by the symbol 2; the number in columns 31-40 is referenced by the symbol 5.

The second card locates the parameters required for the calculation; the format for this card is (10(A1 O5)). The 1st, 7th, 13th, 19th,··· columns contain a BCD symbol (any symbol may be used). The five columns following each symbol give the octal address of the floating point number to which the symbol is to be equated; a listing of the octal address of the available parameters will be supplied with the code.

The third card, punched in the format (20A6), contains the simple arithmetic statements that define the function. Each field must be in the following format: C=A$\circledast$Bb where A, B, and C are any BCD symbols, $\circledast$ is one of the operations in the operation table (below), and b is a blank.

The calculation of the function is initiated by setting symbols 2 through 8 to the numerical values specified on the first card.

Each symbol punched on the second card is set to the number stored at the adjacent octal address. The symbols 0 and b (blank) are set to the numerical value, zero, and the symbol 1 is set to the numerical value 1.0. The arithmetic statements are then executed from left to right. The first blank statement encountered (the test is for a blank in the first column of the field) terminates calculation of the function; the value returned is the last number calculated. If all twenty statement fields are used then the calculation will cease with the twentieth statement, and the result of this statement will be returned as the value of the function. An error in formulating the function will cause an error return; an error return will be treated by the calling routine as if there were no error in the specified optical property determined by the function. This is equivalent to eliminating that specified optical property from consideration.

The function, once defined, may be used as many times as desired by the program. It may be redefined by inserting a subsequent DEFINE n card.

a. Operation Table. The operation symbols used must be listed in the following table. An attempt to use any other symbol will result in an error return. The symbols punched, the equivalent FORTRAN statement, the operation type, and the generated instructions are described in the table below.

Symbols punched	FORTRAN equivalent	op. type	generated instructions
C=A+B	C=A+B	add	CLA A, FAD B, STO C
C=A-B	C=A-B	sub	CLA A, FSB B, STO C
R=P/Q	R=P/Q	div.	CLA P, FDP Q, STQ R
Z=A*P	Z=A*B	mult.	LDQ A, FMP P, STO C
C=A B	C=A	equate	CLA A, NOP B, STO C
Z=A.P	Z=A+ABSF(P)	add mag.	CLA A, FAM P, STO Z

b. Example. Suppose that we wish to constrain the bend in element no. 3, a bending magnet, to be 35°. This type of constraint must be entered by a DEFINE function. We will define function 3 to be $\theta-35^\circ$ where θ is the angle of bend of this magnet in degrees.

The angle of bend for element no. k (a bending magnet) is calculated and stored at XCR(k+1); the XCR array is at location 71243 in COMMON, and XCR(4) is stored at 71240. We enter the following cards:

```
DEFINE 3
35.0
A71240
A=A-2
```

The equivelanet FORTRAN statement is:

FUNCTION3 = XRK(4) - 35.0 .

To enter this condition for the linear programming problem we insert the following CONDITION card

07053 ;

The condition will be labeled as condition no. 7 (arbitrary) and evaluated after element 5 (arbitrary, but must be after element 3).

If we now demand that the entrance and exit angles be the same in addition to the above specification, we define a second function, say function no. 5; α is stored at XPSI(k) and β is stored at XCL(k+1); the locations of α and β are 71335 and 71276, respectively. We enter the following cards to define the function as FUNCTION5=$|\alpha-\beta|$:

```
DEFINE 5
                                   (blank card)
F71335Q71726
Z=F-Q R=0.Z                                                .
```

The equivalent FORTRAN statement is

FUNCTION5 = ABSF(XPSI(k) - XCL(k+1)) .

15. ALTER Cards

The ALTER cards are read in the format (A6, O5, O12, A6, I1, **, 4A6); the ** field is the variable format field. The description of the fields follows.

column	field description
1-6	Name of subroutine--must be in CALL list (BCD text).
7-11	Octal location of word being entered relative to the entry point.
12-23	Octal mask (masked portions of selected word remain unchanged).
24-29	Variable format; this may be any legitimate FORTRAN single field format.
30	Relocation bit; no relocation if blank or zero; address relocated relative to location of altered word if a nonzero integer.
31--	Word being entered, read by variable format.
---	24 characters of text may immediately follow the above field; the location of the text depends upon the length of the field specified in the variable format.

APPENDIX III. NUMERICAL EXAMPLES

The two sample beam systems referred to in Chapter VII have been analyzed numerically both with respect to their linear properties and to their aberrations. The input deck and significant portions of the printed and plotted output are reproduced here. In describing these examples we shall try to demonstrate some of the many types of calculations the code can perform.

The beam system in the first example consists of a quadrupole magnet triplet which is adjusted to provide a point image of a point source. The physcial lengths of the magnets in the triplet are 16 in., 32 in., and 16 in., respectively. Adjacent magnets are separated by 9.25 in. Drift spaces of 275 in. intervene between the source and the effective end of the triplet, and between the other end of the triplet and the image. The beam tube passing through the triplet is eight inches in diameter.

We construct the gradient function first and then determine the effective endpoints and shape coefficients of the magnets. We shall use these data, including the fringing field shape coefficients, to construct the beam system; this beam system is written on a utility tape. We then construct a second beam system which is identical with the first except that the shape coefficients are not included; this beam system is also written on the utility tape. The first beam system is reloaded and adjusted to provide a double focus. We then calculate the aberrations for this system, which includes the fringing field shape coefficients. The second beam system is reloaded and adjusted to provide a double focus. The aberrations are calculated; plots and calculations then follow for several different examples of object-plane phase-space occupation.

We then turn to the second example, for which the beam system, consisting of two quadrupole magnets of 16 in. length, is adjusted to produce a line image of an incoming parallel beam. The bore and separation of the magnets are the same as those in the first example; the numerical values of the effective length, etc. are entered directly. We adjust this system and then calculate and list the aberrations.

A. The Input Deck

Each of the cards in the input deck, which is reproduced at the end of this section, is numbered in columns 78 to 80. Most of the cards perform obvious functions as explained in Appendix II; those that are particularly significant are described.

Card #1 is the required momentum card; this card must immediately follow the * DATA card. Cards #4 through #13 have been inserted to generate internal modifications in the code. Card #14 labels the CRT film, and numbers 15 and 16 set the IF(k) and BOOL switches to the desired initial values. Cards #17 through #21 are required to set up the gradient array; the half-width, 7.38 in., yields the observed effective length for the magnets (V-27). The beam system is loaded from the stored results of SHAPE by cards #25 through #33; this beam system is written on the utility tape, B1, as directed by cards #36 and #37. The beam system is read a second time by cards #38 through #46, dropping the shape coefficients; the initial and final drift distances of 275 in. remain unchanged as a result of placing the -1 on the corresponding cards. This system is written as the second record on utility tape B1 by card #47.

Card #52 assigns a different utility tape. The first beam system is reloaded and adjusted by the FOCUS routine to produce a double focus while maintaining symmetrical gradients (cards #53 through #64). SYSTEM is called twice to list the system properties and to produce the complete sequence of CRT plots. The aberrations are calculated and listed.

Two utility tapes are assigned by card #80. The object-plane parameters are entered on cards #81 through #86. The second system is reloaded and adjusted by cards #90 through #100. Card #108 changes the utility tape assignment for the CRT plots. The remaining cards, through card #135, list the aberrations for several different occupations of object-plane phase space.

Starting with card #206, a new beam system is read. This system is adjusted to produce a focus in the x-z plane and a parallel beam in the y-z plane.

Card #235 places the final CRT identification on the film while card #236 terminates the run, returning control to the monitor.

```
*      DATA                                                                   4P   000
8.0            1700.0          1.717341      0.1                   1.0        4P   001
TITLE                                                                         4P   002
       SAMPLE PROBLEMS FOR THE QUADRUPOLE ABERRATION CODE.                    4P   003
ALTER                                                                         4P   004
STEP  02737             F5.2     0.89    LOWER PROFILE SCALE                  4P   005
ALTER                                                                         4P   006
STEP  03010             F12.9    0.020943951  PI/150 FOR PHASE PLOT           4P   007
ALTER                                                                         4P   008
RESCAN0007300000077777012    453400200000 LXD UDRESS-1,2 REPAIR               4P   009
ALTER                                                                         4P   010
SELECT00052             012    000005070722 IOCD CHIF,,5 FOR TIMING           4P   011
ALTER                                                                         4P   012
SCAN  002140000777777777012    050000000000 SET FOR MIN X ONLY                4P   013
PREID                                                                         4P   014
SENSE                                                                         4P   015
 1       4 16363  1  14        000020000000                                   4P   016
BELL                                                                          4P   017
1      48.0         16.0       0.5           7.38               1.015498      4P   018
2      81.25        32.0       0.5           7.38              -1.02639       4P   019
3      114.5        16.0       0.5           7.38               1.015498      4P   020
       162.5                                                                  4P   021
SHAPE                                                                         4P   022
TITLE                                                                         4P   023
READ BEAM SYSTEM USING DATA DERIVED FROM GRADIENT CURVE JUST CALCULATED       4P   024
READ                                                                          4P   025
 7 .75       .75        .01430    .0093     .00025    4.0       .05           4P   026
DRIFT   275.0                                                                 4P   027
QUAD   1            1                        1            1                   4P   028
DRIFT  1                                                                      4P   029
QUAD   2            2                        2            2                   4P   030
DRIFT  2                                                                      4P   031
QUAD   3            3                        3            3                   4P   032
DRIFT   275.0                                                                 4P   033
TITLE                                                                         4P   034
PUT TWO SYSTEMS ON SAVE TAPE--ONE WITH, ONE WITHOUT FRINGING TERMS            4P   035
SAVTAP11                                                                      4P   036
SAVE                                                                          4P   037
```

```
READ                                                                         4P    038
 7 .75        .75        .01430     .0093      .00025    4.0       .05      4P    039
DRIFT -1                                                                     4P    040
QUAD   1           1                                                         4P    041
DRIFT  1                                                                     4P    042
QUAD   2           2                                                         4P    043
DRIFT  2                                                                     4P    044
QUAD   3           3                                                         4P    045
DRIFT -1                                                                     4P    046
SAVE                                                                         4P    047
SYSTEM                                                                       4P    048
PUNCH                                                                        4P    049
TITLE                                                                        4P    050
ADJUST SYSTEM TO PRODUCE DOUBLE FOCUS.  ASSIGN UTILITY TAPE, RELOAD BEST     4P    051
SAVTAP12                 B2                                                  4P    052
RELOAD1101                                                                   4P   A052
FOCUS                                                                        4P    053
 20001                                                                       4P    054
 40002                                                                       4P    055
 60001                                                                       4P    056
-1                                                                           4P    057
12                                                                           4P    058
22                                                                           4P    059
-1                                                                           4P    060
SAVE                                                                         4P    061
REPEAT0210                                                                   4P    062
FOCUS                                                                        4P    063
SAVE                                                                         4P    064
PUNCH                                                                        4P    065
RELOAD                                                                       4P    066
TITLE                                                                        4P    067
NOW EXAMINE ADJUSTED SYSTEM BY A SERIES OF PLOTS..PHASE AND PROFILE          4P    068
SYSTEM                                                                       4P    069
SENSE                                                                        4P    070
                  20         000020000000                                    4P    071
SYSTEM                                                                       4P    072
TITLE                                                                        4P    073
NOW CALCULATE AND LIST ABERRATIONS FOR THIS SYSTEM                           4P    074
SOLVE                                                                        4P    075
```

```
TITLE
ENTER PHASE SPACE DESCRIPTION AND PLOT ABERRATION PICTURES
SENSE
 1      9017293     04        004527000000
SELECT1213
OBJECT
 .75      .70       .75                 10.0       .75
 .75      .70       .75                 10.0       .75
 .01430   .014      .00572              10.0       .01430
 .0093    .009      .00372              10.0       .0093
 .00025   .0002     .00025              10.0       .00025
STATE
TITLE
LOAD SYSTEM WITH NO FRINGING FIELD TERMS FROM SAVE TAPE , DOUBLE FOCUS
RELOAD1102
DESIGN
 20001                    4.0
 40002                    4.0
 60001                    4.0
-1
12
22
-1
REPEAT0105
DESIGN
PUNCH
EJECT
SYSTEM
EJECT
SOLVE
TITLE
NOW EXAMINE A POINT SOURCE (SET MAXIMUM X AND Y TO ZERO).
SELECT1113
SENSE
                            4527000000
OBJECT
          1.0                                  0
          1.0                                  0
                    .00286
                    .00186

STATE
```

```
TITLE                                                                          4P   118
NOW ELIMINATE MOMENTUM SPREAD AND RE-EXAMINE PLOTS.                            4P   119
OBJECT                                                                         4P   120
                                                                               4P   121
                                                                               4P   122
                                                                               4P   123
                                                                               4P   124
          1.0                                  0                               4P   125
STATE                                                                          4P   126
TITLE                                                                          4P   127
NOW ELIMINATE SPREAD IN Y PRIME--POINT SOURCE WITH ANGULAR SPREAD IN X         4P   128
OBJECT                                                                         4P   129
                                                                               4P   130
                                                                               4P   131
                .00143                                                         4P   132
          1.0                                  0                               4P   133
                                                                               4P   134
STATE                                                                          4P   135
```

```
TITLE                                                                          4P   206
READ NEW BEAM SYSTEM, PRODUCING LINE IMAGE FROM PARALLEL BEAM--DOUBLET          4P   207
SENSE                                                                          4P   208
 1      4016363  1  141       004426000000                                     4P   209
READ                                                                           4P   210
 4 3.0       3.0                                       4.0       0.06          4P   211
4PLUS8  18.16        1.72         0.5                                          4P   212
DRIFT   8.51                                                                   4P   213
4PLUS8  18.16       -1.75         0.5                                          4P   214
DRIFT   275.0                                                                  4P   215
EJECT                                                                          4P   216
SYSTEM                                                                         4P   217
EJECT                                                                          4P   218
DESIGN                                                                         4P   219
 10001                          4.0                                            4P   220
 30002                          4.0                                            4P   221
-1                                                                             4P   222
11                                                                             4P   223
24                                                                             4P   224
-1                                                                             4P   225
SAVE                                                                           4P   226
REPEAT0320                                                                     4P   227
EJECT                                                                          4P   228
DESIGN                                                                         4P   229
SAVE                                                                           4P   230
EJECT                                                                          4P   231
SYSTEM                                                                         4P   232
PUNCH                                                                          4P   233
SOLVE                                                                          4P   234
POSTID                                                                         4P   235
EXIT                                                                           4P   236
```

B. The Printed Output

Each page of the printed output is numbered in the upper right-hand corner. Pages 1, 2, 23, 25, 26, 27, 28, 29, 30, 36, 56, 59, 60, and 61 are reproduced at the conclusion of this section. Most of the output is self-explanatory.

Page 23 is the output resulting from the insertion of the call card, DESIGN, for IF(18)=1. The cost coefficients, basis, primal solution, and constraint errors are listed in the same order as the corresponding linear programming constraint matrix; the first row is the cost row for the primal problem, hence the first row of each of these columns should be ignored. VAR(1) through VAR(N) correspond to rows 2 through N+1 of the constraint matrix; these numbers have been shifted for compatibility with the rest of the program. VAR(N+1) is meaningless; the remainder of the VAR column corresponds to the constraint matrix (Table I), giving the estimated upper bounds on the errors ($\hat{\lambda}_k$ and $\hat{\lambda}$). KOUT(1)≡K=3 indicates an optimal, feasible solution; any other value indicates an error. ITER is the number of linear programming iterations (the number of vertices examined).

Page 27 contains the tolerance coefficients T_i^j; i=1, 4 correspond to the four columns, each of which is arranged in the normal order with respect to j. Page 28 contains the aberration coefficients. The parameters describing the object plane phase space are reproduced at the top of page 29, followed by several characteristic numbers, and the normalized aberration coefficients (normalized according to the numbers in the column, " SCALE FACTOR").

```
(AP)        SAMPLE PROBLEMS FOR THE QUADRUPOLE ABERRATION CODE.             03/25/63    200.08 (18.70 TO GO)  PAGE  1

*** GO TO ALTER .  IF(K)=  0 0 0 0 0 0 0 0 0 0 0 0 0 0 0 0 0 0 0 0 0 0 0 0 0 0 0 0 0 0.  BOOL= 000030000020.  CHIF=    0.
SUBROUTINE STEP   LOC  2737 =ABS..17037          200707534121 HAS REPLACED 200721727024       LOWER PROFILE SCALE

*** GO TO ALTER .  IF(K)=  0 0 0 0 0 0 0 0 0 0 0 0 0 0 0 0 0 0 0 0 0 0 0 0 0 0 0 0 0 0.  BOOL= 000030000020.  CHIF=    0.
SUBROUTINE STEP   LOC  3010 =ABS..17110          173527112460 HAS REPLACED 176722306444      PI/150 FOR PHASE PLOT

*** GO TO ALTER .  IF(K)=  0 0 0 0 0 0 0 0 0 0 0 0 0 0 0 0 0 0 0 0 0 0 0 0 0 0 0 0 0 0.  BOOL= 000030000020.  CHIF=    0.
SUBROUTINE RESCAN LOC    73 =ABS.. 3355          453400202156 HAS REPLACED 050000002156     LXD UDRESS-1,2 REPAIR

*** GO TO ALTER .  IF(K)=  0 0 0 0 0 0 0 0 0 0 0 0 0 0 0 0 0 0 0 0 0 0 0 0 0 0 0 0 0 0.  BOOL= 000030000020.  CHIF=    0.
SUBROUTINE SELECT LOC    52 =ABS.. 2160          000005070722 HAS REPLACED 000004070723     IOCD CHIF,,5 FOR TIMING

*** GO TO ALTER .  IF(K)=  0 0 0 0 0 0 0 0 0 0 0 0 0 0 0 0 0 0 0 0 0 0 0 0 0 0 0 0 0 0.  BOOL= 000030000020.  CHIF=    0.
SUBROUTINE SCAN   LOC   214 =ABS.. 2672          050000077776 HAS REPLACED 030000077776     SET FOR MIN X ONLY

*** GO TO PREID .  IF(K)=  0 0 0 0 0 0 0 0 0 0 0 0 0 0 0 0 0 0 0 0 0 0 0 0 0 0 0 0 0 0.  BOOL= 000030000020.  CHIF=    0.

*** GO TO SENSE .  IF(K)=  0 0 0 0 0 0 0 0 0 0 0 0 0 0 0 0 0 0 0 0 0 0 0 0 0 0 0 0 0 0.  BOOL= 000030000020.  CHIF=    0.

*** GO TO BELL  .  IF(K)=  0 1 0 0 0 0 0 0 4 0 1 6 3 6 3 0 0 1 0 0 1 4 0 0 0 0 0 0 0 0.  BOOL= 000020000020.  CHIF=   -0.

BORE=       8.000000  THERE ARE  3 ELEMENTS.  THERE ARE  1626 GRID POINTS.  SUBROUTINE BELL.
 1 MID,L,FR,BW,EX,ZZ1,ZZ2=    48.000000     16.000000      0.500000      7.380000      1.015498     44.000000     52.000000
 2 MID,L,FR,BW,EX,ZZ1,ZZ2=    81.250000     32.000000      0.500000      7.380000     -1.026390     69.250000     93.250000
 3 MID,L,FR,BW,EX,ZZ1,ZZ2=   114.500000     16.000000      0.500000      7.380000      1.015498    110.500000    118.500000
                                                                                                CRT PLOT NO.  1

*** GO TO SHAPE .  IF(K)=  0 1 0 0 0 0 0 0 4 0 1 6 3 6 3 0 0 1 0 0 1 4 0 0 0 0 0 0 0 0.  BOOL= 000020000020.  CHIF=   -0.
```

```
(&P)        SAMPLE PROBLEMS FOR THE QUADRUPOLE ABERRATION CODE.               03/25/63    200.08 (18.42 TO GO)  PAGE  2

  CALCULATION OF EFFECTIVE MAGNET LENGTHS AND FRINGING FIELD SHAPE COEFFICIENTS FROM INPUT FIELD PLOT


**MAGNET NO.  1--- ZMID=    48.000000 INCHES.  PHISIM=  0.000772193 IN-2.  THETA= 0.504549.  DB/DR=  1.723866 KG/IN.
                                  ENTRANCE           EXIT          TOTAL      (INCHES)
PHYSICAL HALF LENGTH              8.000000        8.000000      16.000000
EFFECTIVE HALF LENGTH             9.758645        8.398185      18.156830
EFFECTIVE LENGTH INCREASE         1.758645        0.398185       2.156830
SHAPE COEFFICIENT                -9.814498        2.596170

LOCATION OF EFFECTIVE ENDS       38.241355       56.398185
REGION OF INTEGRATION--- FROM     0.         TO  60.609845

                                                                                          CRT PLOT NO.  2

**MAGNET NO.  2--- ZMID=    81.250000 INCHES.  PHISIM= -0.000783972 IN-2.  THETA= 0.915247.  DB/DR= -1.750168 KG/IN.
                                  ENTRANCE           EXIT          TOTAL      (INCHES)
PHYSICAL HALF LENGTH             16.000000       16.000000      32.000000
EFFECTIVE HALF LENGTH            16.343945       16.343952      32.687897
EFFECTIVE LENGTH INCREASE         0.343945        0.343952       0.687897
SHAPE COEFFICIENT                -2.916457        2.916432

LOCATION OF EFFECTIVE ENDS       64.906054       97.593952
REGION OF INTEGRATION--- FROM    60.609845   TO 101.890156

                                                                                          CRT PLOT NO.  3

**MAGNET NO.  3--- ZMID=   114.500000 INCHES.  PHISIM=  0.000772193 IN-2.  THETA= 0.504549.  DB/DR=  1.723866 KG/IN.
                                  ENTRANCE           EXIT          TOTAL      (INCHES)
PHYSICAL HALF LENGTH              8.000000        8.000000      16.000000
EFFECTIVE HALF LENGTH             8.398183        9.758647      18.156830
EFFECTIVE LENGTH INCREASE         0.398183        1.758647       2.156830
SHAPE COEFFICIENT                -2.596169        9.814500

LOCATION OF EFFECTIVE ENDS      106.101817      124.258647
REGION OF INTEGRATION--- FROM   101.890156   TO 162.500000

                                                                                          CRT PLOT NO.  4

*** GO TO TITLE .  IF(K)=  0 1 0 0 0 0 0 0 4 0 1 6 3 6 3 0 0 1 0 0 1 4 0 0 0 0 0 0 0 0.  BOOL= 00002000002O.  CHIF=   -0.
```

```
(3P) LOAD SYSTEM WITH NO FRINGING FIELD TERMS FROM SAVE TAPE , DOUBLE FOCUS   03/25/63    200.08 (15.47 TO GO)  PAGE 23

  THE VARIABLE ASSIGNMENT FOR THE FOLLOWING LP ITERATIONS IS....
ELEMENT NUMBER  1  DRIFT   ZL= ZL                    PHI= PHI                       PSI= PSI
ELEMENT NUMBER  2  QUAD    ZL= ZL                    PHI= PHI*(1.0 + VAR(01))       PSI= PSI
ELEMENT NUMBER  3  DRIFT   ZL= ZL                    PHI= PHI                       PSI= PSI
ELEMENT NUMBER  4  QUAD    ZL= ZL                    PHI= PHI*(1.0 + VAR(02))       PSI= PSI
ELEMENT NUMBER  5  DRIFT   ZL= ZL                    PHI= PHI                       PSI= PSI
ELEMENT NUMBER  6  QUAD    ZL= ZL                    PHI= PHI*(1.0 + VAR(01))       PSI= PSI
ELEMENT NUMBER  7  DRIFT   ZL= ZL                    PHI= PHI                       PSI= PSI

  THE  2 CONDITIONS TO BE MET ARE....
CONDITION NO. 22.  DESIRED VALUE=  -0.          .  INITIAL VALUE=   0.54151535E 00.  ERROR=   0.54151535E 00.  WT=  0.1000E 01
CONDITION NO. 12.  DESIRED VALUE=  -0.          .  INITIAL VALUE=  -0.55292778E 01.  ERROR=  -0.55292778E 01.  WT=  0.1000E 01

NO.          SOLUTION          COST. COEFF.      BASIS         PRIMAL SOL.        CONST. ERRORS
 *            VAR(I)              B(I)           JH(I)            X(I)                Y(I)
  1         -0.00399715       0.                    0      -0.22272012E-07      -0.29802322E-07
  2         -0.00224694       0.                    6       0.26919759E 03      -0.12207031E-03
  3          0.               0.                    5       0.30633350E 02       0.24414063E-03
  4         -0.00000060       0.09999999E 01        7       0.30633350E 02      -0.12293458E-06
  5          0.00000004       0.09999999E 01        8       0.26919759E 03      -0.23841858E-06
  6          0.00000004       0.10100000E 02       10       0.10100000E 02       0.

NEW ERROR=         0.00675964   INITIAL ERROR=         6.07079315   CALC. IMPROVEMENT=         0.00000003   VAR FACTOR=  0.998413
INFIX...INFLAG=  4          N= 10         ME=  6         M=  6        MF=  2         MC=  1        NCUT=100       NVER=  0
      KOUT...K=  3  (WANT 3)           ITER=  5       INVC=  5     NUMVR=  1       NUMPV=  7        INFS=  0         JT=  0

*** GO TO REPEAT.  IF(K)=  0 1 0 0 0 0 0 0 9 0 1 7 2 9 3 0 0 1 0 0 0 4 0 0 0 0 0 0 0 0.  BOOL= 004527040020.  CHIF=    0.0

REPEAT THE NEXT   1 CARDS   5 TIMES.

*** GO TO DESIGN.  IF(K)=  0 1 0 0 0 0 0 0 9 0 1 7 2 9 3 0 0 1 0 0 0 4 0 0 0 0 0 0 0 0.  BOOL= 004527040020.  CHIF=    0.0

  THE  2 CONDITIONS TO BE MET ARE....
CONDITION NO. 22.  DESIRED VALUE=  -0.          .  INITIAL VALUE=  -0.65803528E-02.  ERROR=  -0.65803528E-02.  WT=  0.1000E 01
CONDITION NO. 12.  DESIRED VALUE=  -0.          .  INITIAL VALUE=   0.17929077E-03.  ERROR=   0.17929077E-03.  WT=  0.1000E 01

NO.          SOLUTION          COST. COEFF.      BASIS         PRIMAL SOL.        CONST. ERRORS
 *            VAR(I)              B(I)           JH(I)            X(I)                Y(I)
  1         -0.00000133       0.                    0      -0.27049853E-05       0.
  2         -0.00000238       0.                    6       0.80341813E 01      -0.15258789E-04
  3          0.               0.                    5       0.25670392E 02       0.30517578E-04
  4         -0.00000022       0.09999999E 01        7       0.25670391E 02      -0.35762787E-06
  5         -0.00000021       0.09999999E 01        8       0.80341813E 01      -0.48428774E-07
  6         -0.00000022       0.10100000E 02        9       0.10100000E 02       0.

NEW ERROR=         0.00003433   INITIAL ERROR=         0.00675964   CALC. IMPROVEMENT=        -0.                  VAR FACTOR=  0.997925
INFIX...INFLAG=  4          N= 10         ME=  6         M=  6        MF=  2         MC=  1        NCUT=100       NVER=  0
      KOUT...K=  3  (WANT 3)           ITER=  5       INVC=  5     NUMVR=  1       NUMPV=  7        INFS=  0         JT=  0

*** GO TO DESIGN.  IF(K)=  0 1 0 0 0 0 0 0 9 0 1 7 2 9 3 0 0 1 0 0 0 4 0 0 0 0 0 0 0 0.  BOOL= 004527040020.  CHIF=    0.0

  THE  2 CONDITIONS TO BE MET ARE....
CONDITION NO. 22.  DESIRED VALUE=  -0.          .  INITIAL VALUE=  -0.34332275E-04.  ERROR=  -0.34332275E-04.  WT=  0.1000E 01
CONDITION NO. 12.  DESIRED VALUE=  -0.          .  INITIAL VALUE=  -0.               .  ERROR=  -0.               .  WT=  0.1000E 01

NO.          SOLUTION          COST. COEFF.      BASIS         PRIMAL SOL.        CONST. ERRORS
 *            VAR(I)              B(I)           JH(I)            X(I)                Y(I)
  1         -0.00000001       0.                    0      -0.55721726E-09      -0.32672742E-05
  2         -0.00000001       0.                    6       0.21944452E 02       0.23363705E 03
  3          0.               0.                    8       0.21533453E 02      -0.39278083E 03
```

```
(4P) LOAD SYSTEM WITH NC FRINGING FIELD TERMS FROM SAVE TAPE , DOUBLE FOCUS   03/25/63    200.06 (15.44 TO GO)  PAGE 25

*** GC TO SYSTEM.  IF(K)=  0 1 0 0 0 0 0 0 9 0 1 7 2 9 3 0 0 1 0 0 0 4 0 0 0 0 0 0 0 0.  ECOL= 004527040020.  CHIF=    0.0

*****  THE SYSTEM NOW UNDER CONSIDERATION CONSISTS OF THE FOLLOWING ELEMENTS...


K   LENGTH          P= 1700.00 MEV/C.
1  275.0000  DRIFT SPACE
2   18.1568  QUADRUPOLE  MAGNET    PHI=  0.769112E-03  THETA= 0.503541  DB/DR=  1.716985  CL= -0.        CR= -0.
3    8.5079  DRIFT SPACE
4   32.6879  QUADRUPOLE  MAGNET    PHI= -0.782216E-03  THETA= 0.914219  DB/DR= -1.746238  CL= -C.        CR= -0.
5    8.5079  DRIFT SPACE
6   18.1568  QUADRUPOLE  MAGNET    PHI=  0.769112E-03  THETA= 0.503541  DB/DR=  1.716985  CL= -0.        CR= -0.
7  275.0000  DRIFT SPACE

THE TOTAL LENGTH IS  636.0173 INCHES.
                                                                                                  CRT PLOT NO. 23
K=  1  BEAM HALF WIDTHS AT Z=   55.0000 INCHES=  1.086776 INCHES IN X PLANE AND  0.907817 INCHES IN Y PLANE.
K=  1  BEAM HALF WIDTHS AT Z=  110.0000 INCHES=  1.742650 INCHES IN X PLANE AND  1.268475 INCHES IN Y PLANE.
K=  1  BEAM HALF WIDTHS AT Z=  165.0000 INCHES=  2.475831 INCHES IN X PLANE AND  1.707978 INCHES IN Y PLANE.
K=  1  BEAM HALF WIDTHS AT Z=  220.0000 INCHES=  3.234164 INCHES IN X PLANE AND  2.179132 INCHES IN Y PLANE.
K=  1  BEAM HALF WIDTHS AT Z=  275.0000 INCHES=  4.003381 INCHES IN X PLANE AND  2.665203 INCHES IN Y PLANE.

FIRST ORDER SOLUTIONS THROUGH ELEMENT  1                   DCHI=  0.              0.              0.              0.
CHI  0.09999999E 01  0.09999999E 01  0.27500000E 03  0.27500000E 03  0.              0.              0.09999999E 01  0.09999999E 01
VIRTUAL WAISTS...X PLANE--LOC= -275.000 IN., XMAX=  0.7500 IN.          Y PLANE--LOC= -275.000 IN., YMAX=  0.7500 IN.
K=  2  BEAM HALF WIDTHS AT Z=  278.6314 INCHES=  4.034031 INCHES IN X PLANE AND  2.711208 INCHES IN Y PLANE.
K=  2  BEAM HALF WIDTHS AT Z=  282.2627 INCHES=  4.023825 INCHES IN X PLANE AND  2.784766 INCHES IN Y PLANE.
K=  2  BEAM HALF WIDTHS AT Z=  285.8941 INCHES=  3.972867 INCHES IN X PLANE AND  2.886622 INCHES IN Y PLANE.
K=  2  BEAM HALF WIDTHS AT Z=  289.5254 INCHES=  3.881674 INCHES IN X PLANE AND  3.017805 INCHES IN Y PLANE.
K=  2  BEAM HALF WIDTHS AT Z=  293.1568 INCHES=  3.751172 INCHES IN X PLANE AND  3.179644 INCHES IN Y PLANE.

FIRST ORDER SOLUTIONS THROUGH ELEMENT  2                   DCHI=  0.              0.             -0.              0.
CHI  0.87587942E 00  0.11294782E 01  0.25826605E 03  0.32954041E 03 -0.13381942E-01  0.14562293E-01 -0.28041547E 01  0.51341089E 01
VIRTUAL WAISTS...X PLANE--LOC=   90.530 IN., XMAX=  0.2595 IN.          Y PLANE--LOC=  -64.852 IN., YMAX=  0.1424 IN.
K=  3  BEAM HALF WIDTHS AT Z=  294.8584 INCHES=  3.681007 INCHES IN X PLANE AND  3.262906 INCHES IN Y PLANE.
K=  3  BEAM HALF WIDTHS AT Z=  296.5600 INCHES=  3.610848 INCHES IN X PLANE AND  3.346173 INCHES IN Y PLANE.
K=  3  BEAM HALF WIDTHS AT Z=  298.2615 INCHES=  3.540697 INCHES IN X PLANE AND  3.429443 INCHES IN Y PLANE.
K=  3  BEAM HALF WIDTHS AT Z=  299.9631 INCHES=  3.470553 INCHES IN X PLANE AND  3.512717 INCHES IN Y PLANE.
K=  3  BEAM HALF WIDTHS AT Z=  301.6647 INCHES=  3.400417 INCHES IN X PLANE AND  3.595993 INCHES IN Y PLANE.

FIRST ORDER SOLUTIONS THROUGH ELEMENT  3                   DCHI= -0.              0.             -0.              0.
CHI  0.76202759E 00  0.12533723E 01  0.23440866E 03  0.37322074E 03 -0.13381942E-01  0.14562293E-01 -0.28041547E 01  0.51341089E 01
VIRTUAL WAISTS...X PLANE--LOC=   82.022 IN., XMAX=  0.2595 IN.          Y PLANE--LOC=  -73.359 IN., YMAX=  0.1424 IN.
K=  4  BEAM HALF WIDTHS AT Z=  308.2022 INCHES=  3.186528 INCHES IN X PLANE AND  3.854253 INCHES IN Y PLANE.
K=  4  BEAM HALF WIDTHS AT Z=  314.7398 INCHES=  3.079620 INCHES IN X PLANE AND  3.984053 INCHES IN Y PLANE.
K=  4  BEAM HALF WIDTHS AT Z=  321.2774 INCHES=  3.076123 INCHES IN X PLANE AND  3.981063 INCHES IN Y PLANE.
K=  4  BEAM HALF WIDTHS AT Z=  327.8150 INCHES=  3.175922 INCHES IN X PLANE AND  3.845382 INCHES IN Y PLANE.
K=  4  BEAM HALF WIDTHS AT Z=  334.3526 INCHES=  3.382347 INCHES IN X PLANE AND  3.581537 INCHES IN Y PLANE.

FIRST ORDER SOLUTIONS THROUGH ELEMENT  4                   DCHI= -0.              0.             -0.             -0.
CHI  0.60232607E 00  0.11774895E 01  0.23440866E 03  0.37322073E 03  0.29393774E-02 -0.18877193E-01  0.28041547E 01 -0.51341091E 01
VIRTUAL WAISTS...X PLANE--LOC=  -83.959 IN., XMAX=  0.2671 IN.          Y PLANE--LOC=   71.860 IN., YMAX=  0.1401 IN.
K=  5  BEAM HALF WIDTHS AT Z=  336.0541 INCHES=  3.450473 INCHES IN X PLANE AND  3.496862 INCHES IN Y PLANE.
K=  5  BEAM HALF WIDTHS AT Z=  337.7557 INCHES=  3.518607 INCHES IN X PLANE AND  3.412190 INCHES IN Y PLANE.
K=  5  BEAM HALF WIDTHS AT Z=  339.4573 INCHES=  3.586749 INCHES IN X PLANE AND  3.327521 INCHES IN Y PLANE.
K=  5  BEAM HALF WIDTHS AT Z=  341.1589 INCHES=  3.654898 INCHES IN X PLANE AND  3.242856 INCHES IN Y PLANE.
```

```
(4P) LOAD SYSTEM WITH NO FRINGING FIELD TERMS FROM SAVE TAPE , DOUBLE FOCUS   03/25/63    200.08 (15.37 TO GO)  PAGE 26
K=  5  BEAM HALF WIDTHS AT Z=  342.8604 INCHES=  3.723054 INCHES IN X PLANE AND  3.158196 INCHES IN Y PLANE.

FIRST ORDER SOLUTIONS THROUGH ELEMENT  5                      DCHI= -0.            -0.            -0.            -0.
CHI  0.62733389E 00  0.10168848E 01  0.25826603E 03  0.32954042E 03  0.29393774E-02 -0.18877193E-01  0.28041547E 01 -0.51341091E 01
VIRTUAL WAISTS...X PLANE--LOC=  -92.467 IN., XMAX=  0.2671 IN..           Y PLANE--LOC=   63.353 IN., YMAX=  0.1401 IN.
K=  6  BEAM HALF WIDTHS AT Z=  346.4918 INCHES=  3.849418 INCHES IN X PLANE AND  2.993258 INCHES IN Y PLANE.
K=  6  BEAM HALF WIDTHS AT Z=  350.1231 INCHES=  3.936801 INCHES IN X PLANE AND  2.858729 INCHES IN Y PLANE.
K=  6  BEAM HALF WIDTHS AT Z=  353.7545 INCHES=  3.984314 INCHES IN X PLANE AND  2.753245 INCHES IN Y PLANE.
K=  6  BEAM HALF WIDTHS AT Z=  357.3859 INCHES=  3.991477 INCHES IN X PLANE AND  2.675739 INCHES IN Y PLANE.
K=  6  BEAM HALF WIDTHS AT Z=  361.0172 INCHES=  3.958215 INCHES IN X PLANE AND  2.625427 INCHES IN Y PLANE.

FIRST ORDER SOLUTIONS THROUGH ELEMENT  6                      DCHI= -0.            -0.             0.            -0.
CHI  0.60061169E 00  0.79113036E 00  0.27499998E 03  0.27500000E 03 -0.58204059E-02 -0.65132022E-02 -0.99999982E 00 -0.10000002E 01
VIRTUAL WAISTS...X PLANE--LOC=  260.354 IN., XMAX=  0.7173 IN..           Y PLANE--LOC=  241.800 IN., YMAX=  0.6640 IN.
K=  7  BEAM HALF WIDTHS AT Z=  416.0172 INCHES=  3.153025 INCHES IN X PLANE AND  2.071601 INCHES IN Y PLANE.
K=  7  BEAM HALF WIDTHS AT Z=  471.0172 INCHES=  2.359687 INCHES IN X PLANE AND  1.535522 INCHES IN Y PLANE.
K=  7  BEAM HALF WIDTHS AT Z=  526.0172 INCHES=  1.595973 INCHES IN X PLANE AND  1.044870 INCHES IN Y PLANE.
K=  7  BEAM HALF WIDTHS AT Z=  581.0172 INCHES=  0.937331 INCHES IN X PLANE AND  0.702361 INCHES IN Y PLANE.
K=  7  BEAM HALF WIDTHS AT Z=  636.0172 INCHES=  0.750000 INCHES IN X PLANE AND  0.750000 INCHES IN Y PLANE.

FIRST ORDER SOLUTIONS THROUGH ELEMENT  7                      DCHI=  0.            -0.             0.            -0.
CHI -0.99999993E 00 -0.10000002E 01  0.26702881E-04 -0.45776367E-04 -0.58204059E-02 -0.65132022E-02 -0.99999982E 00 -0.10000002E 01
VIRTUAL WAISTS...X PLANE--LOC=  -14.646 IN., XMAX=  0.7173 IN..           Y PLANE--LOC=  -33.200 IN., YMAX=  0.6640 IN.

  THE TRANSFER MATRICES FOR THE SYSTEM ARE---

  XX                     RADIAL                        XX       XX                   VERTICAL                     XX
  XX -0.99999993E 00   0.26702881E-04   0.              XX      XX -0.10000002E 01  -0.45776367E-04  -0.              XX
 XX                                                      XX   XX                                                    XX
XX    -0.58204059E-02  -0.99999982E 00   0.               XX XX    -0.65132022E-02  -0.10000002E 01  -0.              XX
 XX                                                      XX   XX                                                    XX
  XX  0.               0.               1.0             XX      XX  0.               0.               1.0          XX
  XX                                                   XX       XX                                                XX

RADIAL FOCAL LENGTH=  0.17180932E 03 INCHES.  VERTICAL FOCAL LENGTH=  0.15353430E 03 INCHES.      X    XX  XXXX  X
  THE RADIAL OBJECT FOCAL POINT IS LOCATED -0.17180929E 03 INCHES AHEAD OF THE SYSTEM.          X    X X  X  X   X
   THE RADIAL IMAGE FOCAL POINT IS LOCATED -0.17180931E 03 INCHES BEYOND THE SYSTEM.          XXX  X  X  XXXX  XXX
 THE VERTICAL OBJECT FOCAL POINT IS LOCATED -0.15353433E 03 INCHES AHEAD OF THE SYSTEM.         X  XXXXXX X      X
  THE VERTICAL IMAGE FOCAL POINT IS LOCATED -0.15353434E 03 INCHES BEYOND THE SYSTEM.           X      X  X      X

*** GO TO EJECT .  IF(K)=  0 1 0 0 0 0 0 0 9 0 1 7 2 9 3 0 0 1 0 0 0 4 0 0 0 0 0 0 0 0.  BOOL= 004527040020.  CHIF=    0.0
```

```
(MP) LOAD SYSTEM WITH NO FRINGING FIELD TERMS FROM SAVE TAPE , DOUBLE FOCUS   03/25/63    200.08 (15.34 TO GO)  PAGE 27

*** GO TO SOLVE .  IF(K)=  0 1 0 0 0 0 0 0 9 0 1 7 2 9 3 0 0 1 0 0 0 4 0 0 0 0 0 0 0 0.  BOOL= 004527040020.  CHIF=    0.0

TOLERANCE COEFFICIENTS FOR MAGNET NO.  2--PHI=  0.000769109     LATERAL DISPLACEMENT, ROTATION, OR DIPOLE COMPONENT.
                 TERMS IN X                        TERMS IN X'                         TERMS IN Y                        TERMS IN Y'
(1.0) * MU/PHI..-0.380415E 01  SHIFT IN X   -0.875978E-02   (1.0) * NU/PHI.. 0.413411E 01  SHIFT IN Y    0.123640E-01
(XO) *DPHI/PHI..-0.364819E 01  COS(2W)-1    -0.839114E-02   (XO)  * XI/PHI..-0.790675E 01  -0.5*SIN(2W) -0.236288E-01
(XO)  * XI/PHI.. 0.792818E 01  -0.5*SIN(2W)  0.182758E-01   (YO) *DPHI/PHI.. 0.431957E 01  COS(2W)-1     0.129280E-01
(X'O)*DPHI/PHI..-0.103673E 04  COS(2W)-1    -0.238597E 01   (X'O) * XI/PHI..-0.225005E 04  -0.5*SIN(2W) -0.672684E 01
(X'O) * XI/PHI.. 0.225005E 04  -0.5*SIN(2W)  0.518944E 01   (Y'O)*DPHI/PHI.. 0.122741E 04  COS(2W)-1     0.367478E 01

TOLERANCE COEFFICIENTS FOR MAGNET NO.  4--PHI= -0.000782214     LATERAL DISPLACEMENT, ROTATION, OR DIPOLE COMPONENT.
                 TERMS IN X                        TERMS IN X'                         TERMS IN Y                        TERMS IN Y'
(1.0) * MU/PHI.. 0.560831E 01  SHIFT IN X    0.163213E-01   (1.0) * NU/PHI..-0.102682E 02  SHIFT IN Y   -0.334395E-01
(XO) *DPHI/PHI.. 0.358326E 01  COS(2W)-1     0.103751E-01   (XO)  * XI/PHI.. 0.130962E 02  -0.5*SIN(2W)  0.425974E-01
(XO)  * XI/PHI..-0.146550E 02  -0.5*SIN(2W) -0.425974E-01   (YO) *DPHI/PHI..-0.134425E 02  COS(2W)-1    -0.437642E-01
(X'O)*DPHI/PHI.. 0.123128E 04  COS(2W)-1     0.358326E 01   (X'O) * XI/PHI.. 0.450010E 04  -0.5*SIN(2W)  0.146550E 02
(X'O) * XI/PHI..-0.450010E 04  -0.5*SIN(2W) -0.130962E 02   (Y'O)*DPHI/PHI..-0.412777E 04  COS(2W)-1    -0.134425E 02

TOLERANCE COEFFICIENTS FOR MAGNET NO.  6--PHI=  0.000769109     LATERAL DISPLACEMENT, ROTATION, OR DIPOLE COMPONENT.
                 TERMS IN X                        TERMS IN X'                         TERMS IN Y                        TERMS IN Y'
(1.0) * MU/PHI..-0.380415E 01  SHIFT IN X   -0.133819E-01   (1.0) * NU/PHI.. 0.413411E 01  SHIFT IN Y    0.145623E-01
(XO) *DPHI/PHI..-0.238597E 01  COS(2W)-1    -0.839113E-02   (XO)  * XI/PHI..-0.518944E 01  -0.5*SIN(2W) -0.182758E-01
(XO)  * XI/PHI.. 0.672684E 01  -0.5*SIN(2W)  0.236288E-01   (YO) *DPHI/PHI.. 0.367478E 01  COS(2W)-1     0.129280E-01
(X'O)*DPHI/PHI..-0.103672E 04  COS(2W)-1    -0.364819E 01   (X'O) * XI/PHI..-0.225005E 04  -0.5*SIN(2W) -0.792818E 01
(X'O) * XI/PHI.. 0.225005E 04  -0.5*SIN(2W)  0.790675E 01   (Y'O)*DPHI/PHI.. 0.122741E 04  COS(2W)-1     0.431957E 01
```

```
(AP) LOAD SYSTEM WITH NC FRINGING FIELD TERMS FROM SAVE TAPE , DOUBLE FOCUS   03/25/63    200.08 (15.32 TO GO)  PAGE 28

  THE TRANSFER MATRICES FOR THE SYSTEM ARE---

   XX                     RADIAL                  XX       XX                      VERTICAL                 XX
  XX -0.99999993E 00  C.26702881E-04   0.           XX      XX -0.10000002E 01  -0.45776367E-04   0.           XX
 XX                                                  XX   XX                                                  XX
XX   -0.58204059E-C2  -0.99999982E CO   0.            XX XX   -0.65132022E-02  -0.10000002E 01   0.             XX
 XX                                                  XX   XX                                                  XX
  XX  0.              C.               1.0          XX      XX  0.              0.               1.0          XX
   XX                                             XX        XX                                              XX

 RADIAL FOCAL LENGTH=  C.17180932E C3 INCHES.  VERTICAL FOCAL LENGTH=  0.15353430E 03 INCHES.      X    XX  XXXX  X
   THE RADIAL CBJECT FOCAL POINT IS LOCATED -0.17180929E 03 INCHES AHEAD OF THE SYSTEM.           X    X X  X  X   X
    THE RADIAL IMAGE FOCAL POINT IS LOCATED -0.17180931E 03 INCHES BEYOND THE SYSTEM.            XXX  X  X  XXXX  XXX
 THE VERTICAL OBJFCT FCCAL POINT IS LOCATED -0.15353433E 03 INCHES AHEAD OF THE SYSTEM.           X  XXXXXX X      X
  THE VERTICAL IMAGE FOCAL POINT IS LOCATED -0.15353434E 03 INCHES BEYOND THE SYSTEM.              X     X  X     X

     ABERRATICN COEFFICIENTS FCR THIS QUADRUPOLE MAGNET SYSTEM----

 GENERALIZED SPHERICAL ABERRATION
        TERMS IN X                  TERMS IN Y                      TERMS IN X'                    TERMS IN Y'
X'X'X'..C333= -0.554341E 05   Y'Y'Y'..C444= -0.234240F 06   X'X'X'..DC333= -0.161324E 03   Y'Y'Y'..DC444= -0.762826E 03
X'Y'Y'..C443= -0.304661E 06   Y'X'X'..C433= -0.304661E 06   X'Y'Y'..DC443= -0.886626E 03   Y'X'X'..DC433= -0.992160E 03

 GENERALIZED COMA
        TERMS IN X                  TERMS IN Y                      TERMS IN X'                    TERMS IN Y'
XX'X'...C331= -0.483973E 03   YY'Y'...C442= -0.228848E 04   XX'X'...DC331= -0.136125E 01   YY'Y'...DC442= -0.744018E 01
YY'Y'...C432= -0.198432E 04   XY'X'...C431= -0.177325E 04   YX'Y'...DC432= -0.574123E 01   XY'X'...DC431= -0.574054E 01
XY'Y'...C441= -0.886626E C3   YX'X'...C332= -0.992160E 03   XY'Y'...DC441= -0.247989E 01   YX'X'...DC332= -0.321583E 01

 GENERALIZED ASTIGMATISM
        TERMS IN X                  TERMS IN Y                      TERMS IN X'                    TERMS IN Y'
XXX'....C311= -0.146440E 01   YYY'....C422= -0.747490E 01   XXX'....DC311= -0.398694E-02   YYY'....DC422= -0.242615E-01
XYY'....C421= -0.581483E 01   YXX'....C321= -0.581483F 01   XYY'....DC421= -0.161710E-01   YXX'....DC321= -0.187364E-01
YYX'....C322= -0.324956E 01   XXY'....C411= -0.268354F 01   YYX'....DC322= -0.934766E-02   XXY'....DC411= -0.863960E-02

 GENERALIZED DISTORTICN
        TERMS IN X                  TERMS IN Y                      TERMS IN X'                    TERMS IN Y'
XXX.....C111= -0.152909E-02   YYY.....C222= -0.816254E-02   XXX.....DC111= -0.403850E-05   YYY.....DC222= -0.264502E-04
XYY.....C221= -0.958733E-02   YXX.....C211= -0.885579E-02   XYY.....DC221= -0.265138E-04   YXX.....DC211= -0.283781E-04

 GENERALIZED CHRCMATIC ABERRATICN
 SECCND CRDER TERMS IN CELTA *CHI
        TERMS IN X                  TERMS IN Y                      TERMS IN X'                    TERMS IN Y'
X*DELP...C51=  0.245090E 01   Y*DELP...C52=  0.544813E 01   X*DELP...DC51=  0.640712E-02   Y*DELP...DC52=  0.179082E-01
X'*DELP..C53=  0.842174E 03   X'*DELP..C54=  0.167295E 04   X'*DELP..DC53=  0.245090E 01   Y'*DELP..DC54=  0.544813E 01
 THIRD ORDER TERMS IN DELTASQ*CHI
        TERMS IN X                  TERMS IN Y                      TERMS IN X'                    TERMS IN Y'
X*DSQ...C551=  0.368966E-00   Y*DSQ...C552= -0.411663E 01   X*DSQ...DC551=  0.236067E-02   Y*DSQ...DC552= -0.138147E-01
X'*DSQ..C553=  0.218095E C2   Y'*DSQ..C554= -0.122151E 04   X'*DSQ..DC553=  0.368966E-00   Y'*DSQ..DC554= -0.411662E 01

 FRINGING FIELD ABERRATIONS
 THE SECCND ORDER ABERRATIONS DUE TC THE FRINGING FIELD ARE ELIMINATED BY THE CORRECT CHOICE OF THE EFFECTIVE LENGTH.
 THIRD ORDER TERMS IN LAMBDA*LAMBDA*CHI
        TERMS IN X                  TERMS IN Y                      TERMS IN X'                    TERMS IN Y'
LLX.....FLL1=  0.             LLY.....FLL2=  0.             LLX.....DFLL1= -0.             LLY.....DFLL2=  0.
LLX'....FLL3=  0.             LLY'....FLL4=  0.             LLX'....DFLL3=  0.             LLY'....DFLL4=  0.
```

```
(4P) LOAD SYSTEM WITH NC FRINGING FIELD TERMS FROM SAVE TAPE , DOUBLE FOCUS   03/25/63    200.08 (15.31 TO GO)  PAGE 29

         LOWER BOUND    UPPER BOUND      INCREMENT     MEAN VALUE     STAND. DEV   SCALE FACTOR
X"       -0.75000000     0.70000000     0.75000000     0.              10.00000000    0.75000000
Y"       -0.75000000     0.70000000     0.75000000     0.              10.00000000    0.75000000
X'C      -0.01430000     0.01400000     0.00572000     0.              10.00000000    0.01430000
Y'C      -0.00929999     0.00900000     0.00371999     0.              10.00000000    0.00929999
D'/P     -0.00025000     0.00020000     0.00025000     0.              10.00000000    0.00025000

GIVEN PLOT SCALES...                        X,Y=  4.00000000                          X',Y'=  0.05000000
MAXIMA (WITH DISP. AND FRINGE)..           XMAX=  0.75046551    YMAX=  0.75103177   X'MAX=  0.01496018   Y'MAX=  0.01051764
MAXIMUM ABERRATION DISPLACEMENTS...       XAMAX=  0.94159422   YAMAX=  1.35238047
R.M.S. ABERRATION DISPLACEMENTS...         XRMS=  0.05267540    YRMS=  0.07282206    RRMS=  0.08987630
MAXIMUM HALF WIDTHS (TO THIRD ORDER)..   SCALEX=  1.69205973  SCALEY=  2.10341224  SCALER=  2.00000000

THE FOLLOWING COEFFICIENTS ARE NORMALIZED TO THE UNIT HYPERSPHERE

     ABERRATION COEFFICIENTS FOR THIS QUADRUPOLE MAGNET SYSTEM----

 GENERALIZED SPHERICAL ABERRATION
        TERMS IN X                  TERMS IN Y                    TERMS IN X'                   TERMS IN Y'
X'X'X'..C333= -0.162101E-00   Y'Y'Y'..C444= -0.188412E-00   X'X'X'..DC333= -0.471746E-03   Y'Y'Y'..DC444= -0.613584E-03
X'Y'Y'..C443= -0.376807E-00   Y'X'X'..C433= -0.579392E 00   X'Y'Y'..DC443= -0.109659E-02   Y'X'X'..DC433= -0.188685E-02

 GENERALIZED COMA
        TERMS IN X                  TERMS IN Y                    TERMS IN X'                   TERMS IN Y'
XX'X'...C331= -0.742257E-01   YY'Y'...C442= -0.148448E-00   XX'X'...DC331= -0.208772E-03   YY'Y'...DC442= -0.482626E-03
YY'Y'...C432= -0.197921E-00   XY'X'...C431= -0.176869E-00   YX'Y'...DC432= -0.572645E-03   XY'X'...DC431= -0.572576E-03
XY'Y'...C441= -0.575132E-01   YX'X'...C332= -0.152165E-00   XY'Y'...DC441= -0.160864E-03   YX'X'...DC332= -0.493204E-03

 GENERALIZED ASTIGMATISM
        TERMS IN X                  TERMS IN Y                    TERMS IN X'                   TERMS IN Y'
XXX'....C311= -0.117792E-01   YYY'....C422= -0.391030E-01   XXX'....DC311= -0.320699E-04   YYY'....DC422= -0.126918E-03
XYY'....C421= -0.304188E-01   YXX'....C321= -0.467730E-01   XYY'....DC421= -0.845945E-04   YXX'....DC321= -0.150711E-03
YYX'....C322= -0.261387E-01   XXY'....C411= -0.140383E-01   YYX'....DC322= -0.751903E-04   XXY'....DC411= -0.451959E-04

 GENERALIZED DISTORTION
        TERMS IN X                  TERMS IN Y                    TERMS IN X'                   TERMS IN Y'
XXX.....C111= -0.645083E-03   YYY.....C222= -0.344357E-02   XXX.....DC111= -0.170374E-05   YYY.....DC222= -0.111587E-04
XYY.....C221= -0.404465E-02   YXX.....C211= -0.373604E-02   XYY.....DC221= -0.111855E-04   YXX.....DC211= -0.119720E-04

 GENERALIZED CHROMATIC ABERRATION
 SECOND ORDER TERMS IN DELTA *CHI
        TERMS IN X                  TERMS IN Y                    TERMS IN X'                   TERMS IN Y'
X*DELP...C51=  0.459543E-03   Y*DELP...C52=  0.102153E-02   X*DELP...DC51=  0.120133E-05   Y*DELP...DC52=  0.335778E-05
X'*DELP..C53=  0.301077E-02   X'*DELP..C54=  0.388961E-02   X'*DELP..DC53=  0.876196E-05   Y'*DELP..DC54=  0.126669E-04
 THIRD ORDER TERMS IN DELTASQ*CHI
        TERMS IN X                  TERMS IN Y                    TERMS IN X'                   TERMS IN Y'
X*DSQ...C551=  0.172953E-07   Y*DSQ...C552= -0.192967E-06   X*DSQ...DC551=  0.110657E-09   Y*DSQ...DC552= -0.647566E-09
X'*DSQ..C553=  0.194922E-07   Y'*DSQ..C554= -0.710001E-06   X'*DSQ..DC553=  0.329763E-09   Y'*DSQ..DC554= -0.239279E-08

 FRINGING FIELD ABERRATIONS
 THE SECOND ORDER ABERRATIONS DUE TO THE FRINGING FIELD ARE ELIMINATED BY THE CORRECT CHOICE OF THE EFFECTIVE LENGTH.
 THIRD ORDER TERMS IN LAMBDA*LAMBDA*CHI
        TERMS IN X                  TERMS IN Y                    TERMS IN X'                   TERMS IN Y'
LLX.....FLL1=  0.             LLY.....FLL2=  0.             LLX.....DFLL1= -0.             LLY.....DFLL2=  0.
LLX'....FLL3=  0.             LLY'....FLL4=  0.             LLX'....DFLL3=  0.             LLY'....DFLL4=  0.
```

DISTORTION ANC COMA		SPHERICAL ABERRATION AND ASTIGMATISM		PARTIAL SUMS FOR XRMS, YRMS
X	Y	X	Y	
0.CCC03951	0.C0020629	0.00169135	0.00298886	
C.C0000000	0.000CC014	C.00032845	0.00044373	
C.CCC02296	C.CC009181	0.00000057	0.00000637	
0.0CCC0007	0.00000005	0.00059160	0.00139873	
C.CCC01378	0.C0009647	0.00000285	0.00000082	
C.CCC08161	0.C0006517	0.00000192	0.00000455	
C.74999994	0.75000018	0.00000038	0.00000042	
0.CC43653C	0.00488490	0.01430000	0.00930000	
0.75C00032	0.75000060	0.01866530	0.01418490	

CRT PLOT NO. 24
CRT PLOT NO. 25
CRT PLOT NO. 26
CRT PLOT NO. 27

```
(4P) NOW EXAMINE A POINT SOURCE (SET MAXIMUM X AND Y TO ZERO).                03/25/63    200.08 (12.60 TO GO)  PAGE 36

           LOWER BOUND     UPPER BOUND      INCREMENT      MEAN VALUE      STAND. DEV    SCALE FACTOR
X'          0.             -1.00000000      0.75000000     0.              10.00000000     0.
Y'          0.             -1.00000000      0.75000000     0.              10.00000000     0.
X'0        -0.01430000      0.01400000      0.00285999     0.              10.00000000     0.01430000
Y'0        -0.00929999      0.00900000      0.00185999     0.              10.00000000     0.00929999
DP/P       -0.00025000      0.00020000      0.00025000     0.              10.00000000     0.00025000

GIVEN PLOT SCALES...                          X,Y=  4.00000000                          X',Y'=  0.05000000
MAXIMA (WITH DISP. AND FRINGE)..             XMAX=  0.00301115   YMAX=  0.00389004   X'MAX=  0.01430876   Y'MAX=  0.00931267
MAXIMUM ABERRATION DISPLACEMENTS...         XAMAX=  0.53890777  YAMAX=  0.76780483
R.M.S. ABERRATION DISPLACEMENTS...           XRMS=  0.04971971   YRMS=  0.06761657    RRMS=  0.08392885
MAXIMUM HALF WIDTHS (TO THIRD ORDER)..     SCALEX=  0.54191893 SCALEY=  0.77169487  SCALER=  0.70000003

THE FOLLOWING COEFFICIENTS ARE NORMALIZED TO THE UNIT HYPERSPHERE

     ABERRATION COEFFICIENTS FOR THIS QUADRUPOLE MAGNET SYSTEM----

 GENERALIZED SPHERICAL ABERRATION
         TERMS IN X                  TERMS IN Y                    TERMS IN X'                  TERMS IN Y'
X'X'X'..C333= -0.162101E-00   Y'Y'Y'..C444= -0.188412E-00   X'X'X'..DC333= -0.471746E-03   Y'Y'Y'..DC444= -0.613584E-03
X'Y'Y'..C443= -0.376807E-00   Y'X'X'..C433= -0.579392E 00   X'Y'Y'..DC443= -0.109659E-02   Y'X'X'..DC433= -0.188685E-02

 GENERALIZED COMA
         TERMS IN X                  TERMS IN Y                    TERMS IN X'                  TERMS IN Y'
XX'X'...C331= -0.             YY'Y'...C442= -0.             XX'X'...DC331= -0.             YY'Y'...DC442= -0.
YX'Y'...C432= -0.             XY'X'...C431= -0.             YX'Y'...DC432= -0.             XY'X'...DC431= -0.
XY'Y'...C441= -0.             YX'X'...C332= -0.             XY'Y'...DC441= -0.             YX'X'...DC332= -0.

 GENERALIZED ASTIGMATISM
         TERMS IN X                  TERMS IN Y                    TERMS IN X'                  TERMS IN Y'
XXX'....C311= -0.             YYY'....C422= -0.             XXX'....DC311= -0.             YYY'....DC422= -0.
XYY'....C421= -0.             YXX'....C321= -0.             XYY'....DC421= -0.             YXX'....DC321= -0.
YYX'....C322= -0.             XXY'....C411= -0.             YYX'....DC322= -0.             XXY'....DC411= -0.

 GENERALIZED DISTORTION
         TERMS IN X                  TERMS IN Y                    TERMS IN X'                  TERMS IN Y'
XXX.....C111= -0.             YYY.....C222= -0.             XXX.....DC111= -0.             YYY.....DC222= -0.
XYY.....C221= -0.             YXX.....C211= -0.             XYY.....DC221= -0.             YXX.....DC211= -0.

 GENERALIZED CHROMATIC ABERRATION
 SECOND ORDER TERMS IN DELTA *CHI
         TERMS IN X                  TERMS IN Y                    TERMS IN X'                  TERMS IN Y'
X*DELP...C51=  0.             Y*DELP...C52=  0.             X*DELP...DC51=  0.             Y*DELP...DC52=  0.
X'*DELP..C53=  0.301077E-02   X'*DELP..C54=  0.388961E-02   X'*DELP..DC53=  0.876196E-05   Y'*DELP..DC54=  0.126669E-04
 THIRD ORDER TERMS IN DELTASQ*CHI
         TERMS IN X                  TERMS IN Y                    TERMS IN X'                  TERMS IN Y'
X*DSQ...C551=  0.             Y*DSQ...C552= -0.             X*DSQ...DC551=  0.             Y*DSQ...DC552= -0.
X'*DSQ..C553=  0.194922E-07   Y'*DSQ..C554= -0.710001E-06   X'*DSQ..DC553=  0.329763E-09   Y'*DSQ..DC554= -0.239279E-08

 FRINGING FIELD ABERRATIONS
 THE SECOND ORDER ABERRATIONS DUE TO THE FRINGING FIELD ARE ELIMINATED BY THE CORRECT CHOICE OF THE EFFECTIVE LENGTH.
 THIRD ORDER TERMS IN LAMBDA*LAMBDA*CHI
         TERMS IN X                  TERMS IN Y                    TERMS IN X'                  TERMS IN Y'
LLX.....FLL1=  0.             LLY.....FLL2=  0.             LLX.....DFLL1= -0.             LLY.....DFLL2=  0.
LLX'....FLL3=  0.             LLY'....FLL4=  0.             LLX'....DFLL3=  0.             LLY'....DFLL4=  0.
```

```
(AP) READ NEW BEAM SYSTEM, PRODUCING LINE IMAGE FROM PARALLEL BEAM--DOUBLET   03/25/63    200.08 (10.94 TO GO)  PAGE 56

*** GO TO SYSTEM.  IF(K)=  0 1 0 0 0 0 0 0 4 0 1 6 3 6 3 0 0 1 0 0 1 4 1 0 0 0 0 0 0 0.  BOOL= 004426040020.  CHIF=    0.0

*****  THE SYSTEM NOW UNDER CONSIDERATION CONSISTS OF THE FOLLOWING ELEMENTS...

K    LENGTH          P= 1700.00 MEV/C.
 1    18.1600  4POLE+8POLE MAGNET    PHI=  0.486662E-03  THETA= 0.400617  DB/DR=  1.086437  CL= -0.        CR= -0.
                                     PSI=  0.269046E-08  D3B/DR3=   0.500000 GAUSS/IN**3
 2     8.5100  DRIFT SPACE
 3    18.1600  4POLE+8POLE MAGNET    PHI= -0.411681E-03  THETA= 0.368465  DB/DR= -0.919048  CL= -0.        CR= -0.
                                     PSI=  0.269046E-08  D3B/DR3=   0.500000 GAUSS/IN**3
 4   275.0000  DRIFT SPACE

THE TOTAL LENGTH IS  319.8300 INCHES.
                                                                                                   CRT PLOT NO. 47
                                                                                                   CRT PLOT NO. 48
K=  1  BEAM HALF WIDTHS AT Z=     3.6320 INCHES=  2.990375 INCHES IN X PLANE AND  3.009635 INCHES IN Y PLANE.
K=  1  BEAM HALF WIDTHS AT Z=     7.2640 INCHES=  2.961564 INCHES IN X PLANE AND  3.038601 INCHES IN Y PLANE.
K=  1  BEAM HALF WIDTHS AT Z=    10.8960 INCHES=  2.913750 INCHES IN X PLANE AND  3.087085 INCHES IN Y PLANE.
K=  1  BEAM HALF WIDTHS AT Z=    14.5280 INCHES=  2.847240 INCHES IN X PLANE AND  3.155398 INCHES IN Y PLANE.
K=  1  BEAM HALF WIDTHS AT Z=    18.1600 INCHES=  2.762461 INCHES IN X PLANE AND  3.243978 INCHES IN Y PLANE.

FIRST ORDER SOLUTIONS THROUGH ELEMENT  1                        DCHI=  0.              0.              -0.             0.
CHI  0.92082047E 00  0.10813261E 01  0.17678120E 02  0.18649674E 02 -0.86032707E-02  0.90760892E-02  0.92082047E 00  0.10813261E 01
VIRTUAL WAISTS...X PLANE--LOC=  107.031 IN., XMAX= -0.      IN..          Y PLANE--LOC= -119.140 IN., YMAX= -0.      IN.
K=  2  BEAM HALF WIDTHS AT Z=    19.8620 INCHES=  2.718533 INCHES IN X PLANE AND  3.290321 INCHES IN Y PLANE.
K=  2  BEAM HALF WIDTHS AT Z=    21.5640 INCHES=  2.674605 INCHES IN X PLANE AND  3.336663 INCHES IN Y PLANE.
K=  2  BEAM HALF WIDTHS AT Z=    23.2660 INCHES=  2.630676 INCHES IN X PLANE AND  3.383006 INCHES IN Y PLANE.
K=  2  BEAM HALF WIDTHS AT Z=    24.9680 INCHES=  2.586748 INCHES IN X PLANE AND  3.429348 INCHES IN Y PLANE.
K=  2  BEAM HALF WIDTHS AT Z=    26.6700 INCHES=  2.542820 INCHES IN X PLANE AND  3.475691 INCHES IN Y PLANE.

FIRST ORDER SOLUTIONS THROUGH ELEMENT  2                        DCHI= -0.              0.              -0.             0.
CHI  0.84760663E 00  0.11585636E 01  0.25514302E 02  0.27851759E 02 -0.86032707E-02  0.90760892E-02  0.92082047E 00  0.10813261E 01
VIRTUAL WAISTS...X PLANE--LOC=   98.521 IN., XMAX= -0.      IN..          Y PLANE--LOC= -127.650 IN., YMAX= -0.      IN.
K=  3  BEAM HALF WIDTHS AT Z=    30.3020 INCHES=  2.455901 INCHES IN X PLANE AND  3.565061 INCHES IN Y PLANE.
K=  3  BEAM HALF WIDTHS AT Z=    33.9340 INCHES=  2.382326 INCHES IN X PLANE AND  3.635079 INCHES IN Y PLANE.
K=  3  BEAM HALF WIDTHS AT Z=    37.5660 INCHES=  2.321695 INCHES IN X PLANE AND  3.685366 INCHES IN Y PLANE.
K=  3  BEAM HALF WIDTHS AT Z=    41.1980 INCHES=  2.273677 INCHES IN X PLANE AND  3.715647 INCHES IN Y PLANE.
K=  3  BEAM HALF WIDTHS AT Z=    44.8300 INCHES=  2.238012 INCHES IN X PLANE AND  3.725759 INCHES IN Y PLANE.

FIRST ORDER SOLUTIONS THROUGH ELEMENT  3                        DCHI= -0.              0.              -0.             -0.
CHI  0.74600416E 00  0.12419197E 01  0.44369040E 02  0.45177934E 02 -0.27127420E-02  0.38417056E-08  0.11791331E 01  0.80520513E 00
VIRTUAL WAISTS...X PLANE--LOC=  275.000 IN., XMAX= -0.      IN..          Y PLANE--LOC=18250.000 IN., YMAX= -0.      IN.
K=  4  BEAM HALF WIDTHS AT Z=    99.8300 INCHES=  1.790410 INCHES IN X PLANE AND  3.725760 INCHES IN Y PLANE.
K=  4  BEAM HALF WIDTHS AT Z=   154.8300 INCHES=  1.342808 INCHES IN X PLANE AND  3.725760 INCHES IN Y PLANE.
K=  4  BEAM HALF WIDTHS AT Z=   209.8300 INCHES=  0.895205 INCHES IN X PLANE AND  3.725761 INCHES IN Y PLANE.
K=  4  BEAM HALF WIDTHS AT Z=   264.8300 INCHES=  0.447603 INCHES IN X PLANE AND  3.725762 INCHES IN Y PLANE.
K=  4  BEAM HALF WIDTHS AT Z=   319.8300 INCHES=  0.000000 INCHES IN X PLANE AND  3.725762 INCHES IN Y PLANE.
                                                                                                   CRT PLOT NO. 49

FIRST ORDER SOLUTIONS THROUGH ELEMENT  4                        DCHI= -0.              -0.             -0.             -0.
CHI  0.89406967E-07  0.12419207E 01  0.36863064E 03  0.26660934E 03 -0.27127420E-02  0.38417056E-08  0.11791331E 01  0.80520513E 00
VIRTUAL WAISTS...X PLANE--LOC=    0.000 IN., XMAX= -0.      IN..          Y PLANE--LOC=18319.000 IN., YMAX= -0.      IN.

  THE TRANSFER MATRICES FOR THE SYSTEM ARE---

   XX                    RADIAL                       XX       XX                       VERTICAL                       XX
  XX  0.89406967E-07    0.36863064E 03  -0.            XX      XX  0.12419207E 01   0.26660934E 03  -0.              XX
   XX                                                    XX   XX                                                         XX
  XX   -0.27127420E-02    0.11791331E 01  -0.              XX XX    0.38417056E-08   0.80520513E 00  -0.                XX
```

```
(5P) READ NEW BEAM SYSTEM, PRODUCING LINE IMAGE FROM PARALLEL BEAM--DOUBLET   03/25/63    200.08 (10.68 TO GO)  PAGE 59

*** GO TO SOLVE .  IF(K)=  0 1 0 0 0 0 0 0 4 0 1 6 3 6 3 0 0 1 0 0 1 4 1 0 0 0 0 0 0 0.  DCOL= 004426040020.  CHIF=     0.0

TOLERANCE COEFFICIENTS FOR MAGNET NO.  1--PHI=  0.000486657     LATERAL DISPLACEMENT, ROTATION, OR DIPOLE COMPONENT.
                  TERMS IN X                         TERMS IN X'                            TERMS IN Y                          TERMS IN Y'
(1.0) * MU/PHI..-0.317143E 01  SHIFT IN X   -0.103592E-01   (1.0) * NU/PHI.. 0.231877E 01  SHIFT IN Y     0.730811E-02
(X0) *DPHI/PHI..-0.308910E 01  COS(2W)-1    -0.100873E-01   (X0)  * XI/PHI..-0.451449E 01  -0.5*SIN(2W) -0.142202E-01
(Y0)  * XI/PHI.. 0.651016E 01  -0.5*SIN(2W)  0.212708E-01   (Y0) *DPHI/PHI.. 0.238129E 01  COS(2W)-1      0.750934E-02
(X'0)*DPHI/PHI..-0.280325E 02  COS(2W)-1    -0.922192E-01   (X'0) * XI/PHI..-0.415087E 02  -0.5*SIN(2W) -0.132650E-00
(Y'0) * XI/PHI.. 0.575637E 02  -0.5*SIN(2W)  0.189398E-00   (Y'0)*DPHI/PHI.. 0.213181E 02  COS(2W)-1      0.681470E-01

TOLERANCE COEFFICIENTS FOR MAGNET NO.  3--PHI= -0.000411674     LATERAL DISPLACEMENT, ROTATION, OR DIPOLE COMPONENT.
                  TERMS IN X                         TERMS IN X'                            TERMS IN Y                          TERMS IN Y'
(1.0) * MU/PHI.. 0.217143E 01  SHIFT IN X    0.764645E-02   (1.0) * NU/PHI..-0.207685E 01  SHIFT IN Y    -0.730811E-02
(X0) *DPHI/PHI.. 0.171330E 01  COS(2W)-1     0.602921E-02   (X0)  * XI/PHI.. 0.327257E 01  -0.5*SIN(2W)  0.115075E-01
(Y0)  * XI/PHI..-0.526824E 01  -0.5*SIN(2W) -0.185581E-01   (Y0) *DPHI/PHI..-0.252141E 01  COS(2W)-1     -0.887583E-02
(X'0)*DPHI/PHI.. 0.745904E 02  COS(2W)-1     0.263401E-00   (X'0) * XI/PHI.. 0.143530E 03  -0.5*SIN(2W)  0.506578E 00
(Y'0) * XI/PHI..-0.159585E 03  -0.5*SIN(2W) -0.563326E 00   (Y'0)*DPHI/PHI..-0.767152E 02  COS(2W)-1     -0.270650E-00
```

```
  THE TRANSFER MATRICES FOR THE SYSTEM ARE---

   XX                       RADIAL                          XX        XX                         VERTICAL                    XX
  XX  0.89406967E-07   0.36863064E 03   0.                  XX      XX  0.12419207E 01   0.26660934E 03   0.                  XX
 'X                                                           XX  XX                                                            XX
X'    -0.27127420E-02   0.11791331E 01   0.                    XX XX     0.38417056E-08   0.80520513E 00   0.                  XX
 'X                                                           XX  XX                                                            XX
  XX  0.             0.               1.0                   XX      XX  0.               0.               1.0                 XX
   XX                                                       XX        XX                                                       XX

 RADIAL FOCAL LENGTH=  0.36863069E 03 INCHES.  VERTICAL FOCAL LENGTH= -0.26030105E 09 INCHES.       X     XX  XXXX  X
   THE RADIAL OBJECT FOCAL POINT IS LOCATED  0.43466466E 03 INCHES AHEAD OF THE SYSTEM.             X     X X  X  X   X
    THE RADIAL IMAGE FOCAL POINT IS LOCATED  0.32958151E-04 INCHES BEYOND THE SYSTEM.              XXX  X  X  XXXX  XXX
 THE VERTICAL OBJECT FOCAL POINT IS LOCATED -0.20959573E 09 INCHES AHEAD OF THE SYSTEM.             X  XXXXXX X      X
  THE VERTICAL IMAGE FOCAL POINT IS LOCATED -0.32327327E 09 INCHES BEYOND THE SYSTEM.               X      X  X      X

     ABERRATION COEFFICIENTS FOR THIS QUADRUPOLE MAGNET SYSTEM----

 GENERALIZED SPHERICAL ABERRATION
            TERMS IN X                   TERMS IN Y                    TERMS IN X'                   TERMS IN Y'
X'X'X'..C333=  0.504372E 02   Y'Y'Y'..C444= -0.620055E 02   X'X'X'..DC333=  0.169572E-00   Y'Y'Y'..DC444= -0.210344E-00
X'Y'Y'..C443= -0.503179E 02   Y'X'X'..C433= -0.578394E 02   X'Y'Y'..DC443= -0.195692E-00   Y'X'X'..DC433= -0.191480E-00

 GENERALIZED COMA
            TERMS IN X                   TERMS IN Y                    TERMS IN X'                   TERMS IN Y'
XX'X'...C331= -0.239403E 01   YY'Y'...C442= -0.177513E 01   XX'X'...DC331= -0.813265E-02   YY'Y'...DC442= -0.632225E-02
YY'Y'...C432= -0.189554E 01   XY'X'...C431= -0.227382E 01   YX'Y'...DC432= -0.841237E-02   XY'X'...DC431= -0.671606E-02
XY'Y'...C441= -0.258729E 01   YX'X'...C332= -0.170258E 01   XY'Y'...DC441= -0.816924E-02   YX'X'...DC332= -0.676611E-02

 GENERALIZED ASTIGMATISM
            TERMS IN X                   TERMS IN Y                    TERMS IN X'                   TERMS IN Y'
XXX'....C311= -0.274779E-01   YYY'....C422= -0.587517E-01   XXX'....DC311= -0.924949E-04   YYY'....DC422= -0.206890E-03
XYY'....C421= -0.103983E-00   YXX'....C321= -0.711278E-01   XYY'....DC421= -0.346559E-03   YXX'....DC321= -0.234105E-03
YYX'....C322= -0.535877E-01   XXY'....C411= -0.288859E-01   YYX'....DC322= -0.194205E-03   XXY'....DC411= -0.110603E-03

 GENERALIZED DISTORTION
            TERMS IN X                   TERMS IN Y                    TERMS IN X'                   TERMS IN Y'
XXX.....C111= -0.630010E-03   YYY.....C222= -0.920583E-03   XXX.....DC111= -0.209259E-05   YYY.....DC222= -0.310156E-05
XYY.....C221= -0.267486E-02   YXX.....C211= -0.175941E-02   XYY.....DC221= -0.895038E-05   YXX.....DC211= -0.584273E-05

 GENERALIZED CHROMATIC ABERRATION
 SECOND ORDER TERMS IN DELTA *CHI
            TERMS IN X                   TERMS IN Y                    TERMS IN X'                   TERMS IN Y'
X*DELP...C51=  0.137580E 01   Y*DELP...C52=  0.140122E-00   X*DELP...DC51=  0.405813E-02   Y*DELP...DC52=  0.136649E-02
X'*DELP..C53= -0.465579E 02   X'*DELP..C54=  0.553972E 02   X'*DELP..DC53= -0.171182E-00   Y'*DELP..DC54=  0.202503E-00
 THIRD ORDER TERMS IN DELTASQ*CHI
            TERMS IN X                   TERMS IN Y                    TERMS IN X'                   TERMS IN Y'
X*DSQ...C551= -0.374063E-00   Y*DSQ...C552= -0.383427E-00   X*DSQ...DC551= -0.133948E-02   Y*DSQ...DC552= -0.137113E-02
X'*DSQ..C553= -0.225872E 01   Y'*DSQ..C554= -0.215942E 01   X'*DSQ..DC553= -0.800958E-02   Y'*DSQ..DC554= -0.764547E-02

 FRINGING FIELD ABERRATIONS
 THE SECOND ORDER ABERRATIONS DUE TO THE FRINGING FIELD ARE ELIMINATED BY THE CORRECT CHOICE OF THE EFFECTIVE LENGTH.
 THIRD ORDER TERMS IN LAMBDA*LAMBDA*CHI
            TERMS IN X                   TERMS IN Y                    TERMS IN X'                   TERMS IN Y'
LLX.....FLL1=  0.             LLY.....FLL2= -0.             LLX.....DFLL1=  0.             LLY.....DFLL2= -0.
LLX'....FLL3= -0.             LLY'....FLL4= -0.             LLX'....DFLL3=  0.             LLY'....DFLL4= -0.
```

```
(*P) READ NEW BEAM SYSTEM, PRODUCING LINE IMAGE FROM PARALLEL BEAM--DOUBLET   03/25/63    200.08 (10.65 TO GO)  PAGE 61

          LOWER BOUND    UPPER BOUND     INCREMENT     MEAN VALUE      STAND. DEV    SCALE FACTOR
X"        -3.00000000     2.89999998    0.50000000     0.             10.00000000     3.00000000
Y"        -3.00000000     2.89999998    0.50000000     0.             10.00000000     3.00000000
X'C        0.            -1.00000000    1.00000000     0.             10.00000000     0.
Y'C        0.            -1.00000000    1.00000000     0.             10.00000000     0.
D"/P       0.            -1.00000000    1.00000000     0.             10.00000000     0.

GIVEN PLOT SCALES...                        X,Y=  4.00000000                        X',Y'=  0.05999999
MAXIMA (WITH DISP. AND FRINGE)..           XMAX=  0.00000027    YMAX=  3.72576228   X'MAX=  0.00813822   Y'MAX=  0.00000001
MAXIMUM ABERRATION DISPLACEMENTS...       XAMAX=  0.08923147   YAMAX=  0.07235986
R.M.S. ABERRATION DISPLACEMENTS...         XRMS=  0.00754969    YRMS=  0.00694045    RRMS=  0.01025513
MAXIMUM HALF WIDTHS (TO THIRD ORDER)..   SCALEX=  0.08923174  SCALEY=  3.79812214  SCALER=  4.00000000

THE FOLLOWING COEFFICIENTS ARE NORMALIZED TO THE UNIT HYPERSPHERE

     ABERRATION COEFFICIENTS FOR THIS QUADRUPOLE MAGNET SYSTEM----

 GENERALIZED SPHERICAL ABERRATION
         TERMS IN X                      TERMS IN Y                      TERMS IN X'                     TERMS IN Y'
X'X'X'..C333=  0.              Y'Y'Y'..C444= -0.              X'X'X'..DC333=  0.               Y'Y'Y'..DC444= -0.
X'Y'Y'..C443= -0.              Y'X'X'..C433= -0.              X'Y'Y'..DC443= -0.               Y'X'X'..DC433= -0.

 GENERALIZED COMA
         TERMS IN X                      TERMS IN Y                      TERMS IN X'                     TERMS IN Y'
XX'X'...C331= -0.              YY'Y'...C442= -0.              XX'X'...DC331= -0.               YY'Y'...DC442= -0.
YY'Y'...C432= -0.              XY'X'...C431= -0.              YX'Y'...DC432= -0.               XY'X'...DC431= -0.
XY'Y'...C441= -0.              YX'X'...C332= -0.              XY'Y'...DC441= -0.               YX'X'...DC332= -0.

 GENERALIZED ASTIGMATISM
         TERMS IN X                      TERMS IN Y                      TERMS IN X'                     TERMS IN Y'
XXX'....C311= -0.              YYY'....C422= -0.              XXX'....DC311= -0.               YYY'....DC422= -0.
XYY'....C421= -0.              YXX'....C321= -0.              XYY'....DC421= -0.               YXX'....DC321= -0.
YYX'....C322= -0.              XXY'....C411= -0.              YYX'....DC322= -0.               XXY'....DC411= -0.

 GENERALIZED DISTORTION
         TERMS IN X                      TERMS IN Y                      TERMS IN X'                     TERMS IN Y'
XXX.....C111= -0.170103E-01    YYY.....C222= -0.248558E-01    XXX.....DC111= -0.564999E-04     YYY.....DC222= -0.837422E-04
XYY.....C221= -0.722212E-01    YXX.....C211= -0.475041E-01    XYY.....DC221= -0.241660E-03     YXX.....DC211= -0.157754E-03

 GENERALIZED CHROMATIC ABERRATION
 SECOND ORDER TERMS IN DELTA *CHI
         TERMS IN X                      TERMS IN Y                      TERMS IN X'                     TERMS IN Y'
X*DELP...C51=  0.              Y*DELP...C52=  0.              X*DELP...DC51=  0.               Y*DELP...DC52=  0.
X'*DELP..C53= -0.              Y'*DELP..C54=  0.              X'*DELP..DC53= -0.               Y'*DELP..DC54=  0.
 THIRD ORDER TERMS IN DELTASQ*CHI
         TERMS IN X                      TERMS IN Y                      TERMS IN X'                     TERMS IN Y'
X*DSQ...C551= -0.              Y*DSQ...C552= -0.              X*DSQ...DC551= -0.               Y*DSQ...DC552= -0.
X'*DSQ..C553= -0.              Y'*DSQ..C554= -0.              X'*DSQ..DC553= -0.               Y'*DSQ..DC554= -0.

 FRINGING FIELD ABERRATIONS
 THE SECOND ORDER ABERRATIONS DUE TO THE FRINGING FIELD ARE ELIMINATED BY THE CORRECT CHOICE OF THE EFFECTIVE LENGTH.
 THIRD ORDER TERMS IN LAMBDA*LAMBDA*CHI
         TERMS IN X                      TERMS IN Y                      TERMS IN X'                     TERMS IN Y'
LLX.....FLL1=  0.              LLY.....FLL2= -0.              LLX.....DFLL1=  0.               LLY.....DFLL2= -0.
LLX'....FLL3= -0.              LLY'....FLL4= -0.              LLX'....DFLL3=  0.               LLY'....DFLL4= -0.
```

C. The Cathode Ray Tube Display Output

Each plot produced by the computer is dated, containing the same date and time as the corresponding output page. In addition, the plots are numbered (between the date and the time) with the corresponding number appearing on the output page that contains the result of the calculations. All the plots have arbitrary scales which are printed on the plots. Grid lines represent increments of one fifth, tenth, or twentieth of that scale distance.

Plot #1 shows the gradient function constructed by subroutine BELL. Plots #2 through #4 show the division of the scalar potential into $\emptyset_s$ and $\emptyset_c$ as calculated by subroutine SHAPE. In plot #2 each vertical grid line represents an increment of 6.06". The vertical scales of the first four plots are chosen so $\emptyset_s=1$.

Plots #11 through #18 show the phase space distribution after each beam element. The x-x' plane ellipse is distinguished from the y-y' plane ellipse by the appearance of a small "x." The scales for these plots are entered in the seventh and eighth fields of the first card following the call card, READ. In this example,, each vertical line represents an increment of 0.4 in. while each horizontal line represents an increment of 0.0005 radians. Plot #23 shows both the radial and the vertical beam widths through the beam system. The heavy vertical lines separate the constituent elements. The vertical grid lines represent increments of 63.6 in. in this example. All the plots mentioned in this paragraph are produced by the call card, SYSTEM.

Plots #24 through #42 are all produced by subroutine STATE and demonstrate the nature and magnitude of the aberrations. With the exception of plot #25, they all refer to the group of orbits run by SCAN; the bounds on the initial coordinates and slopes are given immediately following the non-normalized aberration coefficients on the printed output. Plots #24 through #27 show the imaging of nine separate source points with a range of angles and momenta. Plots #32, #34, and #35 show the imaging of an axial point source with the same range of angles and momenta as in the previous plots. Plot #36 shows the image of the point source with the momentum spread eliminated. Plot #42 demonstrates the envelope traced out by trajectories in the x-z plane that issue from a point source.

Plots #45 and #48 show the beam envelope for the second system immediately before and after, respectively, adjustment of the system parameters by subroutine DESIGN. Plot #51 shows the beam envelope near the line image in the plane orthogonal to that image.

QUADRUPOLE POTENTIAL PLOT 4P
03/25/63 NO. 1 TIME 200.08

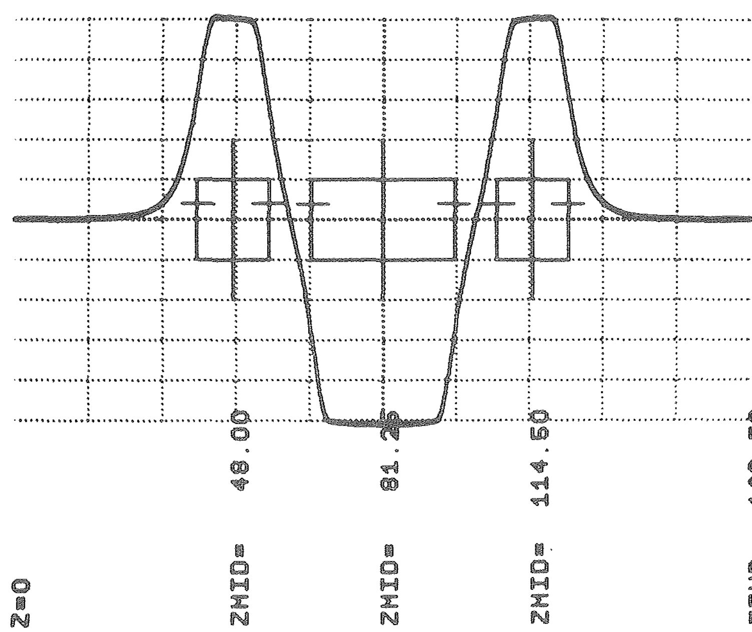

MU-30720

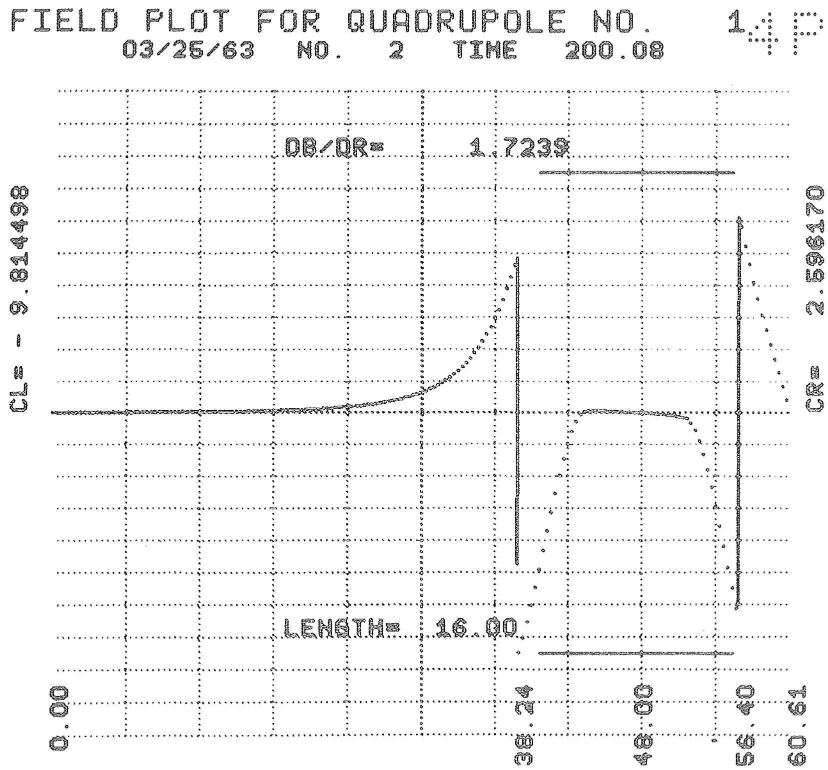

FIELD PLOT FOR QUADRUPOLE NO. 14P
03/25/63 NO. 2 TIME 200.08
DB/DR= 1.7239
LENGTH= 16.00
CL= - 9.814498
CR= 2.596170
0.00
38.24
48.00
56.40
60.61

MU-30721

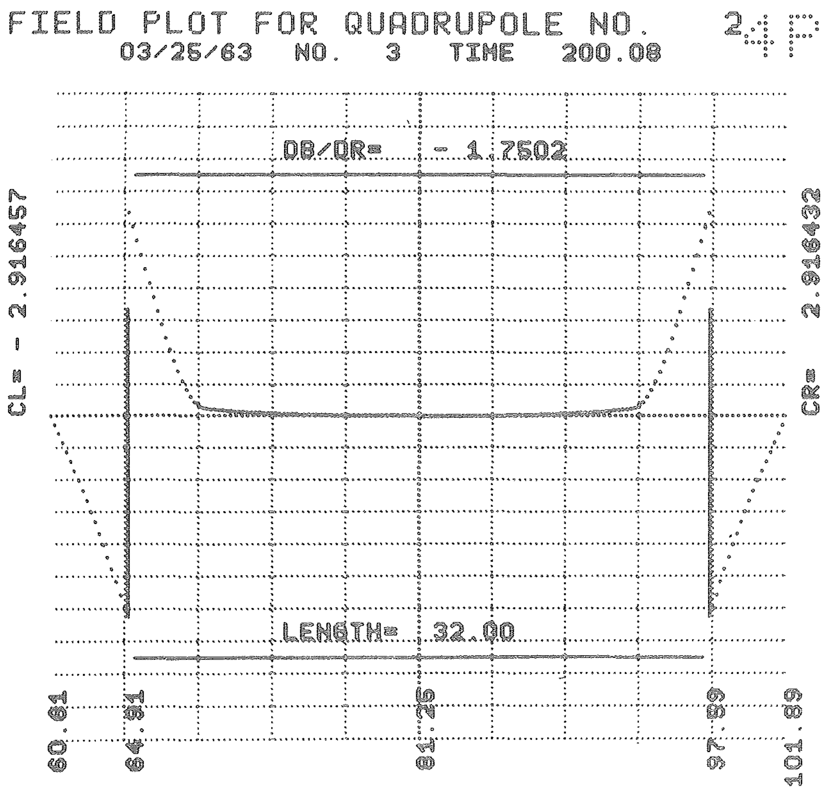

FIELD PLOT FOR QUADRUPOLE NO. 24P
03/25/63 NO. 3 TIME 200.08
DB/DR= - 1.7502
CL= - 2.916457
CR= 2.916432
LENGTH= 32.00
60.61
64.91
81.25
97.89
101.89

MU-30722

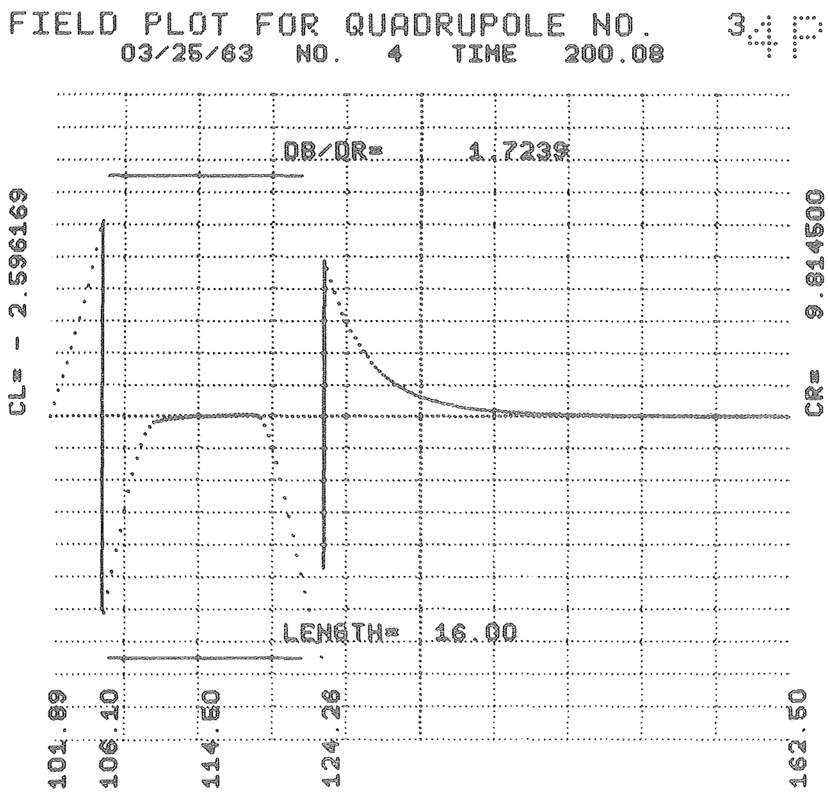
FIELD PLOT FOR QUADRUPOLE NO. 34P
03/25/63 NO. 4 TIME 200.08
DB/DR= 1.7239
CL= - 2.596169
CR= 9.814500
LENGTH= 16.00
101.89
106.10
114.60
124.28
162.50

MU-30723

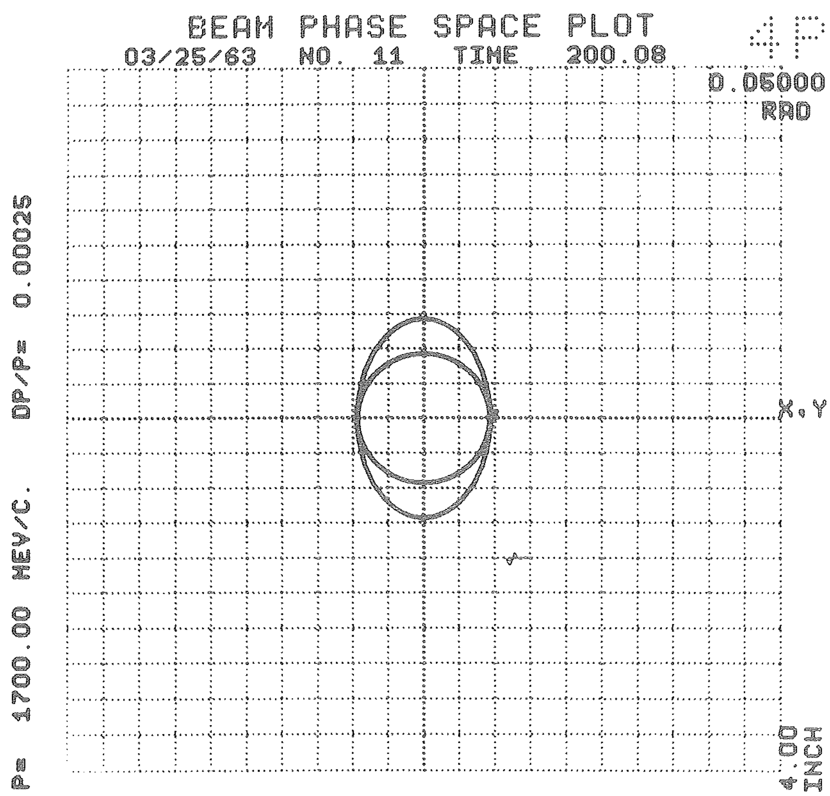
BEAM PHASE SPACE PLOT
03/25/63 NO. 11 TIME 200.08
4P
0.05000
RAD
X,Y
P= 1700.00 MEV/C. DP/P= 0.00025
4.00
INCH

MU-30724

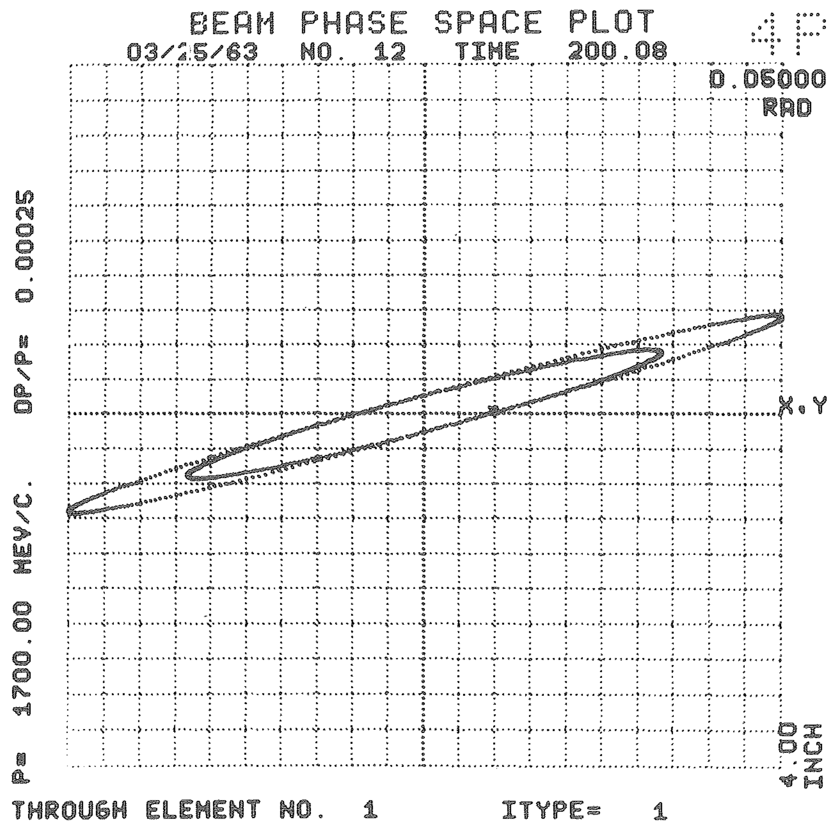
BEAM PHASE SPACE PLOT
4P
03/15/63 NO. 12 TIME 200.08
0.05000
RAD
DP/P= 0.00025
X,Y
P= 1700.00 MEV/C.
4.00
INCH
THROUGH ELEMENT NO. 1 ITYPE= 1

MU-30725

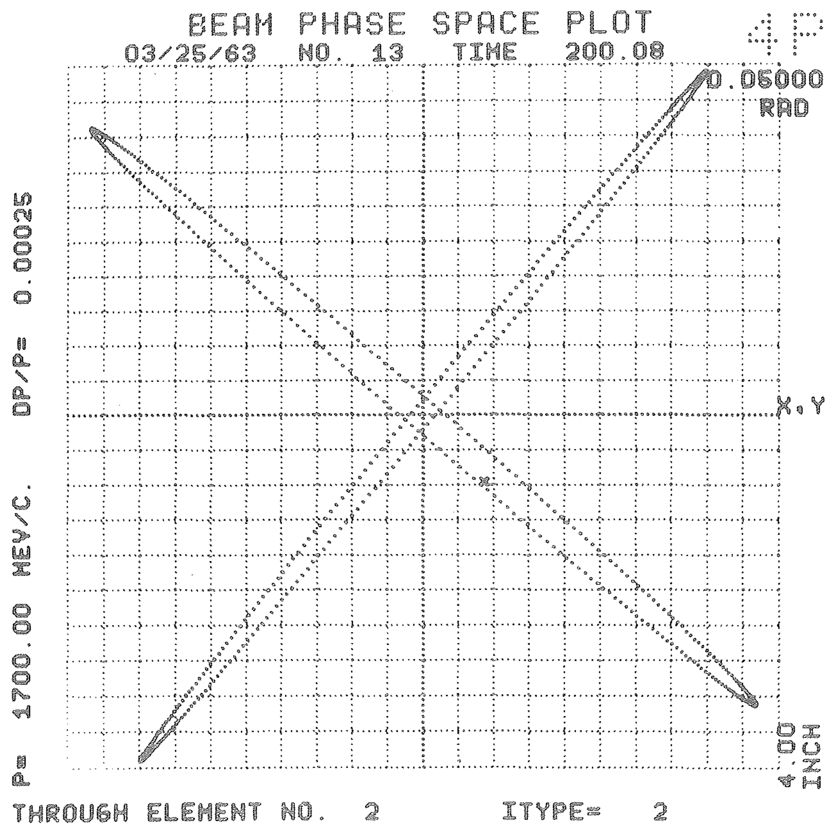
BEAM PHASE SPACE PLOT
4P
03/25/63 NO. 13 TIME 200.08
0.05000
RAD
P= 1700.00 MEV/C. DP/P= 0.00025
X,Y
4.00
INCH
THROUGH ELEMENT NO. 2 ITYPE= 2

MU-30726

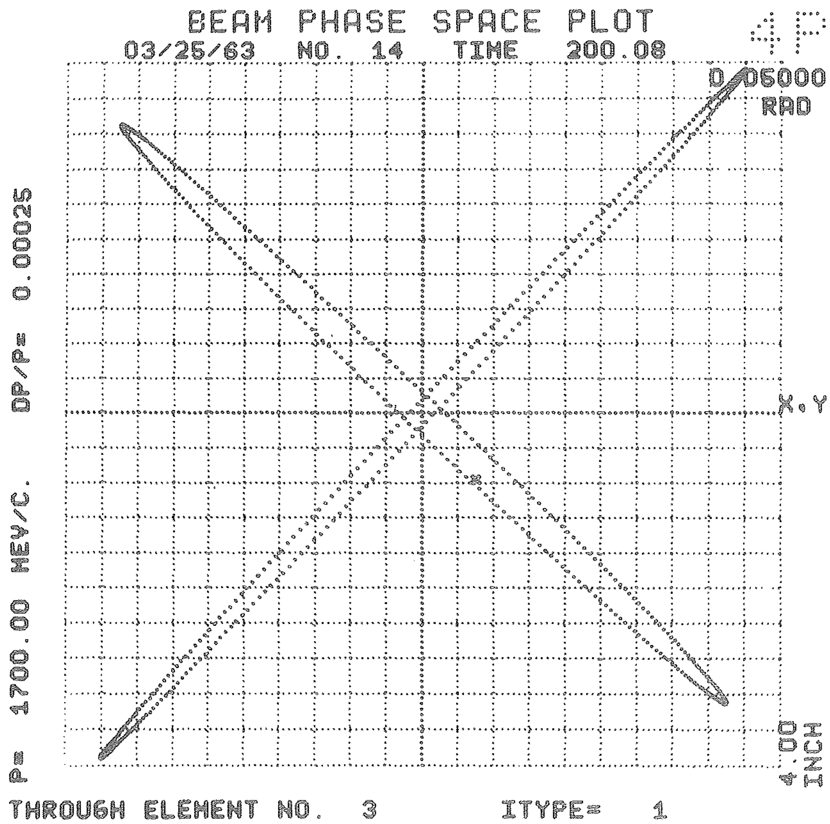
BEAM PHASE SPACE PLOT
03/25/63 NO. 14 TIME 200.08
4P
0.05000
RAD
X,Y
4.00
INCH
P= 1700.00 MEV/C. DP/P= 0.00025
THROUGH ELEMENT NO. 3 ITYPE= 1

MU-30727

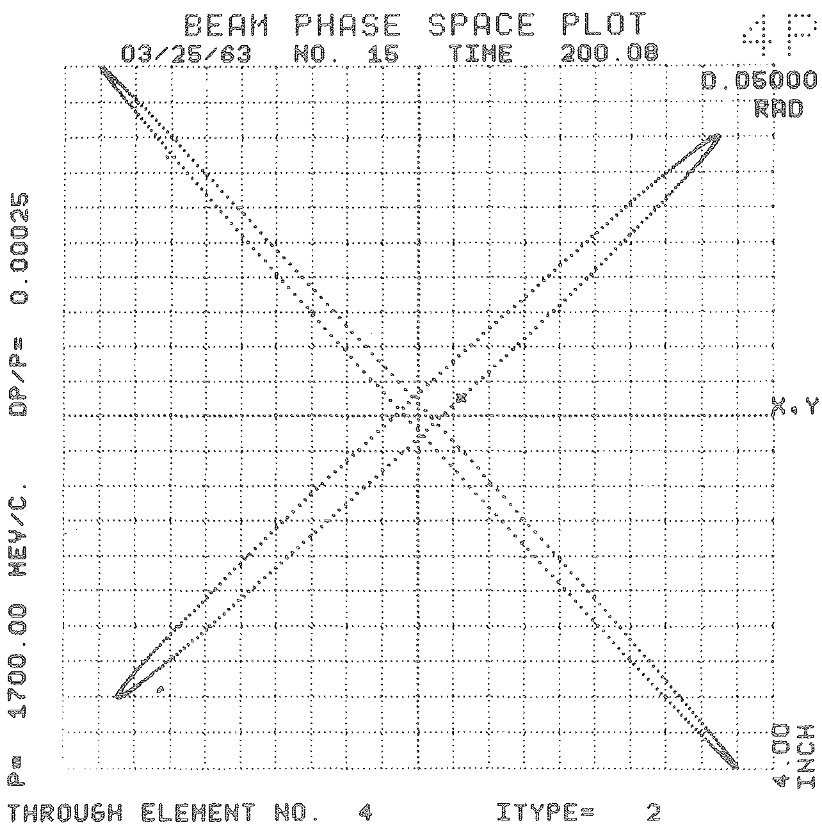

BEAM PHASE SPACE PLOT
4P
03/25/63 NO. 15 TIME 200.08
0.05000
RAD
X,Y
P= 1700.00 MEV/C. DP/P= 0.00025
4.00
INCH
THROUGH ELEMENT NO. 4 ITYPE= 2

MU-30728

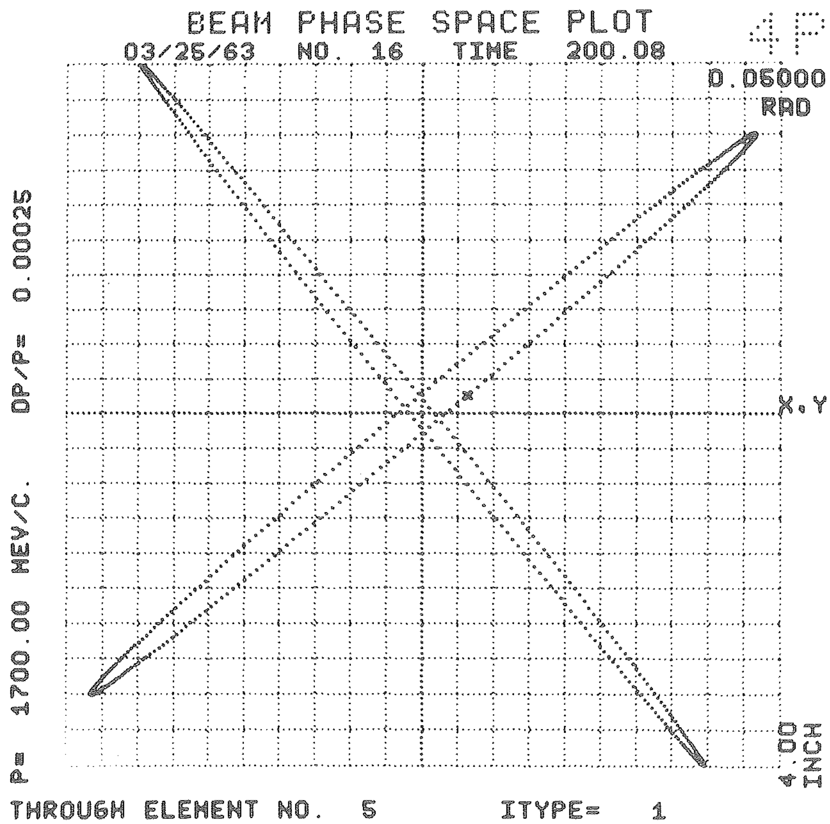
BEAM PHASE SPACE PLOT
4P
03/25/63 NO. 16 TIME 200.08
0.05000
RAD
X,Y
P= 1700.00 MEV/C. DP/P= 0.00025
4.00
INCH
THROUGH ELEMENT NO. 5 ITYPE= 1

MU-30729

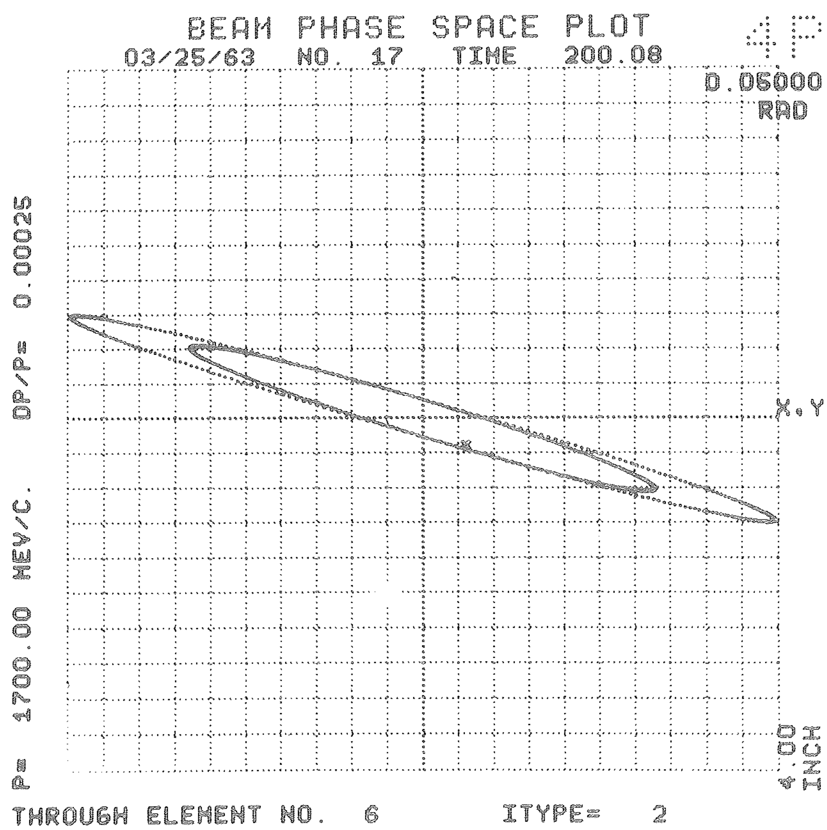
BEAM PHASE SPACE PLOT
4P
03/25/63 NO. 17 TIME 200.08
0.05000
RAD
DP/P= 0.00025
P= 1700.00 MEV/C.
X,Y
4.00
INCH
THROUGH ELEMENT NO. 6 ITYPE= 2

MU-30730

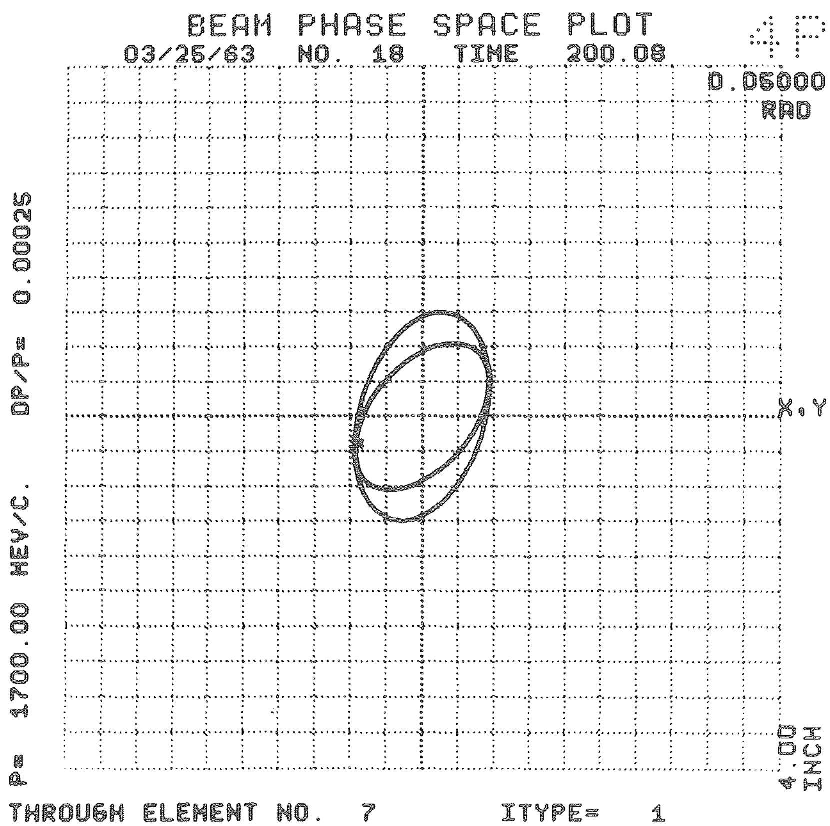
BEAM PHASE SPACE PLOT
4P
03/25/63 NO. 18 TIME 200.08
0.06000
RAD
X,Y
P= 1700.00 MEV/C. DP/P= 0.00025
4.00
INCH
THROUGH ELEMENT NO. 7 ITYPE= 1

MU-30731

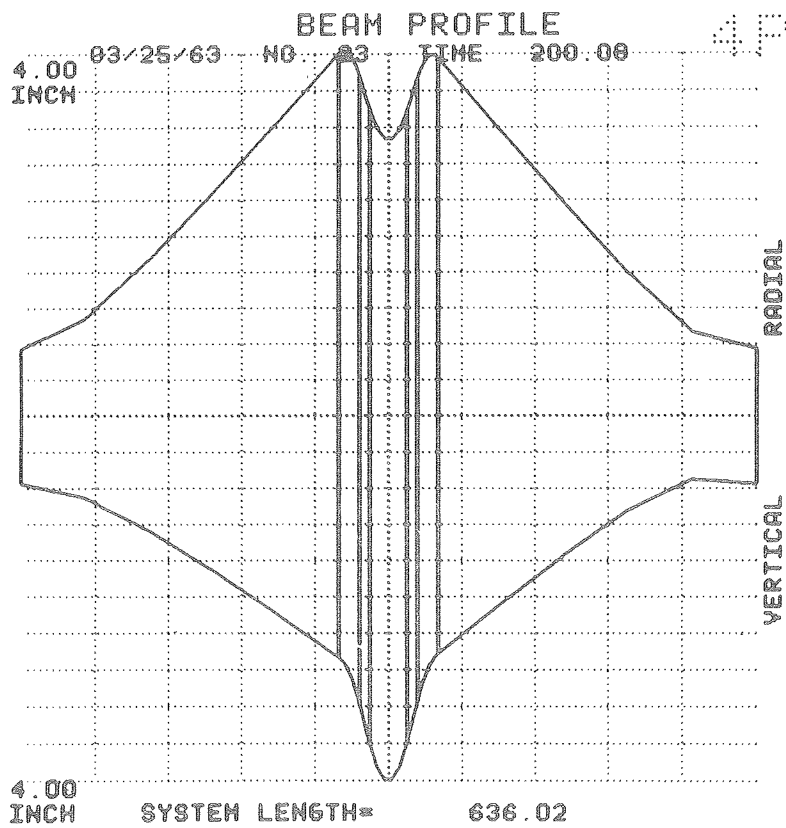
BEAM PROFILE
4P
03/25/63
NO.
TIME 200.08
4.00
INCH
RADIAL
VERTICAL
4.00
INCH
SYSTEM LENGTH= 636.02

MU-30732

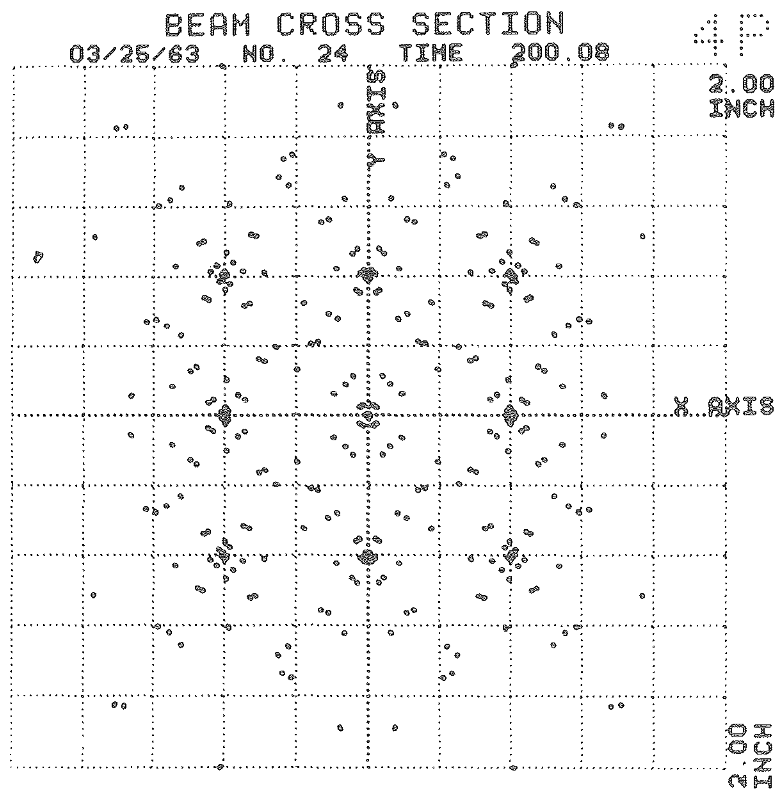
BEAM CROSS SECTION
03/25/63 NO. 24 TIME 200.08
4P
2.00 INCH
Y AXIS
X AXIS
2.00 INCH

MU-30733

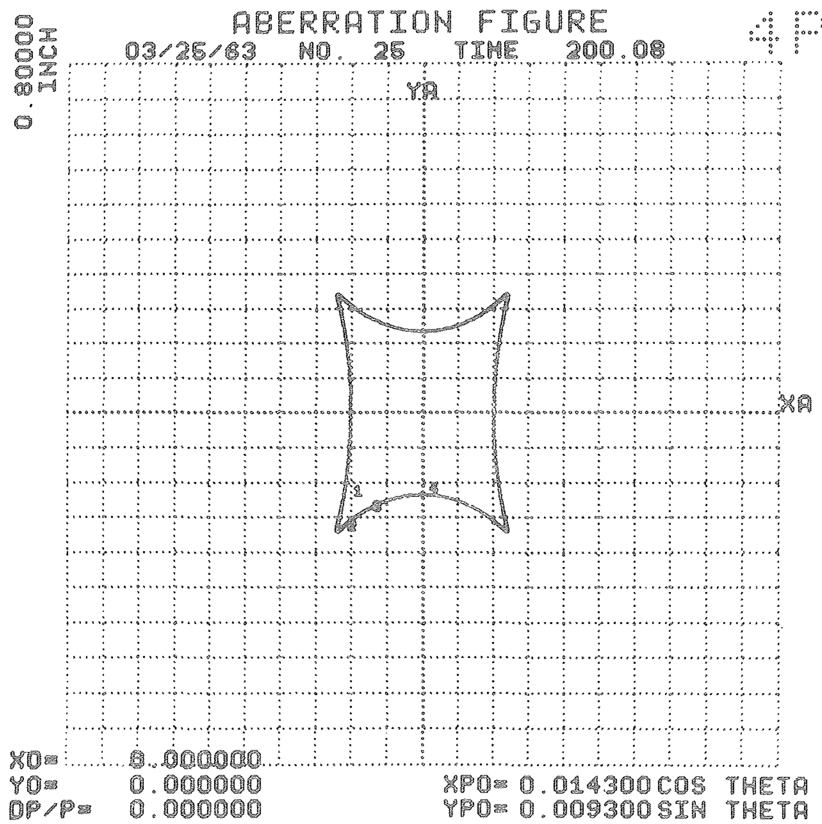
ABERRATION FIGURE
4P
03/25/63 NO. 25 TIME 200.08
0.80000 INCH
YA
XA
XO= 0.000000
YO= 0.000000
DP/P= 0.000000
XPO= 0.014300 COS THETA
YPO= 0.009300 SIN THETA

MU-30734

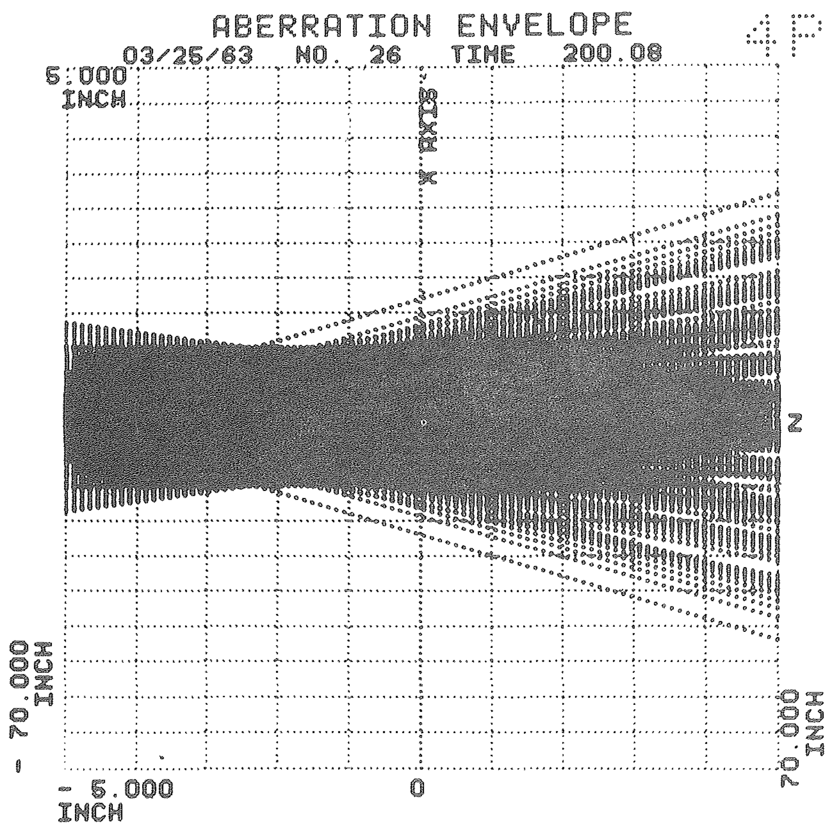
ABERRATION ENVELOPE
4P
03/25/63 NO. 26 TIME 200.08
5.000
INCH
X AXIS
Z
- 70.000
INCH
70.000
INCH
- 5.000
INCH
0

MU-30735

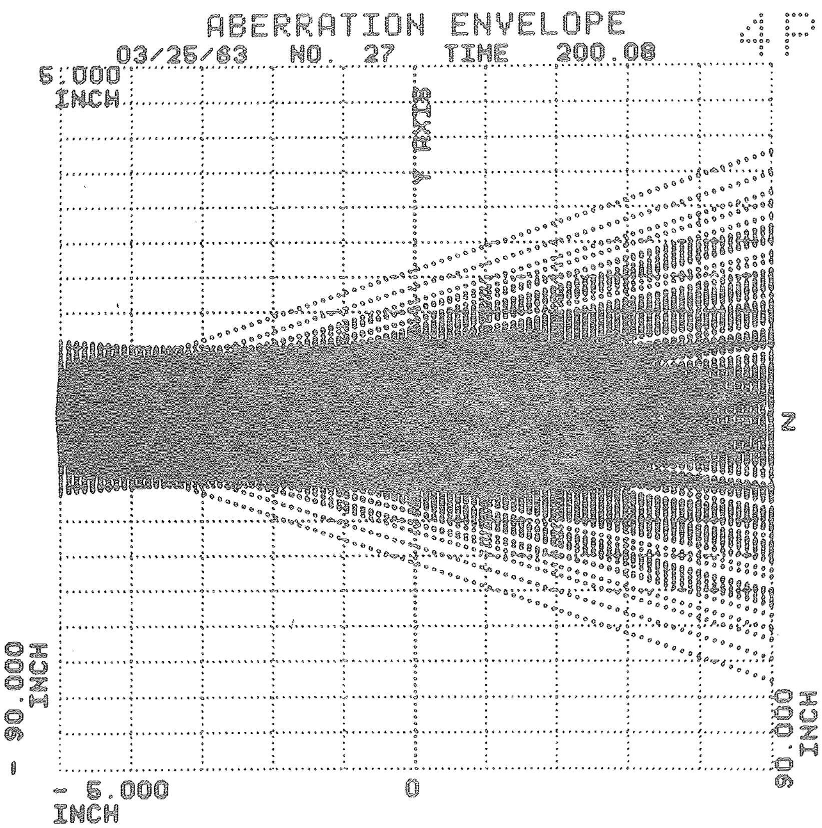
ABERRATION ENVELOPE
4P
03/25/63 NO. 27 TIME 200.08
5.000
INCH
Y AXIS
Z
- 90.000
INCH
90.000
INCH
- 5.000
INCH
0

MU-30736

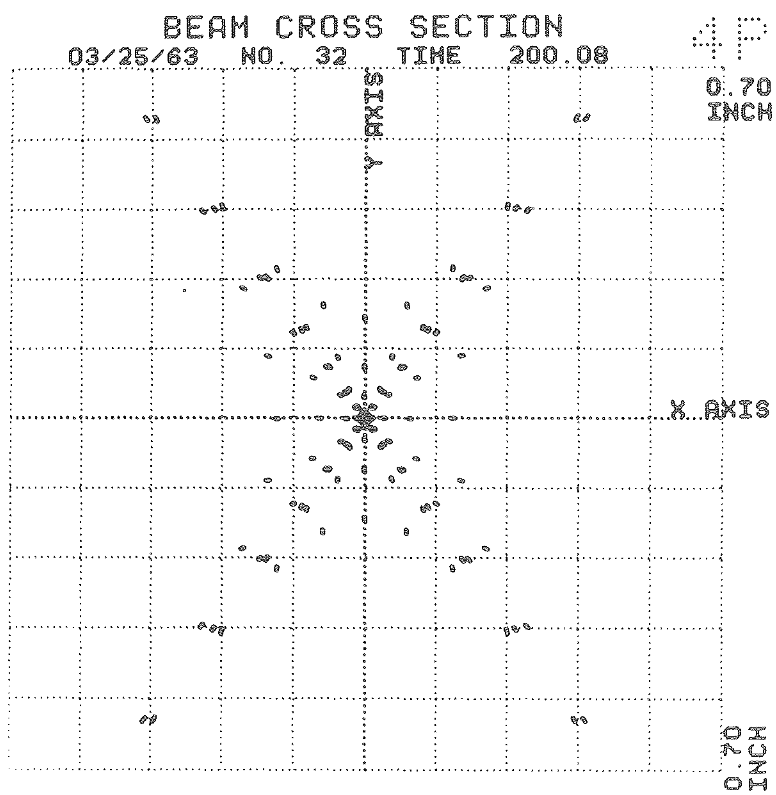

BEAM CROSS SECTION
03/25/63 NO. 32 TIME 200.08
4P
0.70 INCH
Y AXIS
X AXIS
0.70 INCH

MU-30737

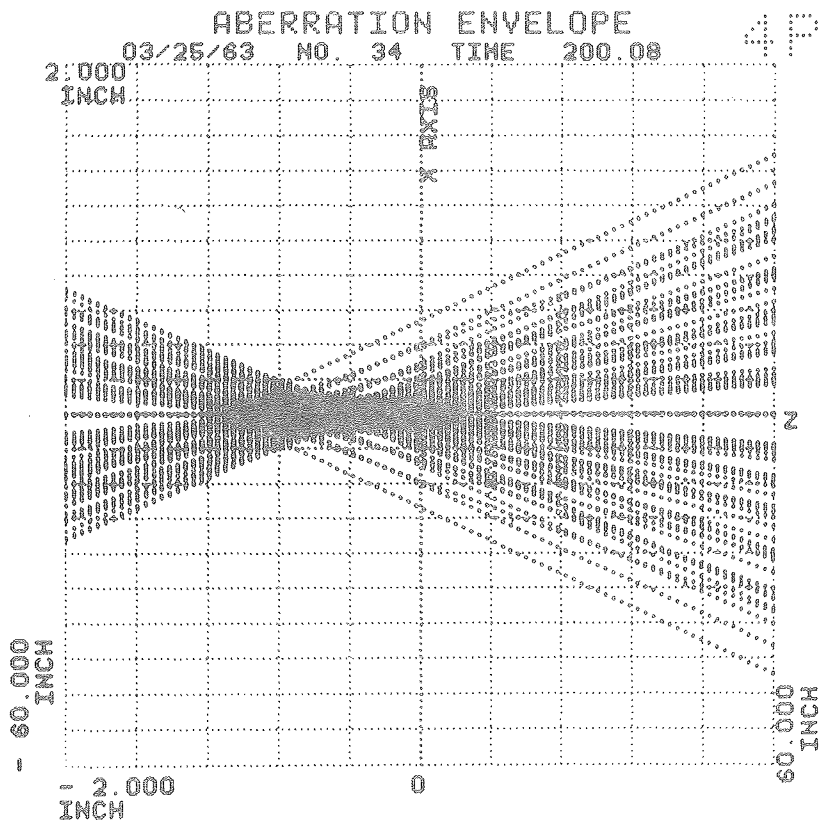
ABERRATION ENVELOPE
03/25/63 NO. 34 TIME 200.08
4P
2.000 INCH
X AXIS
Z
- 60.000 INCH
60.000 INCH
- 2.000 INCH
0

MU-30738

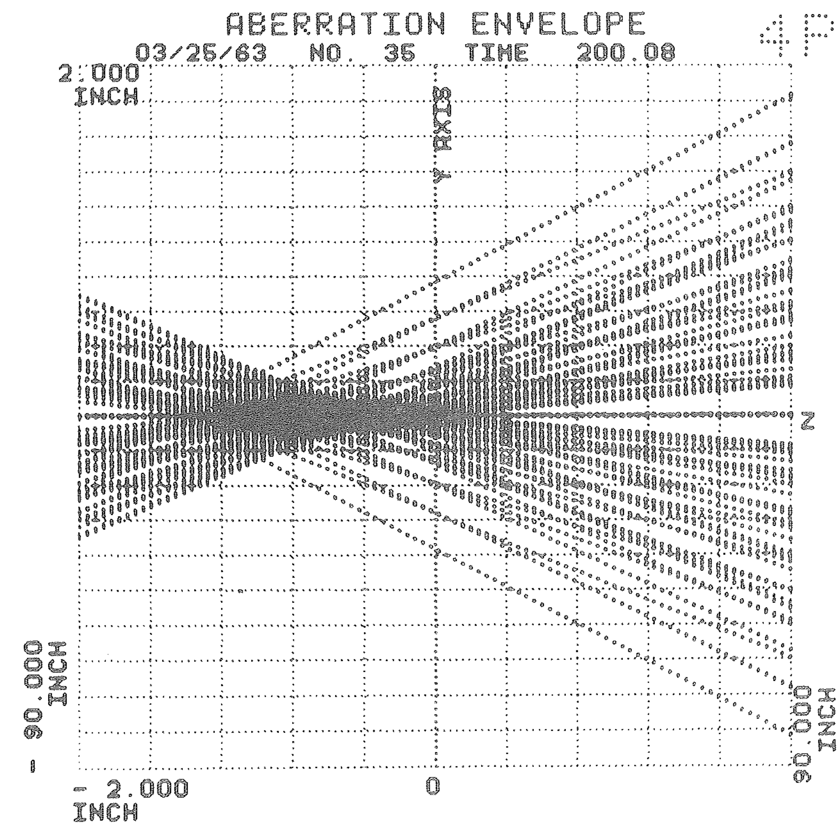
ABERRATION ENVELOPE
03/25/63 NO. 35 TIME 200.08
4P
2.000 INCH
Y AXIS
Z
- 90.000 INCH
90.000 INCH
- 2.000 INCH
0

MU-30739

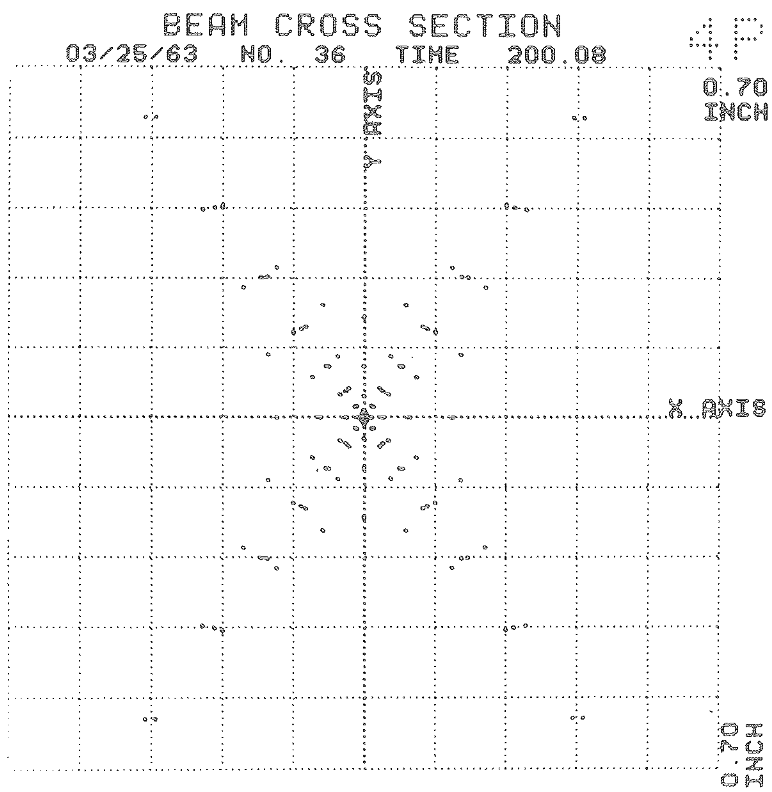

BEAM CROSS SECTION
4P
03/25/63 NO. 36 TIME 200.08
Y AXIS
0.70 INCH
X AXIS
0.70 INCH

MU-30740

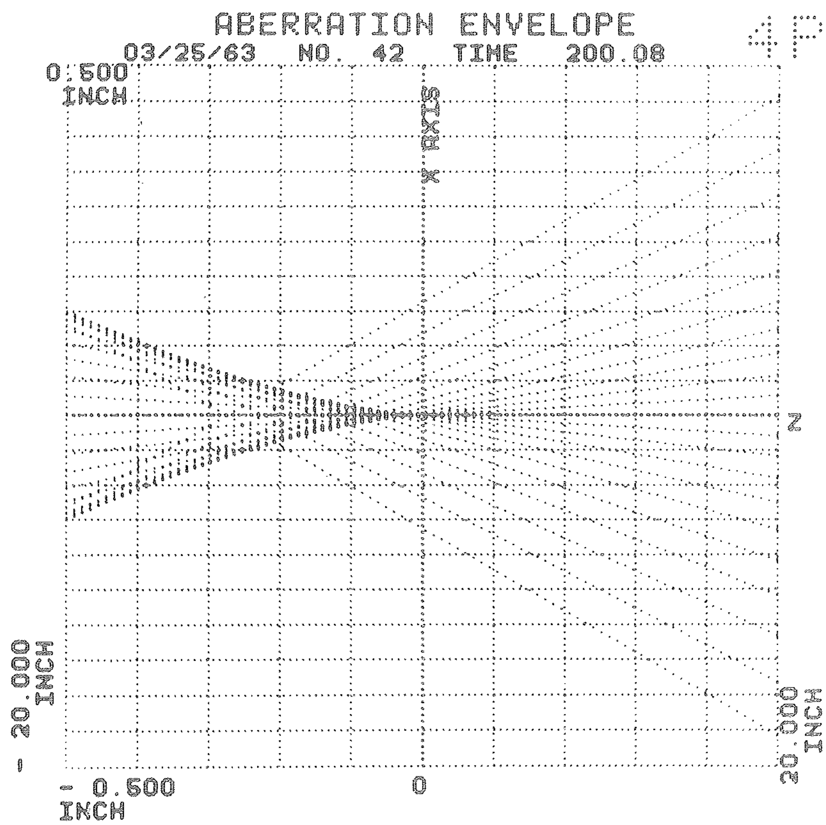

ABERRATION ENVELOPE
4P
03/25/63 NO. 42 TIME 200.08
0.500 INCH
X AXIS
Z
- 20.000 INCH
20.000 INCH
- 0.500 INCH
0

MU-30741

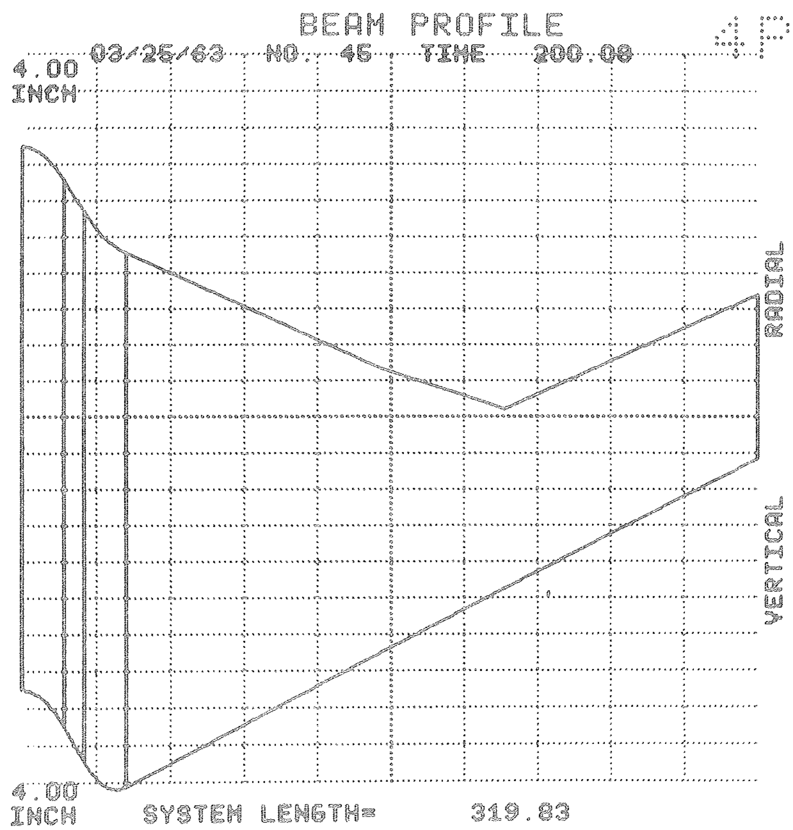
BEAM PROFILE
4P
03/25/63 NO. 45 TIME 200.08
4.00
INCH
RADIAL
VERTICAL
4.00
INCH
SYSTEM LENGTH= 319.83

MU-30742

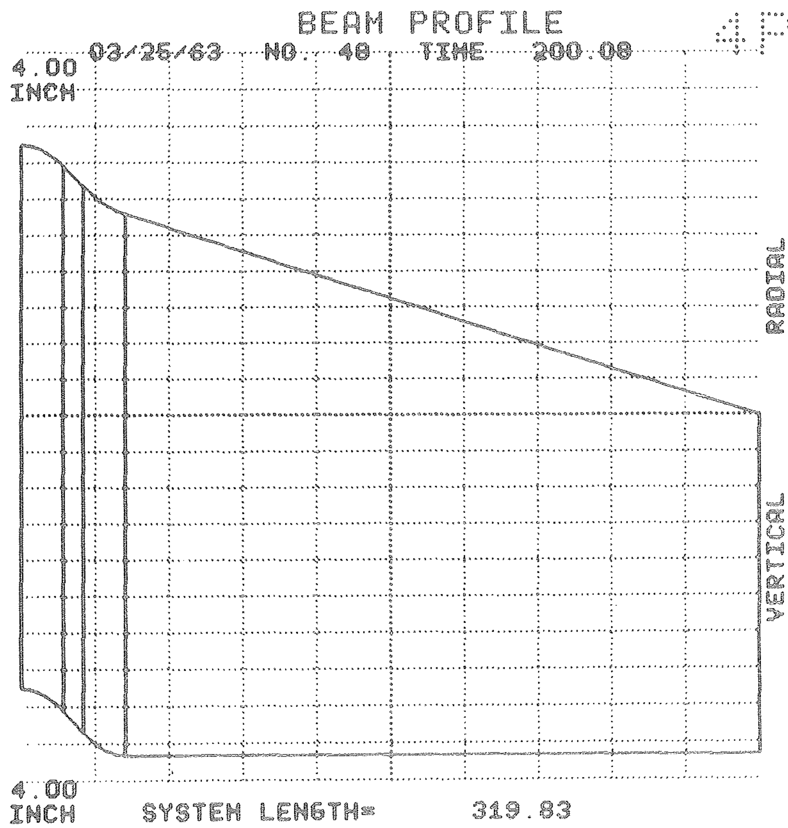
BEAM PROFILE
4P
03/25/63 NO. 40 TIME 200.08
4.00 INCH
RADIAL
VERTICAL
4.00 INCH
SYSTEM LENGTH= 319.83

MU-30743

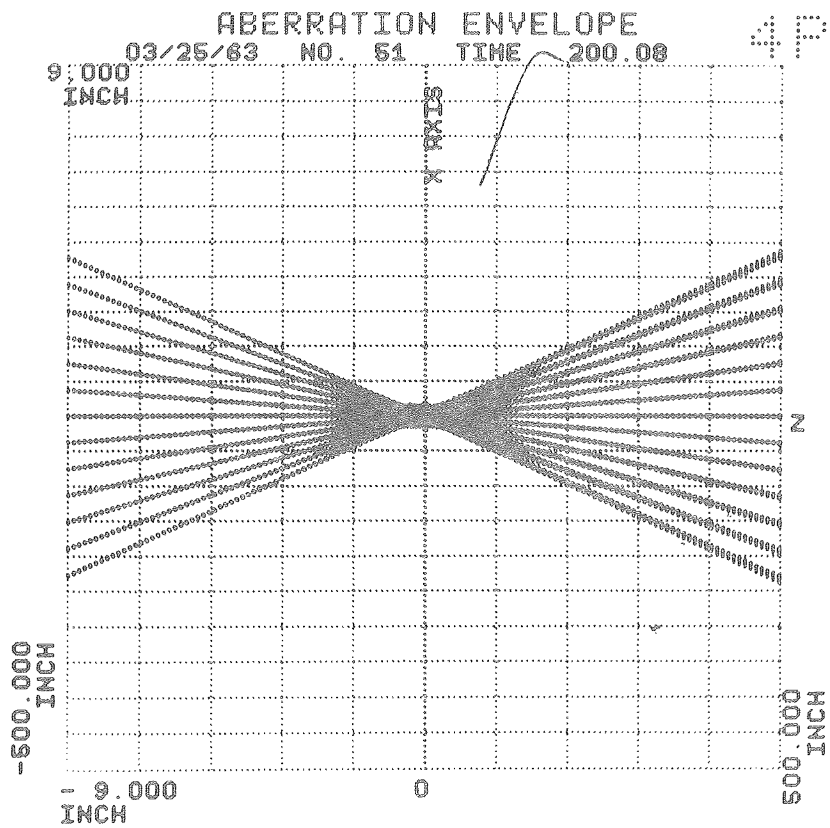

ABERRATION ENVELOPE
4P
03/25/63 NO. 51 TIME 200.08
9.000
INCH
X AXIS
Z
-500.000
INCH
500.000
INCH
- 9.000
INCH
0

MU-30744

PART TWO

ION OPTICAL DESIGN OF HIGH QUALITY EXTRACTED SYNCHROTRON BEAMS WITH APPLICATION TO THE BEVATRON

I. INTRODUCTION TO PART TWO

The desirability of eventually adapting the Bevatron to eject the proton beam was recognized in the earliest stages of the machine's design.

The experimental area around the existing weak-focusing synchrotrons is quite limited. The large increase in available experimental area is perhaps the most important advantage of an external beam over an internal beam.

Positive secondaries are necessarily difficult to extract from the machine when originating from internal targets. An obvious advantage of an external beam is the ability to observe secondaries of positive charge. With an external beam the field surrounding the target may be arbitrarily chosen. For example, it becomes possible to reverse this field, making no other changes, and thus to treat negative particles in the same manner as positive particles.

Being free of the Bevatron, targets in an external beam are observable from nearly any direction.

Materials that are awkward for internal targets due to eight or composition, are available for use with an external beam; liquid hydrogen is an important example.

With an external beam much greater control may be exercised over the optical properties of the beam as its strikes a target.

The total flux impinging upon the target may be accurately monitored; this is important in measuring certain cross sections.

Finally, short-lived secondaries are more easily observed because of the better access to the target.

In 1954, Byron Wright proposed an extraction scheme for the Bevatron which employed an energy-loss target (with no lip) and a single deflection magnet.[15] The energy of the beam passing through the target is reduced enough so that the beam passes into the deflection magnet located one-half betatron wavelength beyond the target. The deflection magnet, located 20 in. inside the target radius, strongly deflects the beam outward, causing it to leave the machine one quadrant beyond the magnet.

A similar one-magnet extraction scheme was independently proposed by O. Piccioni for the Cosmotron.[16] This scheme differs from that proposed by Wright in that a thin "lip" is attached to the energy-loss target. This lip serves to reduce the amplitude of betatron oscillations in the circulating beam before the beam strikes the target; this use of the thin lip was first proposed by E. McMillan.[17] This extraction scheme, employing a single pulsed magnet in a fixed location, has been successfully operating at the Cosmotron for several years.

Experiments under the direction of W. Chupp and G. Lambertson at the Bevatron with the one-magnet system demonstrated that such a system was unsuitable for the Bevatron. Due to the dispersion within the Bevatron, the extracted beam had a radial width of a foot or more; however, this beam must pass through an exit window of 3.5 in. width. Unlike the Cosmotron, the Bevatron magnet surrounds the vacuum chamber, severely restricting the egress of the external beam.

The energy spread in the beam, the Landau effect, is primarily a result of electron Coulomb scattering in the energy-loss target.[18] This spread in energy is characterized by an approximately Gaussian distribution in energy with a long tail toward large energy losses. The Gaussian portion of the distribution represents the statistical distribution of many small losses in energy, a random-walk process. The tail of the distribution is due to occasional very large losses in energy in close collisions with electrons; such large losses cannot be statistically treated in the random-walk manner. The maximum loss is theoretically bounded at about 100 MeV by relativistic considerations. A good treatment of the loss mechanism may be found in Experimental Nuclear Physics.[19] The mechanism of the scattering and energy losses in the lip and target have been analyzed by Mr. M. J. Mitchell (unpublished) at the Rutherford High Energy Laboratory, using a Monte-Carlo method. An additional effect which contributes to the energy spread has not been investigated: a portion of the beam may be scattered, by a single passage through the lip, so that the amplitude of radial betatron oscillation is increased; this portion of the beam may strike the target on the next revolution, leaving the target with greater energy than the remainder of the beam which has passed through the lip many times. The energy spread is significant because synchrotron magnets are powerful momentum analyzers.

The problem of large dispersive spreads at the exit window was solved for the Nimrod proton synchrotron at the Rutherford Laboratory by placing a quadrupole magnet half-way between the target and the deflection magnet.[20] The quadrupole magnet is adjusted to provide energy recombination at the exit window. This solution, although possible for the Nimrod accelerator which has eight straight-sections, is not possible for the Bevatron which has only four straight-sections.

The problem of ejecting a high-quality proton beam from the Bevatron was solved by inserting a second deflection magnet. The energy loss sustained at the target causes the beam to enter a small bending magnet one-half betatron wavelength beyond the target; this magnet, plunged close to the circulating beam, deflects the reduced energy beam further inward into a second and larger magnet which is also plunged. The second magnet, located one quadrant downstream from the first magnet, sharply deflects the beam outward, causing it to emerge one quadrant downstream. Adjacent to each bending magnet is a small current-sheet quadrupole magnet. The first quadrupole magnet is adjusted to provide energy recombination and a vertical focus at the exit window whereas the second quadrupole magnet is adjusted to provide a radial focus near the exit window. All these magnets must be plunged and pulsed so that they will not interfere with the magnetic field at injection.

It is the purpose of this paper to describe the detailed optical studies which resulted in the design of an external beam that is optimized with respect to linear properties, dispersive properties, and aberration properties and which meets engineering requirements of trouble-free operation (pulsed, plunged magnets in high vacuum) at minimum cost. It was determined early in the studies that aberrations can seriously degrade the quality of the beam. A typical example of the magnitude of the aberrations, calculated by the author, is reproduced in II.B.3. Design studies for the Cosmotron and Nimrod accelerators were limited to the use of linear theory, including first order dispersion in the case of the Nimrod. The importance of maintaining a small beam width in the highly nonlinear fringing fields was recognized. One of the primary aims of the study reported here was minimizing the effects of aberrations; for this reason, detailed orbit studies of representative groups of trajectories were conducted with the aid of digital computers. Several innovations due to the author are described; these innovations transferred a very large portion of the work load to the computers, thereby expediting the orbit study.

In Chapter II, we describe the extraction process in terms of linear theory. The digital computer programs developed for the study are described in Chapter III. We next turn our attention to the design of the external beam, describing the design objectives and considerations, the parameters which were to be specified, and the method of solution of the problem. The results of the study are described in IV.D. The behavior of the beam is demonstrated pictorially with the aid of prints of cathode ray tube (CRT) displays generated by the computer. The agreement with experiments is presented at the conclusion of the paper.

The project required the collaberation of many people. Dr. William Wenzel and Dr. Glen Lambertson were responsible for the construction of the external beam; their intimate knowledge of the Bevatron was invaluable in the design of the beam. Dr. Lloyd Smith, Dr. Alper Garren and Dr. Andrew Sessler contributed much to planning the beam. Orbit studies were carried out primarily by the author with the aid of Dr. Sessler, Dr. Garren, and Mr. Herman Owens. Powerful digital computer codes used in the study were a result of efforts by the author, Dr. T. A. Welton, Dr. Gerald Gardner, and Dr. Garren. Mechanical engineering efforts were under the direction of Mr. Jack Gunn, while Mr. E. C. Hartwig was in charge of the electrical engineering work. Experimental measurements were conducted by Mr. K. C. Crebbin under the direction of Dr. E. J. Lofgren and Mr. W. D. Hartsough.

II. THEORY OF EXTRACTION

The extraction of the beam is accomplished by separating protons from the main circulating beam and then deflecting them so that they pass out of the machine. The separation is achieved by passing the circulating beam through an energy loss target; the reduced energy beam leaving the target oscillates radially about the reduced energy equilibrum orbit which lies inside the target radius. The separation between the reduced energy beam and the main circulating beam is greatest at a location one-half betatron oscillation wavelength beyond the target. The amount of separation is proportional to the momentum loss at the target. At the point of maximum separation, a bending magnet is inserted to deflect the reduced energy beam; this bending magnet must not interfere with the circulating beam nor with the magnetic field at injection. Additional magnets may be required to direct and focus the extracted beam. This technique of extraction was proposed by B. Wright for the Bevatron[15] and independently by O. Piccioni for the Cosmotron.[16]

A. One-Magnet Extraction

A single magnet, placed at the point of maximum inward excursion of the reduced energy beam and adjusted to deflect the beam outward, may suffice to extract the beam in some accelerators.

1. The Cosmotron External Beam

A successful external beam has been obtained from the Cosmotron by use of a single pulsed deflection magnet at a fixed location along the internal wall of the machine.[16] At the desired circulating energy the beam is directed into an energy-loss target, that causes the beam to be displaced into the pulsed magnet at the point of maximum inward excursion. This magnet deflects the beam about 3° toward an exit window located on the external wall of the machine at a pumping manifold 75° downstream from the magnet. Steel shims are placed in the fringing field regions to provide the desired optical properties in this region which would otherwise produce divergence in the radial direction. The beam is about six inches wide as it leaves the machine.

This arrangement is possible in the Cosmotron because the pulsed magnet does not interfere in an intolerable way with the magnetic field at injection, although it does result in the loss of about one-half of the maximum circulating beam. Furthermore, the Cosmotron magnet, a "C" type magnet open to the outside, permits great latitude in the placement of steel shims in this outer edge region.

2. One-Magnet System Applied to the Bevatron

During the construction of the Bevatron, a study was made of the future external beam in order that necessary changes in machine design could be made during construction.[15]

This study envisioned a single-magnet extraction scheme which required a 29 MeV energy-loss target and a magnet located three quadrants beyond the target and 20 in. inside the target radius. A deflection of 2.3° would be required to extract the beam one quadrant downstream from this magnet. B. Wright, the author of this study, estimated that 2% of the beam would leave the energy-loss target within an angular range of $\pm 0.01^{\circ}$ with respect to the unscattered trajectory, and would fall on an ellipse six square inches in area located outside the machine; these estimates assume a monoenergetic point-source at the target.

3. Deficiencies in the One-Magnet System

Experiments were conducted with the one-magnet system described above over the period 1956-1959. The beam-width at the exit window was several times the width of the aperture. The width was reduced by moving the energy-loss target closer to the deflecting magnet so that a radial focus occured near the exit window. To compensate for reducing the target-to-magnet distance, the momentum loss sustained at the target was increased; this provided the necessary inward deflection. The beam width was still far larger than the exit aperture. Sample numerical calculations indicated that the beam at the exit window should be on the order of one foot in breadth when dispersive effects were taken into consideration.

The Bevatron, unlike the Cosmotron, has an H type magnet that completely surrounds the vacuum tank, restricting the maximum possible beam width at the exit window to four inches.

Since the entire aperture of the Bevatron is needed at injection, a fixed magnet cannot be used; the magnet must be plunged into position at each cycle of acceleration, and therefore it should be as light as possible.

Shims in the fringing field region, which are needed to prevent intolerable radial defocusing of the beam, cannot be used in the Bevatron owing to its magnet yoke geometry.

Finally, the emerging beam must pass through an entire quadrant before leaving the magnet, thus traversing the defocusing fringing field for a much longer distance than in the Cosmotron; this requires a small exit angle. Experience at the Cosmotron has shown that larger exit angles result in smaller beams.

4. Advantages of the Two-Magnet System

The addition of a second magnet permits a more satisfactory minimization of the dispersive effects. With two magnets, the bending angle at the first magnet is reduced, so that a lighter magnet can be used. Because a smaller magnet may be brought closer to the circulating beam, the required energy loss at the target is reduced. The energy spread due to the Landau effect is smaller for the reduced energy loss.[19]

The addition of a second magnet introduces other degrees of freedom in the choice of focusing parameters. The extra parameters may be chosen to optimize the achromatic properties of the beam system.

B. Two-Magnet Achromatic Extraction

In the remainder of this paper we restrict our attention to the two-magnet system adopted for the Bevatron.

1. Method of Extraction

The first magnet in this system, located at the point of miximum inward excursion of the beam after leaving the energy-loss target, deflects the beam further inward into a second bending magnet, located one quadruant beyond the first magnet, deflects the beam strongly outward so that it passes out of the machine one quadrant beyond the second magnet. The placement of these components is shown in Fig. 9.

a. The Energy-Loss Target

As stated aove, the main function of the energy-loss target is to cause the beam to oscillate inward. The maximum inward deflection is given by

$$\Delta r_{max} = -\frac{2r}{1-n} \frac{\Delta p}{p} , \tag{1}$$

where p and r are the momentum and radius, respectively, of the beam, n is the field exponent, and Δp is the momentum loss in the target. A thin "lip", whose function is to damp the amplitude of radial betatron oscillations, projects from the exterior edge of the target. As the magnetic field is increased after the cessation of acceleration, the circulating beam moves slowly inward toward the target. A proton first passes through the lip during a maximum inward swing; passing through the lip reduces the amplitude of the radial oscillations. The damping of the radial oscillations insures that the protons pass through the entire target once and then enter the gap of the first magnet. Since there is some scattering by the lip, the amplitude of betatron oscillations cannot be reduced indefinitely. The residual betatron amplitude and energy spread result in a finite width of the beam leaving the target.

The beam leaving the target possesses a range of angles due to multiple Coulomb scattering within the target. In addition there is an appreciable spread in momentum because of the Landau effect.[18] The Landau effect is characterized by a large "tail" in the energy distribution, in the direction of large losses. The

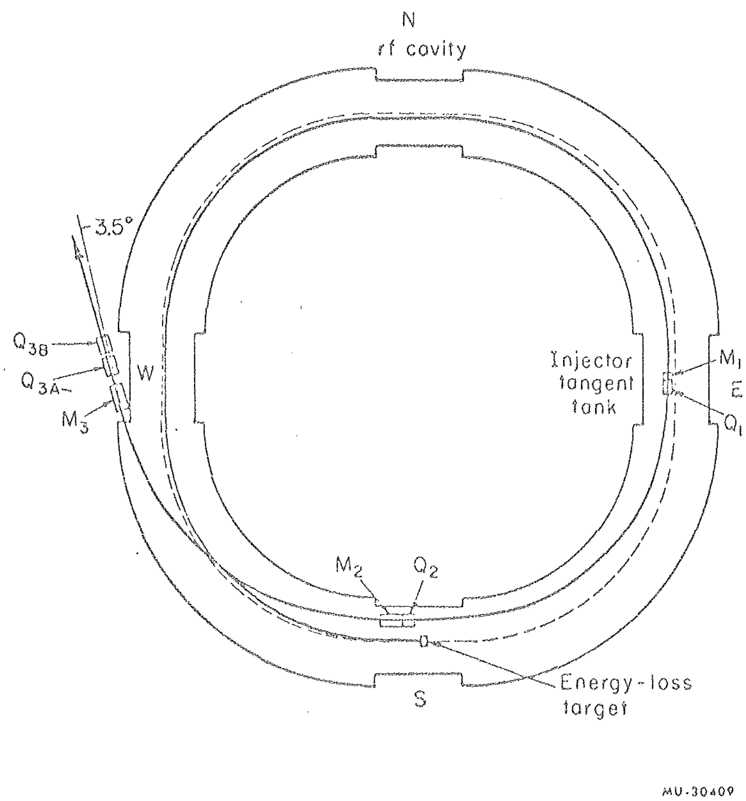

Fig. 9. Schematic diagram of the beam-extraction system of the Bevatron.

width of the energy distribution increases with increasing energy-loss in the target.

b. The First Magnet. The function of th first bending magnet, M_1, is to deflect the reduced energy bea.. further inward into the second bending magnet. The radial location of M_1 depends upon the thickness of the energy-loss target. Adjacent to this magnet is a current-sheet quadrupole focusing magnet, Q_1, that may be adjusted primarily to enhance the energy recombination of the beam. Both of these magnets must be plunged and pulsed so they will not interfere with the beam during acceleration.

c. The Second Magnet. The second bending magnet, M_2, provides the required outward deflection to eject the beam. Its radial location is governed by the strength of M_1. There is also a quadrupole magnet, Q_2, adjacent to this magnet that may be adjusted primarily to minimize the radial spread at the exit window. Both M_2 and Q_2 must also be plunged and pulsed if the maximum beam current is to be achieved. The beam must pass out of the machine through a thin aluminum window located in the west straight section.

d. External Magnets. Additional bending magnets and quadrupole magnets are located outside the vacuum chamber; these magnets are not considered in this paper.

2. Pictorial Phase Space Description of Extraction

The optical considerations in extracting the beam are most easily explained by refering to motion in radial phase space. In Fig. 10 x and Rx'/ν are plotted for a representative set of trajectories comprising the reduced energy beam.

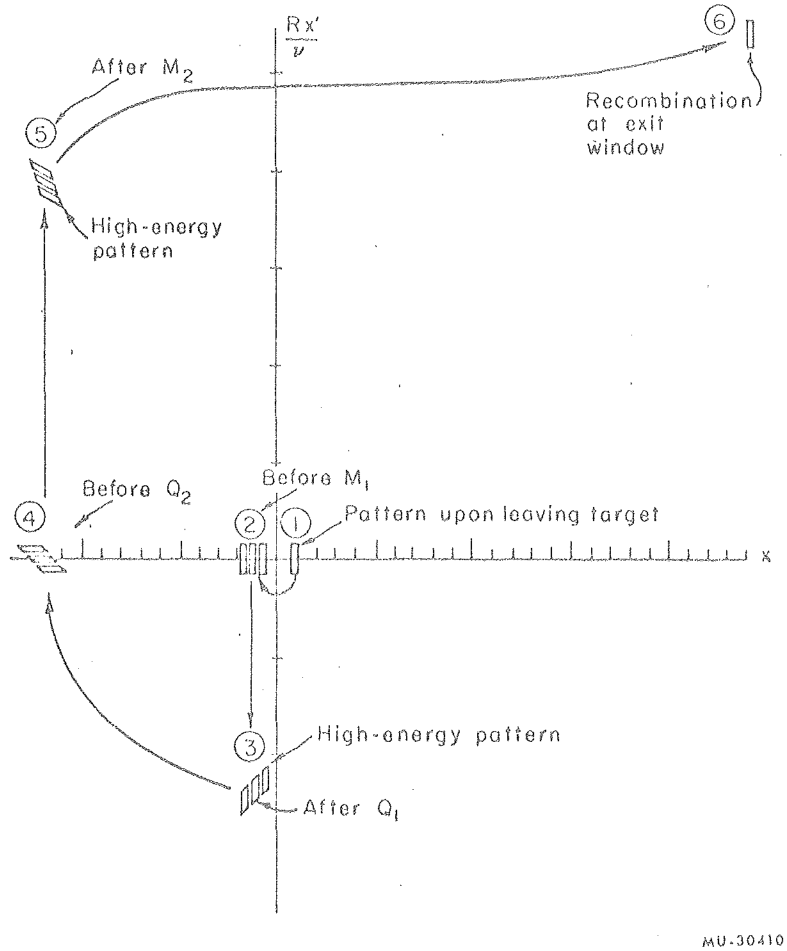

Fig. 10. Configuration pattern motion in radial phase space.

Here x is the displacement of a trajectory from the equilibrum orbit of radius R; ν_r is the radial betatron frequency. We show below that, with this choice of coordinates, representative points rotate about the origin of this figure as the corresponding trajectories move through the Bevatron. The origin of this figure is the configuration point representing the reduced energy equilibrum orbit. The action of a bending magnet is represented by a displacement along the Rx'/ν_r axis. A quadrupole focusing magnet shears a given configuration in the Rx'/ν_r direction; the displacement in Rx'/ν_r is proportional to the displacement in x from the magnet center. It can be shown from the radial betatron equation that motion through the Bevatron corresponds to a rotation of the configuration point about the origin in this figure. Within a synchrotron the approximate linearized equations of motion for displacements from the equilibrum orbits are

$$\frac{d^2x}{ds^2} + \frac{\nu_r^2}{R^2}\, x = \frac{1}{R}\,\frac{\Delta p}{p} \tag{2}$$

and

$$\frac{d^2z}{ds^2} + \frac{\nu_z^2}{R^2}\, z = 0 \quad . \tag{3}$$

where ν_r and ν_z are the radial and axial betatron frequencies, respectively, and s is the path length measured along the equilibrum orbit. The solution to the radial equation is

$$x(s)=x(0)\cos(\nu_r s/R) + (Rx'(0)/\nu_r)\sin(\nu_r s/R) + \frac{\Delta p}{p}\,\frac{R}{\nu_r^2}\,(1-\cos(\nu_r s/R) \;,$$

whence (4)

$$Rx'(s)/\nu_r = -x(o)\sin(\nu_r s/R) + (Rx'(0)/\nu_r)\cos(\nu_r s/R) + \frac{\Delta p}{p}\,\frac{R}{\nu_r^2}\sin(\nu_r s/R) \quad .$$

Thus as the particle moves a distance s in the synchrotron, the representative point rotates through an angle $\Theta = -\nu_r s/R$ in x, Rx'/ν_r space.

The rectangular pattern at (1) in Fig. 10 represents the radial phase space distribution of the beam upon leaving the energy-loss target. Between (1) and (2) the patterns rotate 180° as the trajectories move about 1/2 betatron wavelength from the target to M_1. The three patterns at (2) represent groups of trajectories of three distinct energies corresponding to the Landau spread in energy. The central pattern is the mean energy pattern; The trajectories of lower energy are displaced further from the origin.

The deflection at M_1 and focusing at Q_1 take the patterns at (2) into those at (3). Radial displacements are negligible within the magnets. Since the target is imaged at Q_1, focusing here does not greatly affect the trajectories for a single energy. The focusing strength of Q_1 is chosen mainly to provide energy recombination at the exit window. The deflection at M_1 increases the amplitude of radial betatron oscillations.

One quarter betatron wavelength beyond M_1, the beam is at a maximum inward swing and at an anti-focus. Focusing here strongly affects the radial imaging properties at the exit window while having a lesser effect on energy recombination. Pattern (4) is the beam distribution at the entrance to M_2. A strong outward deflection by M_2 and focusing by Q_2 take the patterns at (4) into those at (5). The deflection at M_1 has produced sufficient displacement at M_2 so that M_2, which must be large to provide the required deflection, does not disturb the circulating beam.

The beam emerges from the Bevatron one quadrant beyond M_2 at the exit window where the distribution is shown by pattern (6). Between (5) and (6) the beam passes through the strongly radially defocusing fringing field of the Bevatron. Ideally, the optical properties of the beam system should provide a radial focus at the exit window with full energy recombination.

In the preceding discussion the vertical properties of the beam have been neglected. The vertical betatron frequency is greater than the radial betatron frequency; thus the vertical image, corresponding to one-half vertical betatron period, will occur before M_1 is reached. Although Q_1 has little influence on the radial focal properties of the beam, it will influence the vertical focal properties. Q_1 must be adjusted to achieve a compromise between the desired achromatic properties of the beam and the desired image in the vertical plane at the window. Q_2 affects the focal properties in the vertical plane, but its strength must be chosen to minimize the radial beam width at the window.

The object of this study was to develop and apply methods for choosing the locations and strengths of the constituent magnets and the location and thickness of the energy-loss target to minimize the size and divergence of the beam at the exit window, and to provide optimal energy recombination at that point. There are many other considerations, mainly those of cost and engineering feasibility, which restrict the choice of parameters.

3. The Inadequacy of the Linear Theory

The linear theory fails to adequately describe the beam geometry due to the relatively large size of the aberrations. Even in the "good" field region between the energy-loss target and the first magnet, where the beam is within three inches of the center of the vacuum tank, large nonlinear effects are observed. This is easily demonstrated by inclusion of the second order terms in the equation for radial motion within a magnet quadrant;

$$\frac{d^2\xi}{d\phi^2} + \xi = \frac{1}{2}\left(\frac{dx}{d\phi}\right)^2 + \delta + k\xi^2 + (2-n)\delta\xi \quad , \qquad (5)$$

where $k=(2n-1-\beta)/\nu_r^2$, $\phi=\nu_r\theta$, $\delta=(p-p_0)/\nu_r^2 p$, $\xi=x/R$, R is the radius of the equilibrum orbit and $B_z(\xi)/B_0=1-n\xi+\beta\xi^2+\cdots$. Here p_0 and B_0 refer to the equilibrum orbit for $\delta=0$.

We can estimate the magnitude and character of the nonlinear effects between the target and M_1 by approximating the right-hand side of the above equation with the linear solution for motion in the Bevatron and then integrate the resulting equation over one-half betatron period. The linear solution is

$$\xi = \xi_0 \cos\phi + \left.\frac{d\xi}{d\phi}\right|_0 \sin\phi, \qquad (6)$$

where ν_r is given by (7)

$$\cos(\pi\nu_r/2) = \cos(\pi\sqrt{1-n}/2) - (L/2R)\sqrt{1-n}\,\sin(\pi\sqrt{1-n}/2)$$

or $\nu_r=\sqrt{1-n}\,(1+4L/4\pi R)+\ldots$; L is the length of the straight section. Here $\xi_0=x_0/R$ and $\frac{d\xi}{ds}=x'=\nu_r\frac{dx}{d\phi}$. At M_1 ($\phi=\pi$ with $\phi=0$ at the target), we find

$$\xi = -\xi_0 + \frac{2}{3}\xi_0^2(1+k) + \frac{1}{3}\left(\frac{d\xi}{d\phi}\right)\bigg|_0^2 (1+4k) + 2\delta - \frac{4}{3}\delta\xi_0(1+k) + \frac{\pi}{2}\delta\left.\frac{d\xi}{d\phi}\right|_0 (2-n+2k)$$

$$+ \delta^2\left[\frac{2}{5} + \frac{8}{3}k + \pi\left(1-\frac{n}{2}\right)\right] + \cdots \quad . \qquad (8)$$

Numerical values of these parameters for typical Bevatron operating conditions are: $\nu_r = 0.68$, $n=0.56$, $\beta = -11.0$, $k=25$; $|\zeta_0| \leqslant 0.000185$, $\left|\frac{d\zeta}{d\phi}\right|_0 \leqslant 0.000176$, and $|\delta| \leqslant 0.00054$.

We find that the centers of the high and low energy patterns are displaced by 0.7 in. from the center of the mean energy pattern at M_1. In addition, the patterns at M_1 are three parallel rectangles by the linear theory, but the second order terms demonstrate that the ends of the patterns (corresponding to trajectories with $x_0' = \pm 1.2$ mr) are actually displaced in the x direction by 0.07 in. relative to their centers. These displacements are 30% of the widths of the rectangles in the x direction. Furthermore, the patterns for the two extremes of energy are tilted with respect to each other and with respect to the pattern for the central energy; at M_1, the spread of the trajectories leaving the target with $x_0' = 1.2$ mr. is 0.2 in. greater than the spread of the trajectories for which $x_0' = -1.2$ mr.

Exact numerical calculations have verified these estimates to within 10%. Even if the remainder of the beam system (from M_1 to the exit window) were free from aberrations, those already present in the "good" field region would double the beam width at the exit window.

As the beam must traverse a large segment of nonlinear fringing field between M_2 and the window, nonlinear effects can certainly be expected to become much worse. Linear theory can only provide crude estimates of the beam behavior. Intelligent choices of adjustable parameters cannot be made without detailed study of the exact trajectories within the Bevatron field.

In the next chapter we discuss the calculational tools that were developed to conduct these detailed studies, and the results are described in the remainder of this paper.

III. NUMERICAL CALCULATION PROGRAMS

Orbit design studies have required the writing of several IBM 704 and 709 digital computer codes. The main code used in this work is the Bevatron Orbit Code (BOC), which calculates detailed trajectories in the Bevatron. Two codes, BEFCYF and DBDT, were written to provide the field data required by BOC. A separate IBM 709 cathode ray tube (CRT) plotting code plots phase space patterns from data calculated by BOC. A series of IBM 709 codes, BEVRMAP, BEVZMAP, BEVRMAX, and BEVZMAX, execute rapid parameter surveys using an extended linear trajectory theory.

A. The Bevatron Orbit Code

1. The Basic Code

The original Bevatron Orbit Code is a modification of the Oak Ridge General Orbit Code No. 1482;[21] this modification was carried out by Dr. T. A. Welton during early 1960. The basic code calculates trajectories in the Bevatron by integration of the following differential equations with Θ as the independent variable:

$$\frac{dr}{d\Theta} = r\ p_r(p^2-p_r^2)^{-1/2}\ ,\quad \frac{dp_r}{d\Theta} = (p^2-p_r^2) - r\ B,\quad \frac{d\Theta}{d\Theta} = 1,$$

$$\frac{dz}{d\Theta} = r\ p_z(p^2-p_r^2)^{-1/2}\ ,\ \text{and}\ \frac{dp_z}{d\Theta} = z\ r\frac{\partial B}{\partial r} - p_r(p^2-p_r^2)^{-1/2}\frac{\partial B}{\partial \Theta}. \tag{9}$$

The Runge-Kutta method is employed using double-precision arithmetic. An interval of 0.5° in Θ constitutes a single Runge-Kutta step. Four point interpolation formulas in r are used to obtain the required field values from stored field data.

Due to the symmetry of the Bevatron, it was necessary to store the field data for only one-half of a quadrant. To obtain the desired accuracy, a grid of 3 in. by 0.25° was chosen, requiring the storage of 7421 values of $B(r,\theta)$ and 7421 values of $dB(r,\theta)/dr$. The field data and the code are all read from a single input tape.

The original code integrates one orbit at a time, printing off-line the trajectory coordinates where desired. Upon completing one orbit, the code reads the initial coordinates of the subsequent orbit.

If at any time the code must be interrupted, it writes a "get-off" tape that, when read by the computer during a subsequent run, continues the calculation in progress when interrupted. The only loss in computer time is that required to write and read this tape.

2. The Modified Code

The Bevatron Orbit Code was extensively modified by the author; its capability was broadened to handle most of the external beam calculations. The modifications made by the author are described in this section.

The output of the code was extended to include on-line printed summaries of each trajectory, printing of the trajectories in terms of "Bevatron coordinates" (rectangular coordinates in the straight sections and polar coordinates, based on the vacuum tank centerline, in the quadrants), and calculation and printing of displacements and slopes relative to one of several stored equilibrum orbits.

Inclusion of bending magnets, quadrupole magnets, and sextupole magnets in the paths of the trajectories was the object of another modification. These magnets may be inserted only at the start of an orbit; the remainder of the orbit proceeds under the action of the Bevatron field along.

The code will now calculate equilibrum orbits for any momentum and will store several equilibrum orbits for reference. The momentum corresponding to an equilibrum orbit at a particular radius may also be calculated.

An important modification, greatly facilitating use of the code, was the addition of the "parameter tape." The coordinates of groups of orbits are stored at a selected azimuth; these coordinates may be referenced as initial coordinates for any subsequent orbits. The selected coordinates of over 300 groups of nine orbits each may be stored. At the conclusion of each run, all the stored coordinates and the group of equilibrum orbits currently in use are written on the "parameter tape." Prior to executing calculations in a subsequent run, this parameter tape is read, reloading the results of every previously calculated orbit. With this feature a representative group of orbits can be calculated between the energy-loss target and M_1 on one day. This same group of orbits can then be run between M_1 and M_2 a number of times on a subsequent day; the effect of varying the strength of Q_1 can then be observed. In the original version of the code, a complete study of a given target location required at least three separate computer runs; between these runs many hours of work with hand calculaters and key punch machines were required to calculate the strengths of the bending and focusing magnets and to insert their effects. With the added features described in this section, preparation time was reduced by 95%.

BOC will calculate and manipulate transfer matrices relative to selected trajectories in the Bevatron; these matrices are used by the linear codes to be described later.

The code calculates the mapping of the radial phase space at one location along the beam to the radial phase space at another location. These maps are produced by backward calculation of groups of orbits whose phase space coordinates are taken from an array (r_i, p_{r_j}); backward orbits are simulated by invoking the azimuthal reflection symmetry of the magnetic field about the midpoint of each quadrant. Such maps are very helpful in understanding aberrations.

For the purposes of the external beam study, the curve in phase space at one azimuth which maps into a single radius at another azimuth is accurately given by:

$$p_r(r) = A + B \cdot r + C \cdot r^2 + D \cdot p. \qquad (10)$$

The code calculates the coefficients A, B, C, and D in this expression from data derived from the mappings. With this expression calculated between M_1 and M_2, and separately between M_2 and the exit window, the strength of both of the bending magnets can be automatically presecribed by the code. The strength of a quadrupole magnet at one azimuth, that minimizes the rms displacement of a representative group of trajectories about the beam optic axis at a second azimuth, may be determined using the above expression. This feature of the code optimizes the strength of Q_2. Nonlinear focusing may be introduced by means of a sextupole magnet; the strength of the sextupole may be optimized in the same sense (minimizing the rms displacements).

A number of error detection routines increase the reliability of the code. All input tapes are written in two indentical parts. Tape reading is checked for accuracy by two methods. In the event of an error, the reading of the first part of the tape is repeated; if the first part cannot be read correctly, the tape is spaced to the second part and the code attempts to read it several times. Errors in running the code result in termination of the orbit in which the error was detected, provided recovery is not possible; the location of the error, the coordinates of the orbit, and the console status is printed. The code then proceeds to initiate calculations on the subsequent orbit.

The modified version of BOC requires a "large" IBM 704 with 32,768 word storage capacity and five or more tape units. The code is entirely SAP coded, making conversion to other computers somewhat tedious. It should be possible to operate the code on a double core IBM 7090 with a simulate routine although this has not been attempted. Upon making minor changes in certain constants, the code can be adapted to any synchrotron.

BOC requires approximately one minute on the IBM 704 to integrate the radial equations through one revolution. If the vertical equations are also integrated, the required time is doubled. An additional 0.25 minute is required for each orbit if the maximum output is desired.

3. The Plot Code

In order to clearly demonstrate the beam behavior, it was desired to plot the radial and vertical phase space pattens traced by the beam at the target, before M_1, after Q_1, before Q_2, after M_2, and at the exit window. These plots consist of the configuration points for representative groups of 27 orbits each, taken from BOC calculations.

The IBM 704 computer at the University of California did not include a cathode ray tube display. Thus a second code was written that reads the parameter tape produced by BOC and then plots the desired information on the CRT attached to the Lawrence Radiation Laboratory IBM 709 computer; a camera records the plotted data on film.

Three choices of plot scale are available to the code and the scale chosen is the largest that will accomodate all the desired configuration points. Each plot requires about eight seconds of IBM 709 time; the plot code will run on the IBM 7090, requiring two seconds per plot.

With the aid of these plots, we can readily determine the beam behavior as a function of each parameter varied. Several plots, chosen from among more than 300 plots, are reproduced in the next section.

4. The Field Codes

Dr. C. Gerald Gardner wrote the two FORTAN IBM 704 codes that prepare the field data for BOC.[22] BEFCYF accepts as input the experimentally measured values of the magnetic field at the median plane of the Bevatron; this data consists of radial and azimuthal profiles within the quadrants and a rectangular array of 1350 values in the tangent tanks. All data were taken from "smoothed curves." BEFCYF produces by interpolation an equivalent set of field values on a polar grid about the geometric center of the Bevatron. DBDT reads the field tape produced by BEFCYF and produces a tape containing the azimuthal derivatives corresponding to the fields produced by BEFCYF. The two tapes are written in the format acceptable by the Oakridge General Orbit Code, #1482, mentioned previously; BOC reads tapes in the same format.

A separate loading routine, written by Dr. Welton and modified by the author, reads the two field tapes and the binary deck for BOC, producing a self-loading binary tape containing BOC and the field values.

In the region where the field is nearly linear the accuracy of the field measurements is approximately 0.5%. This accuracy deteriorates toward the edges of the vacuum tank. Measurements in the fringing field regions of the straight sections are within 3% of the correct values.

B. The Linear Codes

Exact numerical calculation of the beam behavior using BOC is too expensive in terms of computer time to allow complete investigation of the possible choices of external beam parameters, but a simple-minded linear theory that does not take into account the azimuthal and radial variations of the field exponent n is inadequate for this purpose.

A suitable compromise in cost and accuracy is to use the linear approximation for deviations from an exact reference orbit ("optic axis"). The linear approximation allows expressing the deviations from the optic axis in terms of 3x3 transfer matrices. Dr. Alper A. Garren wrote a series of codes for the IBM 709 computer that calculates transfer matrices for arbitrary choices of the strengths of Q_1 and Q_2 and arbitrary target locations. These codes require as input the 3x3 transfer matrices between a "standard target location" (center of the south tangent tank) and M_1, between M_1 and M_2, and between M_2 and the exit window; these matrices are calculated by BOC. The thin lens focusing matrices at Q_1 and Q_2 and the transfer matrix between the arbitrary target location and the standard target location are calculated by the linear codes. These codes execute rapid surveys of the linear beam behavior as the target location and the strengths of Q_1 and Q_2 are varied.

1. Derivation of the Analytic Transfer Matrix to the Standard Target Location

The following derivation of the radial transfer matrix between an arbitrary target location and the standard target location is due to Dr. Garren.

An approximate analytic transfer matrix, that neglects the azimuthal dependence of the amplitude of radial betatron oscillations due to the presence of the straight sections, is derived from the linearized equations given in II.B.2. This matrix operates upon the column vector $\begin{pmatrix} x \\ \frac{R}{\nu_r}\frac{dx}{ds} \\ \frac{\Delta p}{p} \end{pmatrix}$ where x, x', and $\Delta p/p$ are taken relative to the closed (equilibrum) orbit for momentum p_0. The matrix is:

$$M = \begin{pmatrix} \cos \phi & \sin \phi & \frac{R}{\nu_r^2}(1 - \cos \phi) \\ -\sin \phi & \cos \phi & \frac{R}{\nu_r^2}\sin \phi \\ 0 & 0 & 1 \end{pmatrix} , \qquad (11)$$

where $\emptyset = \nu_\nu s/R$ and s is the path length over which the transfer matrix acts.

We want the transfer matrix about the reference orbit (optic axis) between the target and the standard target location. Let X and X' be the displacement and slope of this reference orbit relative to the equilibrum orbit for momentum p_0. If we wish to generalize to cases in which X and X' are not small quantities, then we must expand the matrix as a function of p:

$$M(p) = M(P_0) + \frac{\partial M}{\partial p}\bigg|_{p_0} (p-p_0) + \cdots \quad . \tag{12}$$

Let x, x', and $\Delta p/p$ be taken relative to the reference orbit; then

$$\begin{pmatrix} X+x \\ \frac{R}{\cdot}(X'+x') \\ \frac{\Delta p}{p} \end{pmatrix}_f = \left\{ M(p_0) + \frac{\partial M}{\partial p}\bigg|_{p_0} \Delta p \right\} \begin{pmatrix} X+x \\ \frac{R}{\cdot}(X'+x') \\ \frac{\Delta p}{p} \end{pmatrix}_i \quad . \tag{13}$$

If we now subtract out the reference orbit and collect the remaining terms, we obtain the transfer matrix relative to the reference orbit:

$$\begin{pmatrix} x \\ \frac{Rx'}{\nu_\nu} \\ \frac{\Delta p}{p} \end{pmatrix} = m \begin{pmatrix} x \\ \frac{Rx'}{\nu_\nu} \\ \frac{\Delta p}{p} \end{pmatrix}, \text{ and } m = \begin{pmatrix} \cos\emptyset & \sin\emptyset & \frac{R}{\nu^2}(1-\cos\emptyset - kX_i\emptyset\sin\emptyset + kX_i'\emptyset\cos\emptyset) \\ -\sin\emptyset & \cos\emptyset & \frac{R}{\nu^2}(\sin\emptyset - kX_i\emptyset\cos\emptyset - kX_i'\emptyset\sin\emptyset) \\ 0 & 0 & 1 \end{pmatrix}.$$

The coefficient k is obtained as follows:

$\emptyset = \nu s/R \approx c(1-n)^{1/2}$ for some constant $c=c(s)$;

$$\frac{\partial \cos\emptyset}{\partial p} = -\emptyset\sin\emptyset \left\{ \frac{1}{2}\frac{c}{\emptyset}(1-n)^{-1/2}\left(-\frac{\partial n}{\partial p}\right) \right\} = -k\frac{R}{\nu^2}k\,\emptyset\sin\emptyset ,$$

where $k = \frac{1}{2}\,\frac{\nu^2}{R}\,\frac{1}{1-n}\,\frac{\partial n}{\partial p} \approx \frac{1}{2}\left(1 + \frac{4L}{4\pi R}\right)^2 \frac{1}{R} = \frac{1}{2}\left(1 + \frac{4L}{4\pi R}\right)^2 \frac{1}{p}\,\frac{1}{1-n}\,\frac{\partial n}{\partial R}$,

since $\frac{dp}{p} = \frac{dR}{R}(1-n)$.

A more accurate matrix can be obtained by applying the method of Courant and Snyder[23] to the general linearized equation of motion, the Hill equation, for a synchrotron with azimuthally varying fields. The increase in accuracy amounts to about 10% and is not important here since this matrix is required only for the relatively short distance between the actual target location and the standard target location.

2. Agreement Between the Linear Codes and BOC

The output of the linear codes determines the radial and vertical spreads of the beam at the exit window, the divergence at the window, and the dispersion at the window.

Although this approach gives excellent agreement for the dispersive displacement at the window, it cannot be expected to describe the entire phase space pattern adequately. Even in cases for which approximation indicates that the patterns are exactly the same for the three energies considered, the accurate orbit calculations show that this is almost never true, because of the large second order effects described in Chapter II. However, excellent agreement was found for a few choices of parameters, for which the second order effects are small.

IV. THE OPTICAL DESIGN OF THE EXTERNAL BEAM

We now turn our attention to the solution of the optical design problem of extracting the proton beam. The requirements on the beam are discussed first. We then consider the parameters to be specified, describing the basic effects of their adjustment. Finally, the method of solution, using the numerical calculational tools previously described, is discussed, concluding with the results of the design study.

A. The Design Objectives and Restrictions

1. Optical Properties Required at the Exit Window

The recombination in energy should be as complete as possible in order that the size of subsequent focal spots and the divergence of the beam be minimized. The criterion is that the effective phase space occupied by the entire beam, including residual dispersive and nonlinear effects, should be minimized. The effective occupied phase space area is determined by the area of the smallest simple closed curve, such as an ellipse, that completely encloses the beam. The minimum size of external focal spots is directly related to this area. Although nonlinear effects do not increase the actual occupied phase space area, in general they increase the effective occupied phase space area as defined above. The criterion of effective area is used because linear focusing elements, such as quadrupole magnets, cannot remove aberrations already present in the beam.

The entire beam must pass through the 3.5 in. radial aperture at the exit window. As the beam must travel approximately

100 in. to the first focal elements beyond the exit window, the divergence of the beam should be minimized.

2. Restrictive Mechanical Considerations

In order to obtain full beam intensity all of the internal magnets in the optical system must be plunged and pulsed; stray fields and obstructions are particularly damaging at injection. The magnets M_1, Q_1, M_2, and Q_2 must be constructed to withstand continual plunged operation in high vacuum. These considerations place a premium upon minimizing the size and weight of the magnets. In addition, reliability demands conservative design.

The apertures and fields of the magnets are further restricted so that the main circulating beam will not be perturbed by stray fields. As M_1 and Q_1 must be plunged close to the circulating beam, the stray field must nearly vanish beyond the septum. These restrictions are not as severe for M_2 and Q_2 since they are not plunged quite so close to the beam.

Both of the bending magnets are "C" type magnets with magnetic shields placed between their open sides and the circulating beam. The two quadrupole magnets are Panofsky type (current sheeet) magnets. All of the magnets are water-cooled; even with pulsed operation, the maximum fields are limited by the tolerable temperature rise.

The geometry of the Bevatron (Fig. 9) restricts the azimuthal locations of the magnets. The beam must emerge into the west tangent tank area; thus M_2 and Q_2 must be located in the south tangent tank. M_1 and Q_1 must share the east tangent tank with the injector and the rapid beam ejector. The energy loss target should be in the neighborhood of the south tangent tank (within 90^{o}). The rf cavity fills the north tangent tank.

3. Reduced Energy External Beam

Although the design must be optimized for the full energy, 6.2 BeV, external beam, satisfactory beams must also be obtainable at lower energies. The shape of the Bevatron field is a function of energy with nonlinearities increasing as saturation is approached. The inward deflection at M_1 is approximately inversely proportional to momentum [Eq. (1)]. The initial radial divergence at the target, due to multiple Coulomb scattering within the target, is increased as the momentum is decreased.

Provision must also be made for a continuous beam-spill during acceleration; this can be accomplished by programming the radial position of M_1 and the strengths of all of the magnets so that they "track" the rising Bevatron field.

B. The Adjustable Parameters

There are five independent parameters to be specified, assuming fixed azimuthal positions for the magnets. These parameters are: (a) target azimuth, (b) target thickness, (c) strength of M_1, (d) strength of Q_1, and (e) strength of Q_2. The radial location of M_2 depends upon the strength of M_1. The radial location of M_1 depends upon the target azimuth and target thickness. The strength of M_2 is fixed by the location of the exit window. We now discuss the basic effects of adjusting these parameters.

1. Target Azimuth

Varying the azimuthal location of the target relative to M_1 causes the phase space pattern at M_1 to rotate. The maximum inward deflection is obtained for an azimuthal separation of one-half betatron period; this separation results in the target being imaged at M_1. Changing the target azimuth decreases the deflection and also increases the width of the beam at M_1; however, other properties of the beam may be improved by changing the target azimuth.

2. Target Thickness

Increasing the target thickness results in a larger deflection at M_1; moving M_1 further from the circulating beam relaxes the design requirements, particularly those of gap size and stray field, on this magnet. However this gain is offset by an increase in the energy spread due to the Landau effect.

3. Strength of M_1

Increasing the inward deflection at M_1 results in moving M_2 further from the circulating beam; this relaxes design requirements on M_2, but at the expense of increasing the size of M_1. Another result of changing the radial location of M_2 is to move the beam through a different field region in the Bevatron; this noticeably affects the character of the aberrations. For several choices of the other parameters, it is possible to nearly eliminate the curvature in the phase space patterns at M_2 by the proper choice of the strength of M_1.

4. Strength of Q_1

Q_1 has little effect on the radial imaging properties for monoenergetic beams, for reasons noted in Chapter II. The strength of this magnet must be chosen to optimize both the energy recombination at the window and the vertical divergence at the window. Acceptable vertical divergence at the exit window can be realized only if this magnet is weakly converging in the vertical plane (with focal length greater than 500 in.).

5. Strength of Q_2

The radial beam width at the exit window is very sensitive to the strength of Q_2. For most choices of the other parameters, Q_2 must be weakly convergent in the radial plane.

C. The Method of Solution

During the years 1956 to 1959 several experiments were conducted with single magnet extraction systems. It soon became apparent that only a small fraction of the beam could be extracted with this scheme, for the reasons listed in Chapter II. The mechanism of the energy-loss target was explored, resulting in experimental values for the size and divergence of the reduced energy beam leaving the target. During the next few months, the two magnet scheme, suggested by Dr. Lambertson, was more seriously considered.

The original version of the Bevatron Orbit Code and the field conversion codes, BEFCYF and DBDT, were written in early 1960. Initial theoretical studies were conducted by Dr. Lloyd Smith, Dr. Andrew Sessler, and Dr. Alper Garren.

1. Numerical Orbit Sudies

When BOC became available for use, comprehensive studies of the beam behavior were initiated by Dr. Sessler. Starting with an eleven MeV loss at the target, several azimuthal target locations, near the half-betatron period location, were considered. For each target location, representative groups of orbits were run on BOC with a range of strengths of Q_1. Phase space patterns were plotted at each magnet. Experience soon indicated the focusing requirements at Q_2.

The author worked with Dr. Sessler during the second and third months of the study; a similar numerical exploration was undertaken for a 5 MeV loss target. At the one-half betatron period position, an acceptable solution was found yielding a radial spread of 3.2 in. at the window with an effective increase in occupied phase space area amounting to a factor of four or five.

Upon Dr. Sessler's return to Ohio the author, working with Dr. Garren, continued the exploration of the 5 MeV target. During this period, the ability to determine several parameters (strengths of M_1, M_2, and Q_2) was built into BOC along with the other improvements noted previously; allowing BOC to assign these strengths led to a refinement of the solutions. Three parameters remained: the choice of target location, radial location of M_2, and Strength of Q_2.

2. Linear Parameter Survey

Although an acceptable solution had been determined, the possibility of other totally different solutions existed. The number of cases which could be explored by BOC was limited by cost considerations; each orbit integrated around the Bevatron cost one dollar in computer time. The linear codes, described in III. B., were written to rapidly survey the possible choices of parameters. These codes provide a clearer picture of the functional dependence of the dispersive and focal properties of the beam upon the parameters.

The output of the linear codes incorporated ideas of Dr. Sessler; the primary output consists of dispersive separation in displacement and slope at the window, the monoenergetic pattern widths and divergences, and the total pattern widths and divergences. Hundreds of combinations of choices of target location, focusing at Q_1, and focusing at Q_2 were examined. Promising combinations were further explored with the aid of BOC. Several good solutions were discovered for qualitatively different choices of the parameters.

3. Reduced Energy Survey

The same type of survey described above for 6.2 BeV protons was carried out for 4.2 BeV protons by the author with BOC and by Dr. Garren with the linear codes. The same target was used, resulting in greater divergence of the beam leaving the target at 4.2 BeV than the divergence at 6.2 BeV. The overall increase in effective phase space is greater at 4.2 BeV since the amplitude of betatron oscillations is inversely proportional to momentum [Eq. (1)].

4. Variations to the Basic System

During the course of the study, Dr. William A. Wenzel and Dr. Glen R. Lambertson contributed much to the optical design. Their familiarity with the Bevatron provided keen insight into the nature of the solutions obtained and the adjustments which should be explored. Their aid was invaluable in assessing the engineering feasibility of proposed designs.

During the course of the study, as the requirements upon each magnet became clear, the properties of that magnet were fixed so it could be designed and constructed.

Before fixing the requirements upon any magnet, several novel variations of the extraction scheme were examined.

a. New Window Location. The possibility of extracting the beam about 100 in. upstream from the west tangent tank exit window was considered. Passing through the fringing field over a shorter distance should reduce the radial divergence due to the fringing field. Numerical calculations showed that the slight improvement would not justify cutting the required channel through the magnet iron.

b. Target Location. The linear codes revealed very good solutions for 5/8 to 3/4 betatron period between the target and M_1. Studies with BOC verified the good behavior at the exit window, although aberrations doubled the actual width predicted by the linear codes. These solutions require a larger radial aperture at M_1.

c. Sextupole Magnet. The author proposed inserting a sextupole magnet adjacent to Q_2. Calculations revealed that such a magnet produces marked improvements for those cases characterized by large curvature in the phase space patterns at M_2; for example, the insertion of a sextupole reduces the radial spread of one of the systems mentioned in Paragraph b, above, from 2.6 in. to 1.2 in.. However, several choices of parameters were determined that yielded good beam behavior without the added complication of a sextupole magnet.

d. Radial Placement of M_2. After the aperture requirements at M_2 were established, it was discovered that M_2 could be moved closer to the circulating beam. This change was made after investigations with BOC demonstrated that the aberrations were reduced by decreasing the deflection at M_1; this also reduces the size of M_1. With the new location for M_2, the behavior of the beam as a function of the strength of Q_1 was carefully studied.

D. Conclusions

With a 5 MeV loss target, the initial spread of the beam leaving the target is 0.25 in. (radial) and 0.5" (vertical). The maximum divergence considered in either plane is 1.2 mr. at 6.2 BeV and 1.7 mr. at 4.2 BeV. An energy spread of ± 1.5 MeV is due to the Landau effect. The following results were derived from these initial conditions.

1. Functional Dependence on the Parameters

a. Strength of Q_1. Work with the linear codes demonstrate that the monoenergetic spread at the window is nearly independent of Q_1 for the half-betatron period target location; this was predicted in Chapter II. With Q_2 converging in the radial plane with a focal length of 2000 in., the total radial spread at the window is 3.5 in.

independent of the strength of Q_1. However, the vertical divergence is very sensitive to focusing by Q_1.

For every target location, there exists a strength for Q_2 that renders the total radial spread independent of Q_1; as the target location moves further from the half-betatron period location, the total radial spread at this strength of Q_2 increases.

<u>b. Target Location.</u> The radial beam distribution at M_1 for several target locations is shown in Fig. 11. The two plots at the top of this figure show the radial distribution of the beam leaving the target, with the plot for 6.2 BeV on the left and that for 4.2 BeV on the right.

The second line shows the distributions at M_1 for 6.2 BeV while the third line shows these distributions for 4.2 BeV. The south tangent tank location corresponds to the fourth column from the left; the righthand column corresponds to the east tangent tank location.

Each of these figures is centered on the configuration point for the reference orbit (optic axis). The horizontal axis is the radial displacement; each division is one inch. The vertical axis is the radial divergence; each division is one milliradian. Twenty-seven orbits are plotted representing three initial displacements, three initial angles, and three energies. Mean energy configuration points are labelled by small diamonds; those corresponding to energies 1.5 MeV above and below the mean energy are labelled by the letters "T" and "X", respectively.

Good solutions were obtained for a variety of target locations. The further the target is from the half-betatron

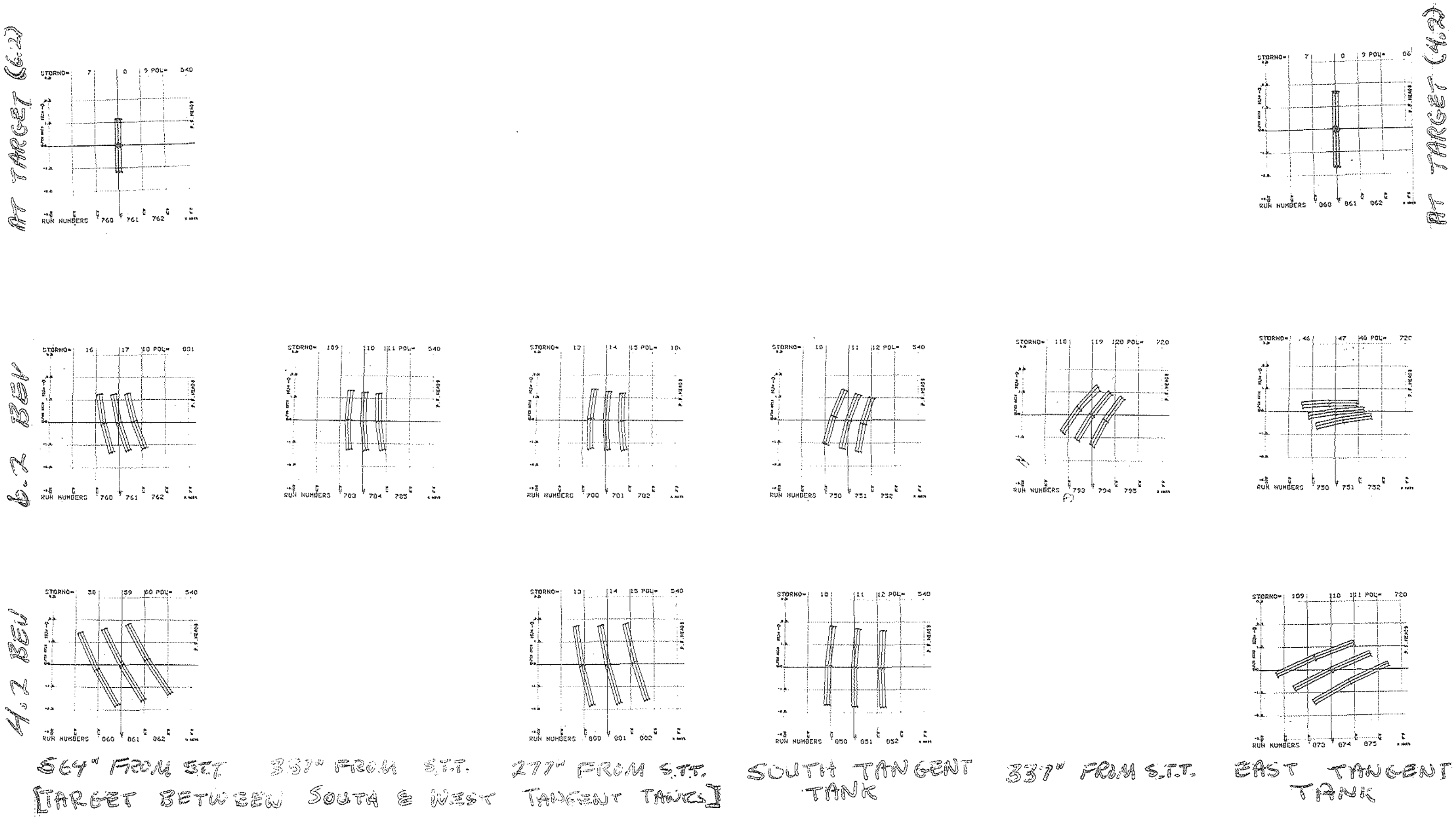

MUB-1888

Fig. 11. Phase space distributions at M_1 for different target locations.

position, the greater the dependence of the radial spread at the window upon Q_1, provided Q_2 is not set to the strength for which Q_1 has no influence. The target was placed in the south tangent tank due to these considerations and because there is an available air-lock at that point (which simplifies target adjustment).

c. Strength of Q_1. Fig. 12 shows the radial dependence upon Q_1 at 6.2 BeV; M_2 is positioned 12.2 in. inside the circulating beam. Each column in thie figure corresponds to a particular choice of parameters. The lefthand column corresponds to strong radial focusing at Q_1; the second column corresponds to no focusing at Q_1, and columns further to the right correspond to increased radial defocusing at Q_1. In each case, Q_2, is chosen to optimize the radial beam distribution at the window. The top row shows the distributions after Q_1; the next three rows show the distributions before Q_2, after M_2, and at the exit window, respectively. The scale divisions for each of these graphs are one inch and one mr. The bottom line shows the distribution at the exit window with the radial scale expanded for clarity; each division in the radial scale corresponds to 0.2 in.

Figure 13 shows a similar study at 4.2 BeV. Note the increased separation of the patterns for different energies. The second bending magnet is positioned 5.5 in. inside the circulating beam for this and subsequent figures.

Figure 14 shows the vertical phase space distribution at 4.2 BeV; the first column corresponds to the first column in Fig. 12, the second column with the fourth column, and the last column with the third column in the preceding figure.

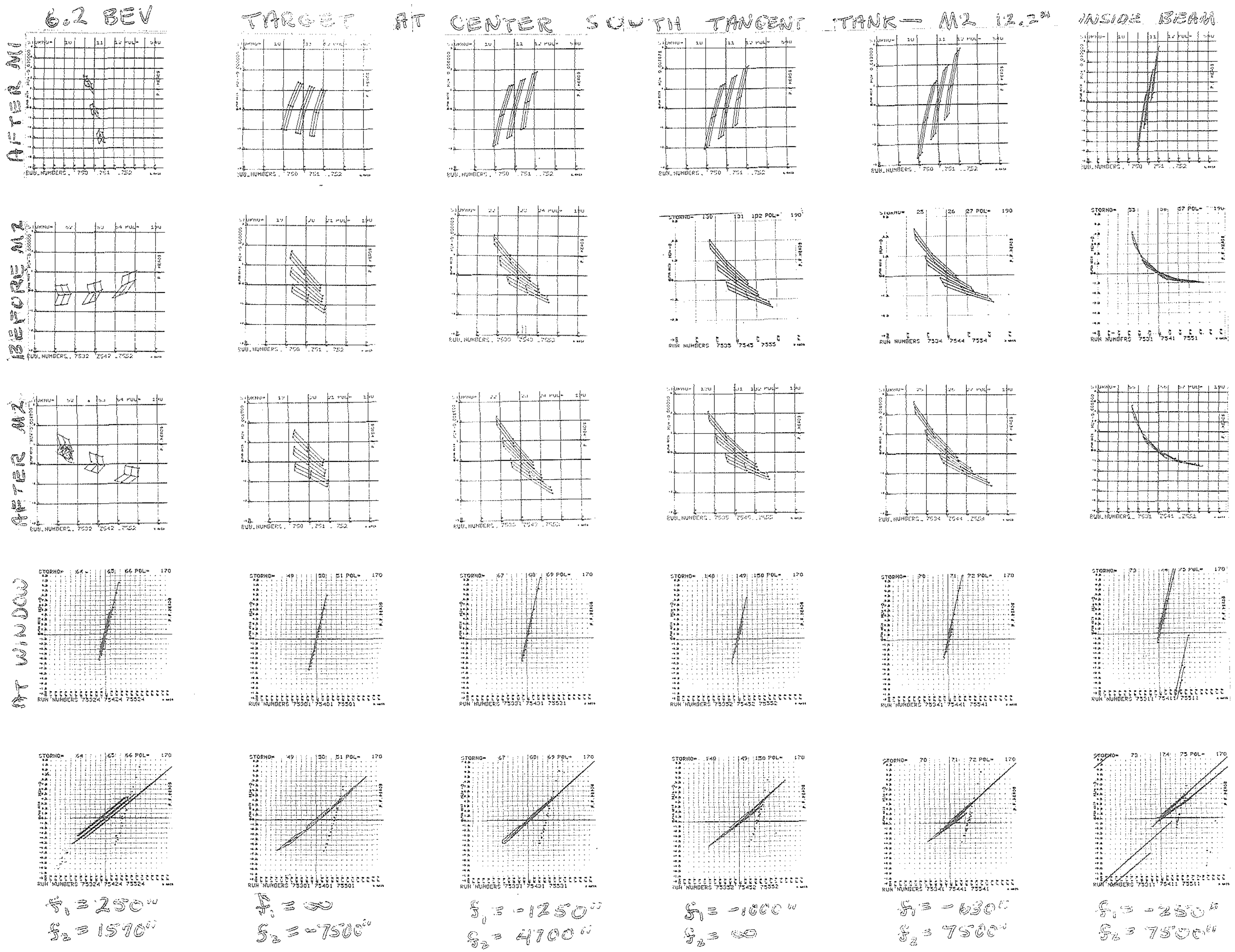

MUB-1889

Fig. 12. Beam at 6.2 BeV from M_1 to window (M_2 12.2 in. in).

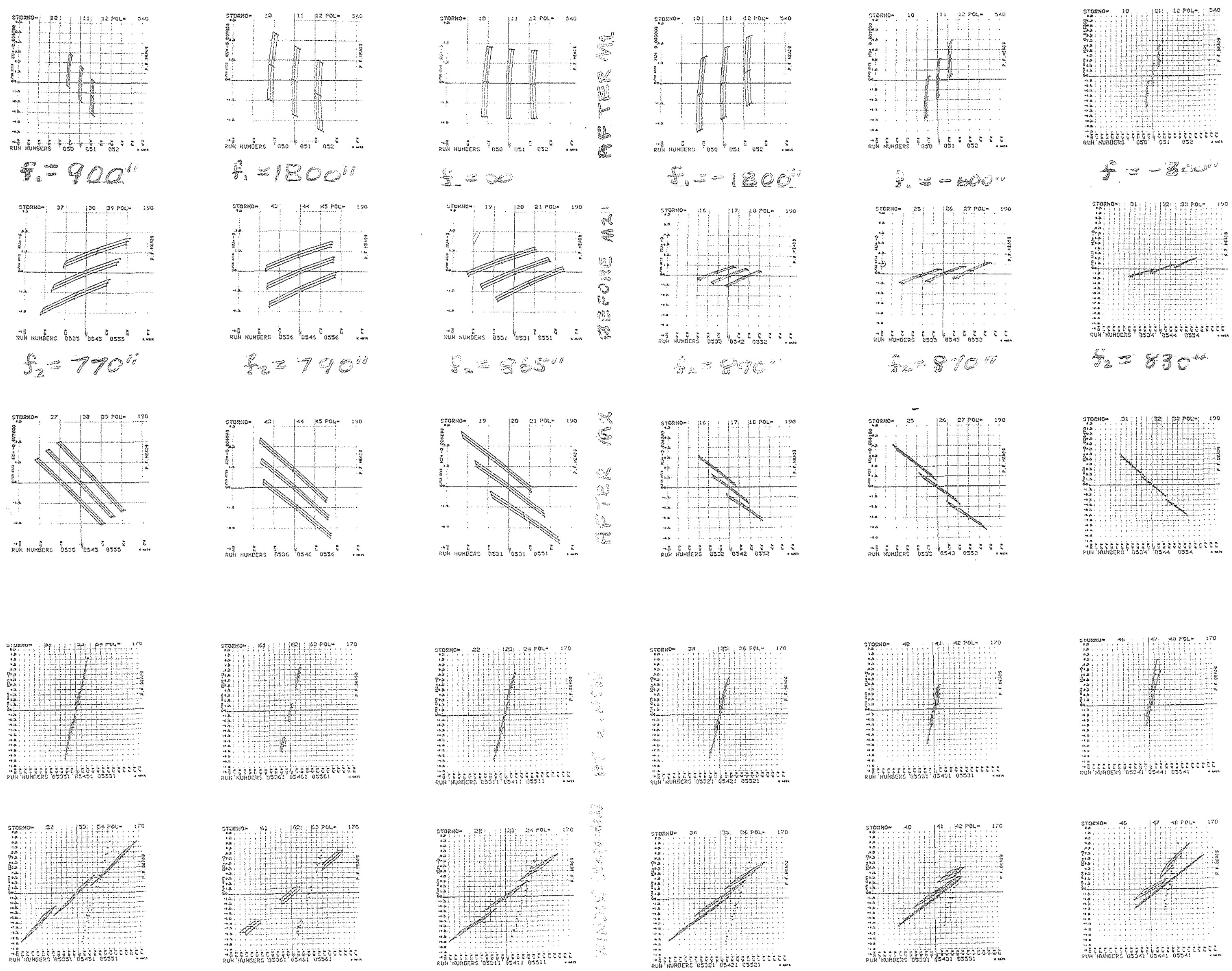

MUB-1890

Fig. 13. Beam at 4.2 BeV from M_1 to window (M_2 5.5 in. in).

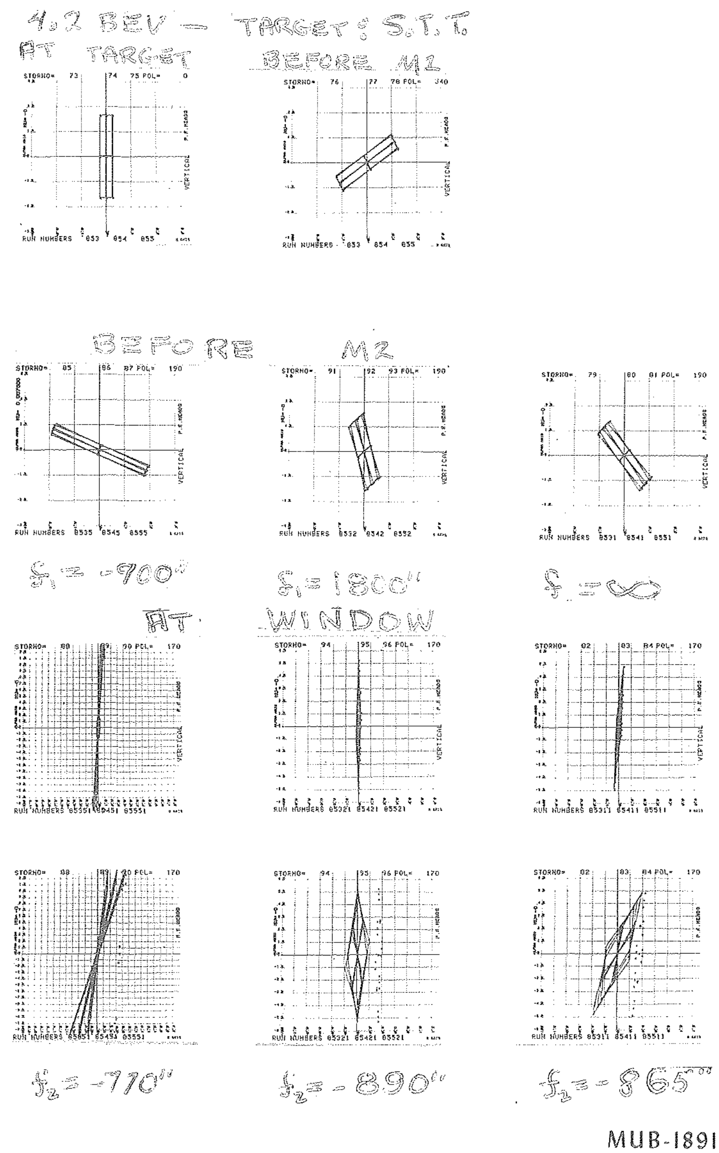

Fig. 14. Vertical phase space patterns at 4.2 BeV.

d. Radial Position of M_2. The second bending magnet is 12.2 in. inside the circulating beam in Fig. 12. Moving this magnet to 5.5 in. inside the circulating beam reduces the aberrations as shown in Fig. 15; the range of focusing at Q_1 is less in this figure than in the preceding figures. The top row shows the radial distributions before Q_2. The bottom two rows show the distributions at the exit window. The best solution is that shown in the fourth column from the left; this solution is described in the next section.

2. The Optimum Solution

The optimum solution, with the target located in the center of the south tangent tank, requires that Q_1 be radially divergent with a focal length of -1200 in. and that Q_2 be radially convergent with the same focal length.

At the exit window, the total radial spread is 1.7 in., the total vertical spread is 0.5 in., and the maximum vertical divergence is $\pm$ 4 mr. The effective occupied phase space area is approximately twice the area occupied by the beam leaving the target.

Vertical apertures of 2 in. at all magnets would barely suffice to pass the beam. Radial apertures of 2.2 in. and 4 in. are required at M_1 and M_2, respectively.

With these apertures, the first magnet pair (M_1 and Q_1) weighs about 300 pounds whereas the second magnet pair with its associated mechanism weighs over four tons. These magnets must be plunged 28 in. in 0.75 second every six seconds, coming to rest within a few thousandths of an inch of the required position.

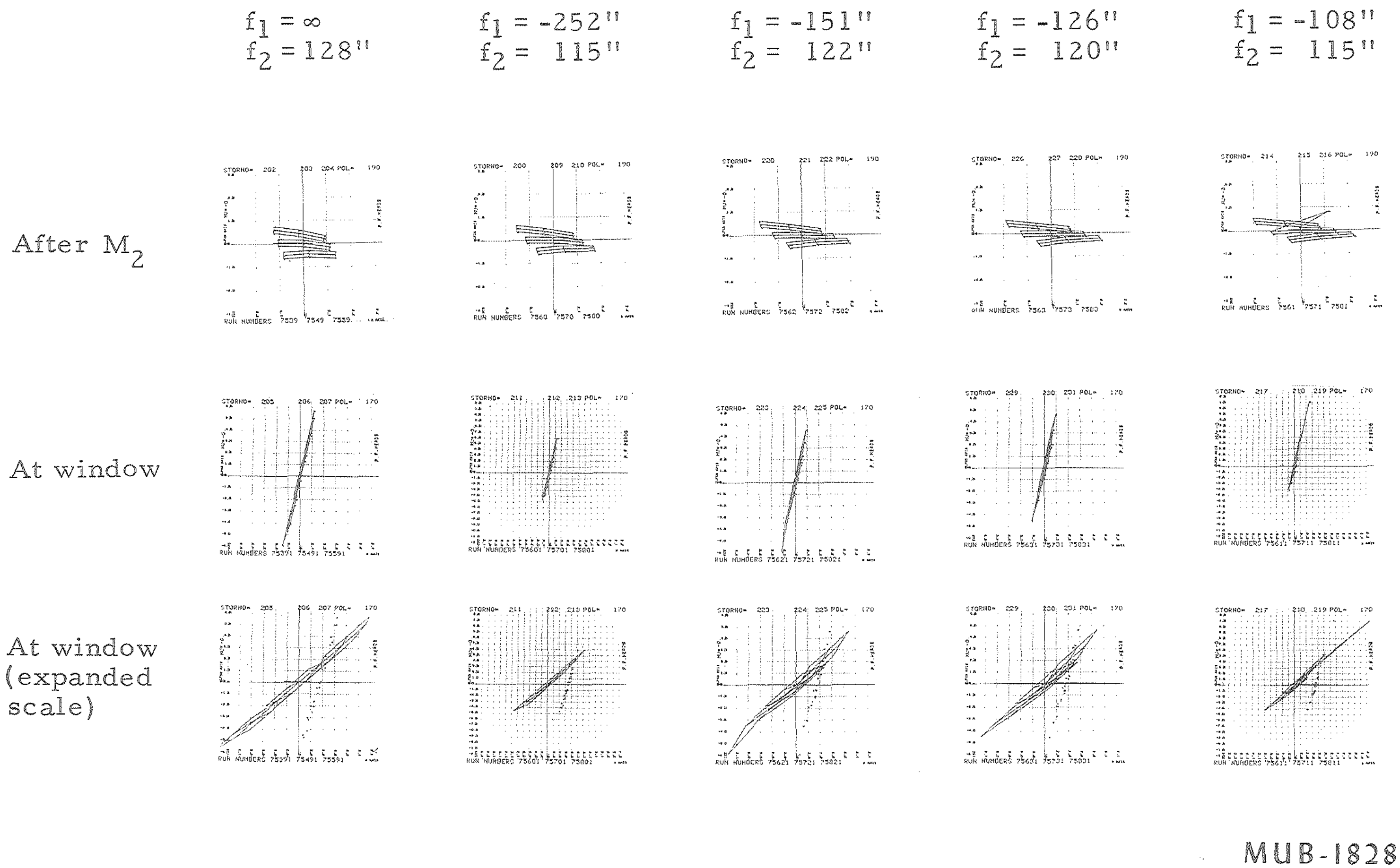

Fig. 15. Beam at 6.2 BeV from M_2 to window (M_2 5.5 in. inside).

3. Comparison with Experimental Results

Measurements of the external beam commenced in early 1963; at this time the beam system was complete through the external bending and quadrupole magnets M_3, Q_{3A}, and Q_{3B}, shown on Fig. 9. No disagreements between theory and experiment have been discovered. The magnet excitations determined in the beam design study produce a well defined beam, agreeing with theoretical predictions within experimental accuracy. Equally well defined beams have been obtained for magnet excitations varying from those that are theoretically optimized; the magnet excitations are not critically defined. No estimate can yet be made as to the portion of the beam successfully extracted. That portion of the beam that is extracted has been focused to an image 0.5 in. (radial) by 0.10 in. (vertical) several feet beyond the external quadrupole magnets Q_{3A} and Q_{3B}. (6.2 BeV).

Figure 16 shows the relative intensity of the extracted beam as a function of radial displacement at the exit window. The measurements were made using two small moveable scintillator counters 5/16 in. in diameter and 2 in. in height; a 14 MeV loss target was used with the full energy beam. The beam width is slightly larger than that calculated; this is due to the larger energy spread obtained from a 14 MeV target (the calculations assumed a 5 MeV loss target). The tails on the intensity distribribution are due to the Landau tail on the energy distribution possibly augmented by scattering off some obstruction upstream.

Figures 17, 18, and 19 are radioautographs of the beam at M_1, M_2, and the exit window, respectively. Polyethylene

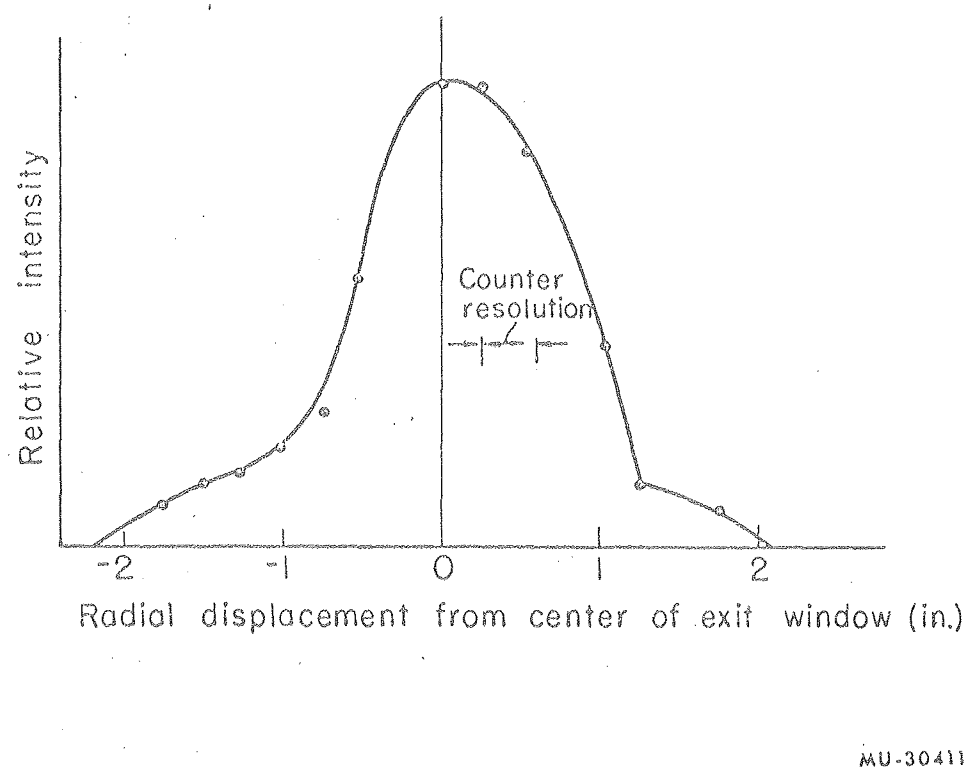

Fig. 16. External beam distribution at exit window.

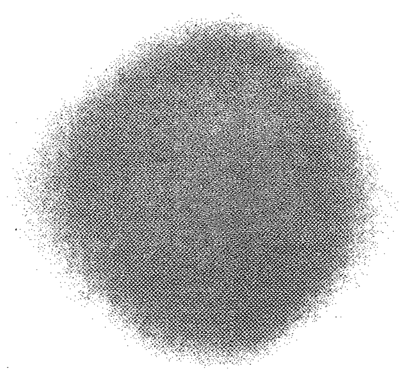

MUB-1896

Fig. 17. Radioautograph of the beam at M_1.

targets are exposed to the beam, removed from the beam, and placed in contact with X ray film for several minutes. Because of the narrow exposure latitude of the film, these pictures do not accurately reflect intensity distributions.

Figure 17 shows a clean separation between the reduced energy beam at M_1 and the energy loss target which is located about two inches to the right of the edge of this picture. The radial and vertical heights are in excellent agreement with theory.

The beam dimensions at M_2 (Fig. 18) are also in excellent agreement with theory. The variation in beam height across the magnet aperture demonstrates the effect of the vertical behavior upon the radial beam path; this is an aberration corresponding to terms in xz, $x'z'$, and r^2 which represent the second order corrections to the vertical equation of motion (3).

Figure 19 shows the beam at the window. The beam is asymmetrically distributed across the gap; this agrees with theory as shown in Fig. 15.

The external beam will be available to experimenters in a few months. Further measurements will be made in the intervening period.

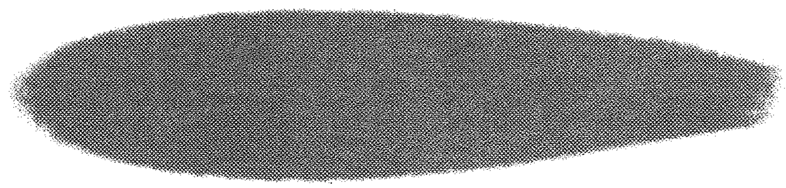

MUB-1895

Fig. 18. Radioautograph of the beam at M_2.

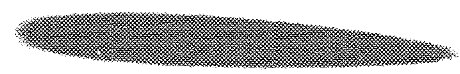

MUB-1897

Fig. 19. Radioautograph of the beam at the exit window.

ACKNOWLEDGEMENTS

I wish to thank Dr. David L. Judd for suggesting the two problems treated in this thesis and for his patient help and encouragement throughout the research and for his critical review of the entire manuscript. I am indebted to Dr. Alper A. Garren and Dr. Jonathan D. Young for their guidance in the application of linear programming techniques to the optimization problems of varying the parameters of a beam system to achieve specified optical properties. Dr. Lloyd Smith was most helpful in the writing of the manuscript.

This work was done under the auspices of the U. S. Atomic Energy Commission.

REFERENCES

1. E.D. Courant, M. S. Livingston, and H. S. Snyder, Phys. Rev. 91, 202 (1953) (letter).
2. E. D. Courant, M. S. Livingston, and H. S. Snyder, Phys. Rev. 88, 1190 (1952)
3. F. Jenkins and H. White, Fundamentals of Optics (McGraw-Hill Book Co., Inc., New York, 1950). Chap. IX.
4. J. C. Burfoot, Third Order Aberrations of 'Doubly Symmetric' System, Proc. Phys. Soc. B67, 523 (1954).
5. E. Reisman, The Imaging Properties of Crossed Magnetic Quadrupoles (Thesis--Cornell University), University Microfilms No. 24773, 1957 (unpublished).
6. P. Grivet and M. Y. Bernard, CERN Laboratory Report (P. S.) MB-6, 1955 (CERN, Geneva) (unpublished).
7. A. Septier, Étude des Champs de Fuite d'une Lentille Quadrupolaire Magnetique, Rend. Acad. Sci. 243, 1026 (1956).
8. P. Grivet and A. Septier, Les Lentilles Quadrupolaires Magnetiques, CERN 58-25, (1958); Nucl. Instr. 6, 126 (1960); Nucl. Instr. 6, 243 (1960).
9. A. Septier, Strong-Focusing Lenses, Advances in Electronics and Electron Physics 14, 85 (1961).
10. K. G. Steffen, in Proceedings of the International Conference on High Energy Accelerators, Brookhaven, 1961 (Brookhaven, New York, 1961), p. 437.
11. V. K. Zworykin, G. A. Morton, E. G. Ramberg, J. Hillier, and A. W. Vance, Electron Optics and the Electron Microscope (J. Wiley and Sons, Inc., New York, 1945), Chap. XVI.

12. H. Goldstein, Classical Mechanics (Addison-Wesley Publishing Co., Inc. Reading, Mass., 1950), Chap. VIII.

13. S. I. Gass, Linear Programming--Methods and Applications (McGraw-Hill Book Co., Inc. New York, 1958).

14. R. J. Clasen, RS MSUB--Linear Programming Subroutine FORTRAN Coded, SHARE distribution #1281 (RAND Corp., Santa Monica, Calif.)(1961).

15. B. Wright, Rev. Sci. Instr. 25, 429 (1954).

16. O. Piccioni, D. Clark, R. Cool, G. Friedlander, and D. Kassner, Rev. Sci. Instr. 26, 232 (1955).

17. E. McMillan, Rev. Sci. Instr. 22, 117 (1951).

18. L. D. Landau, J. Phys. (U.S.S.R.), 8, 201 (1944).

19. Hans A. Bethe and Julius Ashkin, Passage of Radiations through Matter, in Experimental Nuclear Physics, E. Segrè, Ed. (Wiley, New York, 1953), pp. 242-245, 255-258.

20. R. G. T. Bennett and J. W. Burren, An Achromatic System of Extraction for Proton Synchrotrons, J. Nucl. Energy.Pt. C, 3, 14 (1961).

21. M. M. Gordon, T. A. Welton, T. I. Arnette, and H. C. Owens, An IBM 704 Code for Determining Equilibrium Orbits and Properties of Small-Amplitude Oscillations in Cyclotron Fields, Oak Ridge National Laboratory Report ORNL 59-11-2 (Oak Ridge Tenn.) (1959) (unpublished).

22. C. G. Gardner, BEFCYF and DBDT: IBM 704 Codes for Preparing Input for Bevatron Orbit Code (BOC), University of California Radiation Laboratory Report UCRL-9387 (1960) (unpublished)

23. E. D. Courant and H. S. Snyder, Theory of the Alternating-Gradient Synchrotron, Annals of Physics 3, 1 (1958).